



Title: Design, installation, and assessment of a biological winery wastewater treatment system

Gareth A. Holtman
Student number: 210117168

A thesis submitted to the Faculty of Engineering, Cape Peninsula University of Technology, Bellville, in partial fulfilment of the requirements for the Masters of Engineering Degree in Civil Engineering

Bellville
November 2017

Declaration

I declare that this research dissertation is my own unaided work. It is being submitted for the Masters of Engineering Degree at Cape Peninsula University of Technology, Cape Town. It has not been submitted before for any degree or examination in any other University.



(Signature)

Signed in Bellville this ____ 09 ____ day of ____ November ____ 2017

Outcomes

In addition to the material contained in the thesis, the following outcomes were attained during this project:

Publications

1. Welz, P.J., **Holtman G.A.**, Haldenwang, R., Le Roes-Hill, M. (2016) Characterisation of winery wastewater from continuous-flow settling basins and waste stabilisation ponds over the course of one year: implications for biological wastewater treatment and land application. *Water Science and Technology* 74: 2036-2049.
2. Welz, P.J., Mbasha, W., Smith I., Terblanche, G., **Holtman, G.A.**, Le Roes-Hill, M., Haldenwang R. (2017) The influence of grain physicochemistry and biomass on hydraulic conductivity in sand-filled treatment wetlands (submitted to *Ecological Engineering*, July 2017)

Conference presentations

International congresses

1. Smith, I., **Holtman, G.A.**, Haldenwang, R., le Roes-Hill, M., Welz., P.J. Impact of biomass build-up and sand mineralogy on wastewater flow in biological sand filters (13th IWA *Leading Edge Conference on Water and Wastewater Technologies*: Jérez da la Frontera, Spain, 2016). **Poster presentation.**
2. **Holtman, G.A.**, Haldenwang, R., Le Roes-Hill, M., Smith, I., Welz, P.J. Treatment of winery wastewater using a biological sand filtration system (13th IWA *Leading Edge Conference on Water and Wastewater Technologies*: Jérez da la Frontera, Spain, 2016). **Poster presentation.**
3. Welz P.J., **Holtman, G.A.**, Haldenwang, R., Le Roes-Hill, M. Characterisation of freshly settled and ponded winery wastewater. *IWA International congress on winery waste and sustainable viticulture*: Stellenbosch, South Africa, 2015). **Oral presentation.**
4. **Holtman, G.A.**, Haldenwang, R., Le Roes-Hill, M., Welz, P.J. Treatment of winery wastewater using a biological sand filtration system. *IWA International congress on winery waste and sustainable viticulture*: Stellenbosch, South Africa, 2015). **Oral presentation.**

Abstract

Currently in South Africa, most wastewater from small cellars is pH-adjusted and disposed of via land irrigation. This practice can lead to environmental degradation. There is a need for low cost, low maintenance solutions for the treatment of cellar effluent. Constructed wetlands provide such an option. However, the use of plants is problematic because winery effluent can be phytotoxic. After successful initial laboratory-scale experiments, an *in-situ* pilot scale biological sand filter (unplanted constructed wetland) system was designed, installed, and used to treat effluent from a small winery in the Western Cape, South Africa. The system is off-grid, totally self-regulating, and uses a modular approach which allows for the addition and subtraction of filter modules within the system to alter treatment capacity, retention time and/or rest filter modules. The system can be easily integrated into existing settling basins and/or retention ponds at small wineries.

The biological sand filter was operational for 610 days, and showed promising results. The average chemical oxygen demand removal efficiency was 81% (range: 44-98%) with an average effluent of 324 mg/L, and an average flow rate of 413 L/day after the acclimation (start-up) period. The average hydraulic loading rate after the initial start-up period was 143 L/m³ sand day⁻¹ (range: 67-222/m³ sand day⁻¹), with an organic loading rate of 205 gCOD/m³ of sand day⁻¹ (range: 83-338 gCOD/m³ sand day⁻¹) which resulted in an organic removal rate of 164 gCOD/m³ of sand day⁻¹. There was an average of 67% removal of total phenolics, thereby reducing the potential phytotoxicity of the effluent. In addition, there was a 1.6 times increase in calcium concentration, a 29% decrease in the average sodium adsorption ratio, and complete passive neutralisation of the acidic winery wastewater (final effluent pH range: 6.63 – 8.14).

The findings of this study compare well with previous laboratory studies conducted with synthetic and authentic winery effluent. The system can potentially provide a low cost, energy efficient, low maintenance, sustainable means of treating cellar effluent at small wineries. Uptake of this technology may alleviate environmental degradation caused by irrigating land with inadequately treated effluent.

Acknowledgements

I would like to acknowledge the National Research Commission of South Africa for providing funding for this research. I would like to acknowledge the Biocatalysis and Technical Biology research group for the provision of laboratory equipment and work space. I would like to thank my supervisors, Dr P.J. Welz and Prof R. Haldenwang for their time, effort and guidance they have given me and helped me through my Masters. I would like to thank I. Smith for his research and help with the initial design and assistance in installing the system.

Table of Contents

	Page
Declaration	i
Outcomes	ii
Abstract	iii
Acknowledgements	iv
Table of Contents	v
List of Figures	ix
List of Tables	xiii
Abbreviation	xv
Nomenclature.....	xvi
Chapter 1 Introduction	1
1.1 Background and Motivation.....	1
1.2 Research problem	1
1.3 Research Question	1
1.4 Aim, objectives and outcomes	2
1.5 Significance.....	2
1.6 Delineation	2
1.7 Assumptions.....	2
1.8 Summary of methodology.....	3
1.9 Organisation of dissertation.....	3
Chapter 2 Literature review and theory	4
2.1 Introduction	4
2.2 Wastewater	4
2.3 Winery wastewater	4
2.3.1 Composition of winery wastewater.....	5
2.3.1.1 Organic fractions of winery wastewater.....	6
2.3.1.2 Inorganic fractions of winery wastewater	6
2.3.2 Volume of wastewater generated by wineries.....	8
2.4 Current methods used to dispose of untreated winery wastewater.....	8
2.4.1 Irrigation as a means of disposal of winery wastewater	8
2.4.2 Other forms of disposal of winery wastewater	9
2.5 Legislation for the disposal of winery wastewater in South Africa.....	9
2.6 Treatment of winery wastewater	11
2.6.1 Physicochemical processes for the treatment of winery wastewater.....	11
2.6.2 Biological processes for the treatment of winery wastewater.....	11
2.6.3 Waste stabilisation ponds	12
2.6.4 Constructed Wetlands	12
2.6.5 Biological sand filters	16
2.7 Determination of selected operational and performance parameters in biological sand filters	17
2.7.1 Determination of hydraulic retention time	17
2.7.2 Determination of hydraulic loading and organic loading and removal rates	18
2.7.3 Hydraulic pipe flow	18

2.8	Conclusion	19
Chapter 3	Research methodology	21
3.1	Research design.....	21
3.2	Study setting.....	21
3.3	Research methodology	21
3.3.1	Data	21
3.3.1.1	Chemical oxygen demand	21
3.3.1.2	Total phenolics	21
3.3.1.3	Volatile fatty acids.....	22
3.3.1.4	Phosphate	22
3.3.1.5	Total nitrogen.....	22
3.3.1.6	Redox and pH.....	22
3.3.1.7	Total solids, total suspended solids, total dissolved solids and electrical conductivity.....	22
3.3.1.8	Sodium, potassium, calcium, magnesium.....	23
3.3.1.9	Flow rate	23
3.3.2	Research equipment	23
3.3.2.1	Construction and installation of the biological sand filter system	23
3.3.3	Analysis and presentation of results	24
3.3.4	Sampling.....	25
3.3.5	System design	27
3.4	Design Calculations	30
3.4.1	Chemical and physical Analysis of substrate used in biological sand filter	30
3.4.2	Flow calculations for sand filter modules	30
3.4.3	Hydraulic calculation for pipe flow from 500 L tank to filter	31
3.4.4	Design of gravity flow from 5000 L holding tank to 500 L tank	31
3.4.5	Design of pumping main	31
3.4.6	Cost	32
3.4.7	Water usage at the cellar	32
Chapter 4	Results	33
4.1	Design calculation	33
4.1.1	Flow calculations for sand filter modules	33
4.1.2	Hydraulic calculation for pipe flow from 500 L tank to filter	33
4.1.3	Design of gravity flow from 5000 L holding tank to 500 L tank	33
4.1.4	Design of pumping main	34
4.2	Characterisation of winery wastewater	34
4.2.1	Chemical oxygen demand	35
4.2.2	Volatile Fatty Acids.....	36
4.2.3	Total phenolics	37
4.2.4	Total Nitrogen and phosphate	38
4.2.5	Total dissolved solids, total suspended solids and total solids.....	39
4.2.6	Electrical conductivity	40
4.2.7	pH.....	40
4.3	Analysis of influent/effluent to/from the biological sand filter system.....	41
4.3.1	Chemical oxygen demand	41
4.3.2	Volatile fatty acids.....	42

4.3.3	Total phenolics.....	44
4.3.4	Total nitrogen and phosphate.....	45
4.3.5	Inorganic constituents.....	46
4.3.5.1	Sodium	46
4.3.5.2	Potassium.....	47
4.3.5.3	Calcium.....	48
4.3.5.4	Magnesium	50
4.3.5.5	Sodium adsorption ratio	51
4.3.5.6	Cation ratio of soil structural stability.....	52
4.3.5.7	Potassium to sodium ratio	54
4.3.5.8	Electrical conductivity	55
4.3.6	Total solids	56
4.3.7	pH.....	56
4.4	Four hour batch test.....	57
4.4.1	Chemical oxygen demand	57
4.4.2	Volatile Fatty Acids.....	58
4.4.3	Total phenolics	59
4.4.4	Inorganic constituents.....	60
4.4.4.1	Sodium	60
4.4.4.2	Potassium.....	60
4.4.4.3	Calcium.....	61
4.4.4.4	Magnesium	62
4.4.4.5	Sodium Adsorption Ratio	62
4.4.4.6	Cation ratio of soil structural stability.....	63
4.4.4.7	Potassium to Sodium ratio.....	64
4.4.4.8	Electrical conductivity	64
4.4.5	pH.....	65
4.5	Hydraulic analysis of the biological sand filtration system	66
4.5.1	Analysis of the flow rate of the system over the experimental period	66
4.5.2	Hydraulic retention times of biological sand filtration system.....	67
4.6	Hydraulic loading rate and organic loading rate	67
Chapter 5	Discussion.....	69
5.1	Treatment performance of the biological sand filtration system	69
5.1.1	Overall organic removal measured by chemical oxygen demand	69
5.1.2	Volatile fatty acids.....	71
5.1.3	Total phenolics	72
5.1.4	The neutralisation of acidic winery wastewater	73
5.1.5	Salts	74
5.2	Volumetric performance	75
5.2.1	Volume of winery wastewater treated by the biological sand filtration system....	75
5.2.2	The hydraulic retention time	76
5.2.3	The hydraulic conductivity and flow rates.....	77
5.2.4	Organic and hydraulic loading rates	79
5.2.5	Correlation of the flow rate with the influent organic concentration.....	81
5.3	Compliance of treated effluent with legislation	82

5.4	Hydrological data and the effect of precipitation and evaporation on the operation of biological sand filter modules	83
5.5	Operational observations and troubleshooting.....	84
5.6	Financial cost of the system	88
Chapter 6	Conclusions and recommendations	90
6.1	Conclusions	90
6.2	Recommendations and future research	91
References	92
Appendices	98
Appendix A.	Flow calculations for sand filter modules	98
Appendix B.	Integration of flow rate	110
Appendix C.	<i>K</i> values for minor losses.....	113
Appendix D.	Brochure for Aqua-brooks float valve.....	114
Appendix E.	Costing for Biological Sand filter	115
Appendix F.	Published manuscript	117
Appendix G.	Statistical analysis of final effluent flow rate.....	132
Appendix H.	Hydraulic retention time.....	133
Appendix I.	Achieved hydraulic conductivity calculations	135
Appendix J.	Integration of outlet height optimization	136
Appendix K.	Hydraulic and organic loading rate	138
Appendix L.	Correlations of flow rate and chemical oxygen demand.....	139
Appendix M.	Hydrological data and discharge calculation	141

List of Figures

	Page
Figure 2.1	Inputs and wastes generated from typical wine-making processes (adapted from Brito <i>et al.</i> , 2007).....5
Figure 2.2	The energy, operation and maintenance requirement and land constraints of different types of constructed wetlands: Free water surface flow (A), Horizontal sub-surface flow (B), Vertical flow (C) and horizontal subsurface flow with aeration (D) (Adapted from Wu <i>et al.</i> , 2015)13
Figure 3.1	Schematic of the on-site biological sand filter together with existing infrastructure and ledger.24
Figure 3.2	Illustration of existing infrastructure (settling basin) together with sampling points.25
Figure 3.3	Schematic, design notes and valve depiction for pilot biological sand filter system.....28
Figure 3.4	A picture depicting the inlet manifold and float valves for the BSF filter modules plus the 500 L holding tank28
Figure 3.5	A picture showing the set-up of the pipes and control valves that allow the system to be operated in series or in parallel29
Figure 3.6	A picture of the installed BSF system on site: anti-clockwise from top right: solar pump, 5000 L holding tank, 500 L tank and four filter modules with flow control tanks29
Figure 4.1	Pump and System curve for pumping main to 5000 L holding tank34
Figure 4.2	Chemical oxygen demand concentrations measured in samples from the existing settling basin at the inlet, middle and outlet sampling points before commissioning of the BSF system, Apr 2014 – Jan 2015.....35
Figure 4.3	Chemical oxygen demand concentrations measured in the existing settling basin samples taken separately at the inlet, middle and outlet points after the commissioning of the BSF from Feb 2015-June 2016 and the concentrations of pooled samples from the inlet, middle, and outlet sampling points (average) from May-Sep 201636
Figure 4.4	Volatile fatty acid concentrations in samples taken separately from the inlet, middle and outlet sampling points in the existing settling basin from March 2015 - June 2016, and the concentrations in pooled (average) samples from the inlet, middle and outlet points from May - Sep 2016.....37
Figure 4.5	Total phenolic concentrations in samples taken separately from the inlet, middle, and outlet points in the existing settling basin from May 2015-June 2016, and concentrations in pooled (average) samples taken from the inlet, middle and outlet from June 2016 - September 2016.....37
Figure 4.6	Photograph of the settling basin containing winery wastewater with a high concentration of total phenolics on the 20th of August 201638
Figure 4.7	Total nitrogen concentrations in samples taken from the existing settling basin from April 2015 to August 201538
Figure 4.8	Concentrations of total phosphate in samples taken from existing settling basin from April 2015 to August 201639
Figure 4.9	Total dissolved solids, total suspended solids and total solids for inlet and outlet sampling point for existing basin samples taken April 2014 – September 2016.39
Figure 4.10	Electrical conductivity measured in samples taken from the existing settling basin from July 2015 September 2016.....40

Figure 4.11	The pH measured in samples taken from the existing settling basin from April 2015 to September 2016.....	40
Figure 4.12	Samples of Chemical oxygen demand concentration in sample from 5000 L holding tank, 500 L tank and final effluent from February 2015 to September 2016.....	41
Figure 4.13	Chemical oxygen demand concentrations measured in samples from filter outlets 1, 2, 3 & 4 from February 2015 to September 2016	42
Figure 4.14	Volatile fatty acid concentrations measured in samples taken from the 5000 L holding tank, 500 L tank and final effluent from February 2015 to September 2016	43
Figure 4.15	Volatile fatty acid concentrations measured in samples from filter outlets 1, 2, 3 & 4 from May 2015 to September 2016	43
Figure 4.16	Concentrations of total (poly) phenolics measured in samples taken from the 5000 L holding tank, 500 L tank and final effluent from February 2015 to September 2016	44
Figure 4.17	Total nitrogen concentrations in from 5000 L tank and final effluent taken from April 2015 August 2016	45
Figure 4.18	Total phosphate concentrations in samples form 5000 L and final effluent taken from April 2015 to September 2016.....	45
Figure 4.19	Concentrations of sodium measured in samples taken from the 5000 L holding tank, 500 L tank and final effluent from October 2015 to September 2016.....	46
Figure 4.20	Concentrations of sodium measured in samples taken from the filter outlets 1, 2, 3 & 4 from October 2015 to September 2016.....	47
Figure 4.21	Concentrations of potassium measured in samples taken from the 5000 L holding tank, 500 L tank and final effluent from October 2015 to September 2016	47
Figure 4.22	Concentrations of potassium measured in samples taken from the filter outlets 1, 2, 3 & 4 from October 2015 to September 2016.....	48
Figure 4.23	Concentrations of calcium measured in samples taken from the 5000 L holding tank, 500 L tank and final effluent from October 2015 to September 2016.....	49
Figure 4.24	Concentrations of calcium measured in samples taken from the filter outlets 1, 2, 3 & 4 from October 2015 to September 2016.....	49
Figure 4.25	Concentrations of magnesium measured in samples taken from the 5000 L holding tank, 500 L tank and final effluent from October 2015 to September 2016	50
Figure 4.26	Concentrations of magnesium measured in samples taken from the filter outlets 1, 2, 3 & 4 from October 2015 to September 2016.....	51
Figure 4.27	The sodium adsorption ratio calculated from samples taken from the 5000 L holding tank, 500 L tank and final effluent from October 2015 to September 2016	51
Figure 4.28	The sodium adsorption ratio calculated from samples taken from the filter outlets 1, 2, 3 & 4 from October 2015 to September 2016	52
Figure 4.29	The cation ratio of soil structural stability calculated from samples taken from the 5000 L holding, tank 500 L tank and final effluent from October 2015 to September 2016	53
Figure 4.30	The cation ratio of soil structural stability calculated from samples taken the filter outlets 1, 2, 3 & 4 from October 2015 to September 2016	53
Figure 4.31	The Potassium to Sodium ratio calculated from samples taken from the 5000 L holding tank, 500 L tank and final effluent from October 2015 to September 2016	54
Figure 4.32	The Potassium to Sodium ratio calculated from samples taken from the filter outlets 1, 2, 3 & 4 from October 2015 to September 2016	54

Figure 4.33	The electrical conductivity measured in samples taken from the 5000 L holding tank, 500 L tank and final effluent from October 2015 to September 2016.....	55
Figure 4.34	The electrical conductivity measured in samples taken from the filter outlets 1, 2, 3 & 4 from October 2015 to September 2016.....	55
Figure 4.35	Total solids in sample from final effluent form BSF February to September 2016	56
Figure 4.36	The pH measured in samples taken from the 5000 L holding tank, 500 L tank and final effluent from March 2015 to September 2016.....	56
Figure 4.37	The pH measure in samples taken from filter outlets 1, 2, 3 & 4 from May 2015 to September 2016.....	57
Figure 4.38	Chemical oxygen demand concentrations measured in samples taken from all outlets during a 4 hour batch test.....	58
Figure 4.39	Volatile fatty acid concentrations in samples taken from all outlets during the 4 hour batch test	59
Figure 4.40	Total (poly) phenolics concentrations from samples taken from all outlets during the 4 hour batch test. Note: due to similarities in results, the results from final effluent and samples taken from the filter modules are superimposed on one another.....	59
Figure 4.41	Sodium concentration in samples taken from all outlets during a 4 hour batch test	60
Figure 4.42	Potassium concentration in samples taken from all outlets during a 4 hour batch test.....	61
Figure 4.43	Calcium concentrations in samples taken from all outlets during a 4 hour batch test. Note: due to similarities in results, the results from final effluent and samples taken from the filter modules are superimposed on one another.....	61
Figure 4.44	Magnesium concentrations in samples taken from all outlets during a 4 hour batch test.	62
Figure 4.45	Sodium adsorption ratio calculated from samples taken from all outlets during a 4 hour batch test. Note: due to similarities in results, the results from final effluent and samples taken from the filter modules are superimposed on one another	63
Figure 4.46	Cation ratio of soil structural stability calculated from samples taken from all outlets during a 4 hour batch test. Note: due to similarities in results, the results from final effluent and samples taken from the filter modules are superimposed on one another ...	63
Figure 4.47	Potassium to Sodium ratio calculated from samples taken from all outlets during a 4 hour batch test. Note: due to similarities in results, the results from final effluent and samples taken from the filter modules are superimposed on one another	64
Figure 4.48	Electrical conductivity measured in samples taken from all outlets during a 4 hour batch test	65
Figure 4.49	The pH measured in samples taken from all outlets of 4 hour batch test. Note: due to similarities in results, the results from final effluent and samples taken from the filter modules are superimposed on one another.....	65
Figure 4.50	Biological sand filter system flow rate since start-up. The highlighted red marker indicates the flow rate that was measured during the 4 hour batch test.....	66
Figure 4.51	Comparisons of hydraulic loading rates and organic loading rate for BSF from July 2015 to September 2016.....	68
Figure 5.1	The chemical oxygen demand concentration measured in samples taken from the influent and effluent samples plotted against the removal efficiency.....	69
Figure 5.2	The chemical oxygen demand concentration of effluent and average of all four filter modules, including the 4 hour batch test results (August 2015), February 2015 to September 2016.....	70

Figure 5.3	The volatile fatty acids represented in terms of chemical oxygen demand concentration of effluent and average of all four filter modules, including the 4 hour batch test results (August 2015), May 2015 to September 2016.....	72
Figure 5.4	The total phosphorus represented in terms of chemical oxygen demand concentration of the influent and removal efficiency across the system from October 2015 to September 2016.....	73
Figure 5.5	The pH of effluent and average of all four filter modules, including the four hour batch test results (August 2015), April 2015 to September 2016.....	74
Figure 5.6	A schematic of a long section of the water levels obtained in a biological sand filter module, and related infrastructure.....	76
Figure 5.7	The effect of height of sand in the discharge within a biological sand filter using a hydraulic conductivity of 0.044mm/s	78
Figure 5.8	Relationship between effluent flow rate and chemical oxygen demand in influent samples from the influent including a 95% line of confidence	82
Figure 5.9	The relationship between the infiltration rate and the distance from the inlet in a fully saturated biological sand filter with a hydraulic conductivity of 0.044 mm/s	84
Figure 5.10	Photographs of filter module 1-4 on 19 th of February 2015 (A-D), on the 20 th of April 2015 (E-H), on the 25 th of August 2016 at the end of testing (I-L), core samples taken from the inlet channel of filter 3 on the 6 th of May 2016 (M), the hydraulic control tank algal growth or biofilm on the 18 th of April 2016 (N), filter 3 after surface flow had stopped and the picture is showing the microbial blanket on surface of filter on the 18 th of April 2016 (O), filter module 4 after the cellar rinsed bins containing solids into filter (P)	87
Figure 5.11	Photographs of the 500 L tank microbial mat, biofilm, sludge on the 19 th of November 2015 (A), the 500 L tank on the 22 nd of February 2016 (B), on the 1 st June 2016 (C) and on the 25 th of August 2016 (D)	88

Appendices

Figure A.1	Cross-section of a filter module, X represents the height of sand. ($115 \geq x \geq 500$ mm).....	99
Figure A.2	Long-section of a filter module showing fall across filter.	100
Figure A.3	Diagram depiction points used for the calculation of flow rate using the Bernoulli equation	102
Figure D.1	Brochure for Aqua-Brooks float value.....	114
Figure G.1	Results of the statistical analysis of flow rates from the biological sand filtration system.....	132
Figure L.1	Relationships between the following: final effluent flowrate and chemical oxygen demand, influent chemical oxygen demand (5000 L holding tank and average from settling basin)	139
Figure L.2	Correlation between final effluent chemical oxygen demand and final effluent flow rate.....	139
Figure L.3	Correlation between final effluent chemical oxygen demand and 5000 L holding tank COD.....	140
Figure L.4	Correlation between final effluent flow rate and 5000 L holding tank chemical oxygen demand	140

List of Tables

	Page
Table 2.1	General Authorisation in terms of Section 39 of the National Water Act, 2013; Wastewater limit values applicable to the irrigation of any land or property9
Table 2.2	Limits for the purification of waste water or effluent release into Schedule I and other rivers, Government Gazette no 9225 of 18 May 1984.....10
Table 2.3	Comparison of selected biological treatment systems used to remediate winery wastewater.....15
Table 3.1	Sampling schedule.....26
Table 3.2	Mechanical Fractions (%) ($n=3$) of Phillipi sand30
Table 3.3	Filter media particle distribution30
Table 3.4	Available metal (ions)(mg/kg) ($n=3$).....30
Table 3.5	Elemental analysis (%) ($n=3$) of Phillipi sand.....30
Table 3.6	Summarised costing of new biological sand filter system (February 2015)32
Table 3.7	The monthly water used by the cellar converted directly to wastewater consumption.....32
Table 5.1	The monthly water used by the cellar converted directly to wastewater consumption and the percentage treated by the biological sand filter system at a flow rate of 413 L/day....75
Table 5.2	Comparison of operational parameters for selected winery wastewater and olive will wastewater treatment systems81
Table 5.3	Description of problems encountered with the biological sand filtration system and possible mitigating or remedial action table 1 of 285
Table 5.4	Description of problems encountered with the biological sand filtration system and possible mitigating or remedial action table 2 of 286
Table 5.5	Consumable costing and replacement periods for the biological sand filter in the worst-case scenario for a 10 year operational period.....88
Table 5.6	Yearly cost of biological sand filter, for a 10 year period, including inflation of consumables at 6%.....89
Table 5.7	Cost per m ³ of treated effluent using a biological sand filter, for a 10 year period, including inflation of consumables at 6%89

Appendices

Table A.1	Initial Hydraulic conductivity results from constant head by I. Smith98
Table A.2	Hydraulic conductivity results from constant head by I. Smith after 3 months of filtration and control98
Table B.1	Integration of flow rate table 1 of 3.....110
Table B.2	Integration of flow rate table 2 of 3.....111
Table B.3	Integration of flow rate table 3 of 3.....112
Table C.1	K values for various fittings (Adapter from Nalluri et al., 2009; Upadhyay, 2010)113
Table C.2	K values for sudden contraction in circular pipe (Adapter from Nalluri et al., 2009)113
Table E.1	Initial setup costing for biological sand filter treatment system, February 2015.115
Table J.1	Flow rates of biological sand filter for changing outlet heights using a k of 0.044 mm/s 137

Table M.1	The then maximum precipitation instances for Jonkershoek@Manor; G2E013 meteorology station from 13 th of August 1968 to the end of August 2016	141
Table M.2	The average monthly precipitation and evaporation for Jonkershoek@Manor; G2E013 meteorology station in December 2016	141
Table M.3	The integrated flow rate of a fully situated biological sand filter with 100mm of surface water due to precipitation	143

Abbreviation

BSF	Biological sand filter
ca	circa meaning around
CROSS	Cation ratio of soil structural stability
CW	Constructed wetlands
ESP	Exchangeable Sodium Percentage
FE	Final effluent
GAE	Gallic acid equivalent
HSSF	Horizontal subsurface flow
n	Number of
n	Number
RBCOD	Readily biodegradable chemical oxygen demand
SAR	Sodium adsorption ratio
SBCOD	Slowly biodegradable chemical oxygen demand
VFA	Volatile Fatty Acids
WW	Wastewater
WWW	Winery wastewater

Nomenclature

A	Area (m^2)
COD	Chemical oxygen demand (mg/L)
D	Diameter (m)
dh	Changing in height (m)
dl	Change in length (m)
g	Gravity ($9.81 m^2/s$)
h	The head due to pressure (m)
hf	Headloss due to friction or major losses (m)
h_m	Headloss due to minor losses (m)
h_{static}	The static head (m)
h_{total}	The total head within a system (m)
hr	Hours
HLR_A	Hydraulic loading rate across the sectional or surface area of the reactor ($L/m^2/day$)
HLR_V	Hydraulic loading rate for the volume of the reactor ($L/m^3/day$)
HRT	Hydraulic Retention time (days)
K	Hydraulic conductivity/ Coefficient
l	Length (m)
L	Litres
Mt	million tonne/ mega tonne
OLR	Organic loading rate ($gCOD/m^3/day$)
ORR	Organic removal rate ($gCOD/m^3/day$)
p	Pressure energy (Pa)
Pt	Porosity
Q	Volumetric flow rate (m^3/s)
Re	Reynolds number
t	Time
U	Velocity (m/s)
V	Volume (m^3)
ρ	Density (kg/m^3)
ν	Kinematic viscosity (m^2/s)
λ	Friction factor

Chapter 1 Introduction

This chapter presents the rationale for the project and outlines the organisational structure of the thesis.

1.1 Background and Motivation

One of the by-products of making wine is winery wastewater (WWW). Generation of WWW is highly seasonal and the effluent composition and volume changes constantly. In 2016, approximately 1.4 Mt of grapes were crushed by the wine industry of South Africa (South African Wine Industry Statistics, 2016), with the accompanying generation of over 1 billion litres of winery wastewater. The effluent from small wineries is predominantly used for irrigation of pastures. This may result in environmental degradation on several fronts.

There has been a change in the public perception towards greener farming resulting in the need for more environmentally friendly farming techniques within South Africa. Although the vine growing areas in South Africa are situated in water scarce environments, there has been minimal beneficial use of WWW to date. Large co-operatives have a high production of wine and WWW. They have the budget and the quantity of WWW to operate advanced effluent treatment methods. Most of these systems require high initial capital outlay with specialised equipment and design, constant monitoring, maintenance, and skilled technicians to ensure a continuance of the systems' performance. Due to the capital intensive nature of the currently available commercial WWW treatment methods, they are not suited to small wineries. Constructed wetlands (CW) may provide a low maintenance, low energy and economical solution. However, CWs contain plants, and WWW may be toxic to plants (Achakl *et al.*, 2009; Arienzo *et al.*, 2009, a; Masi *et al.*, 2002; Mekki *et al.*, 2007; Sheridan *et al.*, 2014; Vymazal, 2009; Wu *et al.*, 2015), which results in additional maintenance and costs for re-planting. Biological sand filter (BSF) may provide sustainable, low cost, low maintenance and energy efficient systems for the treatment of WW for small wineries.

1.2 Research problem

Small wineries use irrigation as a means of disposal of WWW, which can result in environmental degradation. Despite a wide variety of WW treatment options available, there is no reliable, low maintenance, and cost effective system for the treatment of WWW in South Africa.

1.3 Research Question

Is a horizontal flow BSF system a viable solution for the treatment of WW from a small winery, in terms of performance, maintenance, operation and sustainability?

1.4 Aim, objectives and outcomes

The aim of this research work was to design and validate the performance of a sustainable, cost effective and low maintenance biological treatment process for the treatment of effluent at small wineries in South Africa. The objectives of the project were:

- To design and install a low maintenance, affordable, and sustainable pilot BSF system at a small winery in the Western Cape.
- To monitor the physicochemical parameters of the WWW and the effluent of the BSF system in order to determine treatment performance.
- To validate the performance of the BSF system against the performance of experimental systems treating synthetic and authentic WWW.
- To determine the capital cost of the system, and the cost per liter of WWW treated.

The outcomes were expected to show that the BSF system was affordable, and could adequately treat the WWW to a level where the effluent could be used for irrigation and complied with the national legislation in terms of COD concentration and pH. The outcomes that were achieved were:

- A low maintenance, affordable and sustainable BSF was designed and installed at a small winery in the Western Cape.
- The analysis of the physicochemical parameters of the WWW and BSF system showed that the system was able to significantly improve the quality of WWW.
- The WWW treatment performance of the pilot BSF system was comparable to that of experimental systems previously used to treat synthetic and authentic WWW.
- The cost of installing a BSF system, and the payback cost per liter of treated WWW was determined.

1.5 Significance

To mitigate the adverse effects of applying untreated WWW to land via irrigation, there is a need for low cost, low maintenance treatment options for small wineries within South Africa. In conjunction with previous studies, this work showed that BSF systems may fill this technology gap.

1.6 Delineation

The system was designed (i) to run at a constant flow rate which was expected to gradually reduce due to the build-up of functional biomass (ii) to treat only a portion of the WWW from a small cellar, and (iii) to recirculate effluent back into the head of an existing solids settling basin. The system was not designed to remove sodium and potassium and the effects of the effluent on the environment were not monitored.

1.7 Assumptions

It was assumed that the build-up of functional biomass would not retard the flow to an extent where the treatment of WWW by the BSF system would not be viable. Secondly, it was assumed that characteristics of the WWW would remain in the range that had been previously determined by regular sampling. Thirdly, it was assumed that the infrastructure would not be tampered with or stolen. Fourthly, it was assumed that the effluent would comply with the national legislation pertaining to the release of biodegradable wastewater, other than the sodium adsorption ratio (SAR).

1.8 Summary of methodology

A modular BSF system was designed and installed with four filter modules, holding tank and flow controls. Some assistance with the design concept was provided by the student supervisors, but the student was responsible for all the technical details of the design. An MTech student, Mr I Smith, assisted with the installation of the system.

The efficiency of the system was determined by performing physicochemical and flow analyses. The following parameters were determined on a range of samples, including influent and effluent: chemical oxygen demand (COD), total phenolics, volatile fatty acids, total phosphorus, total nitrogen, total suspended solids and total dissolved solids. The pH and redox potential were also determined. Analysis of the concentrations of sodium, potassium, calcium and magnesium was outsourced. In addition to regular monitoring (typically monthly, and weekly during the crush season), a 4 hour batch test was performed to determine the efficiency of the system with a constant influent. The flow rate of the system was measured on a minimum of a monthly basis.

1.9 Organisation of dissertation

Chapter 1 - Introduction: In this chapter the topic and outcomes are briefly introduced and discussed.

Chapter 2 - Literature review and theory: This chapter contains in-depth discussions of the current literature regarding the merits and shortcomings of current treatment methods for WWWW treatment, the environmental issues caused by the disposal of untreated or partially treated WWWW, and the potential of constructed wetlands (CW) and BSFs for WWWW treatment.

Chapter 3 - Research methodology: This chapter explains the calculations used in the design of the system, and the procedures and analyses used to test the efficiency of the system.

Chapter 4 - Results: The compilation of the measured data is presented in this chapter in the form of figures, graphs, charts, and tables.

Chapter 5 - Discussion: The data presented in Chapter 4 is interpreted and critically discussed in line with relevant available literature.

Chapter 6 - Conclusions and recommendations: In this chapter the results have been summarised and conclusions drawn. Shortcomings of the system are highlighted and recommendations provided.

Chapter 2 Literature review and theory

The literature review provides information about the generation, character, treatment, and disposal of WWW. It also includes a section about the design of BSFs.

2.1 Introduction

While the earth's surface area is covered by approximately 71% water, 96.5% of this is salt water held by the ocean and only 2.5% is fresh water. In turn, 68.7% of the fresh water is in the ice caps and 30.1% is underground, leaving only 1.2% as surface and other fresh water (Perlman, 2017). This gives a representation of the scarcity of fresh water, which is essential for the survival of all land-based biotic species. It is therefore important that this important resource is preserved.

Human activities result in the generation of liquid, solid and gaseous waste that need to be managed to prevent environmental damage (Metcalf and Eddy, 2004). Adequate treatment and responsible disposal of WW contributes towards a cleaner environment and the preservation of this precious resource.

2.2 Wastewater

Wastewater may be defined as “a combination of the liquid or water-carried wastes removed from residences, institutions, and commercial and industrial establishments, together with such groundwater, surface water, and storm water as may be present” (Metcalf and Eddy, 2004). Domestic WW is generated by households and human activity while industrial WW is generated by industrial processes. Sewerage systems were originally developed for sanitation reasons, but nowadays most convey both municipal and industrial effluent to centralised facilities for treatment (Angelakis *et al.*, 2014).

2.3 Winery wastewater

South Africa has a rich agricultural background. One of the focal activities is the cultivation of grapes for making wine. Within South Africa's borders there are close to 600 cellars and 3 314 primary wine producers producing a wide variety of wines (SAWIS, 2016). Within the Western Cape, 510 cellars use almost 1 Mt of grapes for wine making purposes (SAWIS, 2016).

Winemaking relies on the conversion of sugars (mainly glucose and fructose) from the grapes to ethanol, and the formation of organic molecules that enhance the aroma and flavour of the product (Sheridan *et al.*, 2013). One of the problems faced by winemakers is the need to treat and/or dispose of liquid and solids waste generated during the many wine-making activities (Saviozzi *et al.*, 1994). WWW is variable because it is generated from different cellar activities that take place during different times of the year. These include crushing, bottling, cleaning of floors and equipment, cleaning of vats, rinsing of transfer lines, barrel cleaning, dumping of reject wine and product loss, cooling processes, and filtration (Di Stefano *et al.*, 2008; Ioannou *et al.*, 2015; Serrano *et al.*, 2011; Sheridan *et al.*, 2013). The inputs and wastes generated from typical winemaking processes are shown in Figure 2.1.

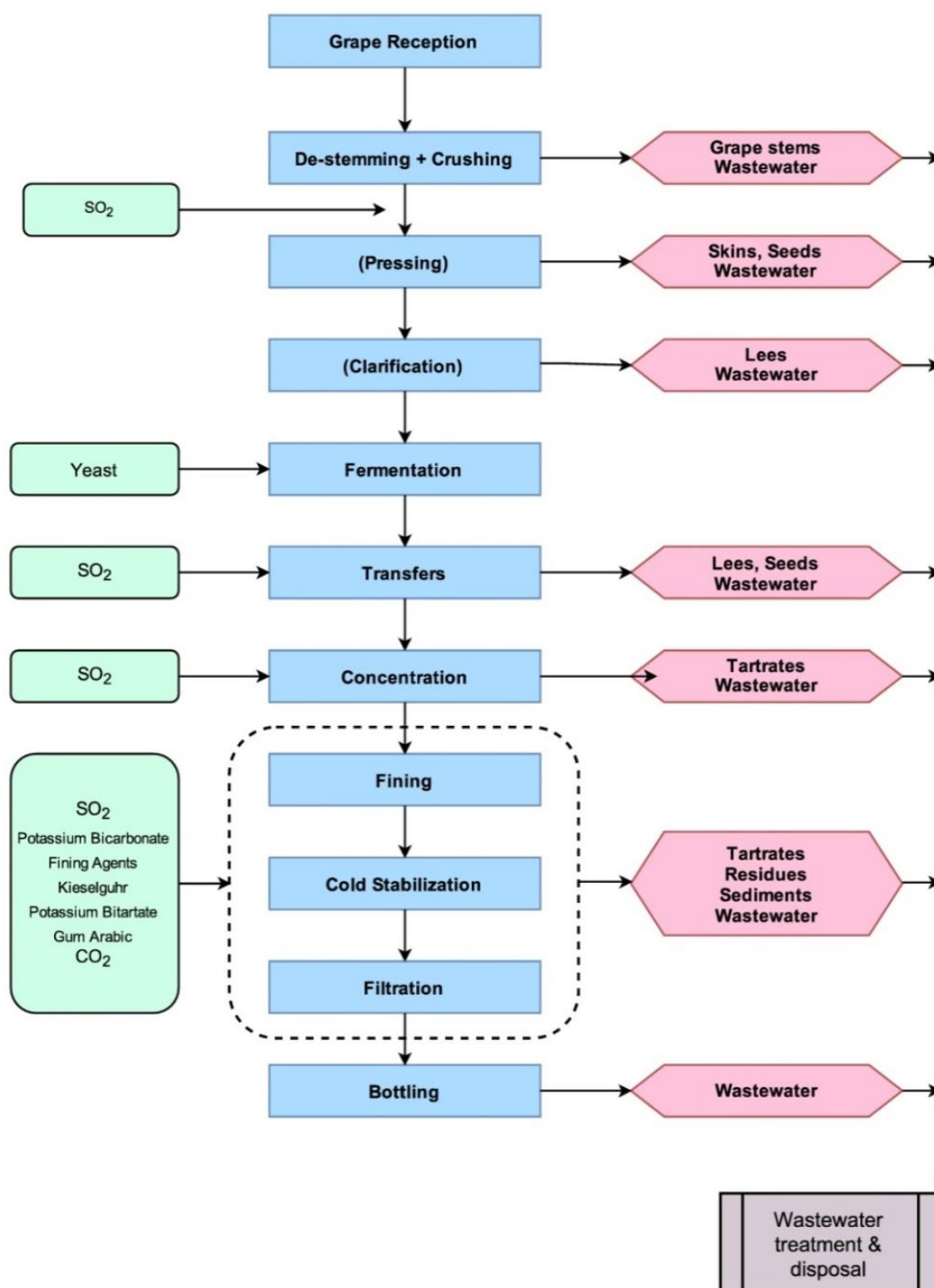


Figure 2.1 Inputs and wastes generated from typical wine-making processes (adapted from Brito *et al.*, 2007).

2.3.1 Composition of winery wastewater

WWW can contain inorganic and/or organic fractions and due to seasonal cellar processes, the character can change from one day to the next (Artiga *et al.*, 2005; Di Stefano *et al.*, 2008; GWRDC, 2011; Mosteo *et al.*, 2006; Petruccioli *et al.*, 2002). The highest volumes and organic load of WWW are found during the peak harvest, which is a 3 to 14 week period (Artiga *et al.*, 2005; Di Stefano *et al.*, 2008; GWRDC, 2011; Mosteo *et al.*, 2006; Petruccioli *et al.*, 2002; van Schoor, 2005).

2.3.1.1 Organic fractions of winery wastewater

Organic waste from the wine industry can be separated into solid waste (grape marc, skins, pips, etc.) and liquid waste. The former can be used for a conditioner for soils, or for the extraction of value added products such as tartaric acid and grape seed extract (Lucas *et al.*, 2010; Sheridan *et al.*, 2013). WWW typically has a high organic content with high concentrations of readily biodegradable compounds (sugar, alcohols, acids, etc.) and/or recalcitrant compounds with high molecular weight [polyphenols, tannins and lignins (Lucas *et al.*, 2010; Serrano *et al.*, 2011; Sheridan *et al.*, 2013)].

Organic compounds present in waste 'consume' oxygen as they decompose, which can lead to oxygen depletion in the aquatic environment (GWRDC, 2011). The test to determine the COD measures the amount of oxygen required to mineralise the organics, and the COD concentration is used frequently as a reference for the quality of WW and a benchmark for regulatory authorities (Andreottola *et al.*, 2009; Aybar *et al.*, 2007; Mosse *et al.*, 2011). The organic COD can be broken up into different fractions with differing degradation rates. Compounds such as alcohols and sugars tend to biodegrade quickly, while compounds which are less degradable, such as phenols and tannins remain in the waste stream (Arienzo *et al.*, 2009a; Mosse *et al.*, 2013; and Vymazal, 2009; Welz *et al.*, 2012). WWW may contain 0.1 to 5% recalcitrant polyphenols and lignins (Vymazal, 2009). The composition of the COD within the WWW should be taken into account when selecting biological treatment systems (Welz *et al.*, 2014; Welz *et al.*, 2012). It has been shown that the COD of WWW can vary significantly, e.g. from 1820 to 11784 mg COD/L (Andreottola *et al.*, 2005), 800 to 12800 mg COD/L (Petruccioli *et al.*, 2002), 600 to 45000 mg COD/L (Shepherd *et al.*, 2001), ≤ 7000 mg COD/L (Sheridan *et al.*, 2010). This shows the importance of determining the COD concentration from each winery on a temporal basis.

2.3.1.2 Inorganic fractions of winery wastewater

The inorganic portion of WWW emanates from cleaning products, and winemaking products used for clarification and filtration (diatomaceous earth, bentonite clay and perlite) (Lucas *et al.*, 2010). WWW is produced by a variety of cellar activities and is generally acidic, but can become alkaline when certain cleaning products are used (GWRDC, 2011).

Cellar cleaning products include potassium hydroxide (KOH), sodium carbonate (Na_2CO_3), sodium hydroxide (NaOH), sodium metasilicate (Na_2SiO_3), tri-sodium phosphate (Na_3PO_4), and phosphoric acid (H_3PO_4). Due to the availability and affordability of sodium hydroxide (NaOH), it is a popular cleaning and disinfection product. However, the use of any cleaning product with a high sodium concentration should be discouraged because sodium can accumulate in the soil and cause sodicity (Di Stefano *et al.*, 2008; Sheridan *et al.*, 2010; van Schoor, 2005). WWW containing NaOH can have a pH as high as 13.5, which is highly caustic. Therefore, citric acid is used to lower the pH due to its cost effectiveness and availability (Di Stefano *et al.*, 2008). Bories *et al.* (2005) found that WWW can contain a significant amount of sodium (Na) and potassium (K) with K:Na ratios of 3:1, and K concentrations at a maximum of 1 000 mg/L.

Due to the threat saline WWW poses on soil structure and soil dispersion, the sodium adsorption ratio (SAR) of the WWW should be monitored if the WW is used for irrigation purposes (Marchuk and Rengasamy, 2010, Ranjbar & Jalali, 2016, Rengasamy & Marchuk, 2011). When a soil has a high sodium content, plant growth can be restricted due to the increased density of clays (Seeling, 2000). Sodium is a monovalent cation and bonds to only one negatively charged soil particle, causing a tight arrangement

of the soil structure, known as dispersion. This results in reduced infiltration and hard, compacted soils when dried. On the other hand, calcium and magnesium are divalent cations which bond to more than one negatively charged soil particle, known as flocculation. This type of bonding creates a matrix within the soil which allows for aeration, infiltration and the penetration of roots (Laurenson & Houlbrooke, 2011; Ranjbar & Jalali, 2016; Rengasamy & Marchuk, 2011; Terragis UNSW, 2016). Potassium has a similar effect on soil properties as sodium, but not to the same magnitude (Arienzo *et al.*, 2009b). The presence of divalent cations can therefore offset the detrimental effects of monovalent cations such as sodium.

The sodium adsorption ratio (SAR) takes into account the concentration of sodium, calcium and magnesium, and is used to indicate the potential for water/WW to cause sodicity in soil (Equation 2.1). In the General Authorisations in terms of Section 39 of the National Water Act, 2013 (Act no. 36 of 1998), hereinafter referred to as the "GA". The current SAR limit for irrigation with biodegradable industrial wastewater is < 5 (Table 2.1). In comparison, the World Health Organization suggests a guideline of 3 to 12 for WW used for irrigation (Olivera and Duart, 2014). The U.S. Salinity Laboratory (1954) determined that soil with a SAR > 13 is sodic (Seelig, 2000) and Horneck *et al.* (2007) state that soils with a SAR < 5, between 5 and 13, and > 13, pose low, medium and high risks, respectively.

The SAR does not take into account the combined additional effect of potassium on soil dispersion, which is relevant for WWW that can contain elevated levels of this cation in addition to sodium, calcium and magnesium (Marchuk & Rengasamy, 2010, Rengasamy & Marchuk, 2011). The CROSS (cation ratio of soil structure stability) is a sodicity indicator that was derived by Rengasamy and Sumner (1998) to overcome this limitation (Equation 2.2). This ratio is more suitable for monitoring the effects of WWW on the soil structure (Marchuk & Rengasamy, 2010, Rengasamy & Marchuk, 2011). Laurenson *et al.* (2012) suggested a maximum CROSS of 20 (with an assumed electrical conductivity of 1.4–2 dS/m) for disposal of WWW to the environment. The authors found an average CROSS of 9.2 (range: 2.5-13.3) in WWW from 8 different wineries in Australia. Another parameter used to determine the potential detrimental effects of sodium on the soil structure is exchangeable sodium percentage (ESP). This uses the relative amount of sodium present in soil compared to other exchangeable ions, shown in Equation 2.3. A suggested ESP of ≥ 6% can be considered sodic although clay soils can show dispersion at lower concentrations (Laurenson & Houlbrooke, 2011; Terragis UNSW, 2016)

If WWW has a high sodicity indicator, mitigating actions should be taken to treat the WWW and ensure the protection of the soil structure (Christen *et al.*, 2010; Marchuk and Rengasamy, 2010, Ranjbar & Jalali, 2016, Rengasamy & Marchuk, 2011).

$$SAR = \frac{Na^+}{\sqrt{0.5(Ca^{2+} + Mg^{2+})}} \quad (2.1)$$

$$CROSS = \frac{(Na^+ + 0.56K^+)}{\sqrt{0.5(Ca^{2+} + 0.6Mg^{2+})}} \quad (2.2)$$

$$ESP = \frac{Na^+}{Ca^{2+} + Mg^{2+} + K^+ + Na^+} \times 100\% \quad (2.3)$$

2.3.2 Volume of wastewater generated by wineries

In order to meet the standards set out in the GA, the quantity of WWW should be monitored to determine the level of treatment required to conform to the applicable discharge limits. Ideally, as with other industries, meters should be installed to determine the volume of WW generated. In spite of this, in South Africa, the amount of WWW is generally estimated from the quantity of water used, even though a portion may not be used for winemaking *per se*. Wineries can produce 1 to 6 litres of WW per litre of wine produced (Ayar *et al.*, 2007; Di Stefano *et al.*, 2008). Large co-operatives produce large volumes of WWW due to the volume of wine produced and/or bottled at these facilities, but can produce a lower ratio of wastewater to wine (Ayar *et al.*, 2007; GWRDC, 2011; Sheridan, 2003).

Using a black box method, Sheridan (2003) estimated that cellars in SA that crush ≤ 500 tonnes of grapes per year consume a yearly average of ≤ 3800 L water/day. Of the current 566 wine cellars in South Africa (SAWIS, 2016), 70% fall into this category. Of these 61% are small wineries that crush < 100 tonnes of grapes per year. Such cellars were estimated to consume < 900 L water/day in 2003. There has been an increasing emphasis on water-saving, particularly due to the 2016/2017 drought in the Western Cape, so there is no reason to suspect that these figures have risen since 2003. It is therefore clear that a substantial number of wineries are small establishments that need to conform to the least stringent legislative requirements for discharge (Table 2.1).

2.4 Current methods used to dispose of untreated winery wastewater

Wineries discharge WWW to the environment or into municipal reticulation systems. Various applicable national and local legislations and by-laws must be adhered to.

2.4.1 Irrigation as a means of disposal of winery wastewater

The most common form of disposal of WWW within South Africa is irrigation to Kikuyu pastures post pH adjustment, which is a popular choice for wineries within South Africa (Mosse, *et al.*, 2011; Mulidzi *et al.*, 2001; Sheridan, *et al.*, 2014; van Schoor, 2005; van Schoor, 2015). The Department of Water Affairs sees this type of non-beneficial irrigation as a wasteful use of water and a loss to the catchment (Sheridan *et al.*, 2014). Ideally, irrigation with WWW should be comparable to irrigating with a fertilizer and water mixture; yet, this is not the case due to seasonal fluctuations and variability in WWW quality and quantity (van Schoor, 2005).

Because a large number of wineries are using irrigation as a means of disposal, an understanding of the level of treatment is required as well as the composition of the WWW. Wineries may irrigate up to 50 m³ of WW to pastures a day if the COD is less than 5 000 mg/L and up to 500 m³ with a COD of less than 400 mg/L. The physiochemical parameters are set out in the Government Gazette Act no. 36, 1998 and the GA (Table 2.1)

One of the problems associated with irrigating with WWW is that large amounts of water are discharged on small areas of land. This results in aggressive leaching of organic components into the ground water and a subsequent retarded degradation of these compounds (Mulidzi *et al.*, 2001). The ability of the soil to adsorb the WWW is often not met and this causes leaching of pollutants offsite (Mulidzi *et al.*, 2001; van Schoor, 2005).

Irrigation of a Kikuyu grass pasture and/or pastures with WWW is the norm in South Africa (van Schoor, 2005). The grass can absorb a large amount of sodium from the soil. On the other hand, the cut grass needs to be disposed of correctly or the potential sodicity will just be relocated elsewhere (Zingelwa & Wooldridge, 2009).

2.4.2 Other forms of disposal of winery wastewater

Evaporation ponds can be used for disposal and treatment of WWW. Similar to sludge drying beds, evaporation from these ponds is enhanced by large surface areas and shallow liquid depths (± 10 cm), (Di Stefano *et al.*, 2008; Sheridan, 2003; Metcalf and Eddy, 2004). Conversely, the shortage of water in vine growing areas makes this technique inappropriate as the natural water resource should ideally be reused beneficially. In addition, evaporation ponds do not actually treat the wastewater, and they require large areas of land in areas where the land value is often high.

The disposal of treated WWW to municipal wastewater treatment plants is a viable option for wineries that are located close to municipal sewerage systems. In such cases, the effluent must conform to specific local municipal discharge limits. The WWW can be released into a watercourse if it has been sufficiently treated in terms of the parameters set in Table 2.2

2.5 Legislation for the disposal of winery wastewater in South Africa

In South Africa, WWW is defined as a “biodegradable industrial wastewater” and wineries which treat and/or dispose of WWW must adhere to the following legislation: Act no. 36 of the National Water act of South Africa of 1998, the National Environmental Management Act of 1998, and the GA. The limits applicable for disposal of different volumes of biodegradable industrial wastewater by means of irrigation are given in Table 2.1.

Table 2.1 General Authorisation in terms of Section 39 of the National Water Act, 2013; Wastewater limit values applicable to the irrigation of any land or property

Quantity of Effluent for irrigation (m ³ /day)	≥ 50	50 ≥ Vol ≥ 500	500 ≥ Vol ≥ 2000
pH	6 ≥ pH ≥ 9	6 ≥ pH ≥ 9	5.5 ≥ pH ≥ 9.5
Electrical conductivity (mS/m)	≥ 200	≥ 200	≤150 mS/m, not ≥70 mS/m than influent
Suspended solids (mg/L)	NA		≥ 25
Chloride as free Cl (mg/L)	NA		≥ 0,25
Fluoride (mg/L)	NA		≥ 1
Soap, oil and grease (mg/L)	NA		≥ 2.5
Chemical oxygen demand (mg/L)	≥ 5000 after removal of algae	≥ 400	≥ 75
Faecal coliforms (CFU per 100 mm ³)	≥ 100000	≥ 100000	≥ 1000
Ammonia (ionised and un-ionised) as N (mg/L)	NA	NA	≥ 3
Nitrate/nitrite as N (mg/L)	NA	NA	≥ 15
Ortho-phosphate as P (mg/L)	NA	NA	≥ 10
Sodium adsorption ratio (SAR)	≥ 5	≥ 5	≥ 5

The disposal limits for treated effluent into schedule I or schedule II rivers or tributaries, as described in Government Gazette 18 May 1984 no 9225, is set out in Table 2.2. Wineries need to adhere to these limits if disposing into a schedule I or II river or tributary.

Table 2.2 Limits for the purification of waste water or effluent release into Schedule I and other rivers, Government Gazette no 9225 of 18 May 1984

	Schedule I rivers and tributaries	Schedule II rivers and tributaries
pH	5.5 ≥ pH ≥ 7.5	5.5 ≥ pH ≥ 9.5
Dissolved oxygen (%)	75	75
Typical (faecal) coli (CFU per 100 mm)	None	≥ 100
Temperature (°C)	≥ 25	≥ 35
Chemical oxygen demand (mg/l)	≥ 30 after chlorine applied	≥ 75 after chlorine applied
Electrical conductivity (mS/m)	≥250 & no higher than 15% of intake water	no higher than 75 mS/m above intake water
Suspended solids (mg/l)	10	90
Sodium (mg/L)	no higher than 50 mg/L above intake water	no higher than 90 mg/L above intake water
Soap, oil and grease (mg/L)	Nil	2.5
Residual chlorine as CP (mg/L)	Nil	0.1
Free & saline ammonia & N (mg/L)	≥ 1.0	≥ 1.0
Nitrate (mg/L)	≥ 1.5	Not defined
Arsenic (mg/L)	≥ 0.1	≥ 0.1
Boron (mg/L)	0.5	≥ 0.5
Total chromium (mg/L)	≥ 0.05	≥ 0.05
Copper (mg/L)	≥ 0.02	≥ 0.02
Phenolic compound (as phenol mg/L)	≥ 0.01	≥ 0.01
Lead (mg/L)	≥ 0.1	≥ 0.01
Soluble ortho-phosphate	≥ 1.0	≥ 1.0
Iron (mg/L)	≥ 0.3	≥ 0.3
Manganese (mg/L)	≥ 0.1	≥ 0.1
Cyanides (mg/L)	≥ 0.5	≥ 0.5
Sulphides (mg/L)	≥ 0.05	≥ 0.05
Fluoride (mg/L)	≥ 1.0	≥ 1.0
Zinc (mg/L)	≥ 0.3	≥ 0.3
Cadmium (mg/L)	≥ 0.05	≥ 0.05
Mercury (mg/L)	≥ 0.02	≥ 0.02
Selenium (mg/L)	≥ 0.05	≥ 0.05
Note	"The waste water or effluent shall contain no constituents in concentrations which are poisonous or injurious to humans, animals, fish other than trout, or other forms of aquatic life, or which are detrimental to agricultural use."	

2.6 Treatment of winery wastewater

In order to dispose of the WWW, some form of treatment is generally required in order to comply with relevant legislation. There are many different methods used to treat WWW, ranging in complexity. Yet, the complexity of the system does not always correlate positively with the final quality of the effluent. This is due to the wide variety and concentrations of contaminants present (Artiga *et al.*, 2005; Di Stefano *et al.*, 2008; GWRDC, 2011; Mosteo *et al.*, 2006; Petruccioli *et al.*, 2002). Van Schoor (2005) mentions that there is no “one fits all” treatment process applicable to all wineries. One of the main goals of the treatment process is to reduce the organic content, which is typically measured as COD (Sheridan, *et al.*, 2014). A comparison and description of a few different biological methods used to treat WWW are shown in Table 2.3.

2.6.1 Physicochemical processes for the treatment of winery wastewater

There are advanced methods used for the treatment of WWW such as ozone-based advanced oxidation (Lucas *et al.*, 2010), heterogeneous photo-Fenton (Mosteo *et al.*, 2016), reverse osmosis by solar photo-Fenton (Ioannau *et al.*, 2013), and photocatalytic advanced oxidation (Navarro *et al.*, 2005). Such systems have small spatial footprints. Then again, they require a high capital outlay and often require skilled personnel to operate, and are therefore generally not applicable for small wineries.

2.6.2 Biological processes for the treatment of winery wastewater

Biological WW treatment systems can be classified as either fixed film systems, where microbial communities form biofilms on physical substrates, or suspended growth systems. Activated sludge systems are the most commonly used suspended growth systems. The biological interaction in an activated sludge system removes contaminants in suspension. These contaminants are then removed with the sludge as it is wasted (Metcalf and Eddy, 2004). Conventional methods used to treat WWW are generally used for larger operations which produce large volumes of WW and do not have the adequate land availability for less intensive methods. The WW can be treated by means of predominantly aerobic or anaerobic biological processes. Common aerobic systems include activated sludge, aerated submerged biofilters, aerobic lagoons, air micro-bubble bioreactors, jet-loop activated sludge reactors, membrane bioreactors, rotating biological contactors and sequencing batch reactors (Ioannou, *et al.*, 2015; Sheridan, *et al.*, 2014; van Schoor, 2005).

Anaerobic biological processes include upflow packed-bed anaerobic digesters, anaerobic fixed-bed reactors, upflow anaerobic filters, anaerobic rotating biological contactors, upflow anaerobic sludge blankets, anaerobic digesters, anaerobic membrane bioreactors (Ioannou, *et al.*, 2015; Sheridan, *et al.*, 2014; van Schoor, 2005). Intensive treatment processes have the potential ability to fully treat the effluent (Sheridan *et al.*, 2014). Yet, due to the nature of these conventional treatment methods, they often cannot handle the changing influent in terms of flow rate, and/or loading rates and/or high concentrations of COD. This often results in inadequately treated WWW (Mosteo *et al.*, 2006; Petruccioli *et al.*, 2002; Serrano *et al.*, 2011). Small to medium wineries cannot reliably operate sophisticated systems as skilled labour is not available and the installation and operating costs of complex treatment systems cannot always be afforded (Di Stefano *et al.*, 2008; Sheridan *et al.*, 2014; van Schoor, 2005).

2.6.3 Waste stabilisation ponds

Due to the sporadic nature of WWW and presence of high concentrations of suspended solids (Di Stefano *et al.*, 2008), surge tanks and holding dams are often used to handle the peak flows and flatten the peaks (GWRDC, 2011; Metcalf and Eddy, 2004; van Schoor, 2005). Primary treatment is used to separate the solid organic material from the waste stream. This makes the WWW easier to treat and results in a potential reduction in odour problems (GWRDC, 2011; Metcalf and Eddy, 2004; van Schoor, 2005). Biological activity will naturally occur within a pond and result in organic degradation as much of this fraction of WWW is highly biodegradable (Ganesh *et al.*, 2010; Serrano *et al.*, 2011). A water stabilisation pond can be retrofitted or adapted to be an aerobic treatment lagoon.

2.6.4 Constructed Wetlands

CWs can provide a solution for smaller wineries as the operation is less labour and energy intensive, they require less maintenance, and are generally more simple and economical to operate than conventional systems (Masi *et al.*, 2002; Serrano *et al.*, 2011; Wu *et al.*, 2015). However, CWs are not always effective for high strength WWW. One option to overcome this is to dilute the WWW (Arienzo *et al.*, 2009a; Wu *et al.*, 2015). Nevertheless, this is not best practice in a water-scarce country like South Africa. One of the main reasons that CWs are sensitive to high strength WWW is that the (poly)phenolics are often phytotoxic (Achakl *et al.*, 2009; Arienzo *et al.*, 2009, a; Masi *et al.*, 2002; Mekki *et al.*, 2007; Sheridan *et al.*, 2014; Vymazal, 2009; Wu *et al.*, 2015).

A CW is an engineered system which employs wetland vegetation, associated microbial communities and a physical substrate such as soil, sand or gravel for the treatment of WW (Masi *et al.*, 2002; Vymazal, 2005; Wu *et al.*, 2015). The beneficial processes which take place in a natural wetland are taken advantage of in a controlled environment with the ability to assimilate fluctuating flows and organic loading (Serrano *et al.*, 2011; Vymazal 2005). A CW can be seen as a system that relies on a symbiosis between the physical substrate, microorganisms and plants, as all work together to treat the WW by means of biotic and abiotic interactions (Ramond *et al.*, 2013). While CWs have been able to handle fluctuating influents (Mosse *et al.*, 2011; Shepherd *et al.*, 2001; Vymazal, 2009), the treatment performance and hydraulic performance of a CW is greatly decreased with high strength WWW and pre-treatment and dilution might be required (Wu *et al.*, 2015).

The main principles of different types of CWs are the same. However, different hydraulic flow types are used for specific purposes (Wu *et al.*, 2014; Wu *et al.*, 2015). For example, the relationship between different CW in terms of land requirements, energy, operation and maintenance requirements is graphically represented in Figure 2.2 (Wu *et al.*, 2015). The most basic form of a CW, which is most similar to a conventional wetland, is a free water surface CW. It is one of the most cost effective CW to construct and operate, is used for advanced treatment but has lower removal efficiencies and can positively attract a variety of wildlife and has the ability to handle fluctuating flows. Conversely, aerated CWs are highly efficient and have a smaller footprint, but are the most energy intensive and capitally intensive. A horizontal subsurface flow (HSSF) CW falls in-between the two, the CW continuously operates fed either within the substrate or on the surface at the inlet. While the footprint is far smaller than a free water surface CW, the cost is greater however it has the advantage of not exposing the WW to humans as the WW runs under the surface of the CW (Knowles *et al.*, 2011; Wu *et al.*, 2015).

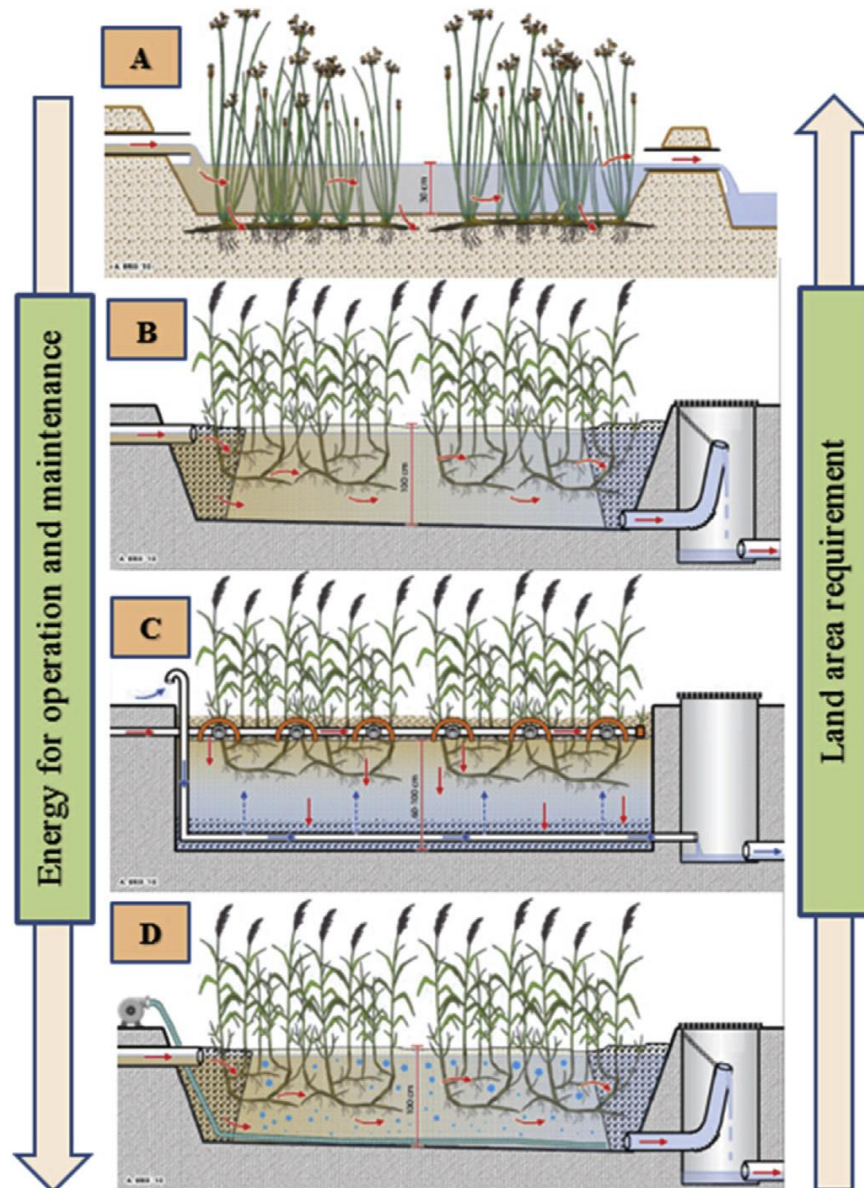


Figure 2.2 The energy, operation and maintenance requirement and land constraints of different types of constructed wetlands: Free water surface flow (A), Horizontal sub-surface flow (B), Vertical flow (C) and horizontal subsurface flow with aeration (D) (Adapted from Wu *et al.*, 2015)

It can be argued that the inclusion of plants in systems treating WWW is not appropriate. They play a very limited role in disinfection and reducing the COD and suspended solids within a CW (Chen *et al.*, 2015; Tanner 2001; von Sperling & de Paoli, 2013). In addition, they require periodic harvesting and the roots facilitate the formation of preferential flow paths which hampers treatment performance. They are also very susceptible to high strength WWW (Achaki *et al.*, 2009; Mekki *et al.*, 2007; Shepherd *et al.*, 2001; Welz *et al.*, 2012). For example, in the United States, Shepherd *et al.* (2001) found positive result with a 97% COD removal from a subsurface flow CW with an influent COD below 5 000 mg/L.

Although CW are used extensively in other parts of the world, only small numbers of CWs currently exist in South Africa (Sheridan *et al.*, 2014). An experimental CW was tested at a distillery in the Western Cape and it was established that the CW successfully treated the distillery WW provided the influent

COD was below 15 000 mg/L. Microbial communities present in the CW were “remarkably robust” (du Plessis, 2007). Mulidzi (2010) treated WWW with a full scale HSSF CW, and achieved 60% and 80% removal with retention times of 7 and 14 days, respectively. He recommended pre-treatment to prevent solids clogging, because > 40% of the COD was particulate.

Arienzo *et al.* (2009a) researched the phytotoxicity of high strength WWW from a single winery (max COD of 17 000 mg/L) on aquatic and non-aquatic plant life. It was found that WWW was extremely phytotoxic, being lethal to garden cress seeds and aquatic plants at dilutions $\geq 50\%$. The authors showed that phytotoxicity could be reduced by the addition of lime, which reduced the COD by 50 % and increased the pH. Still, the actual cause of the phytotoxicity was not determined (Arienzo *et al.* 2009a). Some phenolic compounds that can be present in WWW can be phytotoxic and antimicrobial (Achakl *et al.*, 2009; Mekki *et al.*, 2007; Welz *et al.*, 2012). It is therefore important to monitor the phenolic concentration in treated WWW if it is going to be used for crop irrigation or discharged to the environment.

A potential option for the reduction of phytotoxicity and improved treatment performance of a CW is the recirculation of the WW, the dilution factor is sometimes used to negate the effects of high strength WW (Wu *et al.*, 2014; Wu *et al.*, 2015). Recirculation can increase the aeration of the WW and therefore increase the aerobic microbial activity and result in the additional interaction with the microbes and pollutants and increase treatment performance, however the higher hydraulic loading rates (HRT) could result in solid wash out in vertical flow CW (Wu *et al.*, 2015).

Research has shown that CW are a viable treatment option for WWW and cannot be discarded however due to the phytotoxicity and high strength of WWW plants can be omitted.

Table 2.3 Comparison of selected biological treatment systems used to remediate winery wastewater

Name	Mode/type of growth	Labour intensity/skill	Setup costs	Running costs	Influent COD (mg/L)	COD removal efficiency (%)	Scale	Applicable for small wineries	References
Two-stage fixed bed reactor	Batch/attached	High/medium	High	High	7130 ± 3533	91	Full	No	Andreottola <i>et al.</i> , 2005
Land filter	Batch or continuous/attached	Low/low	Low	Low	2000-4800 (BOD ₅)	57-87	Full	Yes	Christen <i>et al.</i> , 2010
Fixed bed reactor	Batch or continuous/attached	High/medium	High	High	20000 ^d	80	Pilot	No	Ganesh <i>et al.</i> , 2010
Aerated lagoon	Batch/suspended	Low/medium	Medium	Medium	18700	91	Pilot	Yes	Montalvo <i>et al.</i> , 2010
Constructed Wetland	Continuous/attached	Medium/low	Low	Low	2000 – 12000	60-80	Full	Yes	Mulidzi (2010)
Micro-bubble bioreactor	Batch/suspended	High/medium	Medium	Medium	4000-8000	86-99	Lab	No	Oliveira & Duarte, 2011
Jet-loop activated sludge reactor	Continuous/suspended	High/medium	High	High-medium	1400-5900	98-94	Pilot	No	Petruccioli <i>et al.</i> , 2002
Constructed wetland	Batch or continuous/attached	Medium/medium	Low-high ^a	Medium	92-4283	53-93	Full	Yes	Serrano <i>et al.</i> , 2011
Biological sand filter	Batch or continuous/attached	Low/low	Low	Low	2304.4 ± 628.8	98.0	Lab	Yes	Ramond <i>et al.</i> , 2013
					474 – 26333 ^b	81.9-99.8	Lab		Welz <i>et al.</i> , 2011
					234 – 5842 ^c	88.3-100	Lab		Welz <i>et al.</i> , 2012

^a dependent on complexity

^b tested with synthetic readily biodegradable COD: Ethanol

^c tested with synthetic slowly biodegradable COD: Phenolics (vanillin and gallic acid)

^d tested with synthetic winery wastewater

2.6.5 Biological sand filters

It has been found that plant matter has a minimal (if any) effect on organic removal in CWs (Chen *et al.*, 2015; Tanner 2001; von Sperling & de Paoli, 2013), and WWW is phytotoxic (Section 2.3.1.1). This resulted in the introduction of BSFs as a BSF is essentially an unplanted CW. BSFs have been shown to successfully treat olive mill WW, which, like WWW, contains high concentrations of (poly)phenolics (Achak *et al.*, 2009). The use of BSFs as treatment systems for WWW at lab-scale has shown that they may be viable for the treatment of WWW at small wineries (Welz *et al.*, 2011; Rodriguez Caballero *et al.*, 2012; Welz *et al.*, 2012; Ramond *et al.*, 2013; Welz *et al.*, 2011; Welz *et al.*, 2013; Welz *et al.*, 2014; Welz & le Roes-Hill, 2014).

Using experimental BSF systems, Welz *et al.* (2011) reported nearly complete degradation of ethanol with concentrations up to 15800 mgCOD/L (final effluent 58±25 mgCOD/L) and a maximum final effluent concentration of 180 mgCOD/L when the influent was increased to 26333 mgCOD/L. Ramond *et al.* (2013) used the same systems to treat diluted WWW with an influent with a COD of 2304 ± 628 mg/L, and achieved an average removal efficiency of 98%, and Welz & le Roes-Hill (2014) showed a reduction in total phenolics of 76% with a concentration of 2027 mgCOD/L. These initial studies strongly suggested that BSF systems would be effective at full-scale.

BSFs and CWs can both be classified as fixed film systems, where the functional biomass is attached to a physical surface (sand in the case of BSFs). In BSFs, the removal of pollutants is contributed to the biotic and abiotic interaction between the microorganisms and the sand (Welz *et al.*, 2012). Recalcitrant organic chemicals, such as (poly)phenolics, may attach to the substrate and with time may reach saturation point. This can potentially result in harmful chemicals leaching out (Achakl *et al.*, 2009; Mekki *et al.*, 2007; Welz *et al.*, 2012). Though, it has been established that a significant amount of phenolics are degraded by means of biodegradation and mineralisation within a BSF (Welz *et al.*, 2012). When starting-up a BSF system, the addition of wastewater in incremental concentrations allows the functional biomass to acclimate effectively, thereby increasing the COD removal performance (Welz *et al.*, 2011; Welz *et al.*, 2012).

In each CW or BSF, there is a combination of factors (including the physical properties and porosity of the substrate) that dictate a maximum achievable flow rate. It has been established that a decrease in porosity due either solids clogging and/or the growth of functional biomass, impedes the hydraulic flow in unplanted CWs, but that the flow stabilises after 24 months of operation (Brovelli *et al.*, 2011; Ranieri *et al.*, 2013). With the understanding of the processes which occur within a subsurface flow CW and a BSF, a relationship can be determined using the contact time of the contaminants present in the WW and the active microbial biomass within the porous media (Brovelli *et al.*, 2011). With the increase in contact time, the greater the promotion of the biotic and abiotic reactions, this in turn results in greater COD removal efficiencies (Brovelli *et al.*, 2011). The contact time can only be increased by increasing the HRT which is expressed as the volume of reactor divided by the flow. Thus, in order to treat the same volume of WW, a reduction in HRT would require an increase in the volume of the reactor. Conversely, if the contact time is insufficient, the HRT could be increased by reducing the flow rate (Bruch *et al.*, 2014).

The pH of WWW is typically adjusted before discharge. Experimental BSFs have been shown to essentially neutralise synthetic WWW without any chemical intervention (influent pH range: 3.5-4.0; effluent pH range: 6.9-7.6) (Welz *et al.*, 2014).

2.7 Determination of selected operational and performance parameters in biological sand filters

2.7.1 Determination of hydraulic retention time

The physical structure of a porous medium plays an important role in describing the rate at which water flows through the interconnected voids and the void fraction is described as porosity (Gupta *et al.*, 2016). The prime porosity can be defined as the intergranular pore space relative to the volume of a substrate and the effective porosity is less than or equal to the prime porosity and is the void volume which is interconnected and thus allows liquid to pass through the material, the liquid is only a small portion of the volume in the sands ranging from 45-50% in clay to 0-5% in crystalline rocks with sand filling between the two (Cartwright and Hensel, 1995). The volume of liquid in the void fraction of a saturated environment can be determined by multiplying the porosity by the volume of the medium.

Permeability or hydraulic conductivity (K) is an intrinsic value which describes the ability for a substrate to allow fluids to pass through it and is used to determine flows in aquifers, soil filters, water filters in water and WW treatment plants, packed bed chemical reactors, etc. (Darcy, 1856; Gupta *et al.*, 2016). It is affected by the following physicochemical properties: grain size, grain size distribution, pore size and fluid properties, particle shape and arrangement, and mineralogy (Klute and Dirksen, 1986; Fuentes *et al.*, 2004; Wilson, 2009). The K of a substrate can be determined by two standard tests, namely the constant head and falling head methods, which both rely on Darcy's Law and vertical flow (Das, 2000; Klute and Dirksen, 1986).

The velocity through a porous material which is homogeneous has no capillary zones and has a steady state of flow, and can be described by Darcy's velocity or Darcy's Flux (U), which can be determined by multiplying the K by the change in height over the change in length [Equation (2.4)]. The saturated cross-sectional area at the discharge point can then be used in combination with the calculated flux to calculate the discharge rate [Equation (2.5)] (Darcy, 1856; Wilson, 2009). The HRT can then be determined using the volume (V) of liquid within a packed media divided by the flow rate as shown in Equation (2.6) (Metcalf & Eddy 2004).

$$U = -K \frac{dh}{dl} \quad (2.4)$$

$$Q = -KA \frac{dh}{dl} \quad (2.5)$$

$$HRT = V_{liquid} / Q \quad (2.6)$$

2.7.2 Determination of hydraulic loading and organic loading and removal rates

The HLR can be expressed in three ways (i) as the discharge rate of influent divided by the volume of the reactor ($m^3/m^3/d$)[Equation (2.7)], (ii) when the reactor operates in vertical mode the HLR can also be described as surface loading where the discharge rate is divided by the surface area of the reactor ($m^3/m^2/d$)[Equation(2.8)], and (iii) similarly can be written in terms of cross-sectional area when operated in horizontal mode ($m^3/m^2/d$)[Equation (2.9)]. The organic loading rate (OLR) is determined by multiplying the influent flow rate by the influent COD or BOD concentration divided by the volume of reactor (Metcalf and Eddy, 2004; Equation (2.10)). The organic removal rate (ORR) is the quantity of COD removed per unit volume of reactor [Equation (2.11)]. The HLR can be used in conjunction with the organic OLR and ORR for the comparison of different treatment systems irrespective of size and operation parameters. The removal efficiency across a system can be expressed by equation (2.12).

The volume of the reactor is used to determine the HLR, OLR and ORR. In suspended growth systems, the entire reactor volume is occupied by the WW and microorganisms. CWs have large spatial footprints, partly because a considerable portion is occupied by the physical substrate.

$$HLR_V = Q/V_{reactor} \quad (2.7)$$

$$HLR_A = Q/A_{Surface} \quad (2.8)$$

$$HLR_A = Q/A_{cross\ section} \quad (2.9)$$

$$OLR = \frac{COD_{influent} \times Q}{V_{reactor}} \quad (2.10)$$

$$ORR = \frac{\Delta COD \times Q}{V_{reactor}} \quad (2.11)$$

$$RE = \frac{influent - effluent}{influent} \times 100\% \quad (2.12)$$

2.7.3 Hydraulic pipe flow

The total energy within a pipe can be described as (i) the potential energy, or head above an arbitrary datum, (ii) the kinetic energy, and (iii) pressure energy (Nalluri *et al.*, 2009; Upadhyay, 2010). The total energy at point A will be equal to the total energy at point B with continuous flow in a frictionless system with incompressible fluids, which is described as the conservation of energy by the Bernoulli equation (2.13). However, losses occur when a fluid moves within a pipe due to various sources. These losses need to be taken into consideration, warranting a modification in the Bernoulli equation to account for friction and minor losses (2.14).

$$h_1 + \frac{p_1}{\rho g} + \frac{U_1^2}{2g} = h_2 + \frac{p_2}{\rho g} + \frac{U_2^2}{2g} \quad (2.13)$$

$$h_1 + \frac{p_1}{\rho g} + \frac{U_1^2}{2g} = h_2 + \frac{p_2}{\rho g} + \frac{U_2^2}{2g} + h_f + h_m \quad (2.14)$$

The major losses due to friction for steady uniform flows can be determined using the Darcy-Weisbach equation (2.15). The formula can be rewritten in terms of discharge and can be seen in Equation (2.16). λ is co-efficient of friction and can be determined by the Blasius yield relationship for smooth pipes with turbulent flow (2.17). To calculate this the Reynolds number (Re) must be determined for turbulent flows by means of Equation (2.18), using a kinematic viscosity (ν) of water at a specific temperature (Metcalf and Eddy, 2004). The head loss due to friction needs to be determined in order to correctly implement the Bernoulli equation.

$$h_f = \frac{\lambda U^2}{2gD} \quad (2.15)$$

$$h_f = \frac{\lambda/4 \times l \times Q^2}{3.03 \times D^5} \quad (2.16)$$

$$\lambda = \frac{0.3164}{Re^{0.25}} \quad (2.17)$$

$$Re = \frac{UD}{\nu} \quad (2.18)$$

In small systems with many components and fittings the minor losses can amount to greater losses than the friction losses. Minor losses can be expressed as a function of velocity and a specific K value for the particular fitting. This formula is expressed in Equation (2.19) and is a function of velocity, this formula can be rewritten in term of discharge in Equation (2.20). When designing a pumping main the system curve is a function of the static head plus the sum of minor and major losses at different discharges, this can be represented in Equation (2.21). The system curve is used in conjunction with different pump curves to determine the correct pump and duty point.

$$h_{Minor} = \sum K \left(\frac{U^2}{2g} \right) \quad (2.19)$$

$$h_{Minor} = \frac{\sum K \times 8 \times Q^2}{g \times \pi^2 \times D^4} \quad (2.20)$$

$$h_{total} = h_{static} + h_f + h_m \quad (2.21)$$

2.8 Conclusion

In South Africa, water is a scarce natural resource that needs to be protected and preserved. WWW is one of the many waste streams produced by mankind that can pollute the aquatic environment. It is potentially toxic to microbes and plants, and can negatively affect the soil structure. This effluent is difficult to treat due to its unpredictable strength, character and volume.

Within South Africa, many cellars use holding dams, pH dosing with lime and irrigation to grass pastures as a form of treatment and disposal of WWW. This can result in degradation of the soil structure and pollution of streams and ground water. Over 40% of wineries are small, using an average of ≤ 900 L/day of water. For logistical and financial reasons, these wineries cannot operate sophisticated WW treatment systems. There is a need for simple, cost effective systems for WW treatment at these small wineries, as none are currently available.

CWs utilise the beneficial processes originating in natural wetlands to remediate WW, and have been introduced into South Africa as a potential option for the treatment of WWW. There are a variety of CWs, ranging from simple surface flow systems to highly engineered vertical flow systems. CWs with simple operational designs can have relatively low capital, operational and maintenance costs. However, the phytotoxicity of WWW can affect the performance of CWs and result in additional maintenance requirements if the plants need to be removed and/or replaced.

BSFs can be considered as CWs without plants. These systems have been shown to neutralise the pH and effectively reduce the COD and phenolic content of synthetic and authentic WWW of varying concentrations. These systems can be easily incorporated within the existing infrastructure of many small wineries and have the potential to fill the market gap.

Chapter 3 Research methodology

The methodology pertaining to the design, costing and analysis of the performance of the BSF system is discussed in this chapter.

3.1 Research design

An energy-efficient, modular BSF system was designed, installed and optimised at a small winery in the Western Cape of South Africa. The performance of the system was compared to that of similar systems used in previous laboratory-scale experiments using synthetic WWW and the same filter modules and type of sand.

3.2 Study setting

The pilot scale BSF was installed at a small winery producing only red wines within the Stellenbosch wine region of the Western Cape, South Africa. Laboratory work was performed in the Biocatalysis and Technical Biology Research Group's Laboratory at the Cape Peninsula University of Technology Bellville Campus, unless otherwise stated.

3.3 Research methodology

This research was experimental, and required the analysis of the effectiveness of the BSF system treating authentic WWW. The methods used to generate data (*in-situ* measurements and physicochemical analyses) are provided in this section.

3.3.1 Data

Physicochemical data was gathered during the testing and monitoring period of the BSF from February 2015 to September 2016. Analyses (Sections 3.3.1.1 to 3.3.1.9) were performed on the samples taken either on the day of sampling, or frozen after sampling and performed later.

3.3.1.1 Chemical oxygen demand

The COD concentrations were determined using a Merck (Merck®, Whitehouse Station, USA) Spectroquant® Pharo instrument and Merck Spectroquant® cell tests for low, medium and high range samples (cat. no. 1.14895.0001, 1.14541.0001 and 1.14691.0001).

3.3.1.2 Total phenolics

The total phenolics concentrations were determined by using the Folin-Ciocalteu micro method for total phenolics in wine, this was based on the method reported by Slinkard and Singleton (1997) with the use of Merck (Merck®, Whitehouse Station, USA) Spectroquant® Pharo instrument and Merck®Folin-Ciocalteu reagent (Merck®, Whitehouse Station, USA, Cat No: 1.09001.0500). Standards of gallic acid monohydrate (Sigma-Aldrich®, St. Louis, USA Cat No: 27645) were prepared in-house, with concentrations of 5 mg/L, 100 mg/L, 150 mg/L, 250 mg/L and 500 mg/L. A standard graph was prepared plotting adsorption against concentration, and results were determined in gallic acid equivalents or (mgGAE/L) from this plot.

3.3.1.3 Volatile fatty acids

The concentrations of volatile fatty acids were determined using the Hach (Loveland, USA) esterification kits method 8196 kit and in accordance with manufacturer's instructions with some modifications: Three standard concentrations of acetic acid were prepared (945 mg/L, 472.5 mg/L and 236.25 mg/L) and were used to draw a standard graph for the determination of the samples concentrations using a Merck (Merck®, Whitehouse Station, USA), Spectroquant® Pharo instrument. The reagent and sample volumes will be reduced to half of those recommended by the manufacturer. Results were determined in acetic acid equivalents (mgAAC/L).

3.3.1.4 Phosphate

The total phosphate concentrations were determined using a Merck (Merck®, Whitehouse Station, USA) Spectroquant® Pharo instrument and Merck Spectroquant® cell tests (1.14543.0001). This covered the range of PO₄-P from 0.05 to 5.00 mg/L, PO₄³⁻ from 0.2 to 15.3 mg/L-P and P₂O₅ from 0.11 to 11.45 mg/L and followed the relevant controls and standards for the testing procedure in terms of the manufacturer's instructions.

3.3.1.5 Total nitrogen

The total nitrogen concentrations were determined using a Merck (Merck®, Whitehouse Station, USA) Spectroquant® Pharo instrument and Merck Spectroquant® cell tests (1.14537.0001). This covered the range of total nitrogen concentrations from 0.5 to 15.0 mg/L and followed the relevant controls and standards for the testing procedure in terms of the manufacturer's instructions.

3.3.1.6 Redox and pH

The redox potential and pH of the samples was determined by a waterproof handheld CyberScan pH300 meter (Eutech Instruments, Singapore, Cat No: EC-PHWP300/02K). The redox probe (Eutech Instruments, Singapore, Cat No: EC-PHWP300/02K) had the capability of measuring the pH range 2.00-16.00.

3.3.1.7 Total solids, total suspended solids, total dissolved solids and electrical conductivity

The total solids (TS), total suspended solids (TSS) and total dissolved solids (TDS) were determined. The TS, TSS and TDS from sample point 1 & 3 within the settling basin were determined. For TDS, a measured volume of sample was passed through a sintered glass filter with a 0.45 µm cellulose acetate filter paper (Millipore Durapore® membrane filters Cat Number: HVLPO4700) by means of a vacuum pump. The filtrate was collected in a beaker with a known dry mass. The sample was dried in an oven for 24 hours at 180°C and then in a desiccator for 30 min. The difference in mass of the beaker before and after drying was determined, converted, and expressed as the mass of filtrate per L of wastewater.

For the determination of the TSS, the mass of the retentate was used. The dry mass of a beaker was recorded. During the filtration the filter was rinsed with deionised water into the weighed beaker. The samples were dried in an oven at 180°C for 24 hours and then in the desiccator for 30 min. The difference in mass of the beaker before and after drying was determined, converted, and expressed as the mass of retentate per L of wastewater. The TS was calculated by adding the mass of the TDS and TSS.

The TS was alternatively calculated using a known volume of sample placed in a beaker with a known dry mass and dried in an oven at 180°C for 24 hours and then in the desiccator for 30 min.

The electrical conductivity (EC) and TDS was determined both on and off-site by using a hand-held Oakton ECTestr 11 + multi-range, cup-style pocket EC meter (Eutech Instruments, Singapore Cat No: 35665-35). This instrument has the capability of reading EC with a range of 0 $\mu\text{S}/\text{m}$ to 20.00 mS/m .

3.3.1.8 Sodium, potassium, calcium, magnesium

For the four hour batch test, the concentrations of sodium, potassium, calcium and magnesium was determined on unfiltered wastewater samples at Bemlab Pty Ltd. (Somerset West, South Africa) using a Varian® inductively coupled plasma optical emission spectroscopy [MPX ICP-OES Spectrophotometer (Agilent Technologies, Santa Clara, USA)]. The SAR together with the CROSS ratio was determined from these values using Equation 2.1 and 2.2, respectively.

3.3.1.9 Flow rate

The flow rate of the BSF was determined using a bucket, stop watch and a volumetric cylinder. The flow rate at the overall outlet/final effluent pipe of the system was determined by gathering a volume of water in a minute and repeating this three times in order to determine the flow rate.

3.3.2 Research equipment

3.3.2.1 Construction and installation of the biological sand filter system

The BSF system was set up on a small winery within the Stellenbosch wine district. Before the system could be installed earthworks were required to ensure level platforms for the tanks and filter modules. A holding tank (5000 L), tank (500 L), four filter modules (1000 L drinking troughs) and four bins (100 L) were purchased from Nel Tanks (Cape Town, South Africa). The filter module has a length of 1 680 mm and the cross-section is shown in Appendix A; Figure A.1.

The solar powered pump and control system was built off site. A Shurflo 2088-313-145 12 V DC Diaphragm Premium Demand Pump was used to supply the holding tank. A relay connected to a reed switch within the existing retention dam ensured the pump did not run dry. The pump was controlled by a liquid level relay and a probe in the holding tank, ensuring a consistent volume within the holding tank of 2 500 to 3 800 L. The power was supplied by a SD DirectPro EnerSol 140-140 W Solar Panel and SonX RA12 260 Ah -10H 12 V AGM Battery which was controlled by a Phocos CML20 20Amp Charge Controller, a slow blow fuse and a Gewiss 16 amp double throw double pole D cure breaker. The pump was connected to the existing basin which had ten baffles to reduce settleable solids and reduce short-circuit of the WW from inlet to outlet with an approximate basin volume of 45 m^3

A schematic of the system and existing infrastructure is shown in Figure 3.1. The spatial location of the components and the direction of flow are shown, and the design is discussed in more detail in Sections 3.4 & 4.1.

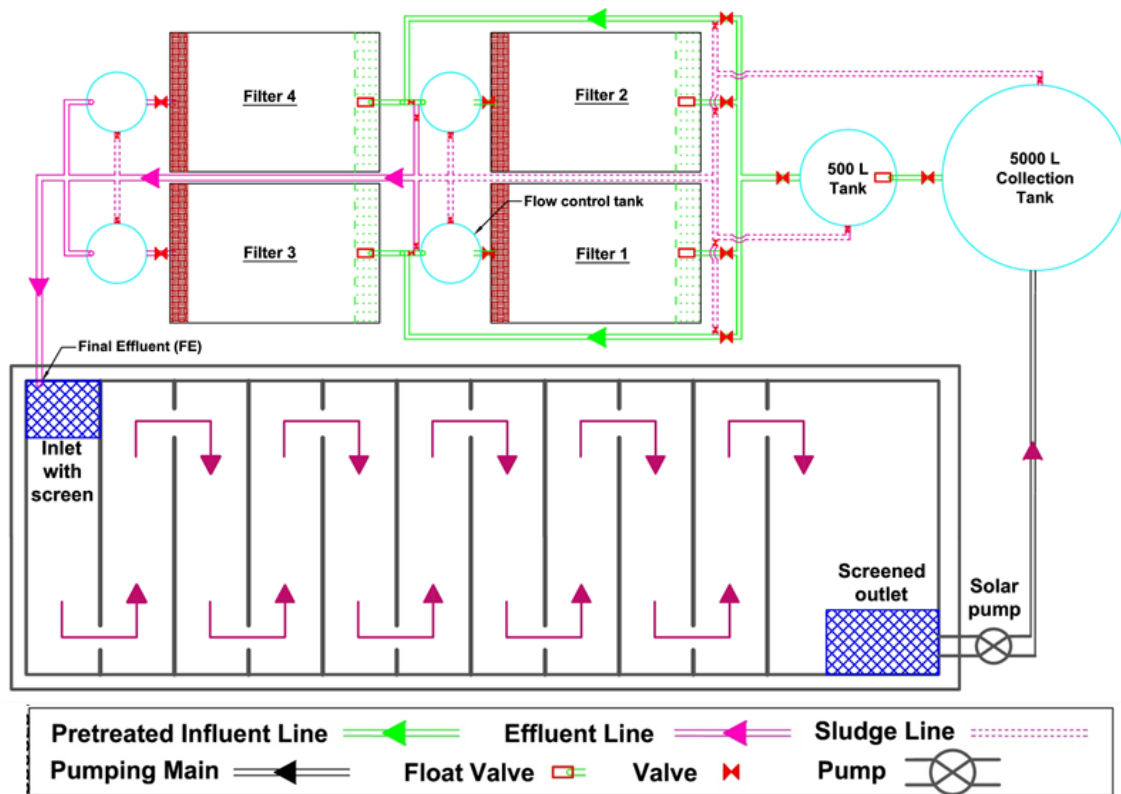


Figure 3.1 Schematic of the on-site biological sand filter together with existing infrastructure and ledger.

3.3.3 Analysis and presentation of results

All the data gathered during the experiments was written in a logbook and transferred to Microsoft Excel. The monthly analyses of the WWT were plotted against time and then against historical data to determine the change in quality of source WW. Concentrations of constituents from the relative sampling points were plotted against time. Removal efficiencies and/or increase or decrease of constituents were calculated from one sampling point to another. The data from the 4 hour tests concentrations were plotted against time. The Pearson's correlation co-efficients between data points were calculated using Microsoft Excel. The same software was used to determine the relationship between samples using a two-tailed paired t-test with a level of significance of 0.05.

Dell Statistica was used to create a matrix graph with true x-y plots in the form of a scatterplot matrix showing the distribution of relationships. This was used to further determine relationships between constituents in a scatter plot with a lineal regression line together with a 95% confidence plot to determine the r value of the regression, called the Pearson's Moment. The data was represented in a summary graph which presents the following statistical analysis: Shapiro-Wilk P, mean, standard deviation, variance, standard error mean, skewness, number, minimum, lower Quartile, medium, upper Quartile, maximum, 95% confidence of standard deviation (lower and upper), 95% confidence of mean (lower and upper), 95% prediction of observation (lower and upper) and non-outlier range. Autocad Civil 3D 2013 Student version was used for the drawing of schematics.

3.3.4 Sampling

Grab samples were taken from all sampling points (Table 3.1). Determination of inorganic concentrations commenced in October 2015. Figure 3.2 shows the location of the sampling points from the existing settling basin (1; Inlet, 2; Middle, 3; Outlet). The samples from the 5000 L holding tank and 500 L tank were taken using a sampling pole after thoroughly stirring the contents of the tank. The samples from the filter modules were taken from a sampling valve that was flushed for 2 seconds prior to sampling. Grab samples were taken from the final effluent pipe. All samples were placed on ice in an insulated container before transportation. Samples were either immediately frozen, or analysed within an hour of receipt in the laboratory.

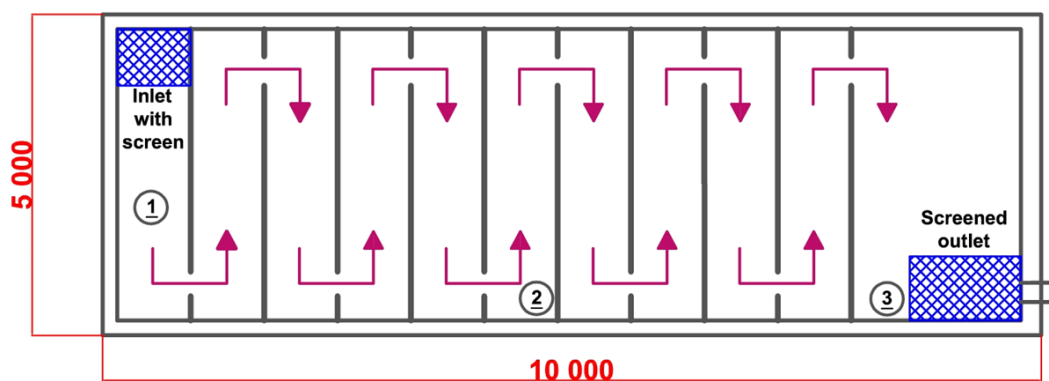


Figure 3.2 Illustration of existing infrastructure (settling basin) together with sampling points.

Table 3.1 Sampling schedule

Sampling point	Period	Occurrence	Analyses	Comment/s
Settling basin: points 1, 2,3	Apr 2014-Feb 2016	Monthly	COD, total phenolics, VFA, total phosphorus, total nitrogen, pH, TS, TSS & TDS	Sampled Weekly in March 2015 during crush. TSS, TDS was deemed unnecessary after 1 year of sampling as it was not relative and the vacuum pump broke therefor only TS was determined.
	Mar-Jun 2016	Bi-weekly	COD, total phenolics, VFA, total phosphorus, total nitrogen, pH & TS	
Settling basin: composite sample	Jun-Sep 2016	Bi-weekly	COD, total phenolics, VFA, total phosphorus, total nitrogen, pH & TS	No correlation between results from 5000 L tank and settling basin. Rationalised to composite samples.
5000 L holding tank 500 L tank	Mar 2015	Once	COD, total phenolics, VFA, total phosphorus, total nitrogen & pH	Additional samples were not deemed necessary during start-up.
	Oct 2015-Apr 2016	Monthly	COD, total phenolics, VFA, pH, sodium, potassium, calcium & magnesium	No sample from 500 L tank in Oct 2015. No samples in Dec 2015 & Jan 2016, settling basin pump broken. No sample in Mar 2016, 5000 L tank obscured.
	May-Sep 2016	Bi-weekly	COD, total phenolics, VFA, pH, sodium, potassium, calcium & magnesium	Sampling schedule increased for more accurate assessment of removal efficiencies.
Filter outlets	Feb, Mar, May 2015	Once	COD, VFA & pH	Additional sampling was not deemed necessary during start-up.
	Nov 2015-Sep 2016	Bi-monthly	COD, VFA, pH, sodium, potassium, calcium & magnesium	Sampling schedule increased for more accurate assessment of removal efficiencies.
Final effluent	Feb 2015-Feb 2016	Monthly	COD, total phenolics, VFA, total phosphorus, total nitrogen, pH, sodium, potassium, calcium, magnesium & flow rate	Sampled Weekly in Mar 2015 during crush. Dec 2015 & Jan 2016 no sample taken as settling basin pump was broken.
	Mar-Aug 2016	Bi-weekly	COD, total phenolics, VFA, total phosphorus, total nitrogen, pH, TS, sodium, potassium, calcium, magnesium & flow rate	TS only measured from June 2016.
5000 L, 500 L, Filter outlets, Final effluent	Aug 2015	Once-off	COD, total phenolics, VFA, pH, sodium, potassium, calcium, magnesium & flow rate	4 hour batch test.

COD = chemical oxygen demand

VFA = volatile fatty acids

3.3.5 System design

The entire system together with the control system was designed by the student and was commissioned on the 23rd of January 2015. A schematic of the BSF together with design notes and valves can be seen in Figure 3.3. The inflow and outflow to and from the 5000 L holding tank was controlled via a liquid level relay and solar pump control system. The holding tank supplied the 500 L tank by means of a float valve. This in turn supplied a constant head of 300 mm on the inlet valves of the filter modules. This set-up allowed the flow to be retarded to the flow achievable by the filter modules. Ball valves were used to allow the gate valves to be flushed. The gate valves and 500 L tank were unnecessary after the addition of the float valves. They were, however, left in place as an additional safety factor. The location of the sampling points for the filters and final effluent can be seen in Figure 3.3.

Figure 3.4 (1) depicts inlet manifold for the filter modules. The float valve (A) in conjunction with the gate valves (B) were used to reduce the risk of overflowing and to maintain a constant head and thus control flow to the filter modules. The PVC ball valves (C) were used to flush the gate valves and inlet piping if blockages occurred. The two ball valves attached to the 500 L holding tank were used as the outlet (D) to the inlet manifold and the lower one (E) was used to drain the tank, which was connected to the overflow of the tank. Both the outlet for the 5000 L holding tank and 500 L tank had raised outlets in order to reduce the chance of sludge entering the pipelines.

The outlet of the filter modules had 25 dm³ of 13.2 mm gravel placed in a ± 150 mm x 150 mm rectangle across the bottom of the filter to aid with drainage and to reduce peripheral flow. A single outlet from each filter module was connected to a flow control tank to maintain a constant outlet height and in turn the height of the WW within the filter. The outlet height could be adjusted within the flow control tank to increase or decrease the flow within the filter module by changing the height of the outlet.

The filter modules were filled with Philippi sand (locally available dune sand) to a height of 420 mm and a channel at the inlet was made to distribute the influent. The system could be operated in parallel or series. When operating in parallel all four filter modules could be supplied with the same influent via the 500 L tank. When additional retention time was required due to poor treatment performance or high strength WW the system was able to operate in series. The effluent from the first filter was supplied to the float valve of the second filter. The control valves for parallel and or series operation can be seen in Figure 3.5. The system was operated in parallel during the experimental period. Figure 3.6 depicts the on-site installation of the entire BSF system.

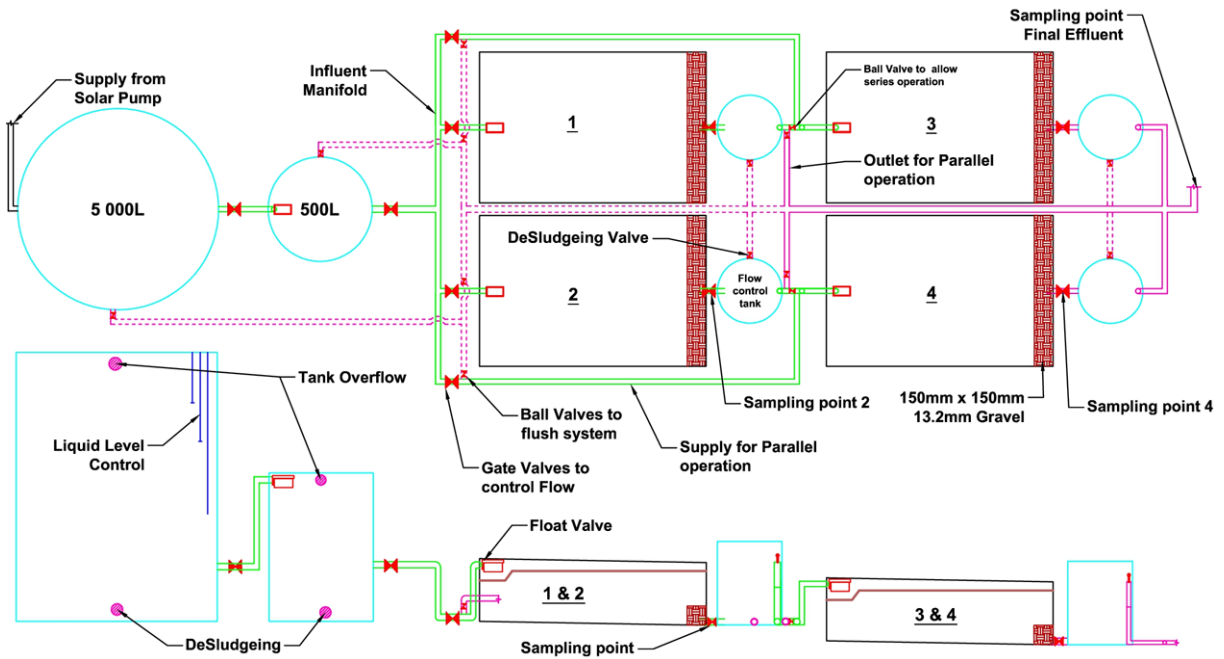


Figure 3.3 Schematic, design notes and valve depiction for pilot biological sand filter system



Figure 3.4 A picture depicting the inlet manifold and float valves for the BSF filter modules plus the 500 L holding tank



Figure 3.5 A picture showing the set-up of the pipes and control valves that allow the system to be operated in series or in parallel



Figure 3.6 A picture of the installed BSF system on site: anti-clockwise from top right: solar pump, 5000 L holding tank, 500 L tank and four filter modules with flow control tanks

3.4 Design Calculations

The achievable flow rates in the BSF were needed to determine the capacity of the system and subsequent designs.

3.4.1 Chemical and physical Analysis of substrate used in biological sand filter

Welz *et al.* (2015) determined the physiochemical properties of Phillipi sand used in this study. The mechanical fraction can be seen in Table 3.2. This represents the broad grading of the sand and its different fractions, with a large majority of sand being medium-sized sand. This is then further broken down and presented in a partial size distribution. This shows the percentage passing the relative sieve size in Table 3.3. The available metal (ions) and elementary analysis can be seen in Table 3.4 and Table 3.5.

Table 3.2 Mechanical Fractions (%) ($n=3$) of Phillipi sand

Size (mm)	Clay <0.005	0.005≤ Silt <0.05	0.05≤ Fine sand <0.10	0.10≤ Medium sand <0.25	0.25≤ Coarse sand <0.5
Fraction	3.9±1.1	1.7±0.6	24.9±3.9	41.8±1.0	27.7±2.1

Table 3.3 Filter media particle distribution

Sieve Size (mm)	2.36	1.18	0.6	0.425	0.300	0.150	0.075	0.0782	0.0553	0.0247	0.0071	0.0050	0.0036	0.0025	0.0015
% Passing	100	95	73	61	39	18	14	14	13	12	9	7	6	5	4

Table 3.4 Available metal (ions)(mg/kg) ($n=3$)

O	K	Cu	Zn	Mn	B	Fe	As
4.6±1.5	7.3±3.1	0.6±0	0.4±0.2	0.5±0.2	0.1±0	12.7±5.1	0.3±0.2

Table 3.5 Elemental analysis (%) ($n=3$) of Phillipi sand

SiO ₂	CaO	AlO ₃	Fe ₂ O ₃	K ₂ O	MgO	Na ₂ O	P ₂ O ₅	TiO ₂
84.59 ± 0.50	7.66 ± 0.03	0.31 ± 0.02	0.07 ± 0	0.15 ± 0	0.15 ± 0	0.21 ± 0	0.03 ± 0.03	0.04 ± 0.01

3.4.2 Flow calculations for sand filter modules

The hydraulic conductivity (K) used is described in Appendix A, Section A. 1 with a K before acclimation ($K_{\max} = 0.286$ mm/s) and 3 months after start up ($K_{\min} = 0.144$ mm/s). To determine the flow within the BSF the cross-sectional area must first be determined. This was achieved by using Equation (3.1) which was determined as a function of the height of sand within the filters trapezoidal shape, Appendix A, Section A.2.1.

$$A = 1070x - 10925 [mm^2] \quad (3.1)$$

After start-up, the flow rates in BSFs and CWs decreases due to the formation of functional biomass. To determine the theoretical discharge from each filter module before and after start-up: The hydraulic conductivities, in the form of Darcy's velocity or Darcy's Flux [Equation (2.4)] was determined. In order to determine Darcy's flux, the following parameters were determined for the filters and K for previous study (i) the maximum and minimum K , (ii) the change in height (ΔH) i.e. the fall from the inlet to the outlet together with the slope along the length of the filter of 1%, (iii) the change in length (Δl) i.e. the length of the filter module. To determine the flow rate across the system, Darcy's law (Equation 2.5) was used with Darcy's flux, and (iv) the cross-sectional area of the saturated sand at the outlet side of the filter. It was assumed that the material was homogeneous, had no capillary zones, and had steady state of flow in terms of Darcy's Law. Permeability or porosity of the sand used in this study was 0.292 ± 0.02 (Welz *et al.*, 2015). Porosity was used to determine the pore volume and in turn the HRT. The theoretical HRT was then calculated using the entire pore volume of the filter and dividing by the discharge as seen in Equation (2.6).

3.4.3 Hydraulic calculation for pipe flow from 500 L tank to filter

The theoretical flow rates from the 500 L tank via the inlet pipe into the filters were calculated using the Bernoulli Equation (2.14) and an integration method and an assumed friction factor (λ). This calculation was used to balance the influent flow to the flow rate of the filter in order to prevent flooding or short-circuiting. The friction factor was used with the Darcy-Weisbach equation (2.15) and the sum of the minor losses (2.19) to determine a new flow rate from pre-determined static head. This flow rate was then used to calculate the Reynolds number (2.18) and therefore a more accurate friction factor using the Blasius yield relationship for smooth pipes with turbulent flow (2.17). Then the new frictional factor was used as the assumed frictional factor until the assumed and calculated frictional factor was the same. The calculation was performed with differing heads and pipe diameters in order to calculate the correct influent flow rate. An example is provided by Appendix A; A. 4, while the complete integration is provided in Appendix B.

3.4.4 Design of gravity flow from 5000 L holding tank to 500 L tank

To supply the 500 L tank with sufficient WWW, the sizing of the pipe between the balancing and holding tank was calculated. To determine the discharge for a 25 mm pipe with an assumed friction of $\lambda = 0.05$ and head of 4 m, the same integrated approach was used as given in Section 3.4.2. The calculations for the integration are provided in Appendix A, A. 4.

3.4.5 Design of pumping main

The pump capacity required to pump the effluent from the existing settling basin to the 5 000 L holding tank was determined. The system curve represents the static head together with the losses due to friction and minor losses. Due to the unknown friction factor an assumed duty point was used to acquire a friction factor to calculate the Reynolds number (2.18). Assumed duty point head of 10.5 m and a flow rate of $0.62 \text{ m}^3/\text{h}$. As the assumed duty point used had turbulent flow together with smooth pipes the Blasius equation (3.9) was used to determine the friction factor via iteration in Appendix A; A.6.4 of $\lambda = 0.03$. The Darcy-Weisbach equation (2.16) was used to determine the loss due to friction together with sum of the minor losses which is written in terms of discharge (2.20) and static head of 9.5 m (2.21). The calculation can be found in Appendix A; 0. The DC Diaphragm Premium Demand Pump curve was supplied by the manufacturer of the Shurflo 2088-313-145 12 V pump.

3.4.6 Cost

To determine the validity of the system in terms of an economical treatment system for WWW the cost of the BSF system was calculated (Table 3.6). A detailed list of the cost of the system is provided in Appendix E.

Table 3.6 Summarised costing of new biological sand filter system (February 2015)

Solar Pump and Controls	R 19965
Pipes and Fittings	R 2947
Tanks and Filters	R 21223
General	R 6000
Total	R 50136

3.4.7 Water usage at the cellar

The monthly water consumption for the cellar can be seen in Table 3.7. It was assumed that the water consumption was directly converted to WW at a ratio of 1:1.

Table 3.7 The monthly water used by the cellar converted directly to wastewater consumption

Month	July	Aug	Sept	Oct	Nov	Dec	Jan	Feb	Mar	Apr	May	June
Water used (m ³ /month)	224	59	41	33	69	31	50	101	162	42	70	100

Chapter 4 Results

4.1 Design calculation

The results of the calculations for theoretical flows are provided in Sections 4.1.1 to 4.1.4.

4.1.1 Flow calculations for sand filter modules

From the calculations described in Section 3.4.2 and calculations in Appendix A; A. 1 - A. 3, the calculated flow rate for one filter at the start of filtration was determined to be 682 L/day/filter module with a velocity of 0.102 m/h, with a HRT of 7.67 hours. Once the K had reduced due to the build-up of functional biomass (acclimation of microorganisms) within the filter module, the new calculated flow rate was 334 L/day/tank, with a velocity of 0.050 m/hr and a HRT of 15.35 Hours. From the flow rate it was approximated that the BSF could treat on average 67% of the WWW generated by the winery.

4.1.2 Hydraulic calculation for pipe flow from 500 L tank to filter

It was initially determined that a 15 mm pipe together a $\frac{3}{4}$ closed gate valve and a head of 200 mm would allow a suitable flow rate to supply the filter modules with 0.709 m³/day and to reduce the flow even further when the K is reduced a 10 mm pipe with a head of 300 mm would achieve a theoretical flow of 309 L/day (Appendix A, A. 4), using the integration approach discussed in section 3.4.2. In spite of this, a small diameter pipe can be prone to clogging and the fittings are not readily available. A 25 mm low density polyethylene pipe was used in conjunction with an Ultra-Low Pressure float valve (Aqua-brooks, Johannesburg, South Africa). The float valve gave the option of slowly trickling in influent with a low pressure and stopping flow in the instance of a blockage. The float valve has a flow of 1500 L/hr at 50 KPa head and brochure is attached in Appendix C.

4.1.3 Design of gravity flow from 5000 L holding tank to 500 L tank

The flow rate from the 5000 L holding tank to 500 L tank was calculated using a 25 mm pipe and a 4 m static head. An integration was done using an assumed friction factor until a calculated friction factor $\lambda = 0.022$ was achieved, calculations can be seen in Appendix A section A. 5. At this point a velocity of 1.817 m/s was calculated and a flow of 3.211 m³/hr which would adequately supply the 500 L tank.

4.1.4 Design of pumping main

The system curve is represented as a function of discharge in equation (4.1) and calculations for this can be seen in Appendix A.6.4. The pump is a Shurflo 2088-313-145 12V DC diaphragm premium demand pump curve in conjunction with the calculated system curve was used to determine the duty point of 9.7 m head and 0.63m³/hr (Figure 4.1). This pump will run for 4.5 hour a day at the start of filtration and will adequately supply the 5000 L holding tank with WWW.

$$h_{total} = 9.5 + 7191194 Q^2 \quad (4.1)$$

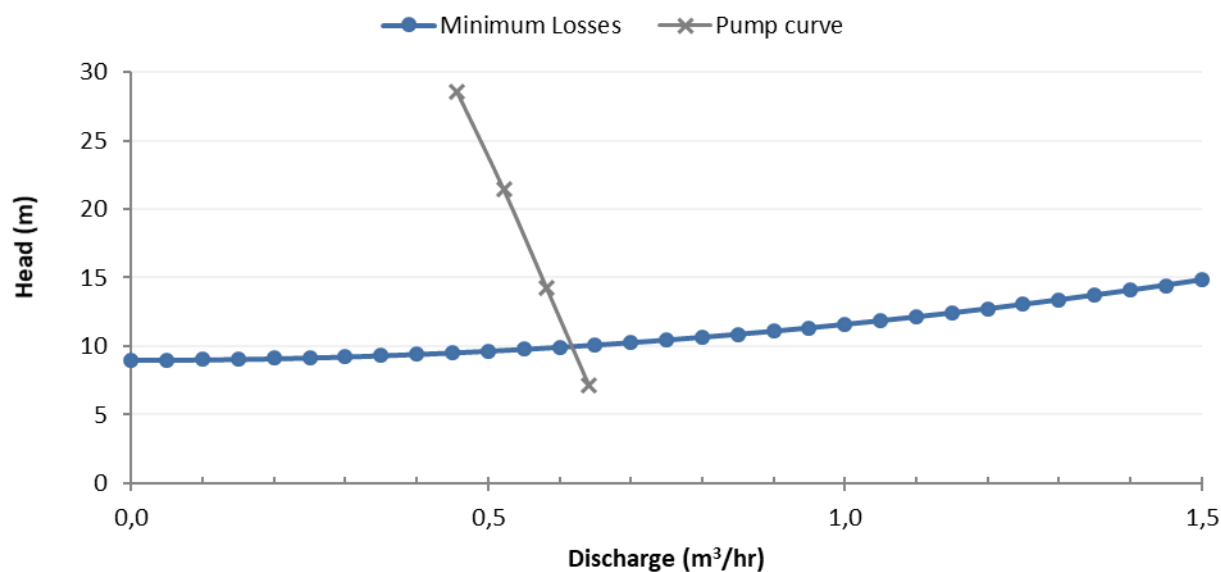


Figure 4.1 Pump and System curve for pumping main to 5000 L holding tank

4.2 Characterisation of winery wastewater

To gain insight into the character of winery wastewater from evaporation ponds and settling basins in the Western Cape, monthly and bi-weekly during crush samples were taken from four sites, including the test site (Table 3.1). Extensive analyses (COD, VFAs, total phenolics, pH, electrical conductivity, sodium, potassium, sugars, ethanol, glycerol and organic acids) were conducted and the results published in Welz *et al.* (2016), this is attached in Appendix F. Only the results of the COD measurements from the test site are included in this thesis.

To evaluate the character of the WWW, samples were taken from the existing concrete settling basin at the test site for 10 months prior to the start-up of the BSF system, and at regular intervals after start-up, according to the schedule provided in Table 3.1.

4.2.1 Chemical oxygen demand

The COD concentrations measured in the samples taken from the three points within the existing basin before the BSF was installed from April 2014 until the end of January 2015 can be seen in Figure 4.2. There was a maximum COD of 7265 mg/L in May which was at the inlet of the basin which also had a minimum of 48 mg/L. The minimum for the entire basin was 28 mg/L. The average COD was 961 mg/L during this period.



Figure 4.2 Chemical oxygen demand concentrations measured in samples from the existing settling basin at the inlet, middle and outlet sampling points before commissioning of the BSF system, Apr 2014 – Jan 2015

The BSF was installed in February 2016. The COD results from samples taken from the settling basin from February 2015 until September 2016 are shown in Figure 4.3. During this period, an average COD of 861 mg/L was recorded with a maximum and minimum from the different sampling points of 2920 mg/L in August 2015 and 31 mg/L in December 2015, respectively. From May until the end of August 2016 composite samples were taken from three points in the settling basin (inlet, middle, and outlet). It was deemed unnecessary to take separate samples from the settling basin as there was no positive correlation with the effluent from the 5000 L holding tank due to the long retention time in the latter. The average COD during this period was 2033 mg/L, which was far higher than previously found. The minimum and maximum were 58 mg/L and 4795 mg/L, respectively. In November 2015, the winemaker retired and a new winemaker took his place, it is possible that the new wine maker followed new cellar practices. If the average of sampling point inlet, middle and outlet are averaged, excluding the composite samples the basin had an average of 694 mg/L.

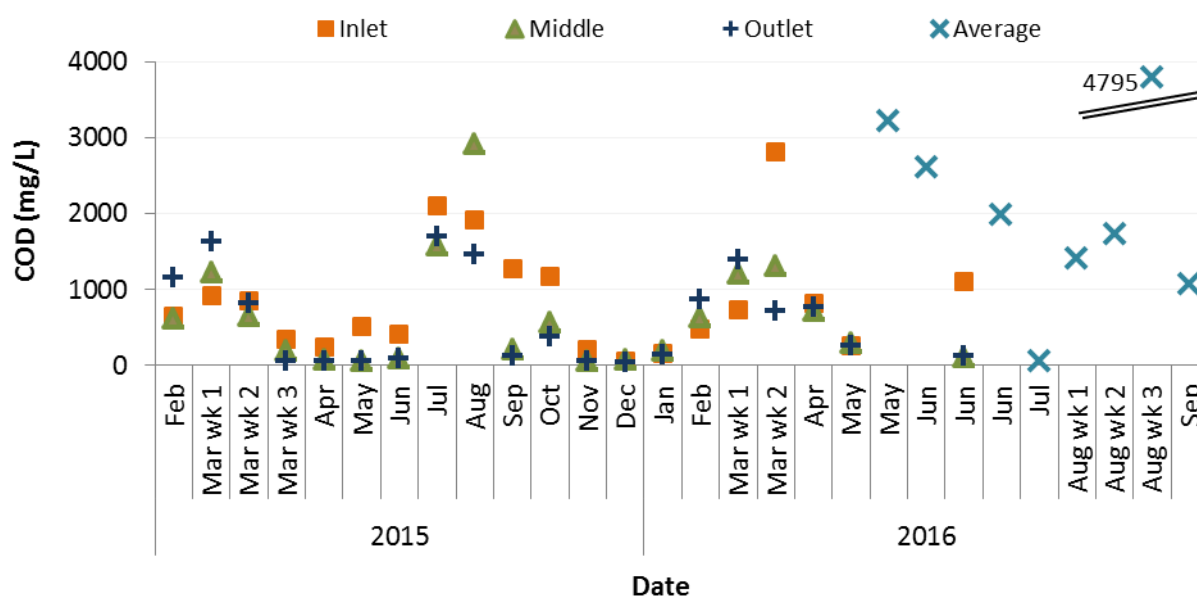


Figure 4.3 Chemical oxygen demand concentrations measured in the existing settling basin samples taken separately at the inlet, middle and outlet points after the commissioning of the BSF from Feb 2015-June 2016 and the concentrations of pooled samples from the inlet, middle, and outlet sampling points (average) from May-Sep 2016

4.2.2 Volatile Fatty Acids

The VFA concentrations fluctuated and can be seen in Figure 4.4. The average VFA concentration in samples taken from the three sampling points (inlet, middle, outlet) until May 2015 was 150 mgAAE/L, with minimum and maximum concentrations of 1.4 and 739 mgAAE/L, respectively. The average concentrations and ranges in samples from the inlet, middle and outlet were 178 mgAAE/L (range: 20-739 mgAAE/L), 114 mgAAE/L (range: 2.4-256 mgAAE/L), and 157 mg/L (range: 1.4-576 mgAAE/L), respectively.

The VFA concentrations in the pooled (inlet, middle, outlet) samples taken from May to August 2016 ranged from 32 to 921 mgAAE/L, with an average of to 339 mgAAE/L.

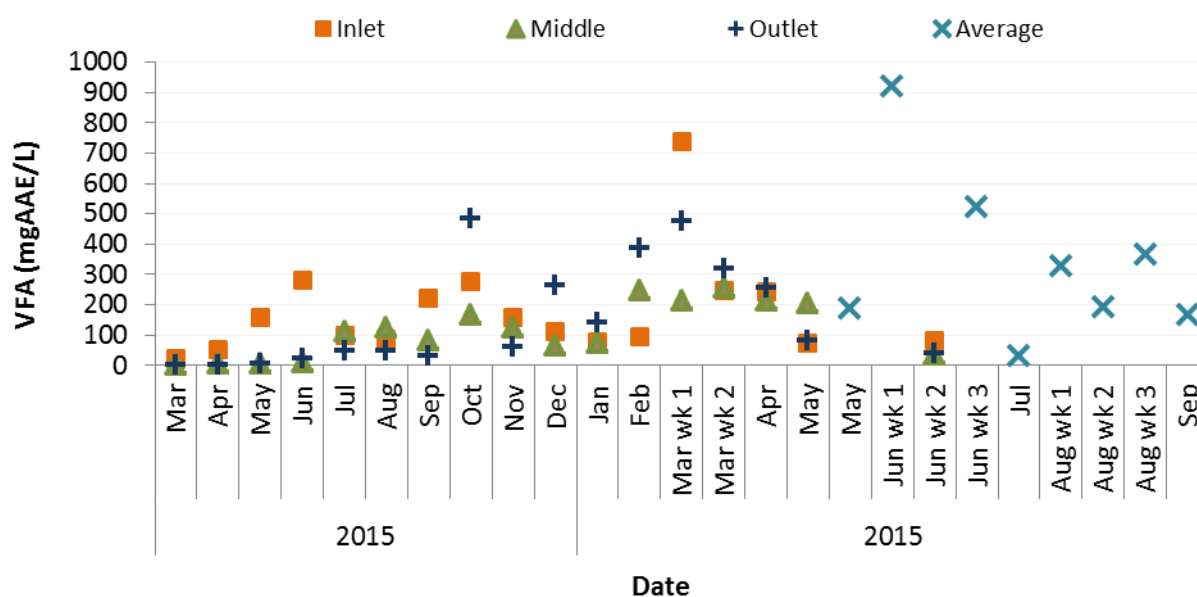


Figure 4.4 Volatile fatty acid concentrations in samples taken separately from the inlet, middle and outlet sampling points in the existing settling basin from March 2015 - June 2016, and the concentrations in pooled (average) samples from the inlet, middle and outlet points from May - Sep 2016

4.2.3 Total phenolics

The average concentration of total phenolics in samples over the entire testing period of 21.4 mgGAE/L (Figure 4.5), while the average concentration in the pooled (average) sample was 39.8 mgGAE/L, with a maximum of 65 mgGAE/L. The highest concentration (64.99 mgGAE/L) of total phenolics was found in August 2016, when the wastewater was heavily contaminated with red wine (Figure 4.6).

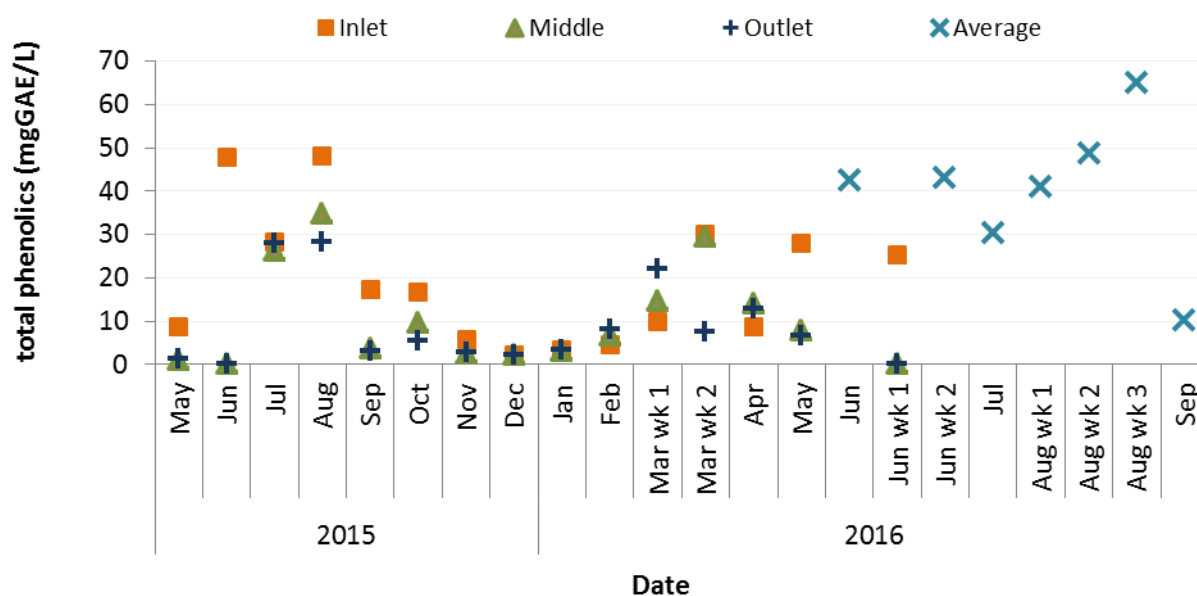


Figure 4.5 Total phenolic concentrations in samples taken separately from the inlet, middle, and outlet points in the existing settling basin from May 2015-June 2016, and concentrations in pooled (average) samples taken from the inlet, middle and outlet from June 2016 -September 2016.

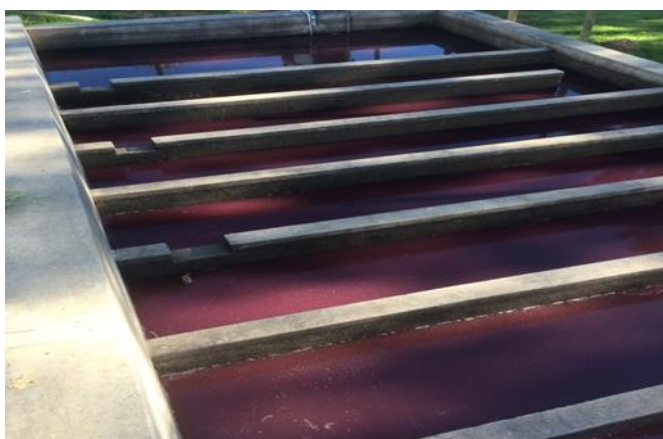


Figure 4.6 Photograph of the settling basin containing winery wastewater with a high concentration of total phenolics on the 20th of August 2016

4.2.4 Total Nitrogen and phosphate

The nutrient concentrations within the WWT showed monthly fluctuations (Section 4.3.4). The average total nitrogen concentration in samples taken from April to December 2015 was of 1.5 mg/L. The average concentrations in samples from the inlet and outlet were 2.2 mg/L and 0.9 mg/L, respectively. The average concentration measured in samples from the inlet was 2.9 mg/L from January to September 2016, with an overall average of 2.2 mg/L and a maximum of 8.9 mg/L (Figure 4.7).

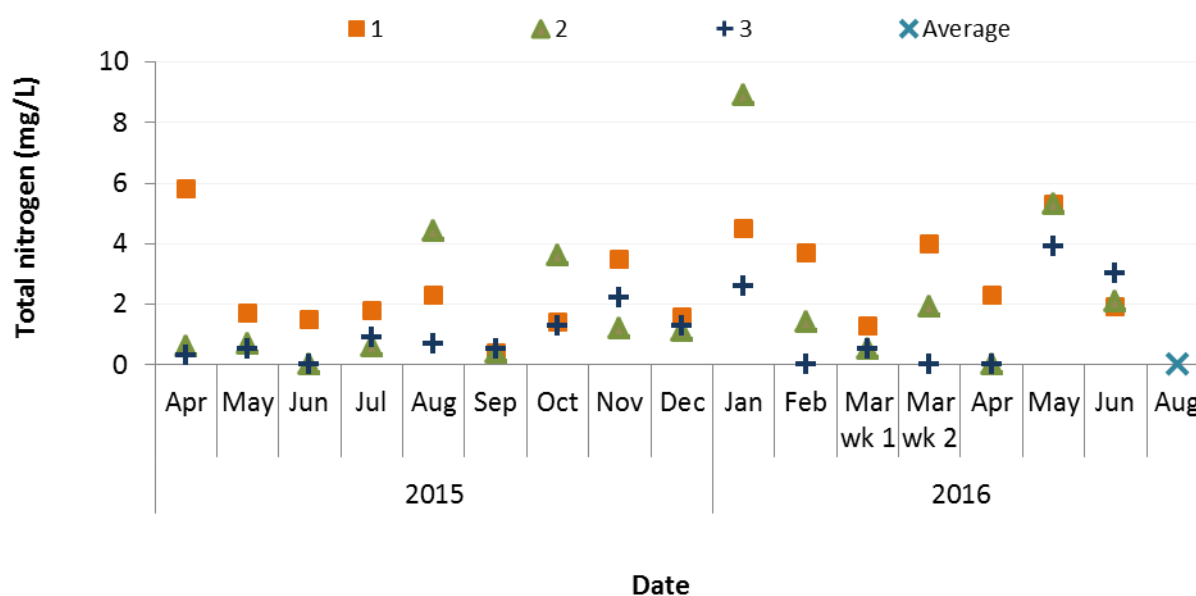


Figure 4.7 Total nitrogen concentrations in samples taken from the existing settling basin from April 2015 to August 2015

The total phosphate (PO_4^{3-}) concentrations fluctuated, with an average concentration of 0.85 mg/L and a maximum concentration of 2.45 mg/L from April to December 2015. Samples taken thereafter had an average concentration of 1.88 mg/L with a maximum of concentration within the inlet of 14.36 mg/L (Jan-Aug 2016). The average for the entire testing period was 1.22 mg/L and excluding the outlier of 14.36 mg/L the average was 0.85 mg/L, there was a minimum average within the middle sampling point of 0.62 mg/L and a maximum at the inlet of 2.13 mg/L and 1.01 mg/L excluding the outlier (Figure 4.8).

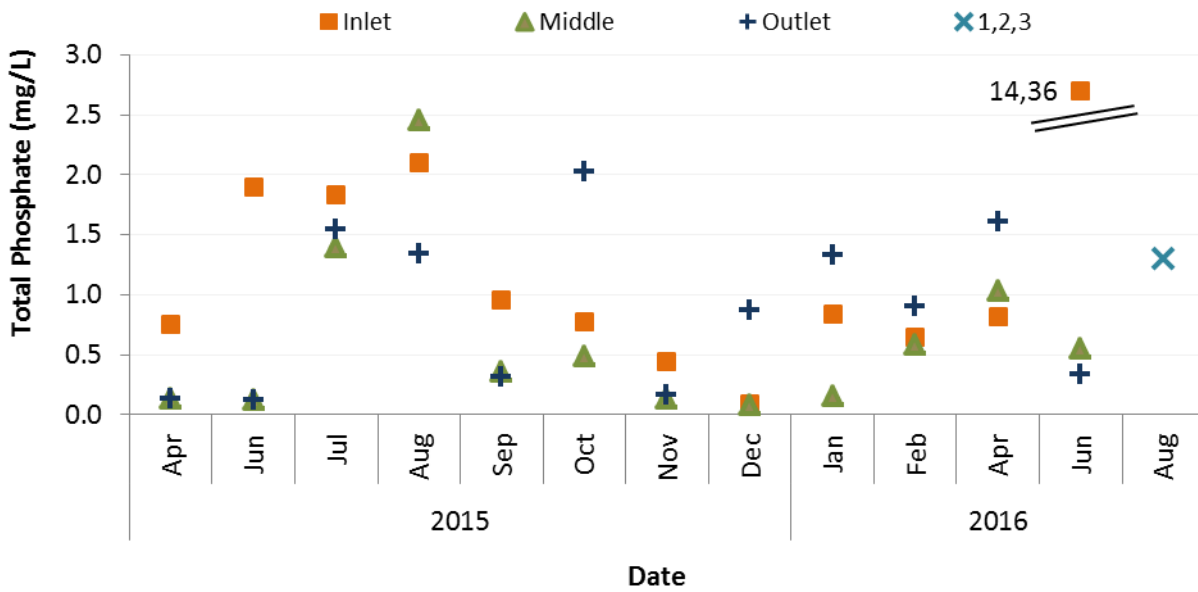


Figure 4.8 Concentrations of total phosphate in samples taken from existing settling basin from April 2015 to August 2016

4.2.5 Total dissolved solids, total suspended solids and total solids

The average TDS and TSS concentrations in the samples taken at the inlet sampling point were 156 mg/L and 1016 mg/L, respectively, while corresponding samples from the outlet sampling point were 127 mg/L and 905 mg/L, respectively (April 2014 to May 2015). The maximum TDS and TSS were 680 mg/L and 2050 mg/L, respectively. The average concentrations of total solids were 824 mg/L and 433 mg/L for the inlet and outlet samples, respectively (October 2015 to September 2016). As seen in Figure 4.9.

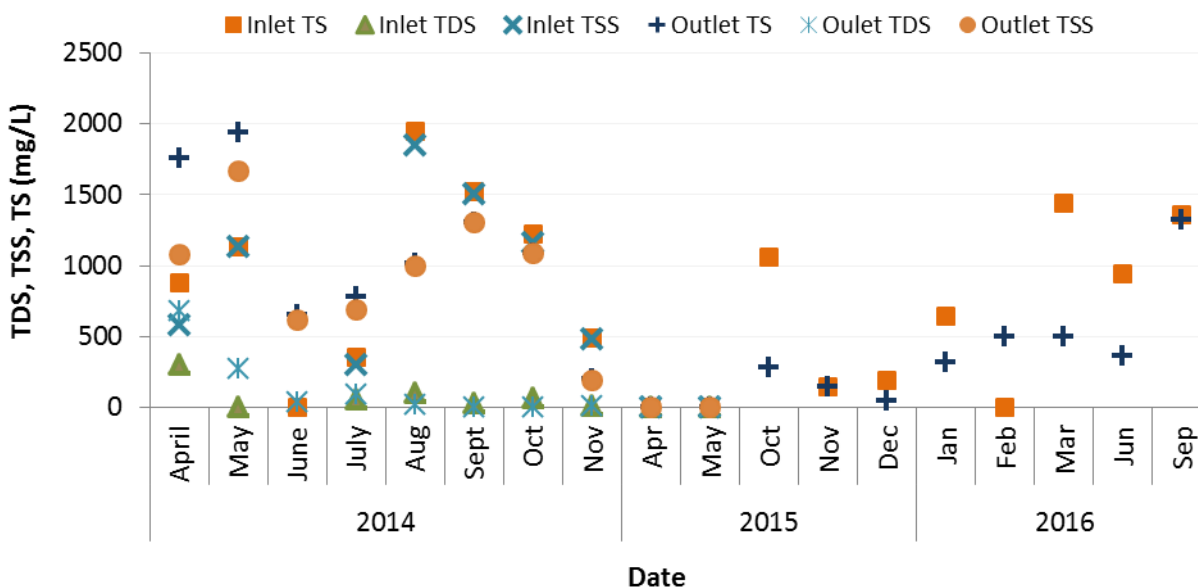


Figure 4.9 Total dissolved solids, total suspended solids and total solids for inlet and outlet sampling point for existing basin samples taken April 2014 – September 2016.

4.2.6 Electrical conductivity

The average EC in the samples was 528 $\mu\text{S}/\text{m}$ with a maximum concentration of 1178 $\mu\text{S}/\text{m}$ in the week 1 of June 2016 and a minimum of 40 $\mu\text{S}/\text{m}$ in November 2015. The time period of sampling is depicted in Figure 4.10.

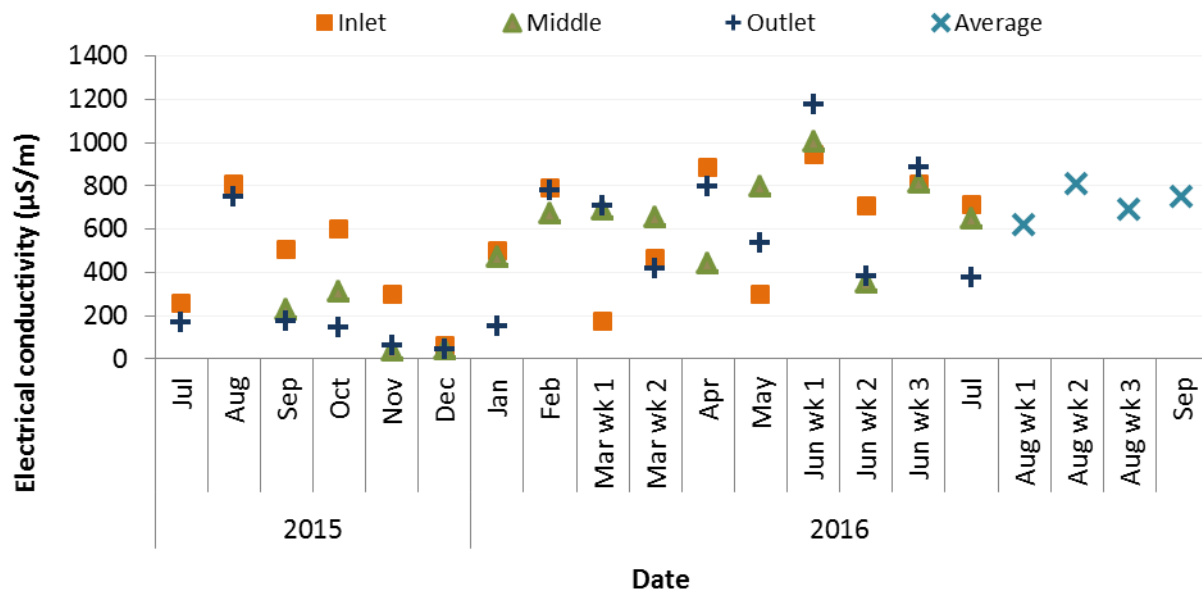


Figure 4.10 Electrical conductivity measured in samples taken from the existing settling basin from July 2015 to September 2016

4.2.7 pH

The pH in the samples ranged from 3.7 to 10.4 during the testing period (Figure 4.10).

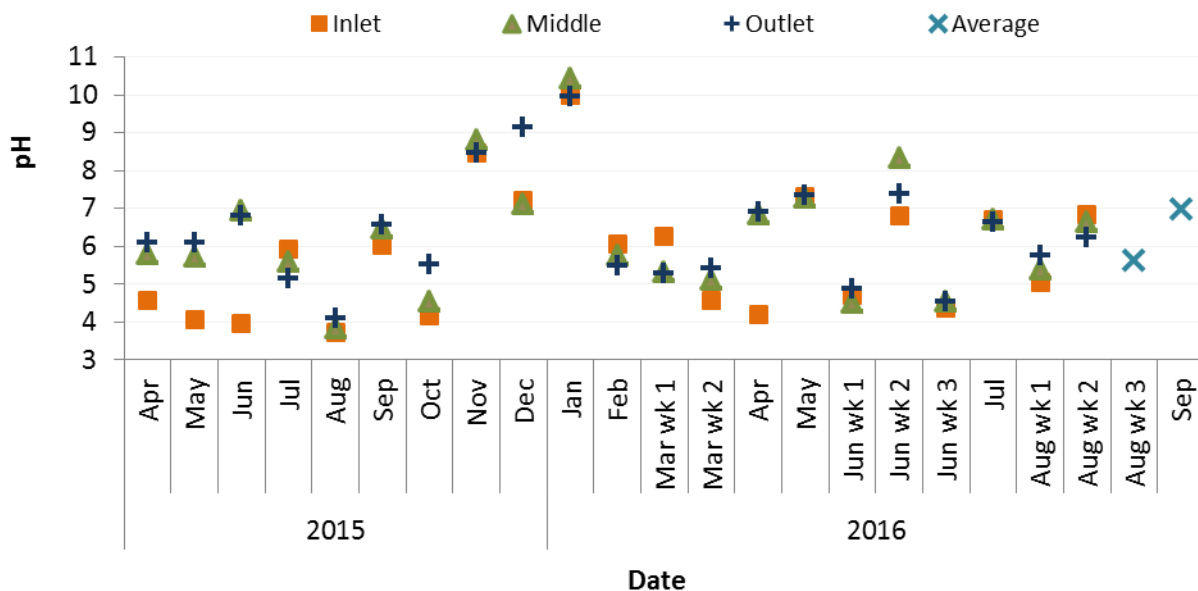


Figure 4.11 The pH measured in samples taken from the existing settling basin from April 2015 to September 2016

4.3 Analysis of influent/effluent to/from the biological sand filter system

The long-term treatment performance of the BSF was analysed by monitoring the influent (from 5000 L holding tank and 500 L flow control tank) and effluent (from filter modules and final effluent).

4.3.1 Chemical oxygen demand

The COD for samples taken for the depicted sampling period from the 5000 L holding tank 500 L tank and Final effluent can be seen in Figure 4.12. Samples taken from the 5000 L holding tank exhibited a range of COD from 424 to 2185 mg/L and an average COD of 1265 mg/L over the entire testing period. From February to September 2016 the average COD concentration was 1324 mg/L for the 5000 L tank. The 500 L tank had a range from 290 – 1551 mg/L.

The COD concentrations measured in the final effluent samples showed and an average of 321 mg/L and a maximum of 831 mg/L from February to November 2015 and an average of 347 mg/L and maximum of 1382 mg/L from February to September 2016. The average COD concentration in samples taken over the entire testing period was 336 mg/L (Figure 4.12).

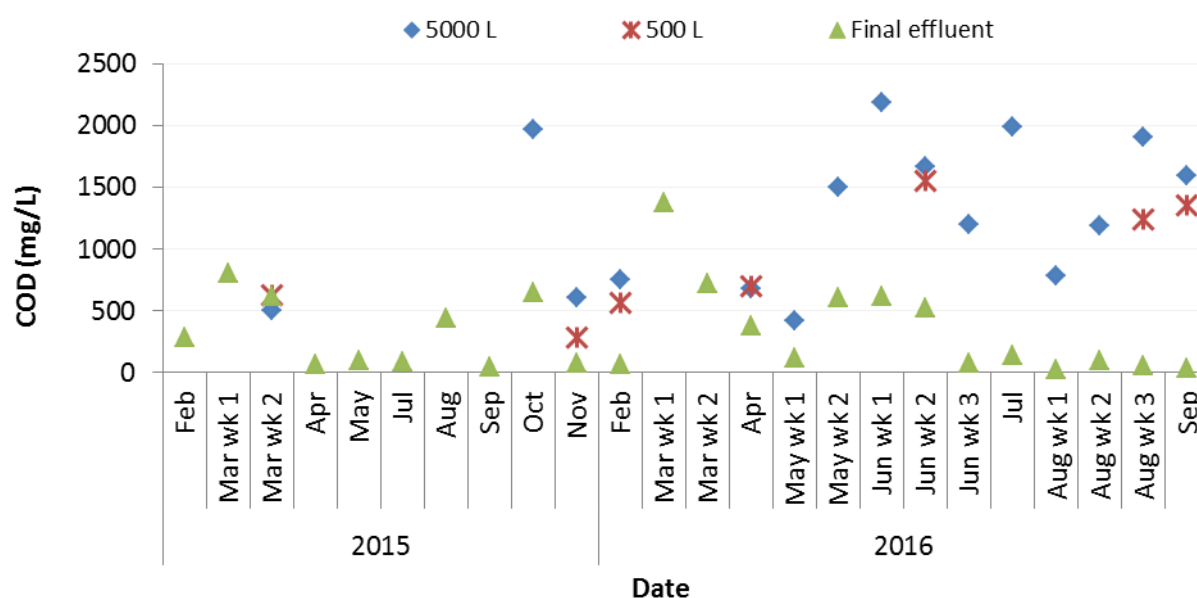


Figure 4.12 Samples of Chemical oxygen demand concentration in sample from 5000 L holding tank, 500 L tank and final effluent from February 2015 to September 2016

Results from the samples taken from the different filter outlets are presented in Figure 4.13. During the 2015 sampling period the maximum COD concentration was found in samples taken from Filter 2 (1332 mg/L), while the maximum COD during 2016 was found in samples taken from Filter 3 (586 mg/L).

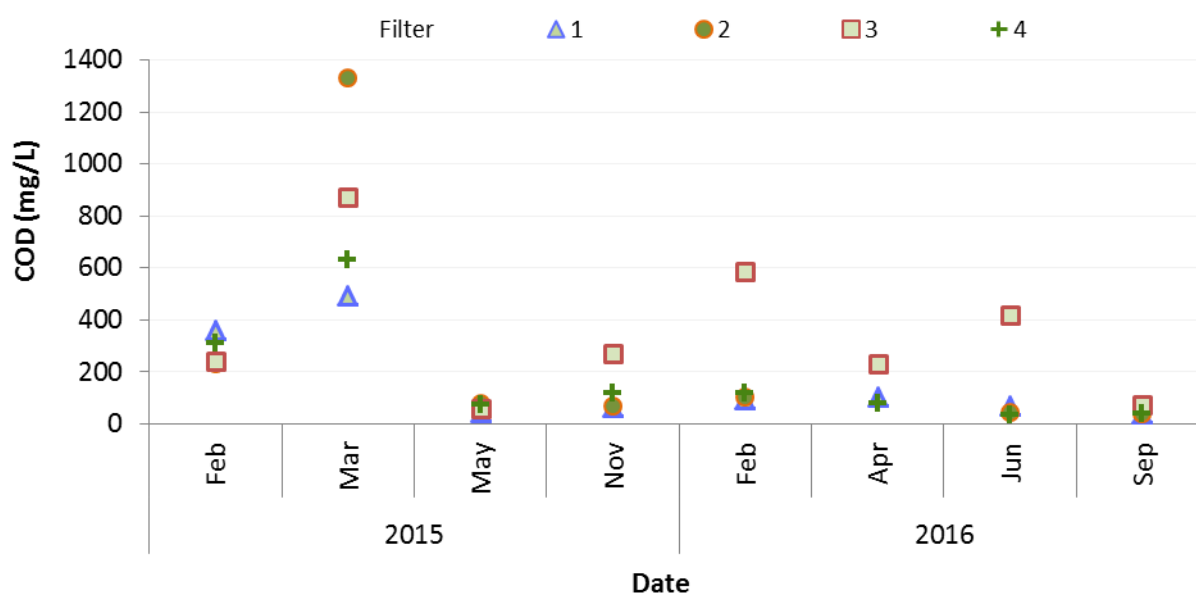


Figure 4.13 Chemical oxygen demand concentrations measured in samples from filter outlets 1, 2, 3 & 4 from February 2015 to September 2016

4.3.2 Volatile fatty acids

The concentrations of VFAs in samples taken from the 5000 L holding tank had a peak concentration of 955 mgAAE/L during 2015. During 2016, samples from the 5000 L holding tank and 500 L tank had maximum concentrations of 1018 mgAAE/L and 923 mgAAE/L, respectively. The average concentrations in samples from the 5000 L holding tank and 500 L tank over the entire sampling period were 525 mgAAE/L and 409 mgAAE/L, respectively (Figure 4.14).

The average concentration of VFAs measured in final effluent samples over the 2015 and 2016 sampling periods were 56 mgAAE/L and 254 mgAAE/L, with a maximum of 254 mgAAE/L and 622 mgAAE/L, respectively. The average concentration of VFAs measured in samples taken over the testing period was 182 mgAAE/L.

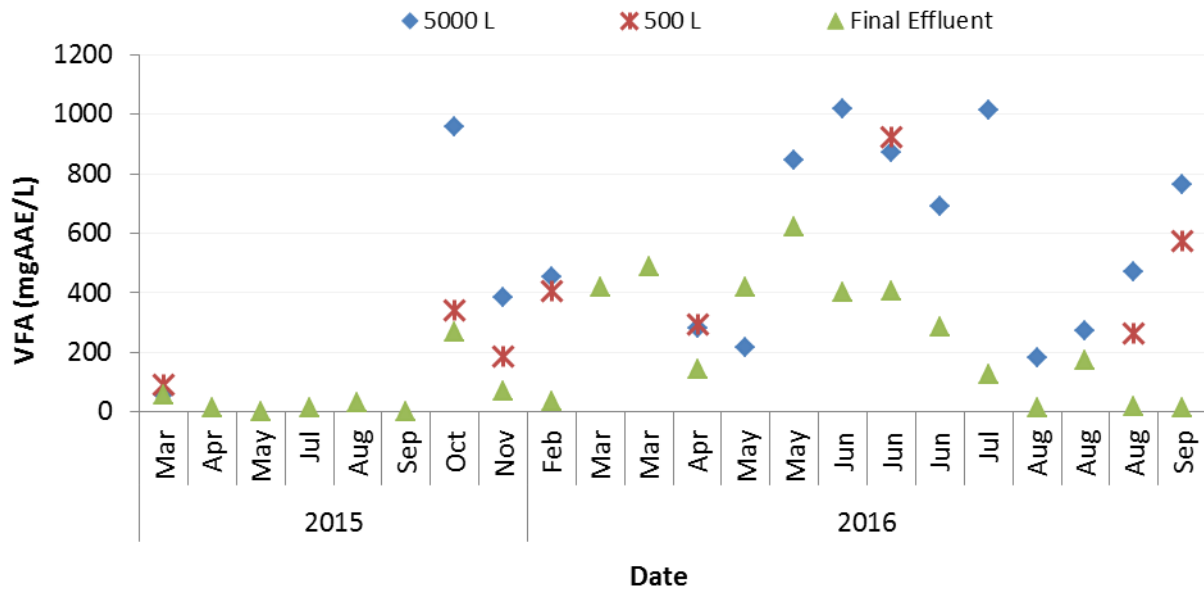


Figure 4.14 Volatile fatty acid concentrations measured in samples taken from the 5000 L holding tank, 500 L tank and final effluent from February 2015 to September 2016

The VFA concentration measured in samples taken from the filter modules were comparatively inconsistent. The highest and lowest concentrations were found in samples taken from Filters 3 and 1, respectively. The maximum concentration measured in samples from Filter 3 was 405 mgAAE/L (Figure 4.15).

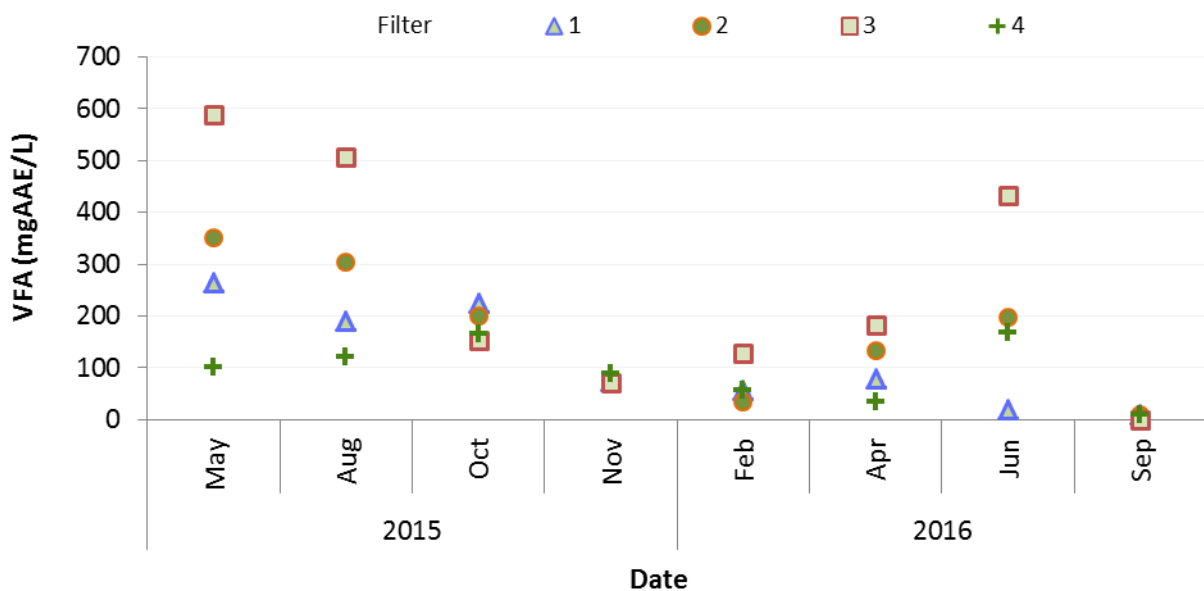


Figure 4.15 Volatile fatty acid concentrations measured in samples from filter outlets 1, 2, 3 & 4 from May 2015 to September 2016

4.3.3 Total phenolics

The total phenolics or (poly)phenolics concentrations measured in samples taken from the 5000 L holding tank and 500 L flow control tank exhibited averages of 21.89 mgGAE/L and 20.24 mgGAE/L, with maximum of 52.78 mgGAE/L and 43.06 mgGAE/L, respectively. In samples of final effluent, the concentration was < 10 mgGAE/L ($n=20$), except for three instances. In two of these, the concentrations were 31.87 and 37.44 mgGAE/L (Figure 4.16).

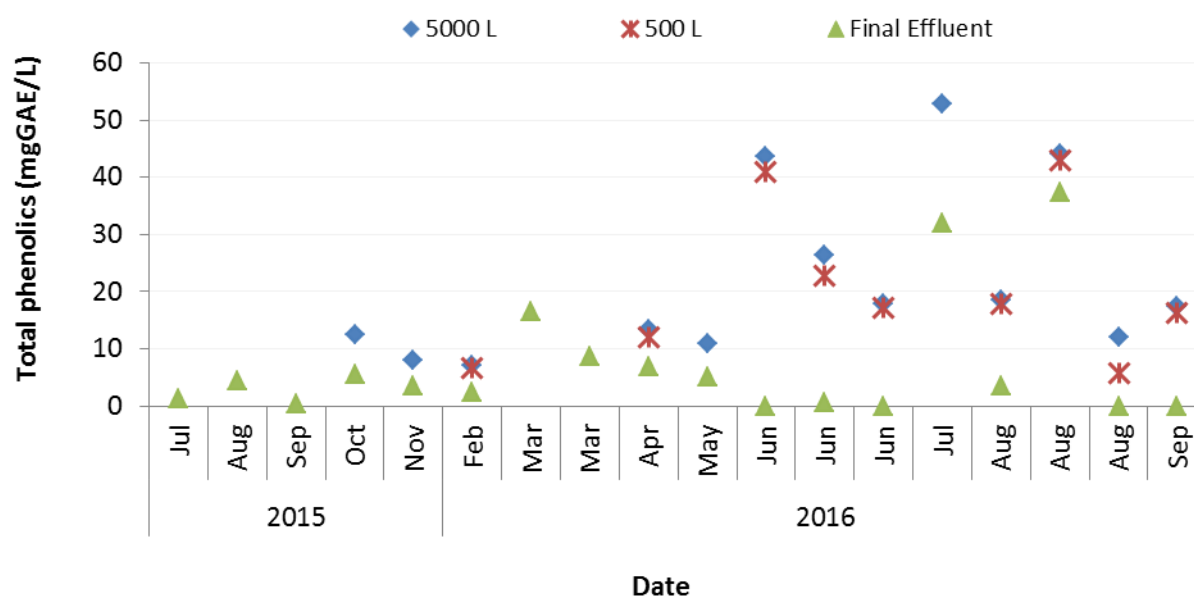


Figure 4.16 Concentrations of total (poly) phenolics measured in samples taken from the 5000 L holding tank, 500 L tank and final effluent from February 2015 to September 2016

4.3.4 Total nitrogen and phosphate

The concentrations of total nitrogen in the final effluent samples were low, with an average of 1.7 mg/L, with a minimum below detectable limit and two spikes of 9.8 mg/L and 3.3 mg/L during the sampling periods, respectively (Figure 4.17).

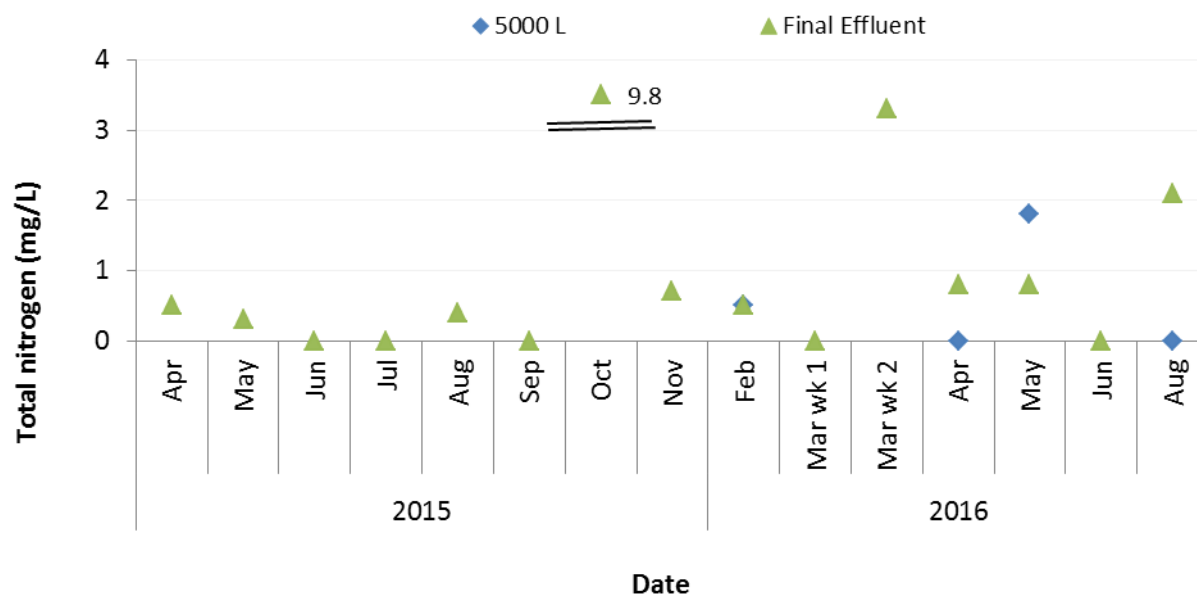


Figure 4.17 Total nitrogen concentrations in from 5000 L tank and final effluent taken from April 2015 August 2016

The phosphate (PO_4^{3-}) concentrations of the final effluent samples ranged from 0.12 to 2.52 mg/L and the maximum in samples from the 5000 L tank sample was 3.57 mg/L (Figure 4.18).

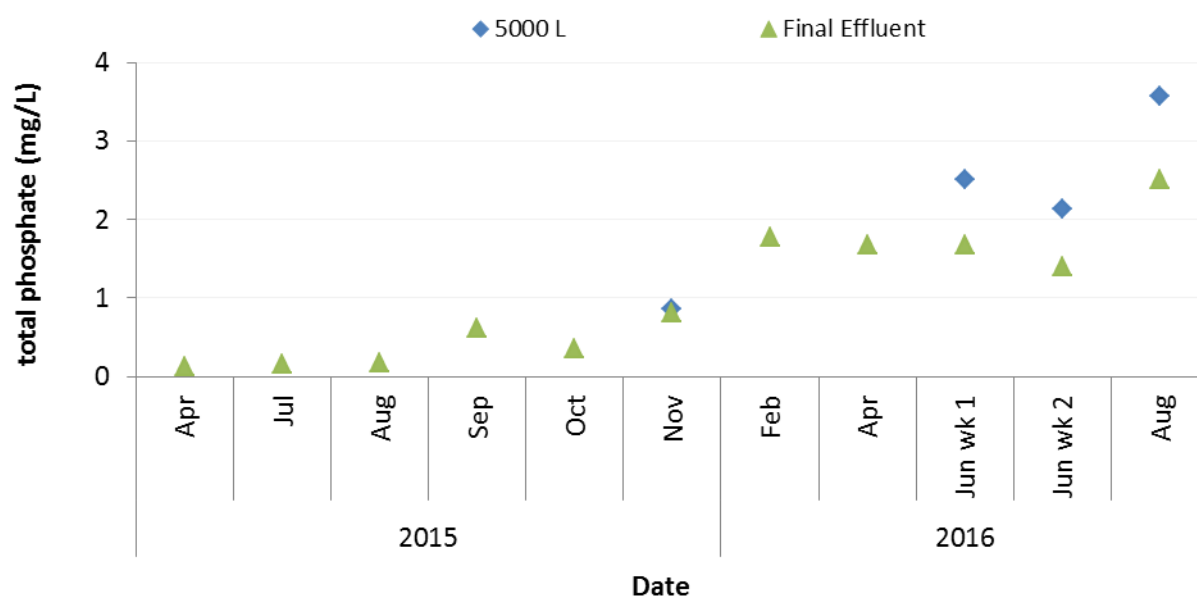


Figure 4.18 Total phosphate concentrations in samples from 5000 L and final effluent taken from April 2015 to September 2016

4.3.5 Inorganic constituents

The concentrations of the monovalent cations, sodium and potassium, and the divalent cations, calcium and magnesium were measured and used to calculate the SAR, CROSS, K:Na ratio and conductivity, as discussed in Sections 4.3.5.1 to 4.3.5.8.

4.3.5.1 Sodium

The sodium concentrations measured in the samples taken from the 5 000 L holding tank and 500 L tank showed increased trends: from 19.1 mg/L to 70.8 mg/L and 6.6 mg/L to 47.2 mg/L, respectively (Figure 4.19). In the final effluent samples, the concentrations ranged from 12.2 to 62.9 mg/L, with an average concentration of 33.2 mg/L (Figure 4.19).

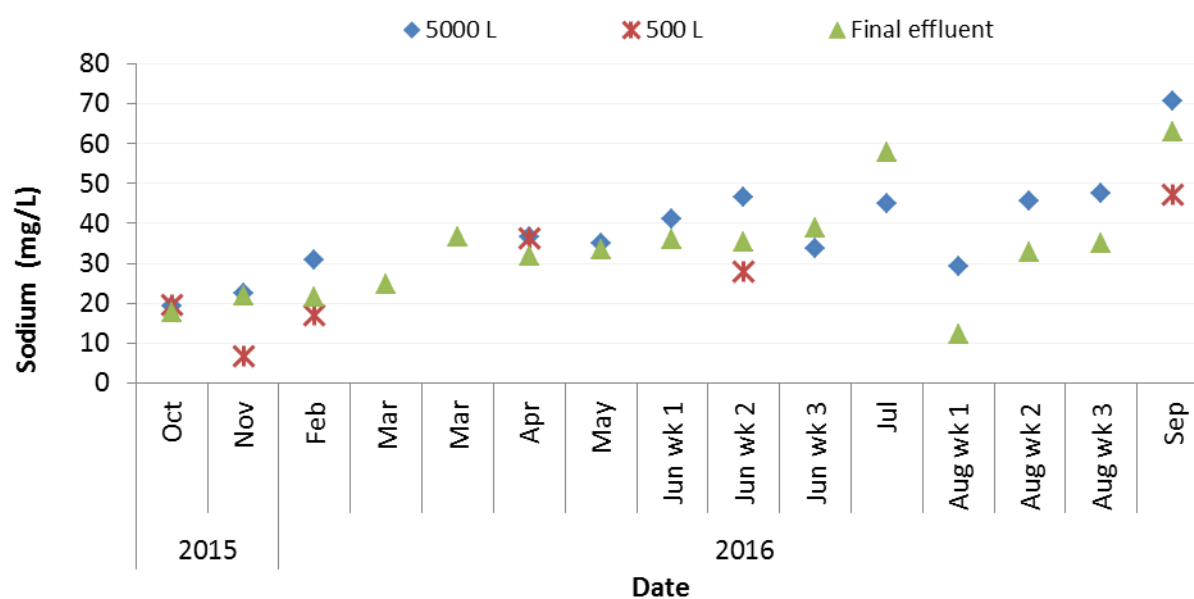


Figure 4.19 Concentrations of sodium measured in samples taken from the 5000 L holding tank, 500 L tank and final effluent from October 2015 to September 2016

In samples from the filter modules (Figure 4.23), concentrations ranged from 10.3 to 106.4 mg/L, with notably higher concentrations being found in samples from Filter 3 (maximum of 106.4 mg/L in February 2016).

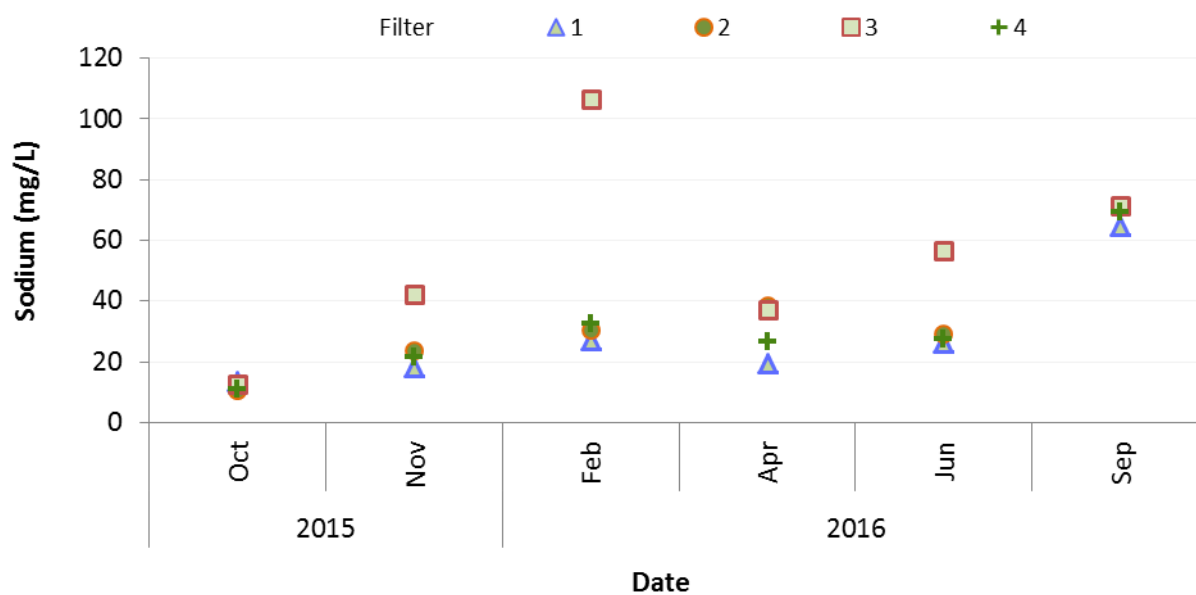


Figure 4.20 Concentrations of sodium measured in samples taken from the filter outlets 1, 2, 3 & 4 from October 2015 to September 2016

4.3.5.2 Potassium

The potassium concentrations measured in the samples taken from the 5 000 L holding tank and 500 L flow control tank ranged from 69.3 to 284.9 mg/L and 20.1 to 149.7 mg/L, respectively, with average concentrations of 167.5 mg/L and 77.3 mg/L, respectively (Figure 4.1.9). The average concentration measured in final effluent samples was 154.9 mg/L, with a maximum of 302.9 mg/l and a minimum of 25.9 mg/L (Figure 4.21).

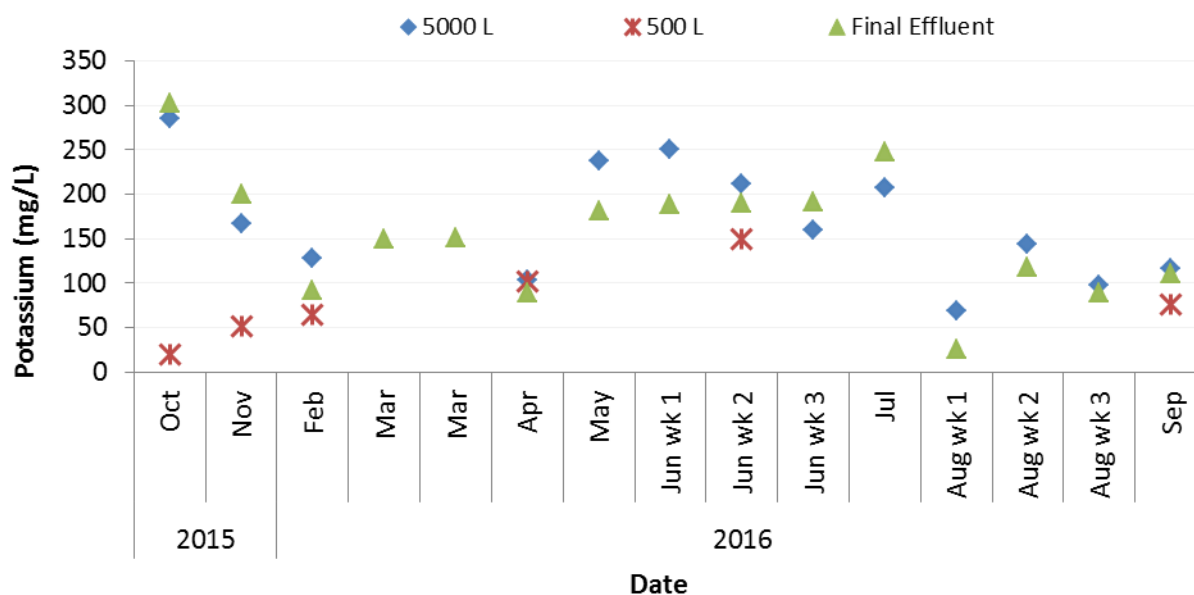


Figure 4.21 Concentrations of potassium measured in samples taken from the 5000 L holding tank, 500 L tank and final effluent from October 2015 to September 2016

The concentrations of potassium in samples from the four filter outlets ranged from 48.0 to 439 mg/L (Figure 4.22), with the maximum from samples from Filter 3 being found during the low flow/resting period. The average concentration in samples from Filter 3 was 268.9 mg/L, while the average in samples from the other filters was 157.8 mg/L.

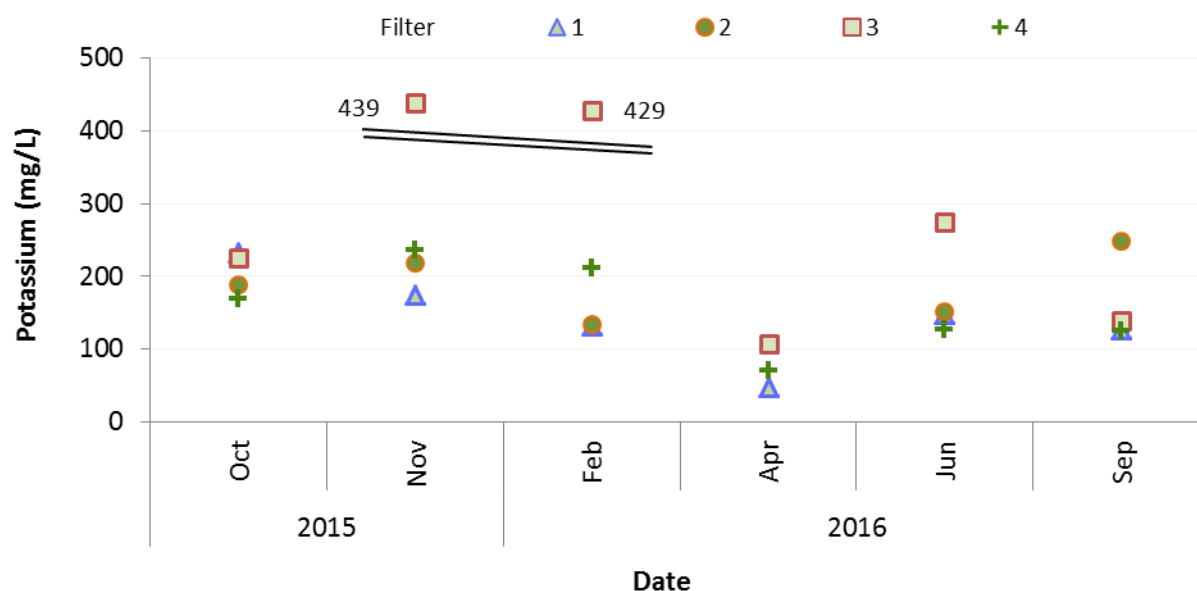


Figure 4.22 Concentrations of potassium measured in samples taken from the filter outlets 1, 2, 3 & 4 from October 2015 to September 2016

4.3.5.3 Calcium

The average concentrations of calcium measured in samples taken from the 5000 L and 500 L were 53.0 mg/L and 35.8 mg/L, respectively (Figure 4.23), with ranges of 21.5 to 104.0 mg/L and 9.6 to 58.7 mg/L, respectively. The concentrations measured in the final effluent samples ranged from 21.9 to 200.3 mg/L, with an average of 91.9 mg/L (Figure 4.23).

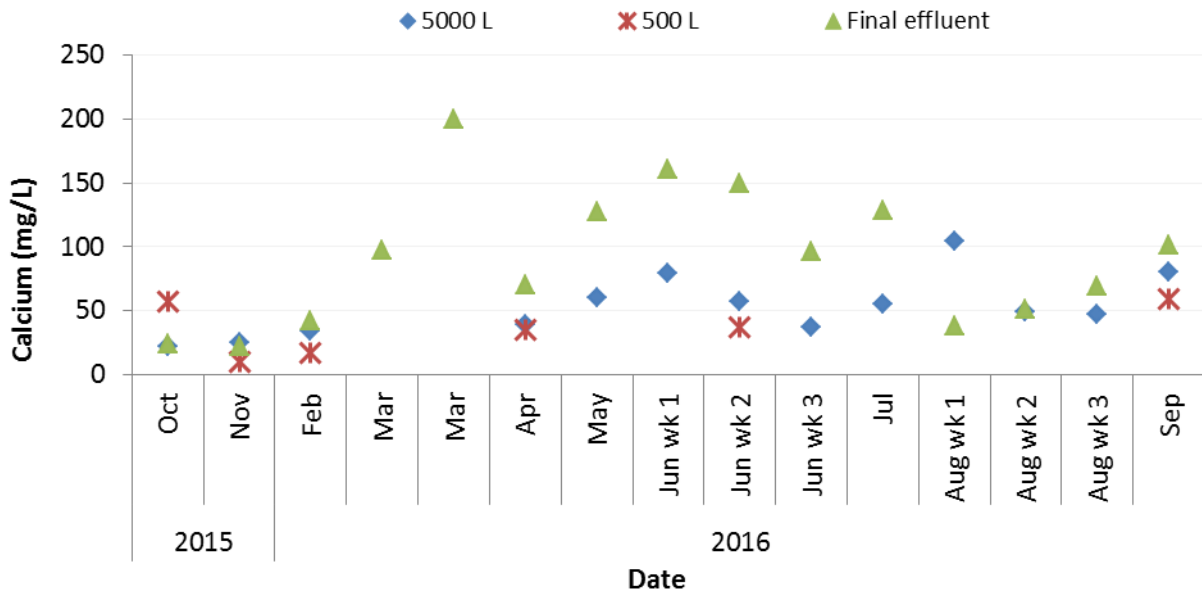


Figure 4.23 Concentrations of calcium measured in samples taken from the 5000 L holding tank, 500 L tank and final effluent from October 2015 to September 2016

The concentrations measured in the samples taken from the filter modules (Figure 4.24), ranged from 2.6 to 168.5 mg/L and exhibited an increasing trend. At the start of the sampling period, the concentrations ranged from 16.0 to 39.8 mg/L, while at the final sampling instance, concentrations ranged from 101.3 to 152.2 mg/L.

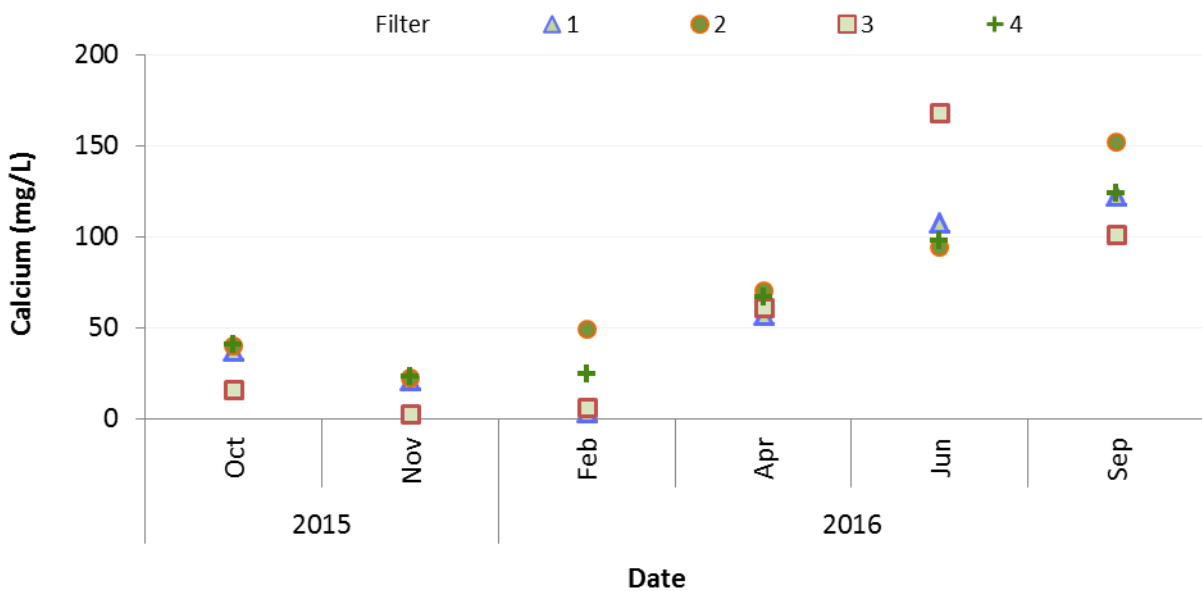


Figure 4.24 Concentrations of calcium measured in samples taken from the filter outlets 1, 2, 3 & 4 from October 2015 to September 2016

4.3.5.4 Magnesium

The concentrations of magnesium measured in samples from the 5000 L holding tank and 500 L tank ranged from 3.9 to 10.2 mg/L and 1.3 to 7.5 mg/L, with averages of 6.4 mg/L and 4.3 mg/L, respectively (Figure 4.25). The concentrations measured in the final effluent samples had an average concentration of 6.2 mg/L with a minimum of 2.6 mg/L and maximum of 10.1 mg/L (Figure 4.25).

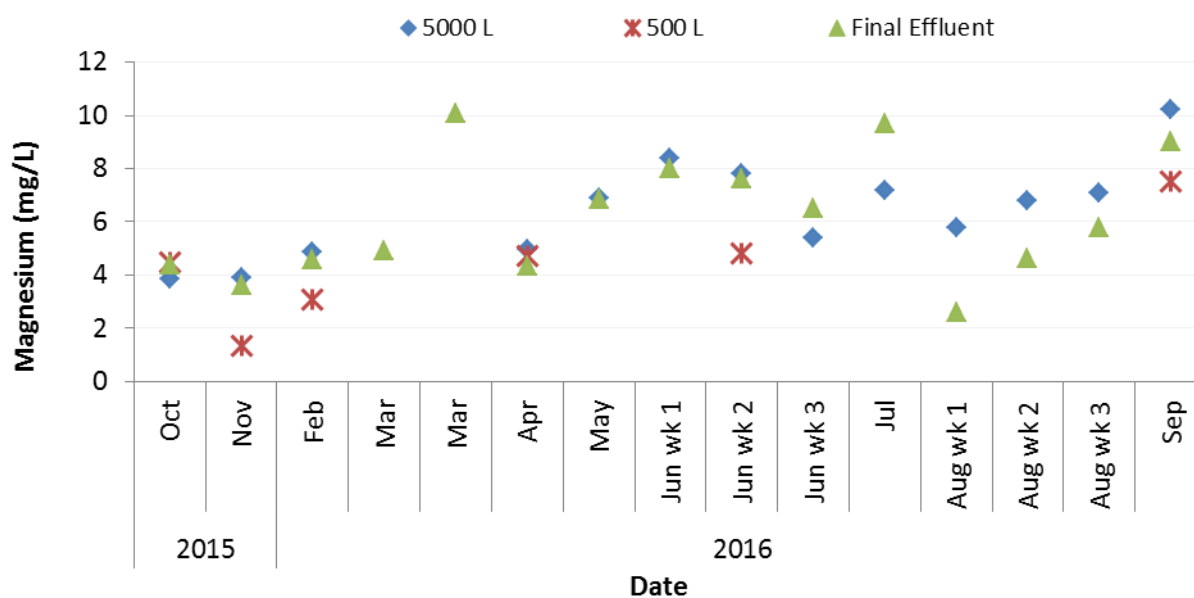


Figure 4.25 Concentrations of magnesium measured in samples taken from the 5000 L holding tank, 500 L tank and final effluent from October 2015 to September 2016

Concentrations of magnesium measured in samples taken from the filter modules were similar for Filters 1, 2 and 4, ranging from 2.9 to 10.7 mg/L and average of 5.2, 5.2 and 5.4 mg/L respectively. Although the range in samples taken from Filter 3 was similar (1.4 to 10.8 mg/L) and similar average of 4.7 mg/L, the trends observed were notably different. The average concentration measured in the samples from all the filter modules was 5.1 mg/L (Figure 4.26).

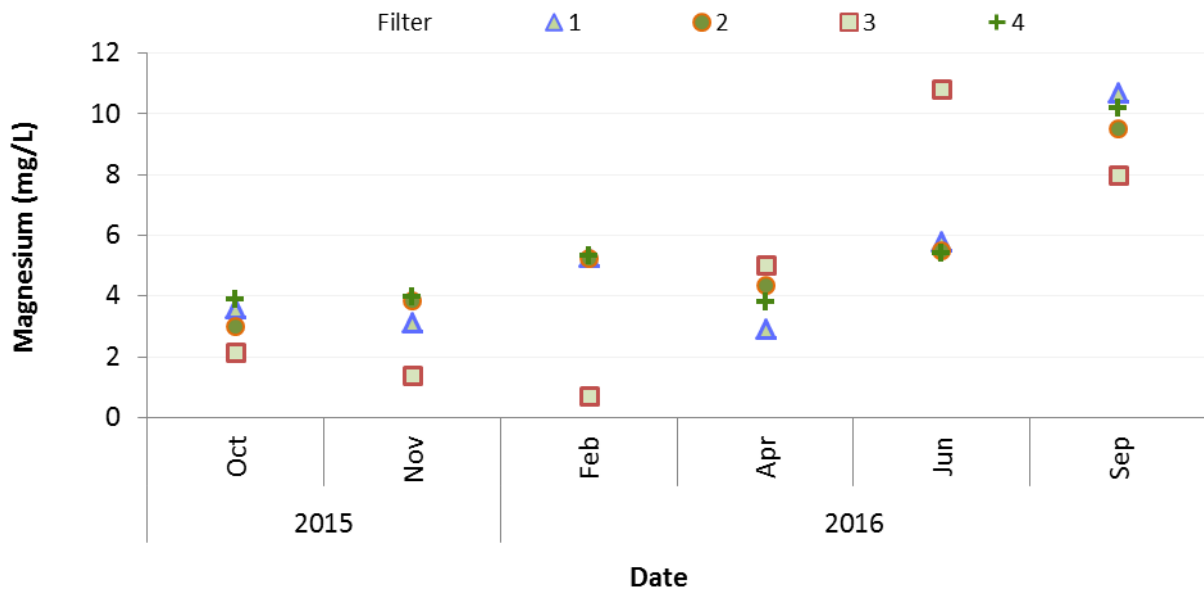


Figure 4.26 Concentrations of magnesium measured in samples taken from the filter outlets 1, 2, 3 & 4 from October 2015 to September 2016

4.3.5.5 Sodium adsorption ratio

The average calculated SAR for samples taken from the 5000 L and 500 L tanks was 1.4 and 1.1, with a range of 0.8 to 2.0 and 0.5 to 1.5, respectively (Figure 4.27). The average SAR calculated for final effluent samples was 0.9, with a range of 0.5 to 1.6 (Figure 4.27).

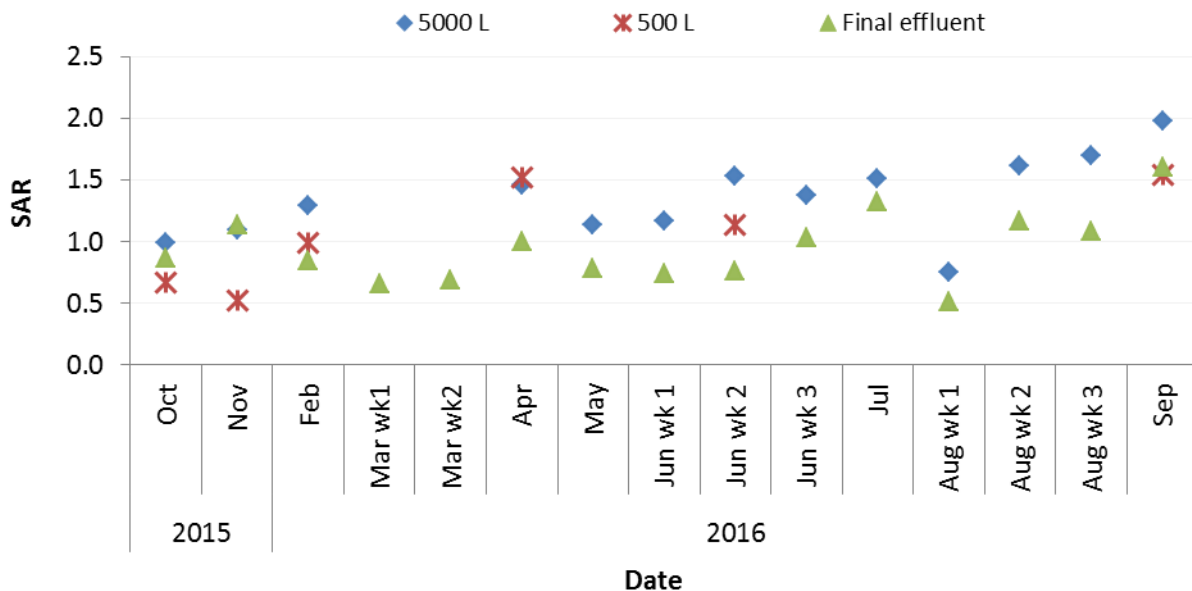


Figure 4.27 The sodium adsorption ratio calculated from samples taken from the 5000 L holding tank, 500 L tank and final effluent from October 2015 to September 2016

The average SAR for samples taken from the filter modules was 1.7 mg/L with minimum and maximum SAR of 0.4 to 10.7 (Figure 4.28). The average SAR from all samples from the filter outlets was 1.1, excluding two outliers of 5.3 and 10.7 from Filter 3.

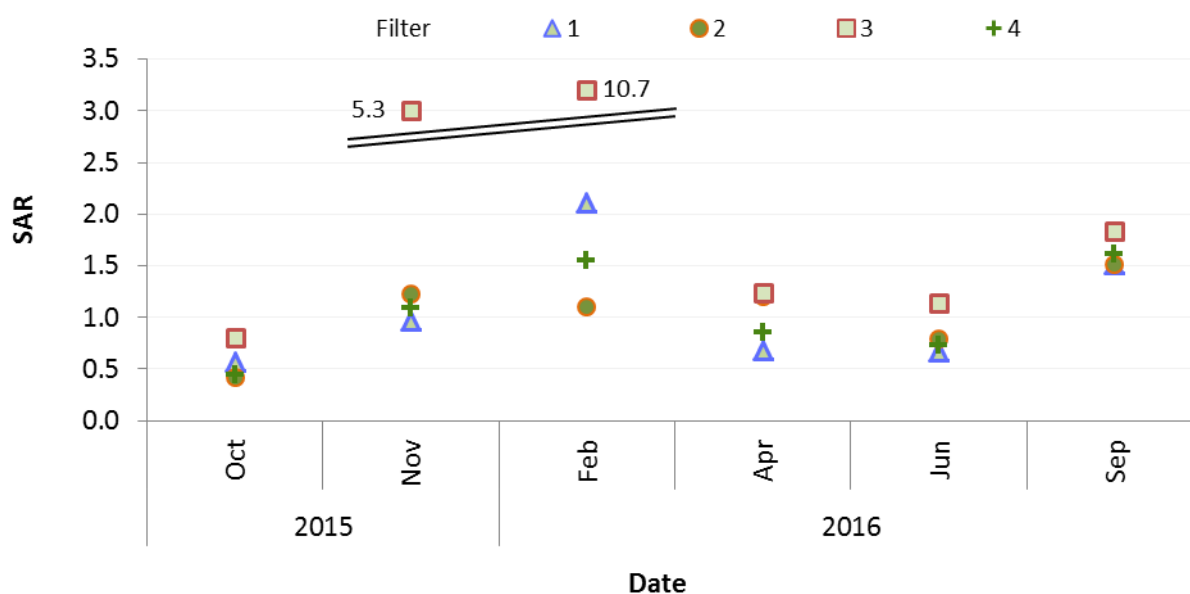


Figure 4.28 The sodium adsorption ratio calculated from samples taken from the filter outlets 1, 2, 3 & 4 from October 2015 to September 2016

4.3.5.6 Cation ratio of soil structural stability

The CROSS values calculated from samples taken from the 5000 L holding tank and 500 L tank had minimum and maximum of 1.9 to 8.7 and 1.3 to 4.6, and averages of 5.0 and 3.3, respectively (Figure 4.29). The CROSS values calculated from final effluent ranged from 1.3 to 8.6 with an average of 3.7 (Figure 4.29).

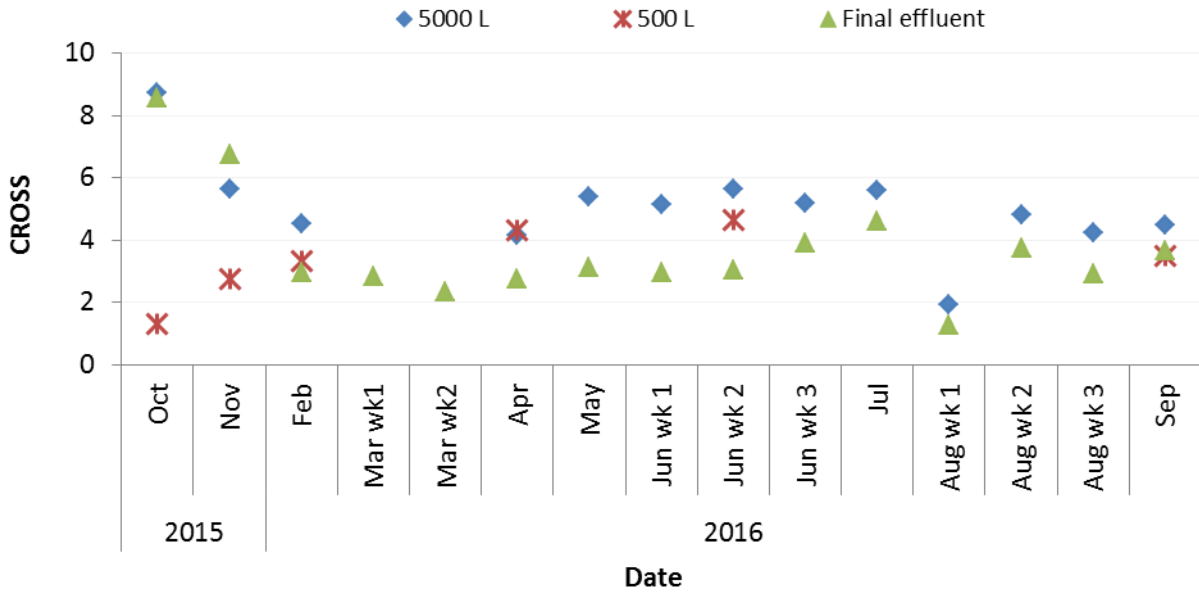


Figure 4.29 The cation ratio of soil structural stability calculated from samples taken from the 5000 L holding, tank 500 L tank and final effluent from October 2015 to September 2016

The CROSS value calculated from all samples taken from the filter modules had an average of 7.3, and 4.7 when two outliers of 36.6 and 36.4 from Filter 3 were removed (Figure 4.30).

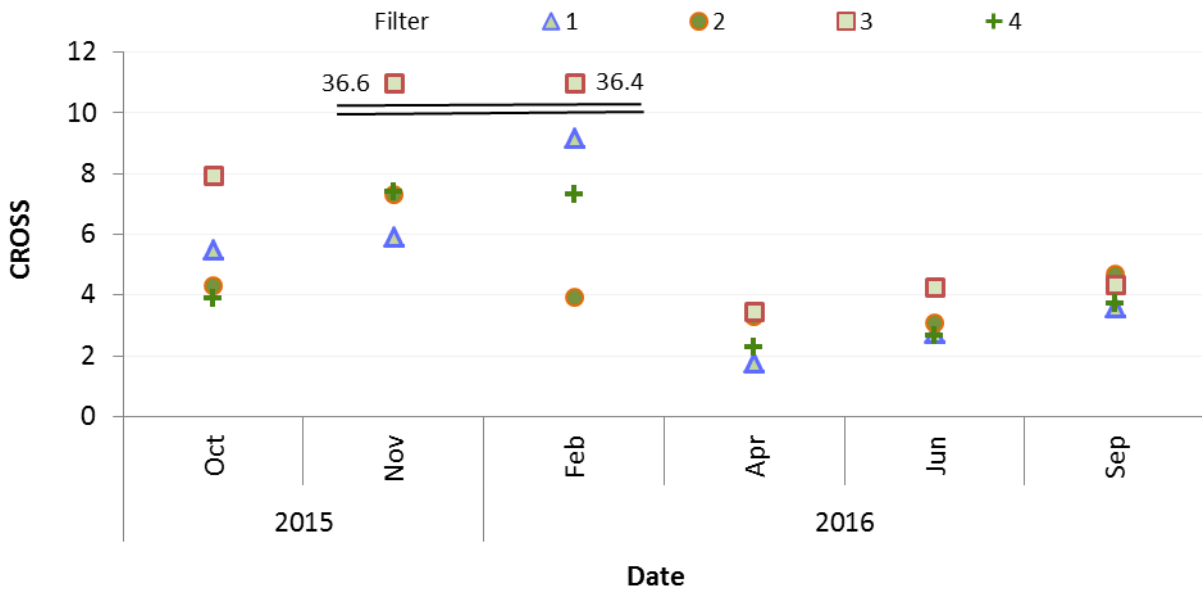


Figure 4.30 The cation ratio of soil structural stability calculated from samples taken the filter outlets 1, 2, 3 & 4 from October 2015 to September 2016

4.3.5.7 Potassium to sodium ratio

The K:Na ratio calculated from samples taken from the 5000 L and 500 L ranged from 1.0 to 8.8 and 1.0 to 4.6, with averages of 3.0 and 2.2, respectively (Figure 4.31). The average ratio calculated from final effluent samples was 3.1, with a range of 1.0 to 10.1 (Figure 4.31).

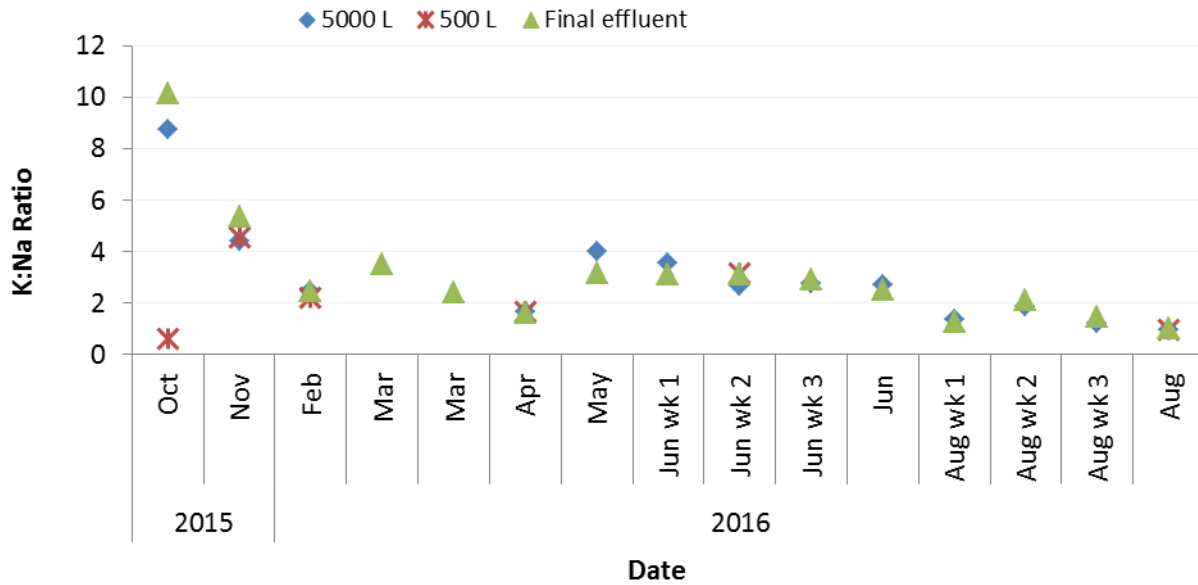


Figure 4.31 The Potassium to Sodium ratio calculated from samples taken from the 5000 L holding tank, 500 L tank and final effluent from October 2015 to September 2016

The ratio for samples taken from the 4 filter modules ranged from 1.1 to 10.8, with an average of 4.1 (Figure 4.32).

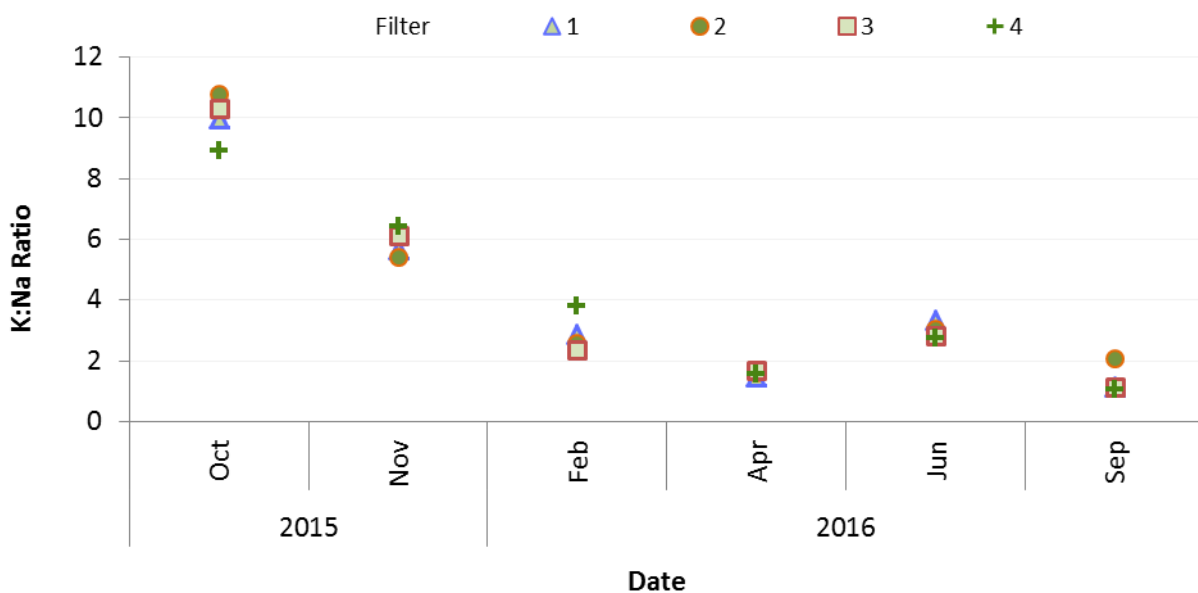


Figure 4.32 The Potassium to Sodium ratio calculated from samples taken from the filter outlets 1, 2, 3 & 4 from October 2015 to September 2016

4.3.5.8 Electrical conductivity

The EC measured in samples taken from 5000 L holding tank and 500 L tank ranged from 346 to 1062 $\mu\text{S}/\text{m}$ and 146 to 995 $\mu\text{S}/\text{m}$ respectively, with averages of 715 $\mu\text{S}/\text{m}$ and 576 $\mu\text{S}/\text{m}$, respectively (Figure 4.33). The EC measured in the final effluent samples had an average of 885 $\mu\text{S}/\text{m}$ with a minimum of 623 $\mu\text{S}/\text{m}$ and a maximum of 1429 $\mu\text{S}/\text{m}$ [Figure 4.33 (C)].

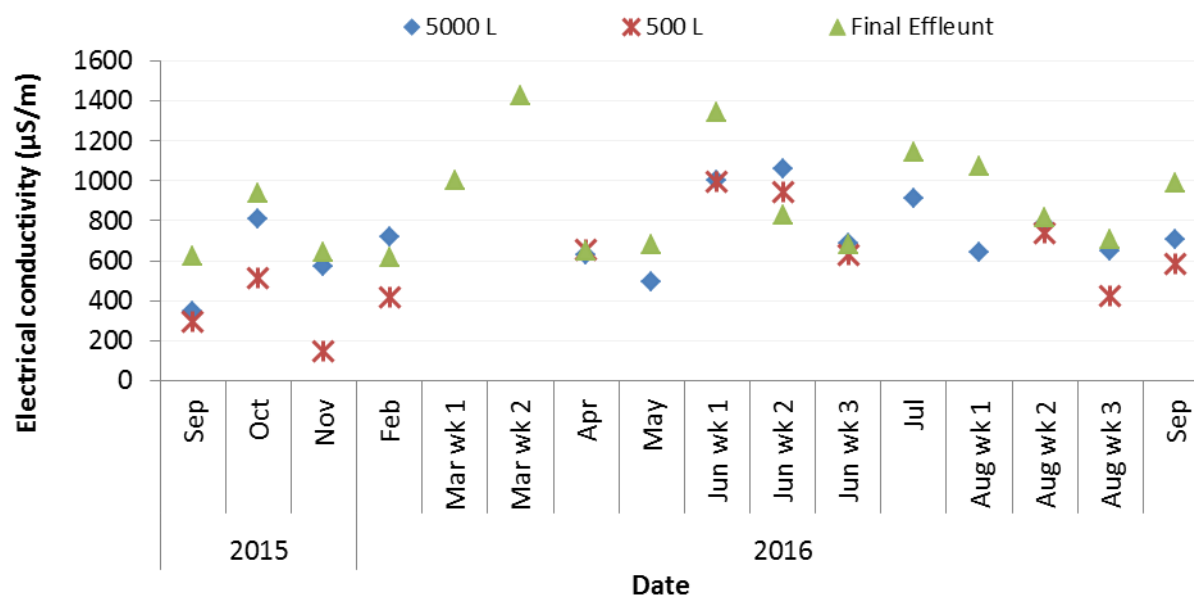


Figure 4.33 The electrical conductivity measured in samples taken from the 5000 L holding tank, 500 L tank and final effluent from October 2015 to September 2016

The EC measured in samples taken from the four filter modules had an average of 1029 $\mu\text{S}/\text{m}$. When the maximum value (4770 $\mu\text{S}/\text{m}$, obtained during the low flow period) was excluded, the average was 890 $\mu\text{S}/\text{m}$ (Figure 4.34).

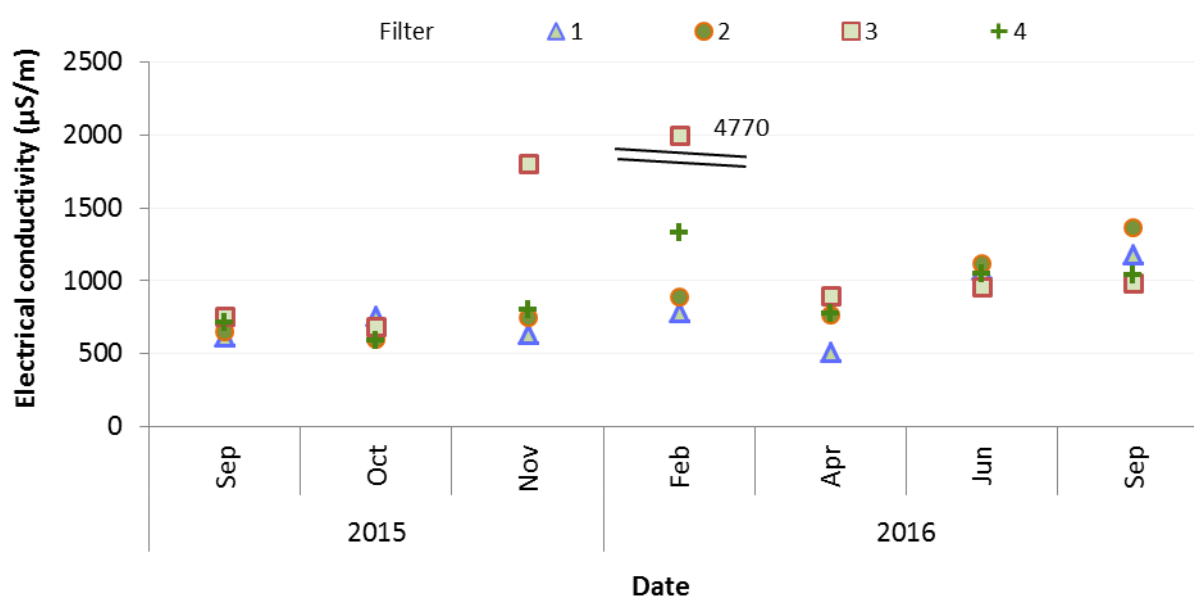


Figure 4.34 The electrical conductivity measured in samples taken from the filter outlets 1, 2, 3 & 4 from October 2015 to September 2016

4.3.6 Total solids

The concentration of total solids measured in the final effluent samples had an average of 908 mg/L with a range of 485 to 1520 mg/L, (Feb to September 2016). This can be seen in Figure 4.35.

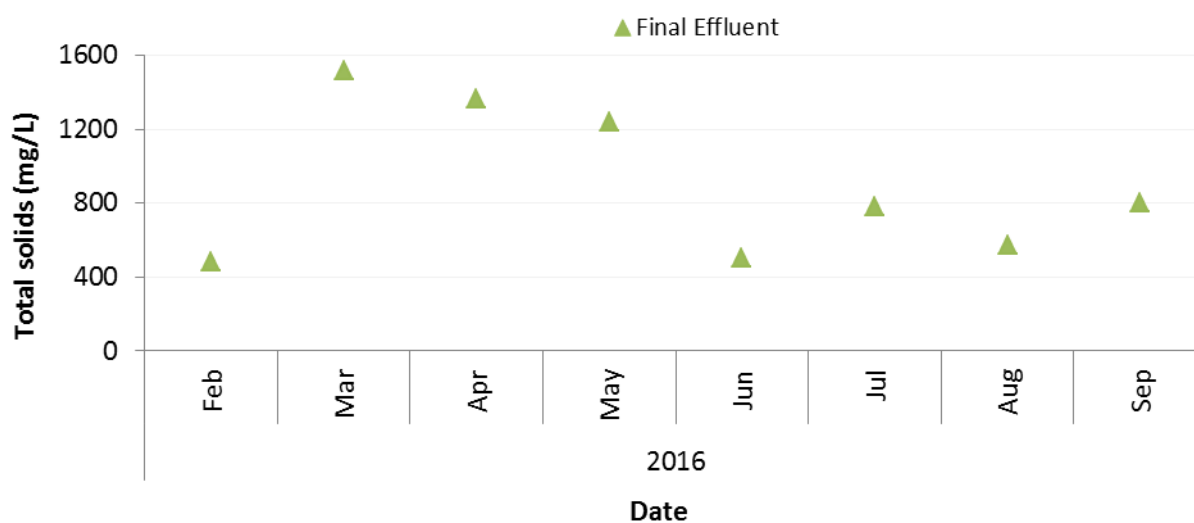


Figure 4.35 Total solids in sample from final effluent form BSF February to September 2016

4.3.7 pH

The pH measured in samples taken from the 5000 L holding tank and 500 L tanks ranged from 4.46 to 7.26 and 4.42 to 6.64, respectively (Figure 4.36). The pH measured in final effluent samples the sampling periods ranged from 6.63 to 8.14, with only two instances when the pH was below 7 ($n=21$) (Figure 4.36).

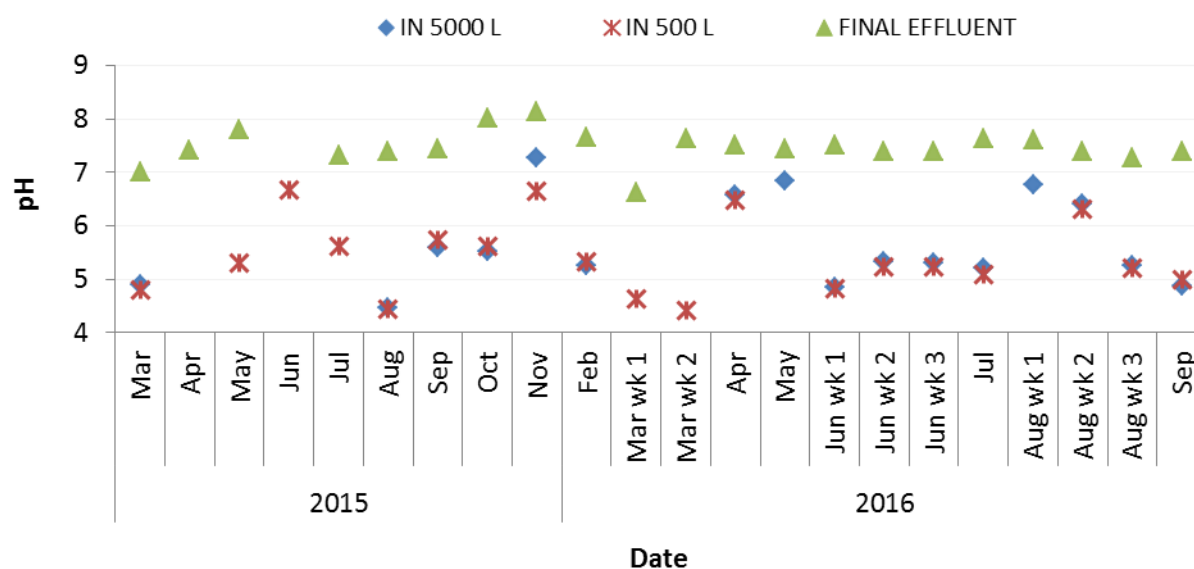


Figure 4.36 The pH measured in samples taken from the 5000 L holding tank, 500 L tank and final effluent from March 2015 to September 2016

Excluding outliers (pH 9.50 to 9.55) from Filter 3, the pH measured in samples taken from the filter modules during the sampling period ranged from 6.64 to 8.39 (Figure 4.37).

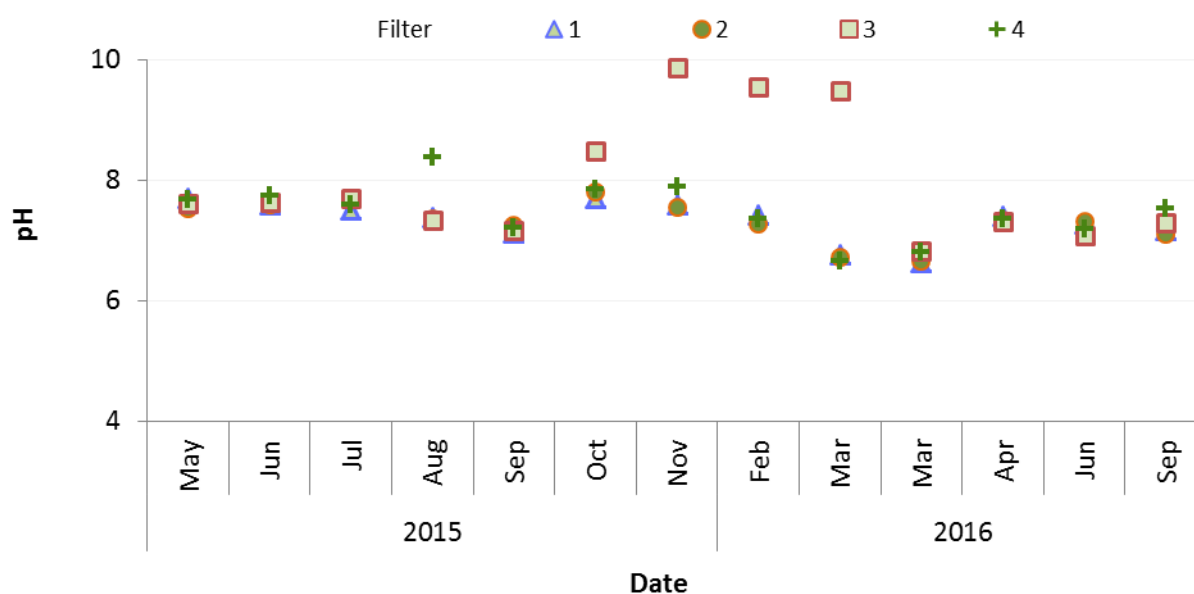


Figure 4.37 The pH measure in samples taken from filter outlets 1, 2, 3 & 4 from May 2015 to September 2016

4.4 Four hour batch test

The results given in Section 4.3 were used to determine the long-term treatment performance of the BSF system. However, by taking grab samples at a particular time point, inconsistencies can come into play because of the long HRT of the BSF system. Determinations of removal performance may be inaccurate when using concentrations measured in influent and effluent samples taken at similar times. To evaluate the effect of snapshot sampling, a batch test was performed on the 21st of August 2015, where samples were taken at hourly intervals over a 4 hour period and results compared. During the 4 hour batch test the flow rate was 398 L/day. The influent was defined as the inflow from the 5000 L tank, with the pump switched off for the duration of the study.

4.4.1 Chemical oxygen demand

There was an overall COD removal efficiency of 72% with an average influent COD concentration of 1263 mg/L. There was a 9% reduction in the COD concentration between the samples taken from influent and the 500 L tank (1149 mg/L). The samples taken from Filter 3 and 4 had the highest and lowest average COD concentrations of all the filters (711 mg/L and 139 mg/L, respectively). The average COD concentration in the final effluent (FE) samples was 360 mg/L and the average from the four filter modules was 413 mg/L, which was slightly higher. The COD concentrations remained consistent in samples taken from each site throughout the testing period (Figure 4.38).

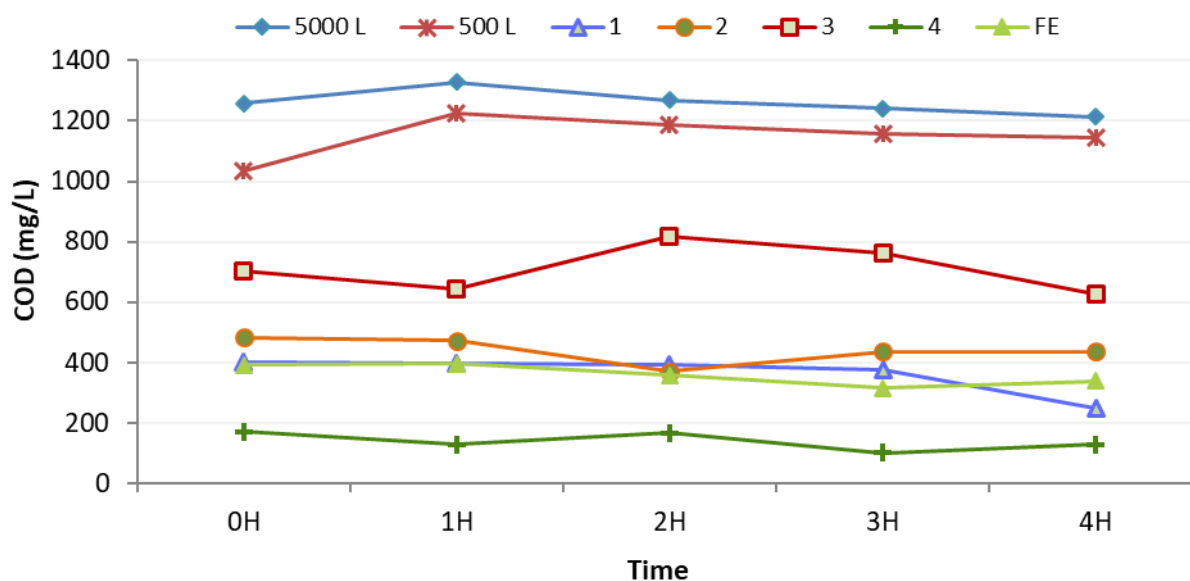


Figure 4.38 Chemical oxygen demand concentrations measured in samples taken from all outlets during a 4 hour batch test

4.4.2 Volatile Fatty Acids

Samples taken from Filter module 3 exhibited the highest average VFA concentration of 442 mgAAE/L, which increased over the testing period (Figure 4.39). This increase in VFA concentration over the testing period was seen at all the sampling locations other than in samples from Filter 1. The samples from Filter 4 exhibited the lowest VFA concentrations, with an average and minimum of 106 and 51 mgAAE/L, respectively. The concentration of VFAs in the samples from the final effluent had an average concentration of 240 mgAAE/L while the combined average from the samples from the filter outlets was 245 mgAAE/L. The samples taken from the 5000 L holding tank and 500 L tanks had average concentrations of 220 and 223 mgAAE/L, respectively.

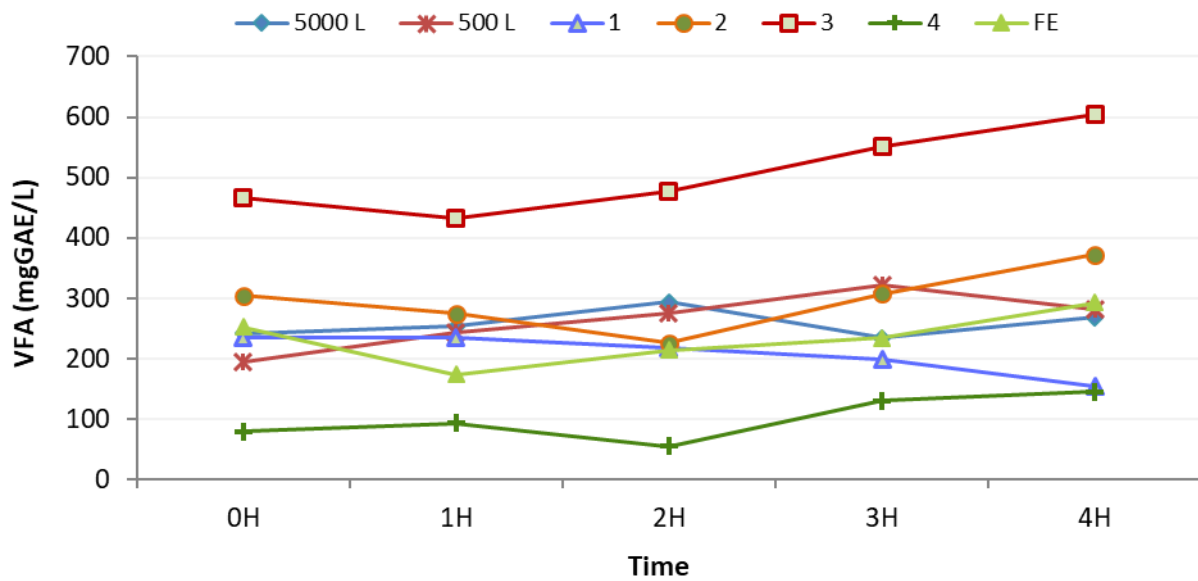


Figure 4.39 Volatile fatty acid concentrations in samples taken from all outlets during the 4 hour batch test

4.4.3 Total phenolics

There was a consistent concentration of total phenolics in samples taken from each site (Figure 4.3.9). There was an average removal efficiency of 75% from the 5000 L holding tank to the final effluent, and the average concentration of total phenolics in the final effluent was 4.7 mgGAE/L.

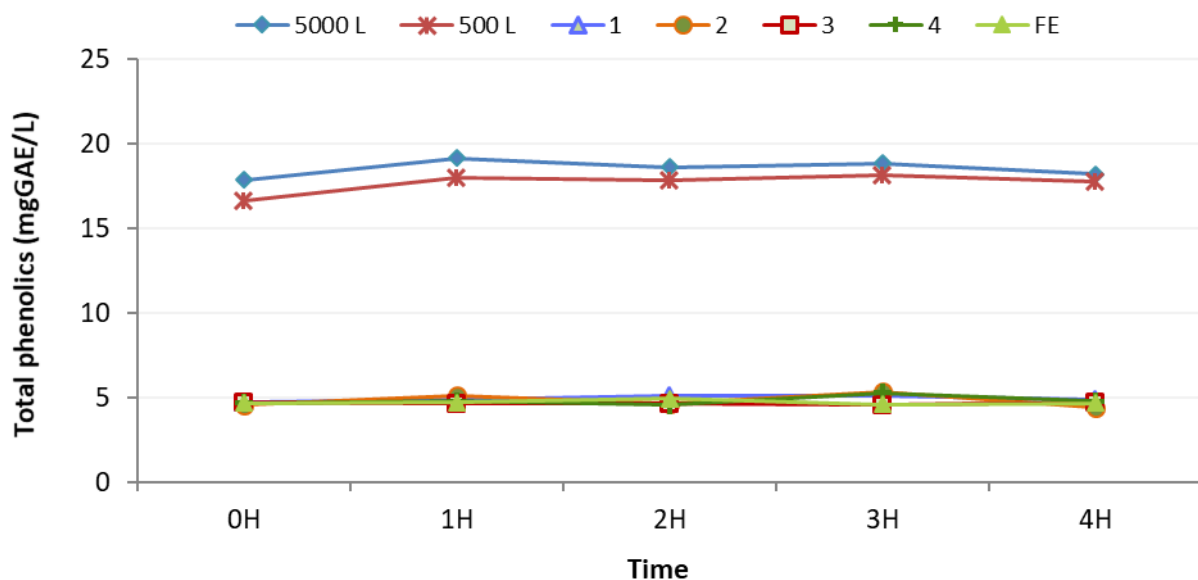


Figure 4.40 Total (poly) phenolics concentrations from samples taken from all outlets during the 4 hour batch test. Note: due to similarities in results, the results from final effluent and samples taken from the filter modules are superimposed on one another

4.4.4 Inorganic constituents

The inorganic constituents measured were sodium, potassium, calcium and magnesium, (Figure 4.41–Figure 4.44) which were also used to calculate the SAR, CROSS, ESP and K:Na ratio (Figure 4.45–Figure 4.47).

4.4.4.1 Sodium

The maximum average sodium concentration was determined in samples taken from Filter 3 (11.20 mg/L), which was higher than the influent from the 5000 L holding tank (9.86 mg/L) (Figure 4.41). The lowest average sodium concentration (7.61 mg/L) was determined in samples from Filter 4, while the concentration in the final effluent was 8.73 mg/L.

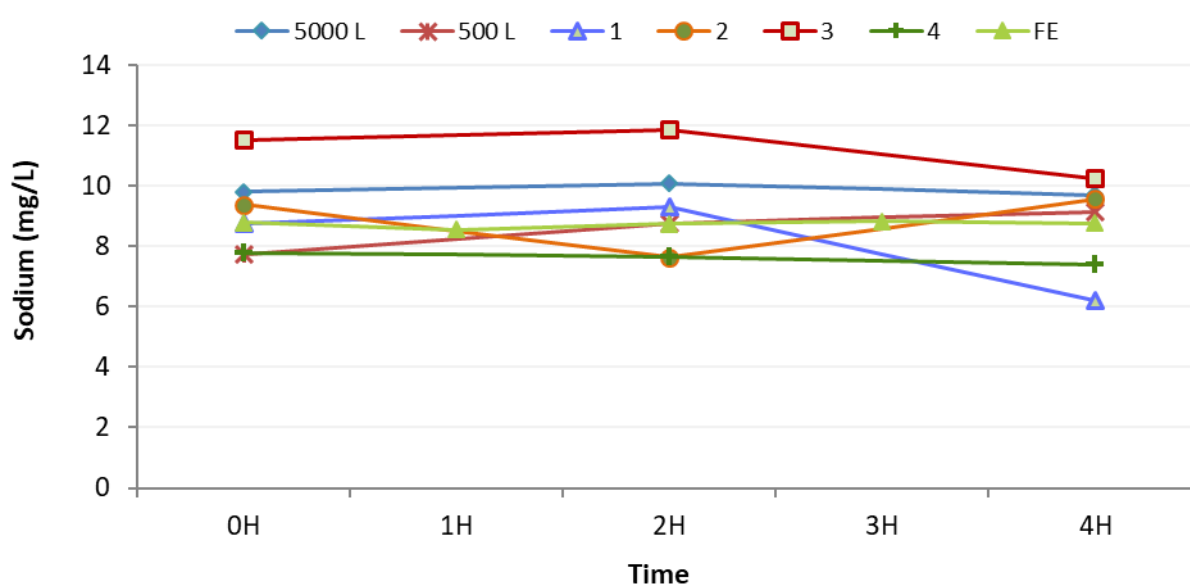


Figure 4.41 Sodium concentration in samples taken from all outlets during a 4 hour batch test

4.4.4.2 Potassium

Samples from the 5000 L holding tank and 500 L tank had substantially higher average concentrations (73.43 and 55.74 mg/L, respectively) than the other samples. The final effluent had an average concentration of 18.28 mg/L, which was a 75% reduction in potassium concentration across the system (Figure 4.42).

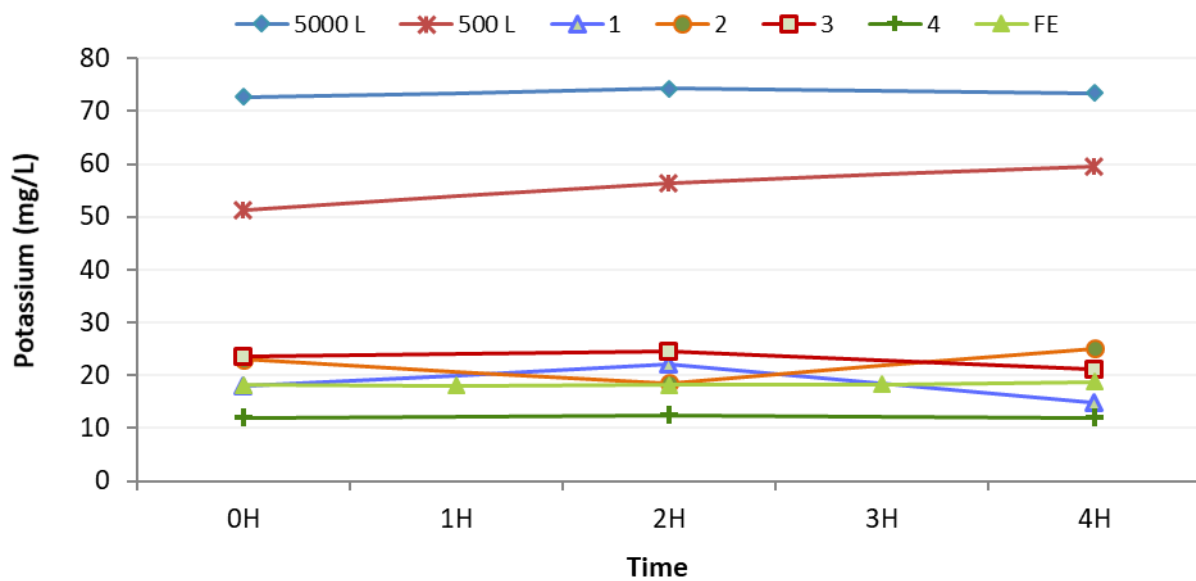


Figure 4.42 Potassium concentration in samples taken from all outlets during a 4 hour batch test

4.4.4.3 Calcium

The calcium concentrations measured in the samples taken from the filters and final effluent (range: 63.97 to 227.84 mg/L) were higher than those in the influent from the 5000 L (19.69 mg/L) and 500 L (19.50 mg/L) tanks, an increase 5 fold increase. Samples taken from Filter 3 exhibited the highest average concentration of 198.1 mg/L, while the samples from the final effluent had an average concentration of 120.39 mg/L which was slightly lower than the average for all four filters (133.25 mg/L) and Filter 4 had the lowest average (69.88 mg/L) (Figure 4.43).

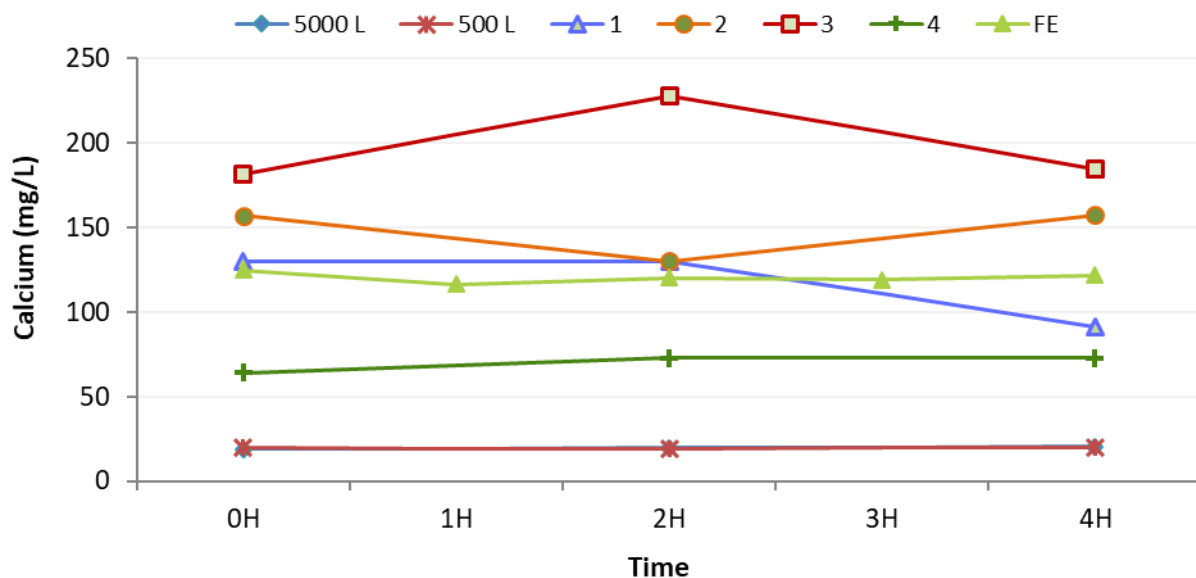


Figure 4.43 Calcium concentrations in samples taken from all outlets during a 4 hour batch test. Note: due to similarities in results, the results from final effluent and samples taken from the filter modules are superimposed on one another

4.4.4.4 Magnesium

The magnesium concentrations in the samples are shown in Figure 4.44. The concentration in the samples from the 5000 L holding tank and 500 L tank exhibited the lowest average concentrations of 1.84 and 1.63 mg/L, respectively. Samples taken from Filter 3 again had the highest concentration (7.53 mg/L) which was more than double that of the average of samples from the final effluent (2.84 mg/L). There was an increase in concentration of 55% across the system.

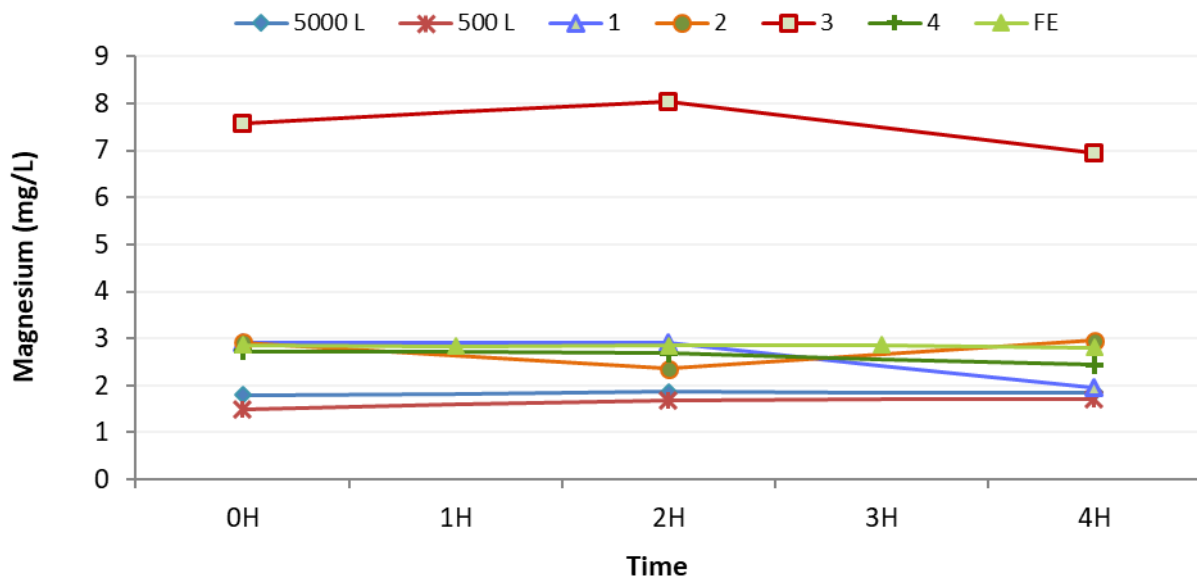


Figure 4.44 Magnesium concentrations in samples taken from all outlets during a 4 hour batch test

4.4.4.5 Sodium Adsorption Ratio

There was a 62% reduction in the SAR in samples from the 5000 L holding tank to the final effluent (average 0.57 to 0.22) (Figure 4.45). The average SAR in samples from the filters ranged from 0.20 to 0.24.

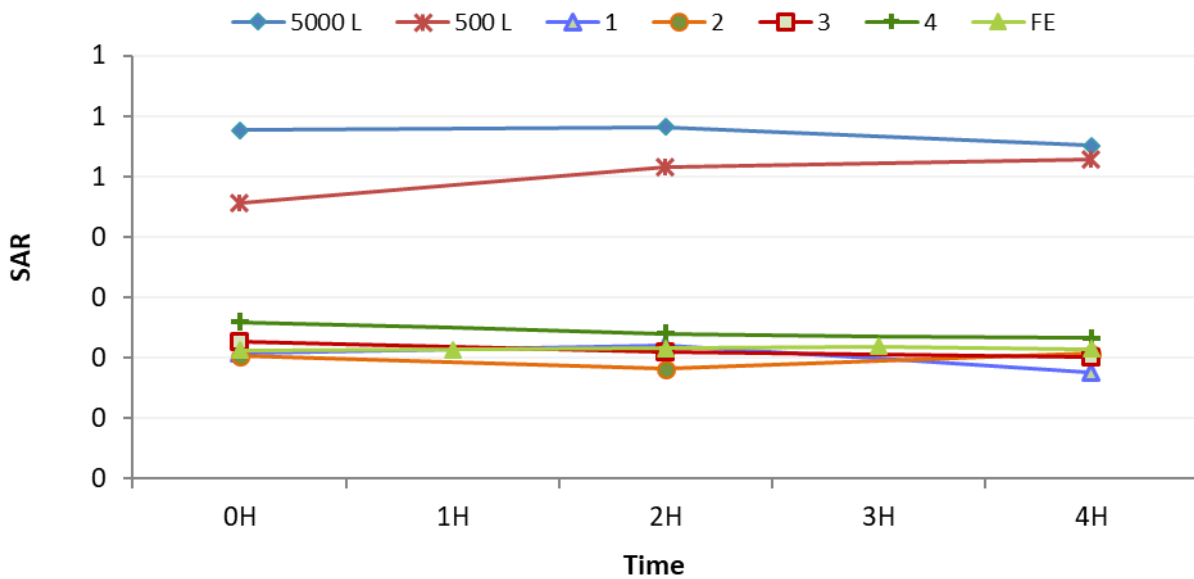


Figure 4.45 Sodium adsorption ratio calculated from samples taken from all outlets during a 4 hour batch test. Note: due to similarities in results, the results from final effluent and samples taken from the filter modules are superimposed on one another

4.4.4.6 Cation ratio of soil structural stability

There was a reduction of CROSS of 82% (Figure 4.46). The 5000 L holding tank had an average concentration of 2.86 which was reduced to 0.52 in the final effluent sample.

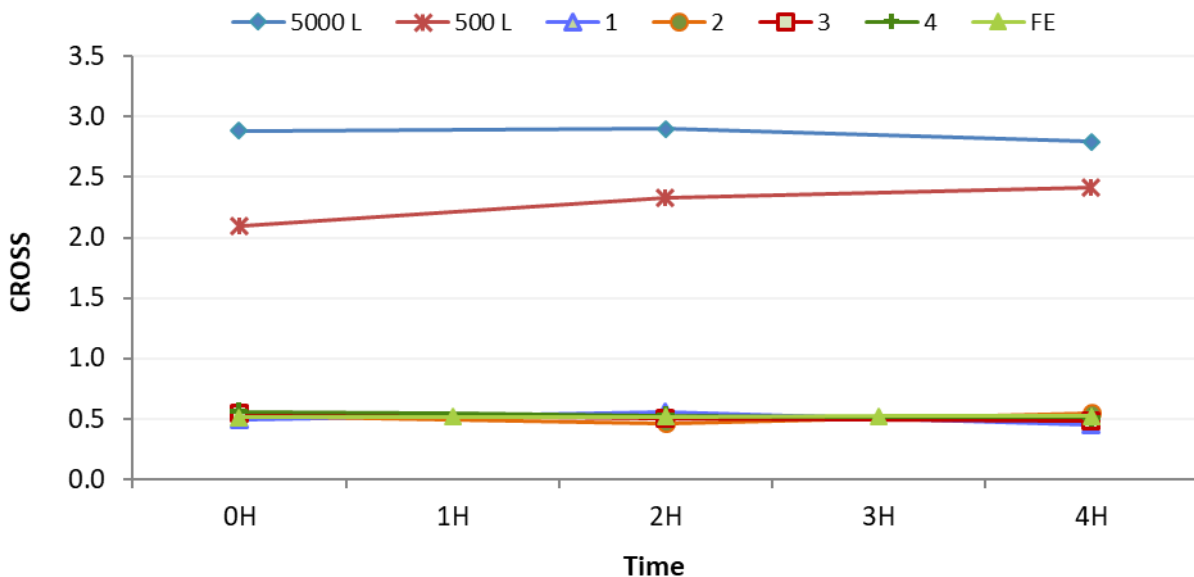


Figure 4.46 Cation ratio of soil structural stability calculated from samples taken from all outlets during a 4 hour batch test. Note: due to similarities in results, the results from final effluent and samples taken from the filter modules are superimposed on one another

4.4.4.7 Potassium to Sodium ratio

There was a 72% reduction K:Na ratio with an average final effluent ratio of 0.52 and an average ratio of 2.86 in the 5000 L tank (Figure 4.47).

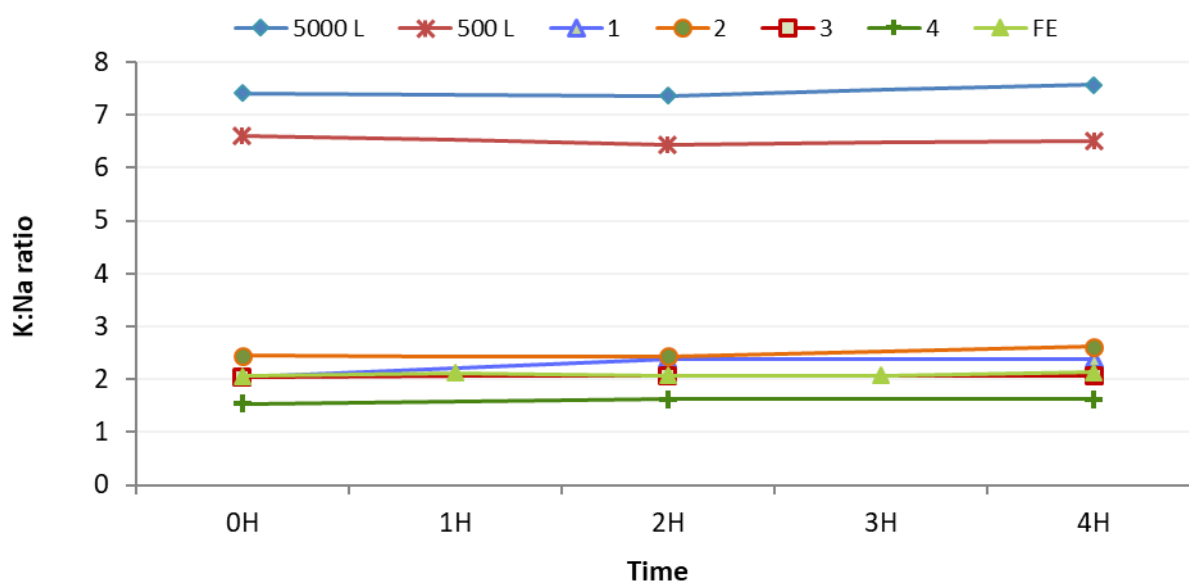


Figure 4.47 Potassium to Sodium ratio calculated from samples taken from all outlets during a 4 hour batch test. Note: due to similarities in results, the results from final effluent and samples taken from the filter modules are superimposed on one another

4.4.4.8 Electrical conductivity

There was a marked increase in the average EC between samples taken from the influent (5000 L tank and 500 L tank 495 and 389 $\mu\text{S}/\text{m}$, respectively) and the filter modules (1053 to 1070 $\mu\text{S}/\text{m}$). Samples taken from the final effluent had a lower average EC (953 μS) compared to samples taken from all the filter outlets (Figure 4.48).

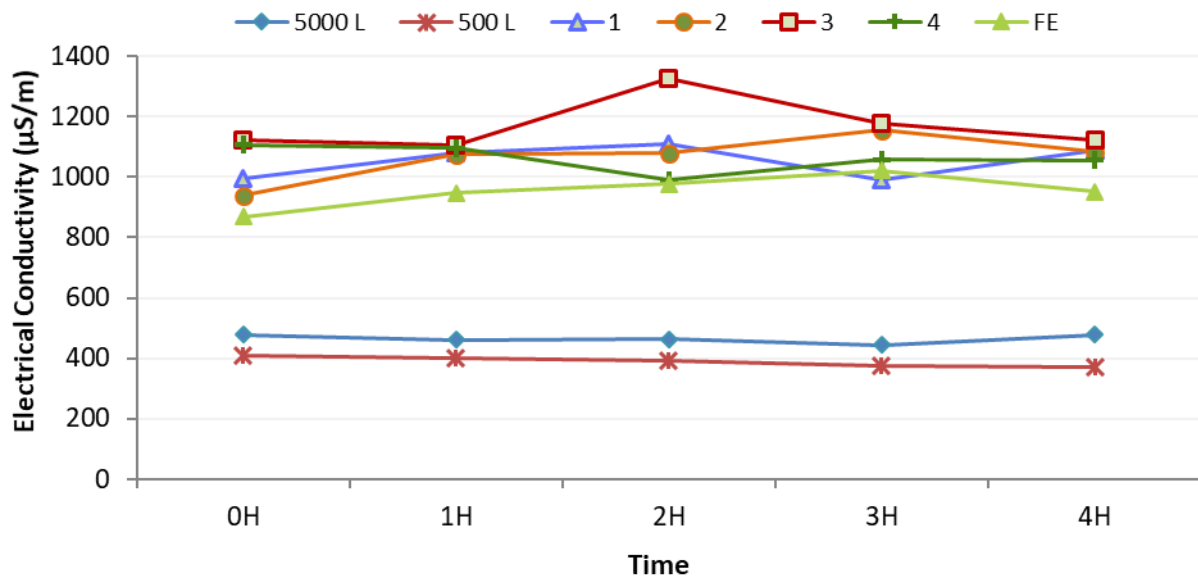


Figure 4.48 Electrical conductivity measured in samples taken from all outlets during a 4 hour batch test

4.4.5 pH

Figure 4.49 shows as the marked increase in pH of the acidic WWW, with the pH of the final effluent samples ranging from 7.36 to 7.57. The pH in the influent samples from the 5000 L holding tank and 500 L tank ranged from 4.19 to 4.71 and 4.25 to 4.40, respectively.

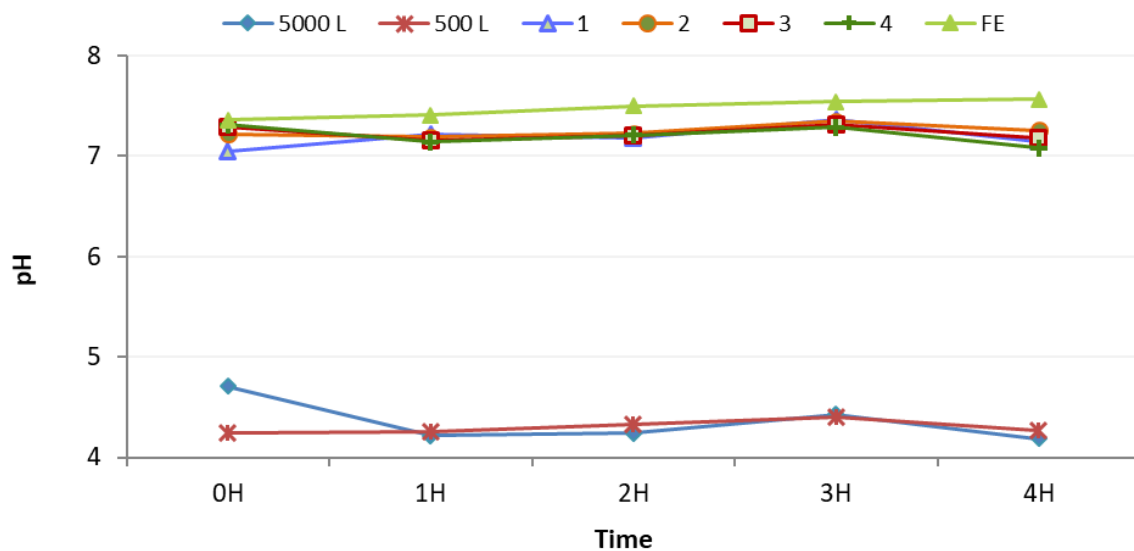


Figure 4.49 The pH measured in samples taken from all outlets of 4 hour batch test. Note: due to similarities in results, the results from final effluent and samples taken from the filter modules are superimposed on one another

4.5 Hydraulic analysis of the biological sand filtration system

4.5.1 Analysis of the flow rate of the system over the experimental period

The flow rates are shown in Figure 4.50. Two methods were initially used to determine flow rates. Firstly, the average monthly volumes of wastewater treated were calculated from the average flow rates (Q). From the data obtained over the entire 610 day study period (02/2015 to 09/2016), an average flow of (i) 636 L/day ($19.1 \text{ m}^3/\text{month}$) was calculated. When the outliers from the start-up period were removed, an average flow of (ii) $13.4 \text{ m}^3/\text{month}$ (441 L/day) was calculated. The flow rates measured during the acclimation period were statistical outliers, this can be seen in Section 5.2.5.

Secondly, from all the measured flow rates (Q), a trapezoidal calculation equation (4.2) was used to estimate the volume of WWT treated between two sampling times (T). When data obtained over the entire 610 day study period was inserted in Equation (4.2), it was estimated that (i) 640 L/day ($19.5 \text{ m}^3/\text{month}$) was treated. However, it was estimated that (ii) $12.8 \text{ m}^3/\text{month}$ (413 L/day) was treated after the acclimation period. This can also be written as $0.140 \text{ m}^3/\text{m}^3$ of sand. This method assumed a linear decrease or increase in flow rate between the two sampling points.

Both of the methods are flawed as they do not depict the actual achieved flow rates. As the exact flow rates between sampling incidences were unknown, the average for the period after acclimation using the trapezoidal method of measuring the flow rate was used (Q of 413 L/day) in all subsequent calculations.

$$\sum Vol_n = Q_{n-1}(T_{n-1}) + 0.5[(Q_n - Q_{n-1})(T_{n-1} - T_n)] \quad (4.2)$$

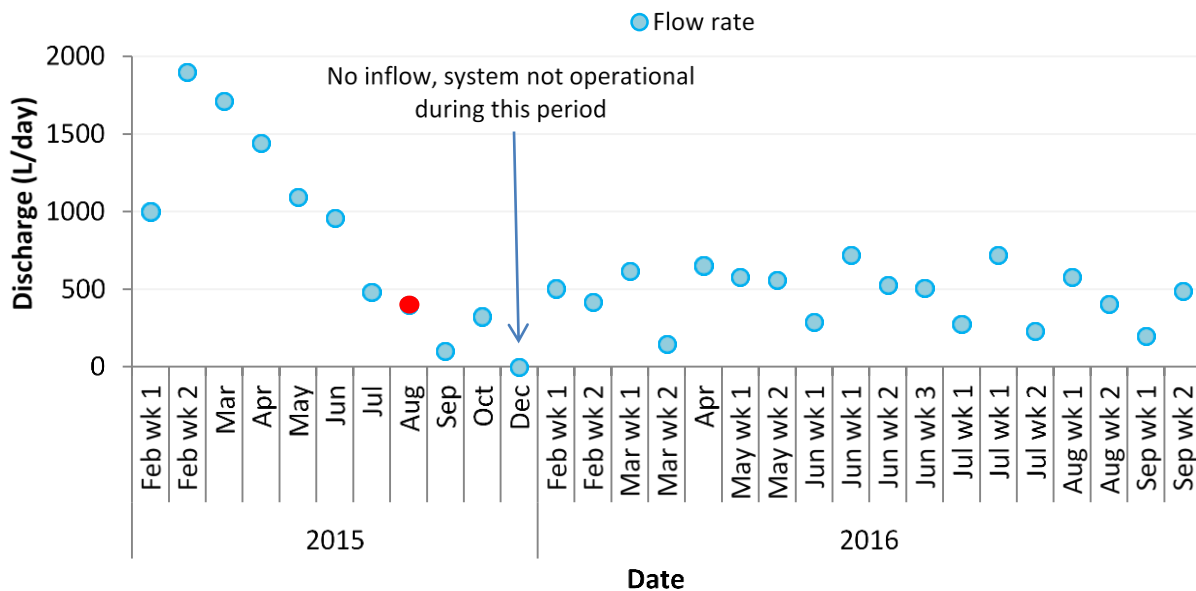


Figure 4.50 Biological sand filter system flow rate since start-up. The highlighted red marker indicates the flow rate that was measured during the 4 hour batch test.

4.5.2 Hydraulic retention times of biological sand filtration system

The HRT was calculated for the initial design for one filter module however the entire BSF system should be taken in to account as the 5000 L, 500 L and hydraulic control tanks contribute to treatment performance and retention times. The HRT was calculated using porosity values determined for Phillipi dune sand (Welz *et al.*, 2015), and therefore only reflect the HRT at start-up. The porosity decreases during operation due to the build-up of functional biomass and solids retention (Peszynska *et al.*, 2016). Peszynska *et al.*, (2016) further developed models in order to determine the growth of biofilm in porous substrate and the hydraulic properties, however the actual measurement of biomass within a treatment system is challenging to determine.

With the initial flow rate of 1900 L/day there was a HRT of 2.4 days for the entire system and 0.45 days for one filter. In comparison, using the average flow rate of 413 L/day (Section 4.5.1), the HRT was determined to be ± 11.2 days for the entire system. The HRT in the 5000 L, 500 L and 100 L outlet tank was respectively 7.4, 1.2 and 0.48 days with a HRT of 2.0 days in a filter module. The time between filling the 5000 L holding tank was 3.1 days between filling, with the average flow rate. The maximum HRT for the system was 23.4 days and 4.4 days in a filter module. The calculations for the average flow rate can be seen in Appendix H in Sections H. 1 and H. 2.

When the BSF was initially instilled the system had a HRT of 2.4 days and a HRT of 0.45 days within one filter module ($Q = 1900$ L/day). After the acclimation period and the decline of the flow rate (413 L/day) the HRT for the system was 11.2 days

4.6 Hydraulic loading rate and organic loading rate

In order to compare the BSF to other treatment systems on a large scale the HLR and OLR must be determined, sample calculations can be seen in Appendix K. The HLR can be calculated using the flow rate, for one filter module, divided by the volume of the filter [Equation (2.7)]. This is done using the cross-sectional area ($A = 0.438\text{m}^2$) multiplied by the length of the filter (1.68m) to calculate the volume. The BSF had an average HLR of 161 L/m^3 of sand day^{-1} from July 2015 to September 2016, after acclimation. There was a maximum HLR during this period of 222 L/m^3 of sand day^{-1} and a minimum of 67 L/m^3 of sand day^{-1} . The HLR can be seen in Figure 4.51. The HLR can also be written in terms of the cross-sectional area of the filter. Using this method an average HLR of 270 L/m^2 was calculated, with a range of 112 to 373 L/m^2 .

The OLR can be calculated by multiplying the HLR by the influent COD, Equation (2.10). The OLR was calculated from June 2015 to the end of sampling. As no samples were taken on the following times the average COD (1265 mg/L) for the 5000 L holding tank will be used; July, August 2015, March 2016. These values will only be used graphically, marked with a red data point, and will not be used for any further calculations. The calculation for the HLR and OLR can be seen in Appendix K for the 25th of August 2016 and follow the method outlined in section 2.7.2. The HLR are plotted against the OLR in Figure 4.51. The average OLR from July 2015 to September 2016 was 205 gCOD/m^3 of sand day^{-1} with minimum and maximum loading rate of 83 and 338 gCOD/m^3 of sand day^{-1} . This too can be rewritten in terms of cross-sectional area of the filter module as an average OLR of 344 gCOD/m^2 of sand day^{-1} with a range of 139 to 568 gCOD/m^2 of sand day^{-1} .

The organic removal rate (ORR) can be calculated using the HLR multiplied by the difference of COD across the system (2.11). This is used to quantify the mass of organics removed by a cubic meter of filtration media in a day. There was an average ORR of 164 gCOD/m³ of sand day⁻¹. The BSF pilot-scale system converted on average 483 gCOD/day.

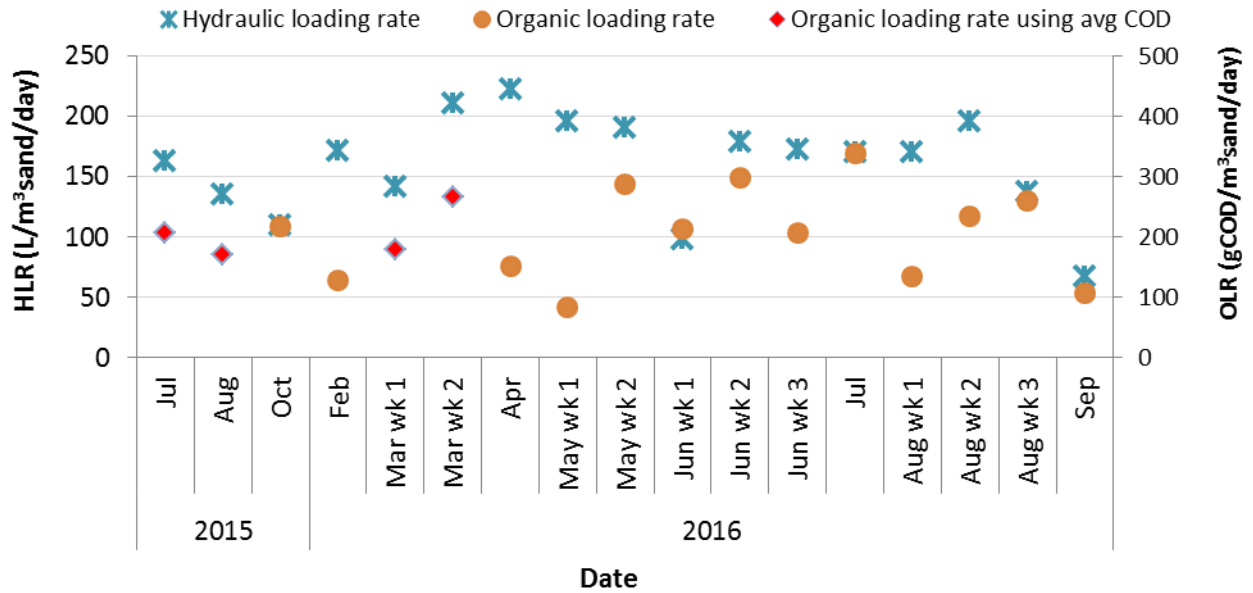


Figure 4.51 Comparisons of hydraulic loading rates and organic loading rate for BSF from July 2015 to September 2016

Chapter 5 Discussion

5.1 Treatment performance of the biological sand filtration system

In order to ascertain whether the BSF system is a viable option for the treatment of WWWW at small wineries, the removal efficiencies of a number of different parameters were determined. The wastewater from the 5000 L holding tank provided the most accurate representation of the influent to the filter modules, and was therefore defined as the 'influent' (see Section 5.1.1 for explanation). Similarly, the final effluent was defined as 'effluent', and the effluent from the outlets of the four filter modules (mean value) was defined as 'filter/s'. This terminology has been used throughout Chapter 5 for ease of interpretation.

5.1.1 Overall organic removal measured by chemical oxygen demand

The COD test is used as proxy for the concentration of organics in wastewater. It is the most widely used parameter employed to assess organic removal performance, and by legislative authorities to assess effluent quality in terms of organic load. In this study, the average COD for the effluent from the BSF system was 336 mg/L ($n=24$) with a range of 28 - 1382 mg/L, with a minimum removal efficiency of 44% and a maximum of 98% ($n=16$). The COD concentration of the influent ranged from 424 to 2185 mg/L ($n=16$). The performance tended to improve with operation time (Figure 5.1), which is promising. However, further research is required to determine whether this trend will continue long-term.

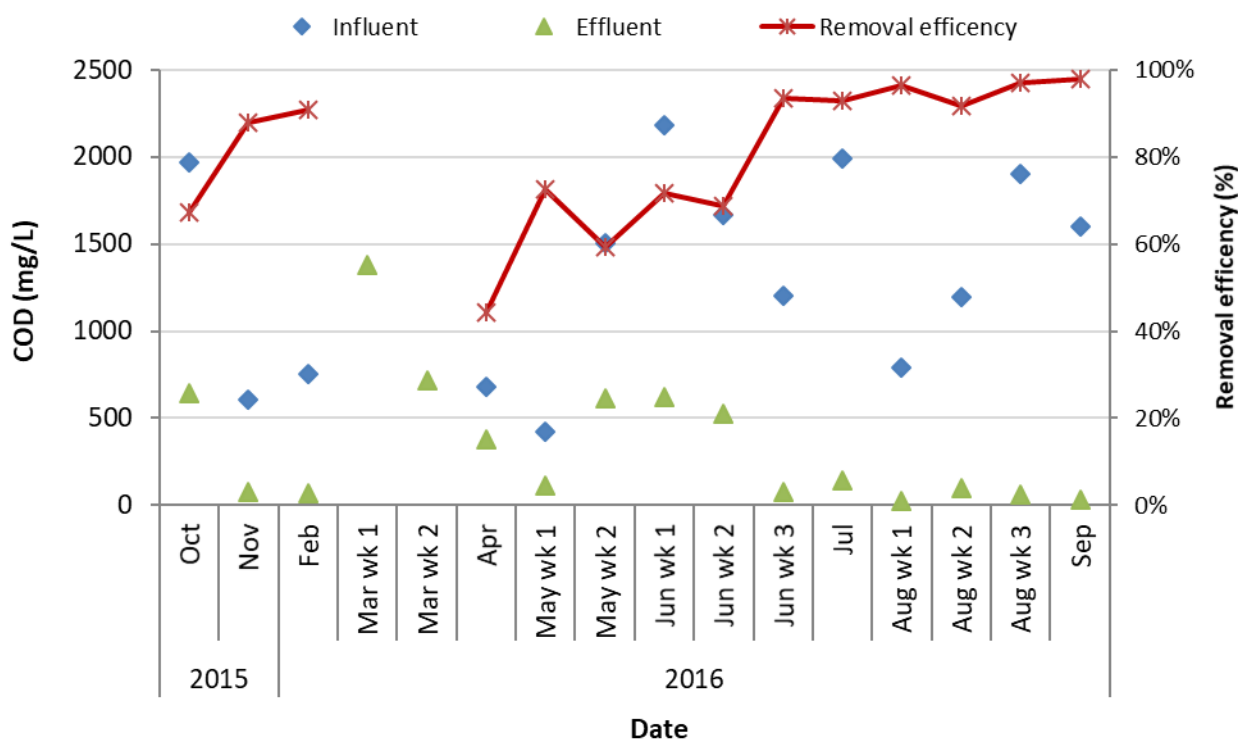


Figure 5.1 The chemical oxygen demand concentration measured in samples taken from the influent and effluent samples plotted against the removal efficiency

A removal efficiency of 74% was achieved during the 4 hour batch test, and constant degradation of COD was noted within the 5000 L holding and 500 L tanks (Figure 4.38). The COD measured in the 500 L tank was 9% less than that in the 5000 L tank during the batch test, and 22% for the testing period ($n=6$).

The effluent COD was compared to the average filter (Figure 5.2). There were instances when the COD in the effluent samples was below or above the minimum or maximum concentrations measured from the filter samples. The average difference was 106 mg/L COD (4.5 - 382 mg/L COD). It was hypothesised that this was due to degradation and accumulation of contaminants within the outlet pipe, as suggested by Ramond *et al.* (2013).

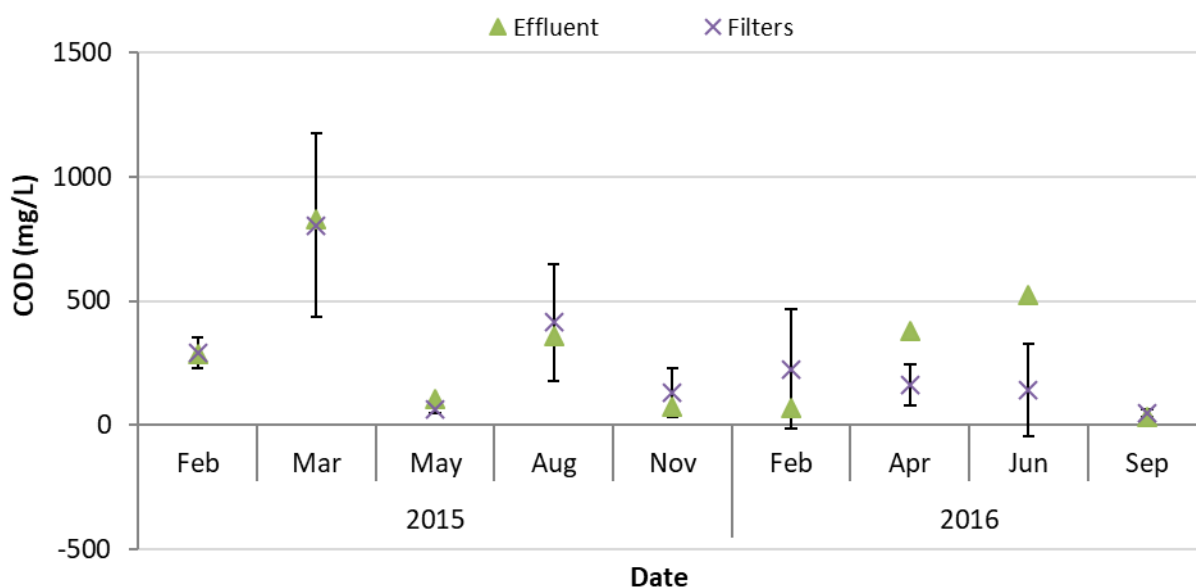


Figure 5.2 The chemical oxygen demand concentration of effluent and average of all four filter modules, including the 4 hour batch test results (August 2015), February 2015 to September 2016

There were large variances in the COD concentrations measured in samples from the settling basin and the influent, with no obvious trends been seen. The 5000 L tank was only filled intermittently (third day on average), while wastewater was continually added and extracted from the settling basin. In addition, the fill cycle in the 5000 L tank took place automatically when the level dropped to 67%, so that there was always residual WWW within the tank. The difference in COD concentrations between the settling basin and influent was not significant (paired 2-tailed t-test; $p>0.5$; $n=15$), but the correlation between the two was low (Pearson co-efficient 0.45). For more accurate interpretation of BSF performance (e.g. removal efficiencies), the WWW from the 5000 L tank was defined as the 'influent' in preference to the WWW from the settling tank (Section 5.1).

The COD concentration in the effluent was significantly lower than that in the influent (paired 2-tailed t-test; $p<0.01$; $n=24$). In this study, there was an 81% and 78% reduction in COD from the 5000 L ($n=16$) and 500 L tank ($n=6$). The removal efficiency for this system is comparable with other treatment systems reported in literature (Table 5.2).

Due to the long HRT within the system it was assumed that the influent was behaving as a rudimentary digester, accounting for the COD removal during the 4 hour batch test. Further analyses will be performed to verify this (e.g. gas analyses, redox measurements, more regular COD testing between fill

cycles). When employing grab sampling, as in this study, an accumulation of residual substrates and metabolites from previous waste streams may skew the removal efficiency calculations as described by Welz & le Roes-Hill (2014). In addition, there was a long HRT in the system, and the fluctuating composition of WWW fed to the 5000 L holding tank may have resulted in vastly different compensations between the sampled influent and effluent. To determine the short-term stability, a batch test was performed which showed minimal variation over the 4 hours.

WWW is a nutrient deficient WW which is often fed with nutrients to assist bioremediation (Artiga *et al.*, 2007; Andreottola *et al.*, 2005; Kalyuzhnyi *et al.*, 2001). For example, researchers have dosed the raw WWW with varying concentrations of nutrients to attain COD:N:P ratios of 502:5:1 (Da Ros *et al.*, 2016), 400:7:1 (Ganesh *et al.*, 2010) and 30-60:2:1 (GWRDC, 2011). No nutrients were added in this study and a COD:N:P ratio for the effluent was 272:1.3:1 ($n=11$). This shows that the BSF operated under nutrient deficient conditions and still maintained a high removal efficiency. It is recommended that further work should be performed on the effect of adding nutrients to the system.

5.1.2 Volatile fatty acids

The average concentration of VFA measured in samples from the influent and settling basin was 565 and 253 mgAAE/L, respectively. Although it appeared that there was an overall increase in the VFA concentration during residence of WWW in the 5000 L tank, there was no consistency in the VFA concentration trends between samples taken from the settling basin and the influent, possibly for reasons outlined in Section 5.1.1. The increase in VFAs in the holding tank could be linked with the notion that the tank acted as a digester. While VFAs are described as being readily biodegradable, acidogenic accumulation can occur when alternative electron acceptors such as oxygen and nitrates are unavailable; high concentrations of VFAs can inhibit sensitive microbial species such as methanogens (Lasko *et al.*, 1997). WWW typically has low concentrations of nitrates (Vymazal, 2009). For example, Welz *et al.* (2016) found that the total nitrogen concentration in the majority of WWW samples taken from 4 wineries over the course of one year were < 10 mg/L. In addition, the long residence time in the 5000 L tank would have led to oxygen depletion. Therefore it could be expected that VFAs would accumulate due to the lack of available electron acceptors.

The average concentration of VFAs in the effluent samples was 191 mgAAE/L, which is equivalent to 204 mg/L COD. This contributed to on average 54% ($n=22$) of the effluent COD. There were four instances where the organic fraction of the effluent mainly consisted of VFAs. There is a lack of knowledge regarding the biological formation and degradation of different substrates within biological WWW (Welz *et al.*, 2014). However, this study supports the results of Welz *et al.* (2011), Welz *et al.* (2014) and Welz & le Roes-Hill (2014) whom showed that VFAs were formed in BSFs from sugars, ethanol and phenolics.

The VFA concentration in samples taken from the filter modules was highest in Filter 3 in all but two occurrences (October, November 2015). This was attributed to that fact that surface pooling occurred, possibly increasing the redox status within the sand substrate. The VFA concentrations in the effluent and filters samples followed a very similar pattern, with the exception of April 2016, when a peak of 433 mgAAE/L was measured in the effluent (Figure 5.3).

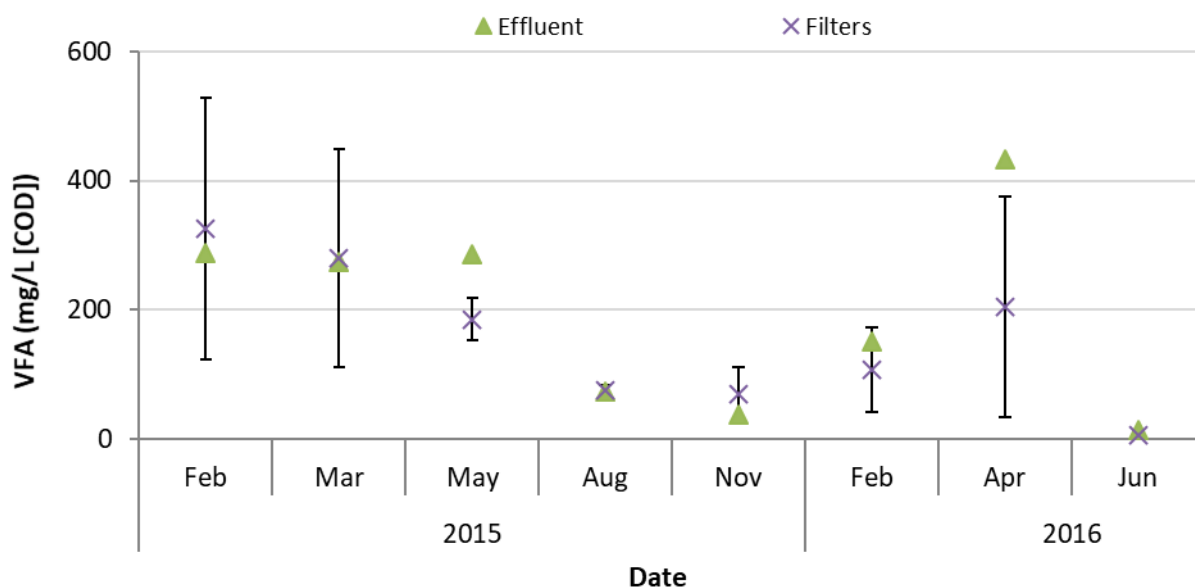


Figure 5.3 The volatile fatty acids represented in terms of chemical oxygen demand concentration of effluent and average of all four filter modules, including the 4 hour batch test results (August 2015), May 2015 to September 2016

When the concentrations of VFAs in the effluent samples were converted to COD terms, the average concentration was 139 mgCOD/L after the acclimation period (July 2015 to September 2016), with a maximum of 936 mg/L in March 2016. If the contribution of VFAs were then removed from the total COD values the average removal rate of non-VFA COD was 95% [67-100% (n=14)].

5.1.3 Total phenolics

The biodegradation of phenolic compounds occurs mainly under anaerobic conditions (Achak *et al.*, 2009). Degradation in olive mill WW has been attributed to bacteria and fungi (D'Annibale *et al.*, 2006; Pradhan and Ingle, 2007). Olive mill WW exhibits significantly higher phenolic concentrations than WWWW, and Achak *et al.* (2009) achieved between 87 and 97% reduction in phenolic content using diluted olive mill WW with an initial concentration of 4.59 g/L. When phenolic compounds are applied to a sand substrate they can be converted into phenolates (for example $C_6H_5O^-$), which can be retained by the cations within the sand to form, for example, iron and aluminium oxide, calcium carbonate and silicates (Achak *et al.*, 2009; Macheiz *et al.*, 1990). The interaction with metals result in the adsorption, adsorption and desorption of phenolics (Tharayil *et al.*, 2006). Oxidation of phenolics can also occur via chemical transformation coupled with iron and/or manganese reduction (Polubesova *et al.*, 2010), or via biodegradation. The sand used in this study mainly consists of silica ($84.59\% \pm 0.50$) and calcium carbonate (7.66 ± 0.03) with 12.7 ± 5.1 mg/kg iron, which could play an important role in chemical adsorption of phenolics. Welz *et al.* (2012) found that approximately half of the phenolics were removed by biodegradation and half via adsorption in acclimated sand microcosms.

Furthermore, the BSF system in this study showed a 67% (n=13) average reduction in the concentration of total phenolics (range 0 to 100%; Figure 5.4). It is possible that phenolics can accumulate in BSFs and leach out if saturated when the rate of biodegradation is exceeded (Achakl *et al.*, 2009; Mekki *et al.*, 2007; Welz *et al.*, 2012).

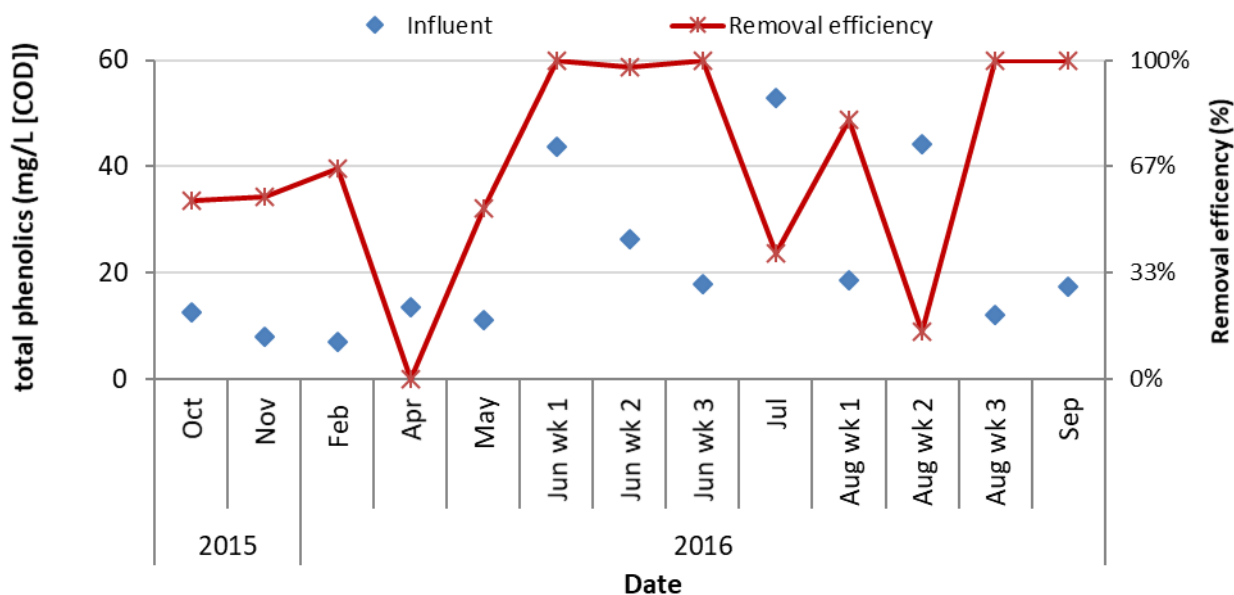


Figure 5.4 The total phenolics represented in terms of chemical oxygen demand concentration of the influent and removal efficiency across the system from October 2015 to September 2016

5.1.4 The neutralisation of acidic winery wastewater

As found in experimental BSF systems (Ramond *et al.*, 2013; Welz *et al.*, 2014; Welz & le Roes-Hill, 2014), the WWW was neutralised within the BSF system. The pH in the holding tank ranged from 4.46 to 7.26, while the pH of the effluent ranged from 6.63 – 8.14 (Figure 5.5). This can be attributed to both abiotic and biotic mechanisms, including dissolution of calcite (calcium carbonate mineral) and/or aluminosilicates from the sand (Millar *et al.*, 2010; Welz & le Roes-Hill, 2014). This is supported by the fact that a 26% increase in calcium concentration from holding tank to effluent was achieved. Neutralisation of synthetic WWW also took place in BSFs containing sand without aluminosilicates or carbonates, suggesting biotic mechanisms (Ramond *et al.*, 2013). Even the formation of VFAs in the system did not lead to an increase in the acidity of the effluent. There were 3 occurrences (highlighted by a red dash circle in Figure 5.5) where the pH values within the different filter outlets were highly variable. There was no flow through the system in December 2015 and January 2016, which may have contributed to the higher pH values in February and March 2016 due to concentration of dissolved calcite within the filters.

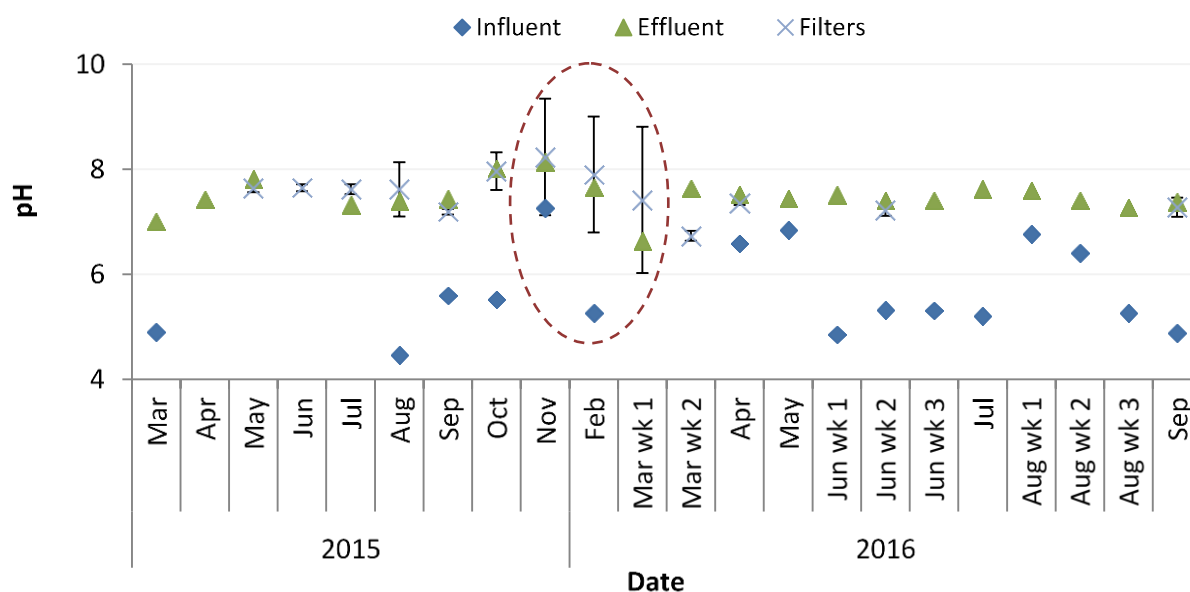


Figure 5.5 The pH of effluent and average of all four filter modules, including the four hour batch test results (August 2015), April 2015 to September 2016

5.1.5 Salts

Jesus *et al.* (2017) found that several physicochemical factors acted simultaneously to remove salts from CWs containing clay, and Ramond *et al.* (2013) found a build-up of sodium within the superficial outlet, but not the inlet of a lab scale BSF. This suggests that sodium, and possibly other inorganic constituents can build up within a BSF during treatment of WWT with high concentrations, and subsequently leach out at a later stage when the concentrations within the influent decrease thus showing an increasing and/or decreasing in concentrations across the filters from snap shot sampled taken at different sampling times. In this study, the temporal concentrations of sodium, potassium and magnesium in the influent and effluent samples were fairly consistent, showing that little to no removal took place.

In contrast, the calcium concentration showed on average 1.6 fold increase from average concentration of 50.6 mg/L (19.7-104.0 mg/L) to 93.7 mg/L (21.9-160.7 mg/L) from influent to effluent. This was attributed to the dissolution of calcite as discussed in Section 5.1.4.

The BSF system achieved an average decrease in SAR (29%) and CROSS (30%) from influent to effluent. This decrease in SAR and CROSS increased the safety of the water for irrigation. All the CROSS values in the effluent were below the limits suggested by Laurenson *et al.* (2012), which were given in Section 2.3.1.2. Although there was a perceived increasing trend in the concentration of sodium in samples taken from the 5000 L, 500 L and final effluent during the sampling period as seen in Figure 4.19, the decrease in SAR was consistent. There are many factors which could have affected this increase from the different cellar practices due to the new winemaker to different cellar activates at different times of the year to the increased scarcity of water. The K:Na ratio within the influent ranged from 1:1 to 8.8:1, with a maximum K concentration of 285 mg/L. The maximum concentration recorded within the effluent was 305 mg/L with a K:Na ratio ranging from 1:1 to 10.1:1. The K:Na ratio therefore sometimes exceed the ratio suggested by Christen *et al.* (2009) of 3:1, but was within the maximum limit of 1000 mg/L. Irrigation using water with high K concentrations can damage the soil structure and reduce

infiltration into soils (Marchuk & Rengasamy, 2010, Rengasamy & Marchuk, 2011). The results tie into the importance of measuring the CROSS, because the commonly used SAR does not take into account the concentration of K, which can also be detrimental to soil structure. Nevertheless, certain plants can uptake K and the crops K demand can be matched to the WW K concentration (Arienzo *et al.*, 2008a). Crops such as banana (*Musasapientum*) and lucerne (*Medicago sativa*) have a remarkable ability to accumulate potassium (Noy & Feinmesser, 1997). There was a noted increase in conductivity across the system which could be attributed to the dissolution of ions with varying electrical conductivity within the substrate which were not measured together with the increase in calcium, however further research must be done.

5.2 Volumetric performance

5.2.1 Volume of winery wastewater treated by the biological sand filtration system

The quantity of WWW generated was compared to the treatment capacity of the pilot system and other similar systems, and is discussed in detail in Section 5.2.4.

The set-up of the BSF system ensured that partial treatment of the WWW can result in improved quality because the effluent was returned to the settling basin, thereby creating a dilution effect. Serrano *et al.* (2011) showed that treated WWW fed to the inlet of a CW treating high strength WWW can successfully improve the negative effects of organic overloading. Using the black box method, Sheridan (2003) determined that a small winery crushing less than 100 tonnes of grapes generates an average of 900 L WWW/day over the course of one year. It was calculated that the pilot BSF system, with an average flow rate of 413 L/day could treat approximately half of this volume.

At the pilot site, the WWW was directly quantified from the volume of water used, and no losses were accounted for. Using this method, an average of 2728 L WWW/day was generated, so that about 17% of the total volume of WWW was theoretically treated. However, there were months with lower and higher water usage/WWW generation, so the treatment capacity varied from month to month (Table 5.1).

Table 5.1 The monthly water used by the cellar converted directly to wastewater consumption and the percentage treated by the biological sand filter system at a flow rate of 413 L/day

Month	July	Aug	Sept	Oct	Nov	Dec	Jan	Feb	Mar	Apr	May	June	Avg.
WW m ³ /month	224	59	41	33	69	31	50	101	162	42	70	100	82
WW L/day	7467	1967	1367	1100	2300	1033	1667	3367	5400	1400	2333	3333	2455
% treated by BSF	6%	21%	30%	38%	18%	40%	25%	12%	8%	30%	18%	12%	17%

5.2.2 The hydraulic retention time

The theoretical HRT calculated using the method discussed in Section 2.7.1 for a single BSF module was 0.32 days, which is relatively short (refer to Appendix A Section A. 3 for calculation). Due to the accumulation of functional biomass within the filter media, a 78% reduction in the system flow rate occurred after start-up. As biological growth occurs within a substrate the following physical properties can change (i) permeability, (ii) porosity, and (iii) mass transport parameters (Peszynska *et al.*, 2016). The change in porosity could not be determined, so using the initial porosity and the average system flow rate after start-up ($Q = 413$ L/day) to calculate the HRT of a single BSF module after start-up was 2.1 days (refer to Appendix H Section H. 1 for calculation)

From on-site observations, it was found that the entire filter modules were not saturated, and the HRT was adjusted accordingly. Small diameter pipes were inserted into the sand medium, and trial holes were dug in order to determine the functional water levels. The saturated zones were then estimated (Figure 5.6). A straight line from the height of the WW at the inlet to that at the outlet using a trapezium long section (or mid-point of long section) was used to determine the volume. The volume of sand within the one percent fall was added to the total functional (saturated) volume of the substrate. The adjusted total volume of functional sand in the filter reduced from 0.736 m³ to 0.617 m³ and the HRT reduced from 2.1 days (50.1 hours) to 1.8 days (42.0 hours) with a flow of 413 L/day. It is acknowledged that the functional saturated zones are in a state of flux. This was not taken into consideration when determining the HRT.

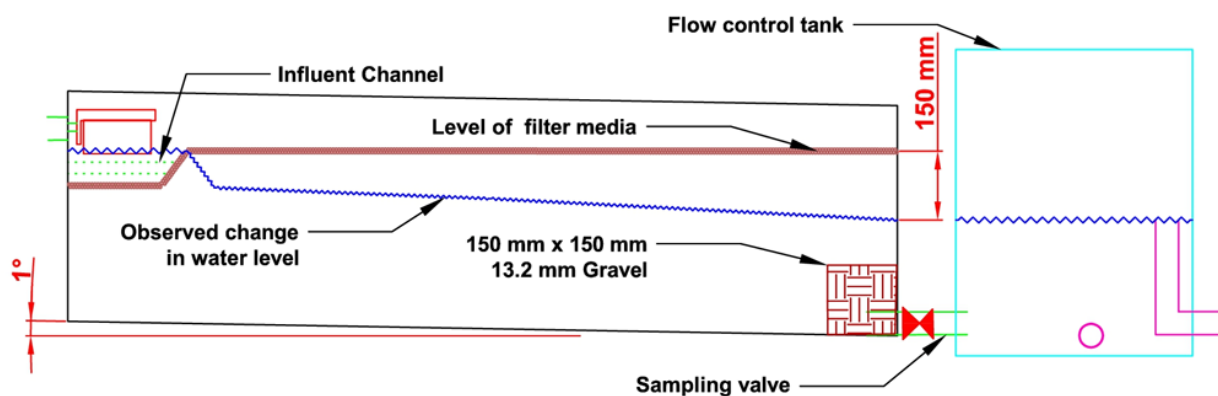


Figure 5.6 A schematic of a long section of the water levels obtained in a biological sand filter module, and related infrastructure

The HRT of 2.1 days for one filter module, achieved after start-up, was significantly shorter than the HRT of other biological systems used to treat WW, including single BSF modules containing river sand (Welz *et al.*, 2011). Yet, the HRT of the entire pilot system, which included the 5000 L holding tank, 500 L balancing tank, filter modules and outlet structure was ± 11.2 days and was comparable to other systems (Table 5.2). For example, a full-scale HSSF CW operated with a HRT of 7 days achieved a COD removal efficiency of 60% (influent COD 2000-12000 mg/L) (Mulidzi, 2010). In laboratory-scale studies using BSFs filled with river (Malmesbury) sand to treat synthetic and authentic WW, COD removal efficiencies of 97.8-99.8% were achieved with a HRT of 22 days (Ramond *et al.*, 2013; Welz *et al.*, 2012). Welz *et al.* (2015) reported 76% reduction in COD with a theoretical HRT of 13 days (± 1 day) in a lab scale BSF using dune (Phillipi) sand, the same type of sand used in this study. In a batch operated anaerobic lagoon, Montalvo *et al.* (2010) achieved a 91% removal efficiency with influent CODs of 8700 and 18700 mg/L and respective HRTs of 30 and 54 days.

5.2.3 The hydraulic conductivity and flow rates

The flow rates achieved during the start-up (acclimation period) gradually decreased and then stabilised for the rest of the study period. Importantly, the filters never clogged completely and continued to function throughout the study period.

A decrease in K in CWs has been attributed to several factors namely: solids entrapment, biofilm clogging, vegetation contribution (in planted wetlands), chemical effects, and clogged matter composition (Knowles *et al.*, 2011). In planted systems, decomposition and humification of the plant matter can clog the pores with organic material, especially at the surface (Siegrist & Boyle, 1987; Varma & Buscot, 2005). Organic material from the WW and plants (in planted systems) serve as a microbial growth substrate, and the amount of microbial biomass/biofilm increases (Varma & Buscot, 2005; Zhao *et al.*, 2017). The microbial biofilm attached to the sand particles reduces the pore size and can also lead to surface sealing, especially at the inlet (Siegrist & Boyle, 1987; Tufenkji, 2007 Metcalf and Eddy, 2004). Liu *et al.* (2003) found a higher amount of biomass accumulation on coarse sand compared to fine sand, based on unit surface area. Large quantities of biomass can plug the interstitial pores and the K can tend towards the K of the biomass itself (Wallace and Knight, 2006). Although the biomass contributes to clogging, the microbial population that is acclimated to a particular WW is the most important functional component for organic biodegradation (Juwarkar *et al.*, 2009; Semple *et al.*, 2007; Welz *et al.*, 2011; Welz *et al.*, 2012).

The K for the Phillipi dune sand used in this study was determined by the constant head method using vertical flow columns (Appendix A) (I Smith, unpublished). The initial K was determined, and thereafter the columns were fed with synthetic WW which resulted in the formation of biomass and the subsequent reduction in K of 51% from 0.286 to 0.140 mm/s after 3 months (Appendix A.1). However, vertical K is not always comparable with horizontal K , but this is dependent on the type of substrate and the packing of the material (Cartwright & Hensel, 1995; Ritzema, 1994).

Darcy's equation (Section 3.4.2), was used to determine the theoretical horizontal K in the BSF system (refer to Appendix I for calculations). At start-up, the system flow rate was 1900 L/day and the calculated K was 0.199 mm/s. After 4 months, the theoretical K reduced by 42% to 0.115 mm/s with a flow rate of 1094 L/day. The theoretical K values obtained were less than those determined experimentally by the constant head method, but the 42% reduction due to clogging was less. After 4 months, the flow rate/ K continued to drop, with an average of flow rate of 413 L/day recorded between July 2015 and September 2016, which translated into a theoretical K or 0.044 mm/s, which is a 78% reduction. The lowest recorded flow rate was 144 L/day, which was converted to a theoretical K of 0.015 mm/s.

An integration method was used to determine the most favourable height of the outlet to achieve the optimal discharge rate (Using method described in Section 3.4.2, calculations can be seen in Appendix J and Table J.1). With a K value of 0.044 mm/s, an outlet height of 223 mm and a fall of 197 mm theoretically gives a flow of 110 L/day.filter⁻¹. From the observations of the change in water level shown in Figure 5.6, approximately 23% of the volume of sand was unused due to the design of the system. This excludes the loss of treatment due to potential preferential flow patterns within the filter module. The fall across the filter which was chosen for this study was 150 mm. Comparing this to the calculated optimum fall across the system of 197 mm showed a theoretical difference of 0.005 m³/dayfilter⁻¹ which

is only a 5% difference in flow rate. This additional flow should be weighed against the difference in theoretical volume of sand within the BSF being occupied by WW. The lower the outlet, the less sand is in contact with WW, which effectively translates to a reduction in the theoretical HRT. Manipulating the outlet height could have an adverse effect on the WW treatment performance, and further research should be performed to optimise the outlet height.

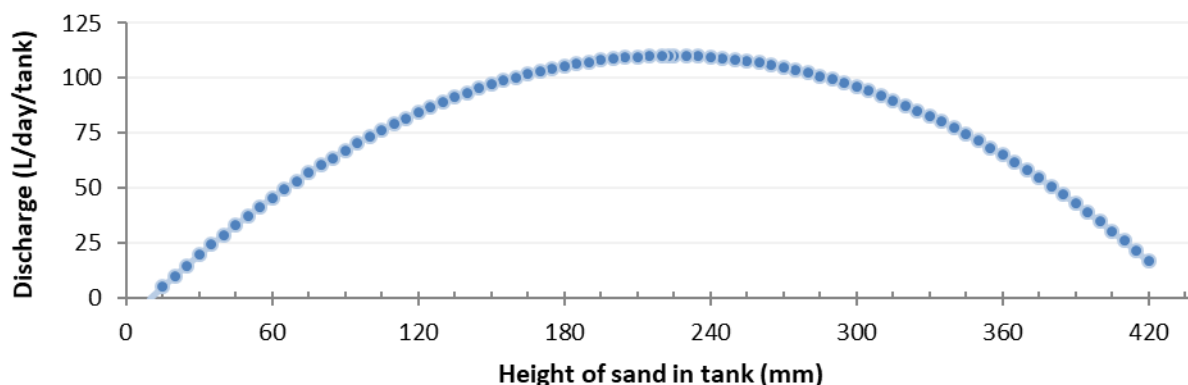


Figure 5.7 The effect of height of sand in the discharge within a biological sand filter using a hydraulic conductivity of 0.044mm/s

Caselles-Osorio and Garcia (2006) reported a 36% reduction in the relative inlet K compared to the outlet K due to biofilm clogging in a HSSF CW fed with WW containing glucose. It was further reported that the relative outlet K was the same within in a duplicate CW fed with starch. The duplicate CW had an accumulation of starch. Nevertheless, the inlet and outlet relative K was the same. It was assumed that the readily biodegradable nature of glucose could have caused the growth of additional biomass. It was concluded that different WW can result in different biomass formation rates.

Mace and Amrhein (1999) showed that synthetic drain water applied to soil reduced the K of the soil. This was largely reversible with the application of surface gypsum when the SAR was 1-8, but irreversible plugging occurred due to clay dispersion and internal swelling when the SAR was 5-8. This suggests that sodium in the WW could contribute to the reduction in K in BSF systems, but further research is required to verify this.

A mitigating option and operational possibility for the reduction of clogging within a HSSF CW is intermittent operation, which has the ability to reverse clogging (Nguyen, 2001) and the ability to mineralize sludge or clogged material on surface layers and restore the infiltration rate to subsurface layers (Batchelor & Loot 2007; Knowles *et al.*, 2011). Achak *et al.* (2009) showed that resting a sand filter dosed with olive mill WW for 3 days resulted in regeneration of the K and both Achak *et al.* (2009) and McKinley *et al.* (2011) hypothesised that the hydraulic and organic loading rates could be adjusted to reduce the effects of clogging. In spite of this, the biomass is seen as a positive within the system as the functional microbial communities which are acclimated to the particular WW are seen as functional microbial groupings which have the ability to treat WW by means of biodegradation (Juwarkar *et al.*, 2009; Semple *et al.*, 2007; Welz *et al.*, 2011; Welz *et al.*, 2012). Further research to determine the best operational parameters, such as mode of operation, to manage biomass accumulation is recommended.

5.2.4 Organic and hydraulic loading rates

Two of the parameters used to determine and compare the treatment performance are the HLR and OLR. These parameters can be used to show the quantity and strength of organics applied to the system and subsequent removal of organics in terms of ORR. In literature, the HLR and/or OLR is often calculated using only the surface or cross-sectional area (m^2), but the use of total reactor volume (m^3) allows better comparison between different systems. For example, a slender vessel can have a high cross-sectional loading rate but relatively low overall loading rate, while the converse is true for a wide, shallow vessel.

The influent COD, COD removal efficiency, HLR, OLR and HRT for this study was compared to other systems used for the treatment of WWW and olive mill WW (Table 5.2). The BSF pilot-scale system operated under comparable OLR, with the exception of a two-stage fixed bed reactor described by Andreottola *et al.* (2005).

Achak *et al.* (2009) used a vertical flow sand filter for the treatment of 50% diluted olive mill WW, with a starting HLR of as 68.2 L/m^3 of sand day^{-1} , which decreased to 5.0 L/m^3 of sand day^{-1} over a 10 week period. The HLR reduction was due to the accumulation of biomass and high suspended solids within the WW and resulted in the experiment being terminated. The COD reduction for the first 4 weeks was $> 70\%$ and increased to $> 90\%$ after the 6th week (Achak *et al.*, 2009). This followed a similar trend to the treatment performance of the BSF in this study, as the efficiency improved with time.

Andreottola *et al.* (2005) showed a full-scale two-stage fixed bed bioreactor treating WWW removed 91% of the COD. The system has a treatment capacity of 100000 population equivalent installed at a winery producing 350 tons of grape a year (30% red, 70% white). The fixed bed reactor was filled with polypropylene spherical shaped media with a void ratio of 95% ($d=110 \text{ mm}$). This system achieved high removal efficiencies with high organic loading but is not a viable treatment option for a small winery within South Africa due to the high set-up costs and skills requirement.

Montalvo *et al.* (2010) reported on a two adjacent pilot-scale batch fed aeration lagoon treating 790 L/day and 170 L/day, respectively. While both ponds removed 91% of the COD with comparable OLR to the BSF system used in this study, it can be assumed that the long retention time and cost of aeration makes the system less economical.

Mulidzi (2010) achieved 60% and 80% COD removal for a CW with retention times of 7 and 14 days, respectively. The results compared with those found with the BSF system. However, the additional complexity and maintenance of a CW cannot be negated.

Ramond *et al.* (2013) reported removal efficiencies of 98% by an experimental BSF fed bi-weekly with WWW (COD of $2304 \pm 628.8 \text{ mg/L}$), with an OLR of 16.4 gCOD/m^3 of sand day^{-1} . Although a high removal efficiency was achieved, the OLR and HLR was low due to the low K of the river sand used in the system.

Rozema *et al.* (2016) showed 98.9% removal of COD treating a combination of WWW (4250 L/day) and domestic WW (12435 L/day) with a 4 cell vertical flow CW. The system operated at a relatively low OLR compared to the BSF in this study. A large portion of the WW was domestic, making comparison between the two difficult. The presence of domestic WW may enhance microbial activity because of the addition of nutrients to WWW (which has a high carbon to nitrogen ratio). A disadvantage of adding domestic wastewater is the potential introduction of pathogens.

Serrano *et al.* (2011) reported an average COD reduction of 73.3% across a two-stage CW fed by a hydrolytic upflow sludge bed for the treatment of WWW mixed with domestic WW from a cellar producing up to 315 KL of white wine per year. The system achieved an average HLR of 19.5 mm/day and surface OLR of 30.4 g/m²day⁻¹. The OLR for the first stage vertical flow CW achieved a 29-70% reduction in COD with a hydraulic loading rate of 30.7 – 332.9 L/m³ day⁻¹. Comparing the results of the first stage to the BSF for this study shows similar OLR. However, the addition of a second stage horizontal flow CW increased the removal efficiency. Similar results may be obtainable if the BSF modules are operated in series.

Welz *et al.* (2011) using incremental loading of a synthetic WW (ethanol) with an OLR ranging from 3.4 to 187.3 gCOD/m³ of sand day⁻¹ (theoretical COD = 474 – 26333 mg/L) achieved almost complete organic degradation with a maximum effluent COD of 365 mg/L under the highest influent concentration in an experimental BSF. The synthetic WW only contained ethanol, which is a readily biodegradable organic molecule (Malandra *et al.*, 2003; Serrano *et al.*, 2011). This could explain why the removal efficiency was higher than that in the in-situ pilot system used in this study. Welz *et al.* (2011) found that a higher ORR could be achieved when the ethanol concentration was incrementally increased (incremental priming). Incremental priming enhanced the COD removal efficiency and the stability of a BSF by allowing the bacterial communities to gradually adapt to the WW (Welz *et al.*, 2011, Welz *et al.*, 2012). This is challenging to perform on-site as the influent strength cannot be controlled. To overcome this, the initial flow rate, and consequently OLR of the BSF system used in this study could have been reduced by increasing the outlet height. The rate could then have been slowly increased by lowering the outlet height, effectively achieving incremental priming.

Table 5.2 Comparison of operational parameters for selected winery wastewater and olive mill wastewater treatment systems

Process description	COD Influent (mg/L)	COD removal efficiency (%)	HLR (L/m ³ day ⁻¹)	OLR (gCOD/m ³ day ⁻¹)	tHRT (days)	References
Sand Filter* Lab Scale	30830 ± 1690	>70 - 90	5.0 -68.2 [#]	2102.6 – 154.1 [#]	7 – 101 [#]	Achak <i>et al.</i> , 2009
Two-stage fixed bed reactor	6957 ± 4300	Total: 91 Stage 1: 80 Stage 2: 51	NG	Stage 1: 2400 (200-8000) Stage 2: 1300 (200-4500)	NG	Andreottola <i>et al.</i> , 2005
Pilot-scale fed-batch aerated lagoons	1:8700 2:18700	91 91	29 [#] 15.7 [#]	137 [#] 294 [#]	30 54	Montalvo <i>et al.</i> , 2010
Full-Scale HSSF	1: 2000 - 12000 2: 2000 - 12000	60 80	25 [#] 50 [#]	75± 450 [#]	7 14	Mulidzi (2010)
Experimental BSF	2304.4 ± 628.8	98	7.1 [#]	16.4 [#]	22	Ramond <i>et al.</i> , 2013
CW VF WWW and Domestic WW	2117	98.9	22 mm/day 23 [#]	34 g/m ² day ⁻¹ 48 [#]	NG	Rozema <i>et al.</i> , 2016
CW two-stage (VF/HF)	VF: 1558 ± 1023 HF: 711 ± 769	73.3 VF: 29-70 HF: 13-79	VF: 77-215 mm/day 55-154 [#] HF: 13-36 mm/day 1.3-3.6 [#]	VF: 43-466 g/m ² day ⁻¹ 30.7 – 332.9 [#] HF: 3.6–55 g/m ² day ⁻¹ 0.4-5.5 [#]	NG	Serrano <i>et al.</i> , 2011
Experimental BSF	15800 ^a 7587 ^a	99.5 - 99.8 97.9 - 95.7	7.1 [#] 7.1 [#]	112 54	22 22	Welz <i>et al.</i> , 2011
Pilot BSF	1265	81% (44-98%)	161	205	11	This study

^a tested with synthetic readily biodegradable COD: ethanol

* 50% Olive mill wastewater and 50% domestic wastewater

[#] Calculated from information given in article NG = Not given

VF = Vertical Flow

HF = Horizontal flow

HSSF = Horizontal subsurface flow

tHRT = theoretical hydraulic retention time

5.2.5 Correlation of the flow rate with the influent organic concentration

It was hypothesised that there would be a correlation between biomass clogging and the concentration of organic (food) present for microbial growth. The relationships between the measured flow rate, the effluent, and the COD were therefore investigated (Appendix L, Figure L.1-L.4). Only values obtained after the start-up period were considered because Ramond *et al.* (2012) have shown that it takes 90 days for the microbial communities to acclimate to the prevailing conditions in BSFs. There was a statistically significant negative correlation between the effluent flow rate and the influent COD from the influent ($r = -0.7$, $p < 0.01$; Figure 5.8), supporting the hypothesis.

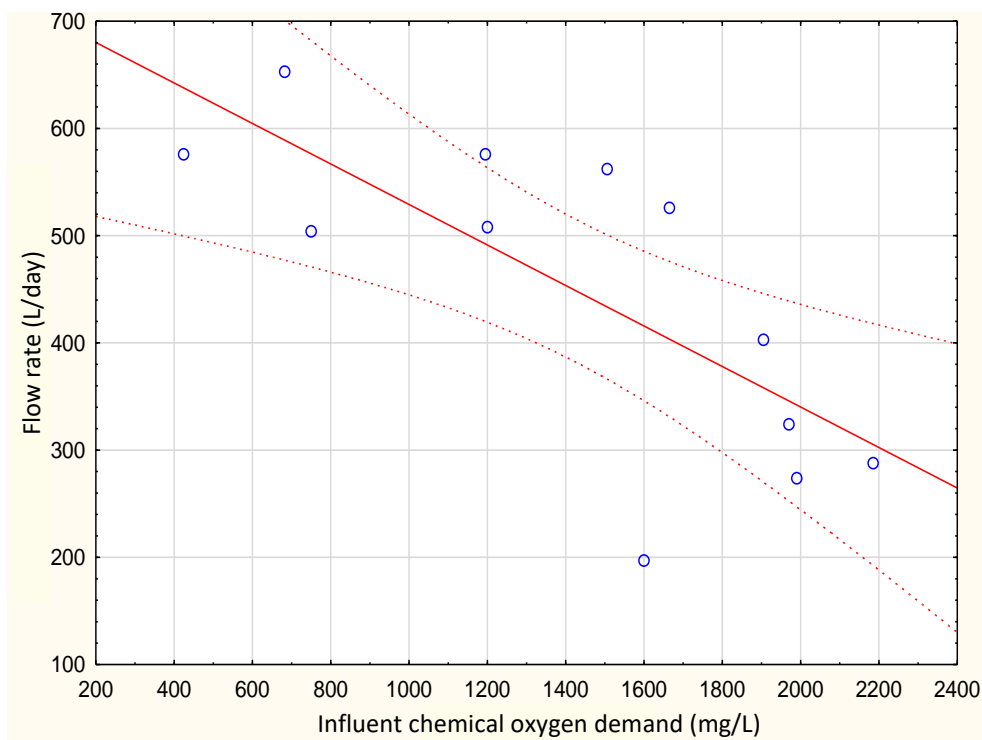


Figure 5.8 Relationship between effluent flow rate and chemical oxygen demand in influent samples from the influent including a 95% line of confidence

5.3 Compliance of treated effluent with legislation

Within South Africa, effluent must conform to the amended GA (2013) in terms of Section 39 of the National Water Act, 1998. The winery used in this study used $< 50 \text{ m}^3\text{WW/day}$ for irrigation, and was therefore subject to the relevant GA limits for irrigation of biodegradable industrial wastewater of this volume (Table 2.1).

In terms of COD, all the effluent concentrations complied with the legislative requirements ($\leq 5000 \text{ mg/L}$; Figure 4.12), but so did every sample from the influent (5000 L holding tank) (Figure 4.12). All of the samples from the settling basin but one adhered to the GA (maximum values of 7265 mg/L; Figure 4.2, Figure 4.3).

Although the SAR was reduced by the BSF system (Section 4.3.5.5; Figure 4.27 & Figure 4.28), all samples from the influent were < 2 , and complied with the GA limit of ≤ 5 .

The pH of the effluent complied with the legislative limits (Figure 4.36 & Figure 4.37), but 68.9% and 65.2% of the samples from the 5000 L holding tank and the settling basin (average), respectively, did not (Figure 4.11 & Figure 4.36). 68.9% and 60.9% of samples from the 5000 L tank and settling basin exhibited lower pH values in terms of the GA limit of 6 to 9. In addition, 4.43% of samples from the settling basin exhibited higher pH values than the GA Limits.

In terms of electrical conductivity, 100% of samples of influent and effluent samples complied with the GA limit of ≤ 200 ms/m. It was not envisioned that a BSF would remove salts from the waste stream, but rather be used with a tandem sustainable treatment system, such as phytoremediation system, to take up salts.

The faecal coliforms were not enumerated in the effluent as this was outside the scope of the research.

Although the untreated WWW from the study site complied with the GA in terms of COD and SAR, the reduction of these after treatment should still be seen in a favourable light from an environmental perspective. The results showed that in terms of the current legislation, the system is a viable treatment option for removal of COD and pH neutralisation at this winery.

The system is envisaged as a pre-treatment of effluent before irrigation, and therefore not all of the parameters listed in the GA for release of effluent into a schedule 1 river or tributary were measured (Table 2.2). With the exception of SAR and pH, the parameters that were measured in the effluent from the BSF system did not generally comply with the stringent limits as seen in Figure 4.12, Figure 4.16, Figure 4.17, Figure 4.18, Figure 4.19, Figure 4.27, Figure 4.33, and Figure 4.36.

5.4 Hydrological data and the effect of precipitation and evaporation on the operation of biological sand filter modules

The ability of the BSF to handle a storm with high intensity precipitation is important. The top 10 instances of precipitation since 1984, together with monthly averages of precipitation and evaporation can be seen in Appendix M. The maximum recorded precipitation was 190.8 mm/day on 11th of April 1993, but no hourly data was available, so peaks could not be ascertained.

From the available data, the potential ability of the filter to handle precipitation was evaluated, (calculations seen in Appendix M, using Darcy's equation, outlined in Section 3.4.2). The filter has an available freeboard of approximately 100 mm which works out to approximately 200 L. If the filter is filled to the top and a K of 0.043 mm/sand is used with a potential head of 250 mm, the flow rate would equate to 11 L/hr from the inlet across the length of the filter. On the other hand, if the filter is fully saturated, the water has a shorter distance to travel. Therefore, using a point 0.100 m and 0.020 m away for the outlet, a theoretical flow rate of 185 L/hr and 927 L/hr was calculated.

This data can be converted to a rainfall intensity or infiltration rate of 6 mm/hr, 95 mm/hr and 474 mm/hr, respectively. The calculations can be seen in Section M. 2 and Table M.3 with the integration of the different points at a spacing of 0.020 m. The change in infiltration due to the distance from the inlet can be graphically seen in Figure 5.9. Therefore, once the filters' 100 mm of freeboard is occupied by precipitation, the filter should overflow when the rainfall intensity is above the average infiltration rate of 6 - 474 mm/h. The filters should theoretically be able to handle a severe storm without overflowing. This was confirmed by the fact that there was no evidence of overflow during the study period.

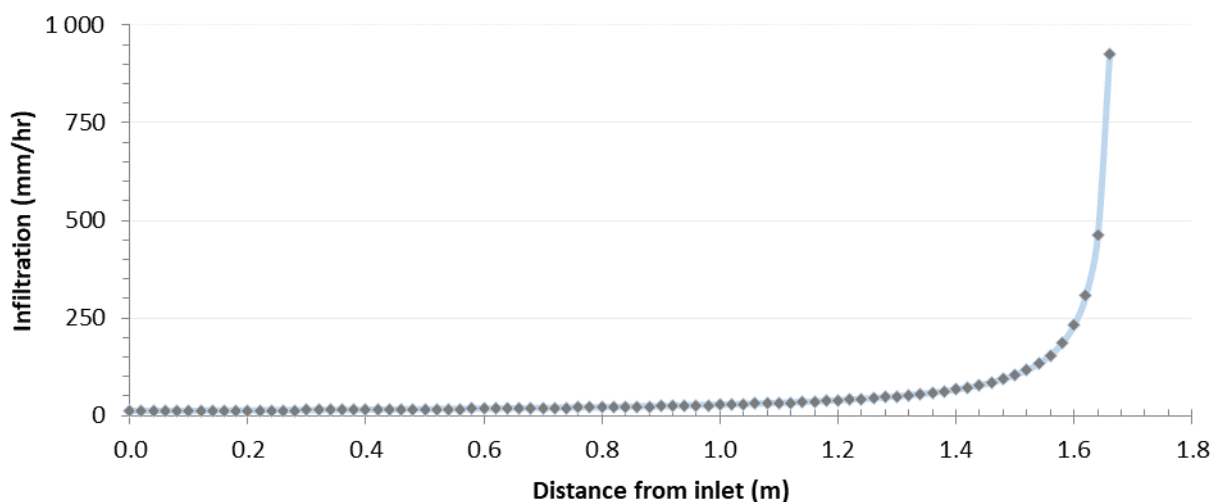


Figure 5.9 The relationship between the infiltration rate and the distance from the inlet in a fully saturated biological sand filter with a hydraulic conductivity of 0.044 mm/s

As the BSF is open to the environment, so not only will precipitation have an effect the concentration of the WWT within the filter, but so too could evaporation. While precipitation will dilute the concentration, evaporation will increase the concentration of constituents within the BSF. The rate at which evaporation of water from porous media (e.g. soil and rock) takes place is affected by several environmental factors together with the physical characteristics of the substrate such as the hydraulic conductivity, capillary characteristics, and thickness of the layers (Shokri *et al.*, 2010; Wilson, 2009). Salt can raise the level of water within a clay substrate due to capillary reactions and the evaporation results in the concentration of salts, which may reduce removal efficiencies (Jesus *et al.*, 2017). In this study, the loss due to evaporation was not taken into account as the filters had a relatively small surface area of water and the effects were assumed to be negligible on the final effluent.

5.5 Operational observations and troubleshooting

Due to the nature of the pilot system there were some general observations, highlights and problems encountered during the operation of the BSF system. Where possible, problems will be addressed during the design of future systems (Table 5.3, Table 5.4, Figure 5.10, Figure 5.11). Possible remedial actions are outlined in Table 5.3 and Table 5.4.

The sand did not clog over the operational period, although the casing of Filter 3 did suffer excessive bulging, resulting in temporary surface flow (Figure 5.10, C, K, O). This filter also showed the highest tendency for plant and microbial growth within the surface water (Figure 5.10, G).

In terms of visible changes, the colour of the sand at the surface of filters 1, 2 & 4 only changed at the inlet, where it became darker than the original sand (Figure 5.10). The discoloration did not penetrate the deeper layers of the sand, as evidenced by core samples that were taken on the 18th of April 2016 (Figure 5.10M).

There was either intermittent or permanent microbial growth on the surface of the tanks and/or in the pipes of the system. In some instances, these led to operational problems and clogging of the pipes (Figure 5.11).

The change in WW level across the filter resulted in a large volume of sand which is was not used (effective dead space). This reduced the treatment capacity of the entire system. There was possibly a longer retention time of wastewater in Filter 3 and 4 due to a longer pipe length from the 500 L balancing tank than Filter 1 and 2. Filter 3 did not perform as well as the other Filters, strongly suggesting that surface flow is undesirable.

Table 5.3 Description of problems encountered with the biological sand filtration system and possible mitigating or remedial action table 1 of 2

Date of First occurrence	Description	Occurrences	Remediation/ mitigating actions
February 2015	Bulging of filter modules when sand was applied. Excessive bulging occurred when filter modules were filled too high. Therefor a height of 420 mm was chosen. However Filter 3 still bulged excessively.	Permanent	The filters could be filled lower or partially buried to reduce the pressure on the tank.
February 2015	Long retention time within outlet structure and possibly a poor extraction of treated WW from the filter module due to singular outlet and a possible reduction in usable volume.	Permanent	Decrease the size of the outlet structure and increase the amount of outlet fittings within the outlet side of the filter.
March 2015	Foam/sludge/microbial mat floating on the surface of the WW within the 5000 L and 500 L tank. No negative effect unless sludge clogs pipes [Figure 5.11(A-D)].	Permanent	None.
March 2015	Build-up of algae floating on the surface and growing on the walls of the flow control tank [Figure 5.10 (N)]. The algal sometimes entered the effluent pipe and caused partial blockages.	Permanent	Removal of algae from surface water bi-weekly. Future tank to be UV resistant. A floating ring around the outlet pipe could reduce the amount of floating algae entering the effluent pipe.
March 2015	Rat-tailed maggots assumed to be Hover Fly (<i>Eristalinus taeniops</i>) were found within the inlet channel of the BSF. They were also found within the settling basin.	Mainly in spring and summer with no consistency.	None.
March 2015	Growth of plants and grass within the filter module.	Permanent.	Monthly removal of plants from filter bed.
March 2015	Distinct smell coming from the 5000 L holding tank and 500 L balancing tank when taking off the lid. The BSF did have a slight smell however only slight	Permanent.	None

Table 5.4 Description of problems encountered with the biological sand filtration system and possible mitigating or remedial action table 2 of 2

Date of First occurrence	Description	Occurrences	Remediation/ mitigating actions
April 2015	The gradual collapse of the inlet channel and the observed thickening and saturation of the inlet channel with organic material.	Permanent.	The reformation of inlet channel by increasing the depth of the channel and reducing width by hand. This could reduce the chance of humification and the possible degradation of affected substrate.
November 2015	Clogging of effluent pipe.	Low	Disconnect pipe and rinse with fresh water.
November 2015 June 2016	An oily type substance floating on the surface of Filter 2 and 3 inlet channel. The substance gave a rainbow effect on the surface of the water as it refracted the light.	Low	None
January 2016	Livestock climbed into the BSF and walked on the sand.	Low	Fence the area to reduce the chance of outside interference.
March 2016	The clogging of the Aqua-Brooks float due to the very low flow rate resulted in accumulation of microbial growth on the small opening in the outlet of the valves. The valve within the 500 L tank clogged. However, the filter modules valves did not clog.	Low	The float valves should be held fully open for 2 minutes monthly and be cleaned every 6 months to reduce the chance of clogging.
April 2016	Major disturbance of the sand within Filter 2 and 4 due to winemaker rinsing bins into filter module. This resulted in a high amount of suspended solids and can be seen in Figure 5.10 (P)	Low	The sand was re-levelled and the inlet channel was reformed.
April/May 2016	After an extended period of surface flow within filter module 3. the surface flow halted. No additional media was added to the filter yet there was visible microbial growth on the surface of the filter (Figure 5.10 O). The exact mechanism which ceased the surface flow is unknown.	Low	None
July 2016	Field mice used the sand underneath the filter modules as a burrow in April 2015. They removed the sand under the filter and the filters sunk into the ground. This could lead to the introduction of preferential flow paths as the bottom of the tank is no longer level.	Permanent	There should be some form of protection against this, possibly a base material used for filling instead of compacted sand.

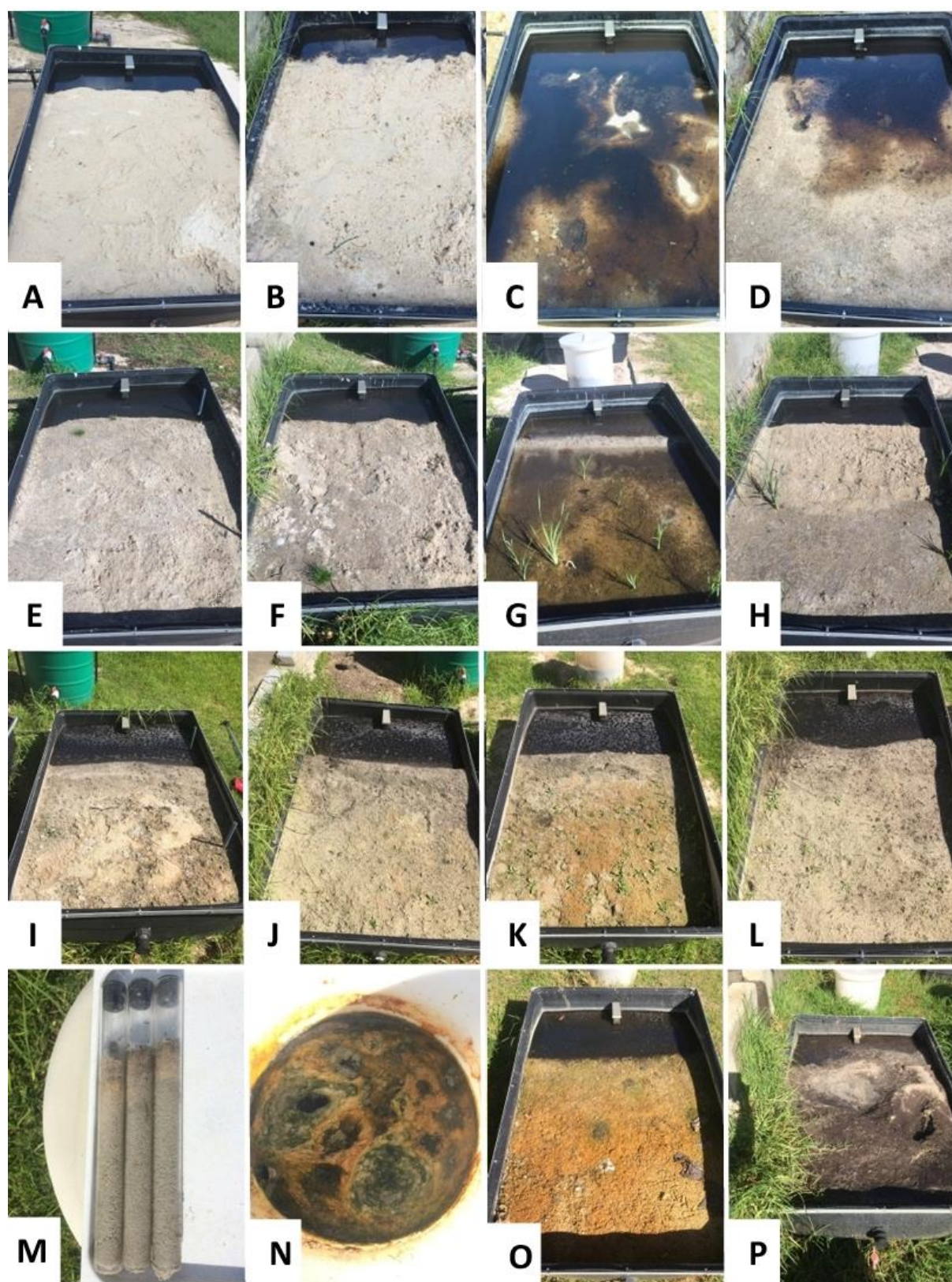


Figure 5.10 Photographs of filter module 1-4 on 19th of February 2015 (A-D), on the 20th of April 2015 (E-H), on the 25th of August 2016 at the end of testing (I-L), core samples taken from the inlet channel of filter 3 on the 6th of May 2016 (M), the hydraulic control tank algal growth or biofilm on the 18th of April 2016 (N), filter 3 after surface flow had stopped and the picture is showing the microbial blanket on surface of filter on the 18th of April 2016 (O), filter module 4 after the cellar rinsed bins containing solids into filter (P)

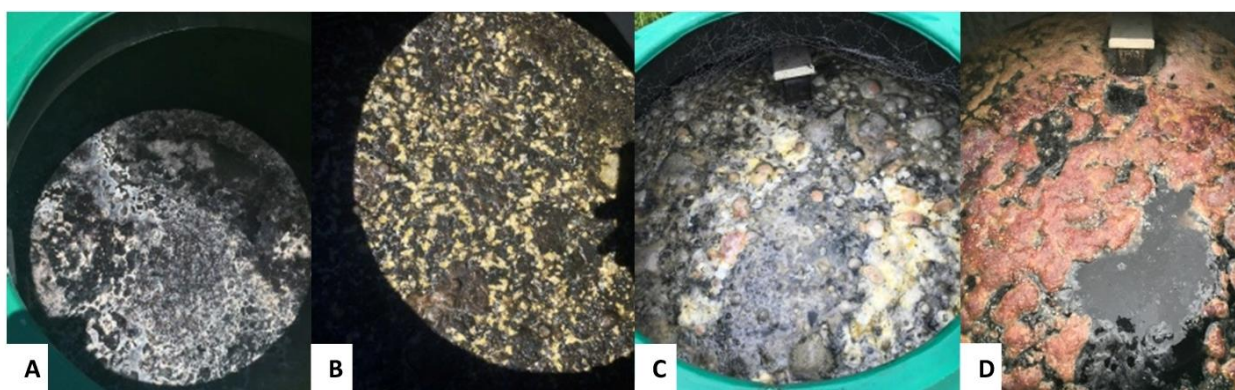


Figure 5.11 Photographs of the 500 L tank microbial mat, biofilm, sludge on the 19th of November 2015 (A), the 500 L tank on the 22nd of February 2016 (B), on the 1st June 2016 (C) and on the 25th of August 2016 (D)

5.6 Financial cost of the system

In order to determine the financial validity of the system, the capital expenditure, installation, maintenance and operation costs were taken into consideration. The system did not require any running costs (no energy or chemicals) over 610 days, and maintenance requirements (approximately 30 minutes bi-weekly of unskilled labour) could theoretically be performed by existing staff and therefore easily absorbed by the winery. The costs were therefore attributed to the capital and installation costs of R50 136 (updated to reflect costs in February 2017), summarised in Section 3.4.6, with a detailed breakdown in Appendix E.

If the capital outlay of the system is linearly distributed over a 10 year period, the system would cost R5013 per year or R167 per month. However, there will be an additional maintenance and consumable costs to replace parts of the system. The following estimates for replacement periods of the different items are: sand (every 3 years), batteries (every 5 years) and the pump (every 5 years), in the worst-case scenario. This must be considered together with inflation (6%) of the consumable items only. The distribution of the costs can be seen in Table 5.5. This would equate to a yearly replacement cost of R7529 for the first year, and the following years can be seen in Table 5.6. When the sand requires replacing, at current cost, this was estimated as R 6000 (for replacement of sand, disposal of spent sand and labour). It must be noted that the sand was not clogged after the 610 day period of this project, and the system is still operational as of August 2017. For the 11th year the running cost would be R7578, which would be the inflated cost of the consumables only.

Table 5.5 Consumable costing and replacement periods for the biological sand filter in the worst-case scenario for a 10 year operational period

Description	Costs	Replacement Period (years)	Cost per year	Cost per m ³ with flow of 413 L/day
Replacement of sand	R 6000	3	R 2000	R 13
Replacement of Battery	R 6618	5	R 1324	R 9
Replacement of Pump	R 4540	5	R 908	R 6
Other permanent components	R 32978	10	R 3298	R 22
Total	R 50136		R 7529	R 50

Table 5.6 Yearly cost of biological sand filter, for a 10 year period, including inflation of consumables at 6%

Years	1	2	3	4	5	6	7	8	9	10
Infrastructure	R 3298	R 3298	R 3298	R 3298	R 3298	R 3298	R 3298	R 3298	R 3298	R 3298
Consumables	R 4232	R 4485	R 4755	R 5040	R 5342	R 5663	R 6003	R 6363	R 6745	R 7149
Total	R 7529	R 7783	R 8052	R 8338	R 8640	R 8961	R 9300	R 9661	R 10042	R 10447

Using the monthly cost of the system including the additional maintenance and replacement costs of consumables and a flow rate of 413 L/day the system would cost R 50/m³ of WW, the yearly distribution of this cost can be seen in Table 5.7, which includes inflation of the consumables at 6% per year.

Table 5.7 Cost per m³ of treated effluent using a biological sand filter, for a 10 year period, including inflation of consumables at 6%

Years	1	2	3	4	5	6	7	8	9	10
Infrastructure	R 22	R 22	R 22	R 22	R 22	R 22	R 22	R 22	R 22	R 22
Consumables	R 28	R 30	R 32	R 33	R 35	R 38	R 40	R 42	R 45	R 47
Total	R 50	R 52	R 53	R 55	R 57	R 59	R 62	R 64	R 67	R 69

The financial saving for using a solar pump and completely offline system cannot be negated. Assuming only a 0.75 Kw pump is used for this system with a flow rate of 1.5 m²/hr and a cost of electricity of R2.10 Kw/hr the monthly electricity cost would be R17.35 per month and R211 per year. If this is converted to a cost R0.58 per m³ comparing this to the cost for the solar system at R15 per m³ shows a high financial deficit due to the solar system. This is due to the high initial cost of the solar system plus the possibly inflated replacement costs of the solar consumables.

Chapter 6 Conclusions and recommendations

6.1 Conclusions

In South Africa, WWW is a problem that has not been sufficiently addressed, particularly at small to medium sized wineries. Although the WW from some small wineries falls within the GA guidelines for 'beneficial' irrigation, greener practices, water scarcity and the heightened need for environmental protection requires increased implementation of simple and affordable WWW treatment technologies.

This study involved comprehensive characterisation of the WWW and monitoring of physicochemical parameters to assess the performance of a BSF system treating WWW at a small winery in the Western Cape, South Africa.

Highlights of the study in terms of system performance include:

(i) The system improved the effluent quality by reducing the COD by 81% (range:44-98%) with an average influent concentration of 1265 mg/L (range:424-2185 mg/L). The system treated 413 L/day WWW on average after start-up with a HLR of 143 L/m³ sand day⁻¹ (range: 67-222/m³ sand day⁻¹). The OLR of 205 gCOD/m³ of sand day⁻¹ (range: 83-338 gCOD/m³ sand day⁻¹) competes well with other methods available for treating WWW.

(ii) The phenolic content of the WWW was reduced by 67%, and there was a 29% decrease in the SAR. WW with a high SAR can cause sodicity, which has an adverse effect on soil structure, and phenolics are potentially toxic to plants and microbial populations. The BSF system thus reduced the potential impact of the WWW on the receiving pasture.

(iii) The BSF system effectively neutralised the generally acidic WWW without the addition of chemicals.

(iv) The factors described in (i)-(iii) led to a reduction in the potential microbial toxicity, phytotoxicity, and sodicity of the WWW, rendering it more suitable for irrigation. In addition, the COD concentration, SAR, pH and EC in all the effluent samples adhered to the applicable GA for < 50 m³WW/day for irrigation.

(v) The BSF modules did not clog, and produced a stable flow rate after the acclimation period. There was a strong negative correlation between *K* and the OLR i.e. the *K* decreased during periods of high organic loading and increased again during periods of low organic loading. The increase was assumed to be attributable to degradation of accumulated organic solids and biomass. As expected, there was also a significant reduction in the *K* of the filters after start-up due to the build-up of functional biomass. In spite of this, the flow rate was still satisfactory, and biomass plays a crucial role in the treatment of WWW. The initial reduction in *K* should therefore not be viewed as a negative.

- Results of this study strongly suggest that a BSF system may present a viable treatment solution for WW treatment at small wineries. The pilot system tested was affordable and sustainable, requiring minimal maintenance and inputs, and no significant economic inputs after installation.

6.2 Recommendations and future research

It is recommended that ongoing research should be conducted on the physicochemical treatment and hydraulic performance of the system to establish longevity. This can be achieved by monitoring:

(i) The COD and phenolic removal performance, (ii) The effluent flow rates, and (iii) WW neutralisation, including the rate of calcite dissolution from different areas within the sand matrix.

Future designs should focus on (i) allowing a greater volume of the sand matrix to be used by reducing the 'low flow' and dead zones, (ii) avoiding surface flow and short circuiting, (iii) preventing bulging of the filter modules by changing the casing to a stronger material, half-burying the modules, and/or providing a concrete base, (iv) minimising algal growth by using tanks and pipes impermeable to sunlight, (v) decreasing the retention time, for example, by increasing the number of outlets or changing the mode of operation to vertical flow.

It is possible that digestion takes place in the holding tank. It is recommended that this is investigated further with a view to optimisation. For example, the effect of mixing by stirring or the provision of an angular inlet at the bottom of the tank.

It is recommended that research should be conducted on the effect of the OLR, biomass and SAR on K and HRT.

Different modes of operations should be explored (continuous v/s batch mode). For example, the use of batch mode could increase the redox potential within the currently generally anaerobic system and enhance bioremediation rates. Resting periods introduced as part of batch-mode operation have also been shown to assist with hydraulic flow in constructed wetlands, and requires further investigation in BSFs treating WWW. Vertical flow should also be explored to take advantage of the ability to achieve higher flow rates and redox potential.

References

- Achak, M., Mandi, I. & Quazzani, N., 2009. Removal of organic pollutants and nutrients from a olive mill wastewater by a sand filter. *Journal of Environmental Management*, 90 (2009), 2771-2779.
- Andreottola, G., Foladori, P., Nardelli, P. & Denicolo, A. 2005. Treatment of winery wastewater in a full-scale fixed bed biofilm reactor. *Water Science Technology*, 51 (1), 71–73.
- Andreottola, G., Foldari, P., Ziglio, G., 2009. Biological treatment of winery wastewater: an overview. *Water Science Technology*, 60 (5), 1117-1125.
- Angelakis, A. N., Kavoulaki, E., & Dialynas, M. G. 2014 Sanitation and Stormwater and Wastewater Technologies in Minoan Era. In: Evolution of Sanitation and Wastewater Management through the Centuries (A. Angelakis and J. Rose, Eds). IWA Publishing, London, UK, Ch. 1: 1-24.
- Arienzo, M., Christen, E.W., Quayle, W., Kumar, A., (b) 2009. A review of the fate of potassium in the soil–plant system after land application of wastewaters. *Journal of Hazardous Materials* 164(2-3), 415–422.
- Arienzo, M., Christen, E.W., Quayle, W.C., 2009. (b) Phytotoxicity testing of winery wastewater for constructed wetlands treatment. *Journal of Hazardous Materials*, 169 (1-3), 94–99.
- Artiga P., Carballa M., Garrido J.M., Mendez R., 2007, Treatment of winery wastewaters in a membrane submerged bioreactor. *Water Science and Technology*, 56(2), 63–69
- Artiga, P., Ficara, E., Malpei, F., Garrido, J.M. & Mendez, R. 2005. Treatment of two industrial wastewaters in a submerged membrane bioreactor. *Desalination*, 179 (2005), 161-169.
- Aybar, M., Carvallo, M., Fabacher, F., Pizarr, G., Pasten, P., 2007. Towards a benchmarking model for wastewater treatment and disposal. *Water Science Technology*, 56(2), 153-160.
- Batchelor, A., Loots, P., 1997. A critical evaluation of a pilot scale subsurface flow wetland: ten years after commissioning. *Water Science and Technology* 35 (5), 337–343
- Bories, A., Sire, Y. & Collin, T., 2005. Odorous compounds treatment of winery and distillery effluents during natural evaporation in ponds. *Water Science and Technology*, 51 (1), 129-136.
- Brito, A.G., Peixoto, J., Oliveira, J.M., Oliveira, J.A., Costa, C., Nogueira, R. & Rodrigues, A., 2007. *Brewery and Winery Wastewater Treatment: Some Focal Points of Design and Operation*, in Oreopoulou, V. & Russ, W., (eds.) 2007, Utilization of By-Products and Treatment of Waste in the Food Industry. New York: Springer Science - Business Media p 109-131.
- Brovelli, A., Carranza-Diaz, O. & Barry, D.A., 2011. Design methodology accounting for the effects of porous medium heterogeneity on hydraulic residence time and biodegradation in horizontal subsurface flow constructed wetlands. *Ecological Engineering*, 37 (2011), 758-770.
- Cartwright, K., & Hensel, B.R.. (1995). Hydrogeology. In: Daniel, D.E. (ed) Geotechnical Practice for Waste Disposal. 1st ed. Chapman & Hall, London, England:
- Caselles-Osorio, A. and García, J., 2006 Performance of experimental horizontal subsurface flow constructed wetlands fed with dissolved or particulate organic matter *Water Research.*, 40 (19), 3603–3611
- Chen, Y., Wen, Y., Tang, Z., Huang, J., Zhou, U. & Vymazal, J., 2015. Effects of plant biomass on bacterial community structure in constructed wetlands used for tertiary wastewater treatment. *Ecological Engineering*, 84 (2015) 38-45.
- Christen, E.W., Quayle, W.C., Macoux, M.A., Arienzo, M. & Jayawardane, N.S., 2010. Winery wastewater treatment using land filter technique. *Journal of Environmental Management*. 91 (2010), 1665-1673.
- D’Annibale, A., Quaratino, D., Federici, F., Fenice, M., 2006. Effect of agitation and aeration on the reduction of pollutant load of olive mill wastewater by the white-rot fungus *Panus tigrinus*. *Biochemical Engineering Journal*, 29 (2006), 243–249.
- Darcy, H. 1856. Les fontaines publiques de la ville de Dijon. Paris: Dalmont.
- Dell Statistica. USA: Dell Inc., 2017. Windows.

-
- Department: Water and Sanitation, Republic of South Africa, (2016) Department of Water and Sanitation, [Online] Available at <http://www.dwa.gov.za/Hydrology/Verified/HyDataSets.aspx?Station=G2E013> [Accesses 12 December 2016]
- Di Stefano, N., Quayle, W., Arienzo, M., Zandona, R., Blackwell, J. & Christen, E. 2008. *A low cost land based winery wastewater treatment system: Development and preliminary results* [Online] Available: <http://www.clw.csiro.au/publications/science/2008/sr43-08.pdf> [2015, June 30].
- du Plessis, K. 2007 *Wetlands consistently clean up organic effluents* [Online]. Available: <http://www.wineland.co.za/technical/wetlands-consistently-clean-up-organic-effluents> [2015, July 25].
- Ganesh, R., Rajinikanth, R., Rajinikanth, J.V., Ramanujam, R.A. & Torrijos, M., 2010. Anaerobic treatment of winery wastewater in fixed bed reactors. *Bioprocess and Biosystems Engineering*, 33 (5): 619-628.
- Government Gazette. (1998) *Act no. 36 of the National Water act of South Africa of 1998* [Online]. Available: http://www.energy.gov.za/files/policies/act_nationalwater36of1998.pdf [2015, March 12]
- Government Gazette. (2008) *Act no. 59 of the National Environmental Management: Waste Act of 2008*. [Online]. Available https://www.environment.gov.za/sites/default/files/legislations/nema_amendment_act59.pdf [2015, April 15]
- Government Gazette. (2013) Revisions of General Authorisation in terms of Section 39 of *Act no. 36 of the National Water act of South Africa of 1998* [Online]. Available: <http://faolex.fao.org/docs/pdf/saf126916.pdf> [2015, June 29].
- Grape and Winer Research and Development Cooperation, 2011, *Winery Wastewater Management and Recycling Operational Guidelines*. [Online]. Available <https://www.wineaustralia.com/getmedia/72627da6-d28a-42f2-b600-28fdd5a6c85c/Operational-Guidelines.pdf> [2015, April 15]
- Gupta, A., Alam, J., Muzzammil, M., 2016. Influence of thickness and position of the individual layer on the permeability of the stratified soil. *Perspectives in Science*, 8 (2016), 757-759.
- Horneck, D.A. Ellsworth, J.W. Hopkins, B.G. Sullivan, D.M. and Stevens R.G., 2007, *Managing Salt-affected Soils for Crop Production*. Oregon State University, November 2007. Oregon State University: Pacific Northwest Extension publication. 24.
- Ioannou, L.A., Michael, C., Vakondios, N., Drosou, K., Xekoukoulotakis, N.P., Diamadopoulou, E., Fatta-Kassinos, D., 2013 Winery wastewater purification by reverse osmosis and oxidation of the concentrate by solar photo-Fenton. *Separation and Purification Technology*, 118 (2013): 659–669.
- Ioannou. L.A., Li Puma. G. & Fatta-Kassinos. D., 2015. Treatment of winery wastewater by physicochemical, biological and advanced processes: A review. *Journal of Hazardous Materials*, 286 (2015): 1001-108.
- Fuentes, J.P., Flury, M., Bezdicsek. D.F., 2004. Hydraulic properties in a silt loam soil under natural prairie, conventional tillage and on-till *Soil Science Society of America Journal.*, 68 (2004), pp. 1679–1688
- Jesus, J.M., Cassoni, A.C., Danko, A.S., Fiuza, A. & Borges, T. 2017. Role of three different plants on simultaneous salt and nutrient reduction from saline synthetic wastewater in lab-scale constructed wetlands, *Science of The Total Environment*. 576 (2017), 447-455
- Juwarkar, A., Singh, S. & Mudhoo, A. 2009. Comprehensive overview of elements in bioremediation. *Reviews in Environmental Science and Bio/Technology*. 9(3) 215–288.
- Kalyuzhnyi S., Gladchenko M., Sklyar V., Kizimenko Y., Shcherbakov S., 2001, One and two stage upflow anaerobic sludge bed reactor pre-treatment of winery wastewater. *Applied Biochemistry Biotechnology*. 90(2), 107–123
- Klute, A., & C. Dirksen. 1986. Hydraulic conductivity and diffusivity: Laboratory methods. p. 687–734. In A. Klute (ed.) *Methods of soil analysis*. Part 1. 2nd ed. ASA, Madison, Wageningen the Netherlands
- Knowles, P., Dotro, G., Nivalla, J. & Garcia, J. 2011. Clogging in subsurface-flow treatment wetlands: Occurrence and contributing factors. *Ecological Engineering*. 37 (2011) 99–112
- Lasko, D., Schwerdel, C., Bailey, J., Saue, U., 1997. Acetate-specific response in acetate-resistance bacteria: an analysis of protein patterns. *Biotechnology Progress*. 13(5), 519–523.
-

-
- Laurenson, S. & Houlbrooke, D., 2011. Winery wastewater Irrigation- the effect of sodium and potassium on soil structure [Online]. Available: http://www.marlborough.govt.nz/sitecore/shell/Controls/Rich%20Text%20Editor/~/_media/Files/MDC/Home/Environment/Land/Soils/Winery_wastewater_Irrigation-the_effect_of_sodium_and_potassium_on_soil_structure.ashx [2016, February 2]
- Laurenson, S., Houlbrooke, D. & Styles, T., 2012. Determination of soil dispersion in response to changes in soil salinity under winery wastewater irrigation [Online]. Available: http://www.marlborough.govt.nz/sitecore/shell/Controls/Rich%20Text%20Editor/~/_media/Files/MDC/Home/Environment/Land/Soils/AgResearch_Client_Report_for_Marlborough_District_Council.ashx [2015, February 8]
- Liu, Q., Mancl, K. and Tuovinen, O. 2003. Biomass accumulation and carbon utilization in layered sand filter biofilm systems receiving milk fat and detergent mixtures. *Bioresource Technology*, 89(3), 275-279.
- Lucas, M.S., Peres, J.A., Li Puma, G., 2010. Treatment of winery wastewater by ozone-based advanced oxidation processes (O₃, O₃/UV and O₃/UV/H₂O₂) in a pilot-scale bubble column reactor and process economics. *Separation and Purification Technology*, 72 (2010), (235–241)
- Mace, J.E. & Amrhein, C., 1991. Leaching and Reclamation of a Soil Irrigated with Moderate SAR Waters. *Soil Science Society of America Journal*, 13 (1), 199-204.
- Malandra, L., Wolfaardt, G., Zietsman, A., Viljoen-Bloom, M., 2003. Microbiology of a biological contactor for winery wastewater treatment. *Water Research* 37 (17), 4125–4134.
- Marchuk, A.G. & Rengasamy, P., 2010. *Cation ratio of soil structural stability (CROSS)*. [Online] Available: <http://iuss.org/19th%20WCSS/Symposium/pdf/1194.pdf> [2016, January 12].
- Masi, F., Conte, F., Martinuzzi, N. & Pucci, B., 2002. Winery high organic content wastewaters treated by constructed wetland in mediterranean climate. Unpublished paper delivered at the IWA 8th International Conference on Wetland Systems for Water Pollution Control, September, Arusha.
- McKinley, J.W. and Siegrist, R.L., 2011, Soil Clogging Genesis in Soil Treatment Units Used for Onsite Wastewater Reclamation: A Review. *Environmental Science and Technology*, 41 (24), 2186–2209,
- Mekki, A., Dhoub, A. & Sayadi, S., 2007. Polyphenols dynamics and phytotoxicity in a soil amended by olive mill wastewaters. *Journal of Environmental Management*, 84 (2007), 134-140.
- Metcalf and Eddy, Inc. 2004, *Wastewater Engineering: Treatment, Disposal and Reuse*. 4th edition. The McGraw-Hill Companies. New York, New York.
- Montalvo, S., Guerrero, L., Rivera, E., Borja, R., Chica, A. & Martin, A., 2010. Kinetic evaluation and performance of pilot-scale feed-batch aerated lagoon treating winery wastewater. *Bioresource Technology*, 101 (2010), 3452-3456.
- Mosse, K.P.M. Patti, A.F. Smernik, R.J. Christen, E.W. Cavagnaro, T.R., 2011. Physicochemical and microbiological effects of long- and short-term winery wastewater application to soils. *Journal of Hazardous Materials*, 201-202, 219-228.
- Mosse, K.P/M., Lee, J., Leachman, B.T., Parkikh, S.J., Cavagnaro, T.R., Patti, A.F. & Steenwerth, K.L., 2013. Irrigation of an established vineyard with winery cleaning agent solution (simulated winery wastewater): Vine growth, berry quality, and soil chemistry. *Agricultural Water Management*, 123 (2013), 93-102.
- Mosteo, R., Ormad, P., Mozas, E., Sarasa, J. & Ovelleiro, J.L., 2006. Factorial experimental design of winery wastewaters treatment by heterogeneous photo-Fenton process. *Water Research*, 40 (8), 1561-1568.
- Mulidzi, A.R., 2010. Winery and distillery wastewater treatment by constructed wetland with shorter retention time. *Water Science and Technology*, 61(10): 2611-2615
- Mulidzi, R. Laker, G. van Schoor, L.G. & Louw, L., 2002. Fate of organic components of winery effluents in soils [Online]. Available: <http://www.wineland.co.za/technical/fate-of-organic-components-of-winery-effluents-in-soils> [2015, June 29].
- Nalluri, C., Featherstone, R., Marriott, M. and Nalluri, C. (2009). Nalluri & Featherstone's Civil engineering hydraulics. 5th ed. Oxford, U.K.: Wiley-Blackwell.
- Navarro, P., Sarasa, J., Sierra, D., Esteban, S., Ovelleiro, J.L., 2005, Degradation of wine industry wastewaters by photocatalytic advanced oxidation. *Water Science Technology*, 51 (1), 113–120.
-

-
- Nguyen, L., 2001. Accumulation of organic matter fractions in a grave-bed constructed wetland. *Water Science and Technology*. 44 (11–12), 281–287.
- Noy, J., Feinmesser, A., 1997 The use of wastewater for agricultural irrigation, in: H.I. Shuval (Ed.), *Water Renovation and Reuse*, Academic Press, New York, 1997,73–92.
- Oliveira, M. & Duarte, E., 2011, Winery Wastewater Treatment - Evaluation of the Air MicroBubble Bioreactor Performance, Mass Transfer - Advanced Aspects, Dr. Hironori Nakajima (Ed.), InTech, [Online] Available : <http://www.intechopen.com/books/mass-transfer-advancedaspects/winery-wastewater-treatment-evaluation-of-the-air-micro-bubble-bioreactor-performance> [2015, September 03].
- Olivera, M., Duarte, E., 2014. Integrated approach to winery waste: waste generation and data consolidation. *Frontiers of Environmental Science and Technology*. 1-9.
- Perlman, H., 2017. The USGS Water Science School. [ONLINE] Available at: <https://water.usgs.gov/edu/earthhowmuch.html>. [Accessed 12 October 2016].
- Peszynska, M., Trykozko, A., Iltis, G., Schlueter, S. & Wildenschild, D., 2016, Biofilm growth in porous media: Experiments, computational modeling at the porescale, and upscaling. *Advances in Water Resources*, 95 (2016), 288–301
- Petruccioli, M., Duarte, C.J., Eusebio, A. & Federici, F., 2002. Aerobic treatment of winery wastewater using a jet-loop activated sludge reactor. *Process Biochemistry*, 37 (2002), 821-829.
- Polubesova, T., Eldad, S., Chefetz, B., 2010. Adsorption and oxidative transformation of phenolic acids by Fe(III)-Montmorillonite. *Environmental Science & Technology*, 44 (11), 4203–4209.
- Pradhan, N., Ingle, A.O., 2007. Mineralization of phenol by a *Serratia plymuthia* strain GC isolated from sludge sample. *International Biodeterioration and Biodegradation* 60, (2007), 103–108.
- Ramond, J.-B. , Welz, P.J., Tuffin, M.I., Burton, S.G. & Cown, D.A., 2013. Assessment of temporal and spatial evolution of bacterial communities in a biological sand filter mesocosm treating winery wastewater. *Journal of Applied Microbiology*, 115 (2013), 91-101.
- Ranieri, E., Gorgoglionea, A. & Solimenob, A., 2013. A comparison between model and experimental hydraulic performances in a pilot-scale horizontal subsurface flow constructed wetland. *Ecological Engineering*, 60 (2013) 45-49.
- Ranjbar, F. & Jalali, M., 2016. The combination of geostatistics and geochemical simulation for the site-specific management of soil salinity and sodicity. *Computers and Electronics in Agriculture*, 121 (2016) 301–312.
- Rengasamy P., & Sumner M.E. 1998. Processes involved in sodic behaviour, *Sodic Soils. Distribution, Properties, Management, and Environmental Consequences*. (Sumner ME, Naidu R, Eds.), 35-50. New York Press, New York.
- Rengasamy, P. & Marchuk, A., 2011. Cation ratio of soil structural stability (CROSS). *Soil Research*. 49 (3) 280-285
- Ritzema, H.P. 1994. Drainage Principles and Applications. International Institute for Land Reclamation and Improvement (ILRI). Publication 16. Second revised edition 1994. Wageningen, The Netherlands
- Rodriguez Caballero, A., Ramond, J.B., Welz P.J. (2012) Treatment of high ethanol concentration wastewater by constructed wetlands: enhanced COD removal and bacterial community dynamics. *Journal of Environmental Management* 109: 54-60.
- Rozema, E.A., Rozema, L.R. & Zheng, Y., 2016, A vertical flow constructed wetland for the treatment of winery process water and domestic sewage in Ontario, Canada: Six years of performance data. *Ecological Engineering*. 86 (2016), 262-268
- SAWIS. 2016. *South African Wine Industry Statistics (no.40)*. [Online] Available: http://www.sawis.co.za/info/download/Book_2016_engels_final_web.pdf [2017, April 05]
- Seelig, B.D. 2000. Salinity and Sodicity in North Dakota Soils. EB-57. North Dakota State University, Fargo, ND.
- Semple, K., Doick, L., Wick K. & Harms, H. 2007 Microbial interactions with organic contaminants in soil: definitions, processes and measurement. *Environmental Pollution*. 150(1) 166–176.
- Serrano, L., de la Varga, D., Ruiz, I. & Soto, M. 2011. Winery wastewater treatment in a hybrid constructed wetland. *Ecological Engineering*, 37 (2011), 744-753.
-

-
- Shepherd, H.L., Grismer, M.E. & Tchobanoglous, G., 2001. Treatment of high-strength winery wastewater using a subsurface-flow constructed wetland. *Water Environment Research*, 73 (4), 394-403.
- Shepherd, H.L., Grismer, M.E., Tchobanoglous, G., 2001. Treatment of high-strength winery wastewater using a subsurface-flow constructed wetland. *Water Environment Research*, 73 (4), 394-403.
- Sheridan, C. 2003. A critical process analysis of wine production to improve cost efficiency, wine quality and environmental performance. Unpublished Masters of Science Thesis. Stellenbosch: University of Stellenbosch
- Sheridan, C. Hildebrand, D. Glasser, D. 2014. Turning Wine (Waste) into Water: Toward Technological Advances in the Use of Constructed Wetlands for Winery Effluent Treatment. *AIChE Journal*. 60 (2),420-431.
- Sheridan, C., Glasser, D., Hildebrandt, D., Petersen, J. & Rohwer, J., 2010. An Annual and Seasonal Characterisation of Winery Effluent in South Africa. *South African Journal of Ecology and Viticulture*, 32 (1)
- Shokri, N., Lehmann, P. & Or, D., 2010, Evaporation from layered porous media, *Journal of Geophysical Research*, 60(B06204), 1-12
- Siegrist, R. L. 1987. Soil Clogging During Subsurface Wastewater Infiltration as Affected by Effluent Composition and Loading Rate. *Journal of Environmental Quality* 16, 181-187.
- Slinkard, K., Singleton, V.L., 1977. Total phenol analysis: automation and comparison with manual methods. *American Journal of Enology and Viticulture*, 28, 49-55.
- Tanner, C.C., 2001. Plants as ecosystem engineers in subsurface-flow treatment wetlands. *Water Science and Technology*, 44(11-12), 9-17.
- Terragis UNSW (2016). Exchangeable Sodium Percentage (ESP). [online] Available at: http://www.terragis.bees.unsw.edu.au/terraGIS_soil/sp_exchangeable_sodium_percentage.html [Accessed 15 Oct. 2016].
- Tharayil, N., Bhowmik, P.C., Xing, B., 2006. Preferential sorption of phenolic phytotoxins to soil: implications for altering the availability of allelochemicals. *Journal of Agricultural and Food Chemistry*, 54 (8), 3033-3040.
- Tufenkji, N., 2007. Modelling microbial transport in porous media: traditional approaches and recent developments. *Advances in Water Resources*. 30 (6-7), 1455-1469.
- UN-Water, 2015, Wastewater Management UN-Water Analytical Brief, [ONLINE] Available at: http://www.unwater.org/fileadmin/user_upload/unwater_new/docs/UN-water_Analytical_Brief_Wastewater_Management.pdf [Accessed 12 October 2016].
- Upadhyay, A. 2010. Fluid mechanics (Hydraulics). 1st ed. New Delhi, India: S.K. Kataria & Sons.
- van Schoor, L.H. 2005. *Guidelines for the management of wastewater and solid waste at existing wineries* [Online]. Available: <http://www.ipw.co.za/content/guidelines/WastewaterApril05English.pdf> [2015, March 03]
- van Schoor, L.H., 2015. An introduction to Agri-Industrial wastewater: Origin to end-use. Unpublished paper delivered at the 7th IWA Specialized Conference of Sustainable Viticulture, Winery Wastes & Agri-Industrial Wastewater Management. 4 November, Stellenbosch.
- Varma, A. and Buscot, F. 2005. *Microorganisms in Soils: Roles in Genesis and Functions*. 1st ed. Berlin, Heidelberg: Springer-Verlag Berlin Heidelberg.
- von Sperling, M. & de Paoli, A.C., 2013. First-order COD decay coefficients associated with different hydraulic models applied to planted and unplanted horizontal subsurface-flow constructed wetlands. *Ecological Engineering*, 57 (2013), 205-209.
- Vymazal, J., 2005. Horizontal sub-surface flow and hybrid constructed wetlands systems for wastewater treatment. *Ecological Engineering*, 25 (2005), 478-490.
- Vymazal, J., 2009. The use constructed wetlands with horizontal sub-surface flow for various types of wastewater. *Ecological Engineering*, 35, (2009) 1-17.
- Wallace, S.D., Knight, R.L., 2006. Small-scale constructed wetland treatment systems: feasibility, design criteria, and O&M requirements. Water Environment Research Foundation (WERF), Alexandria, Virginia.
- Welz, P.J. & Le Roes-Hill, M., 2014. Biodegradation of organics and accumulation of metabolites in experimental biological sand filters used for the treatment of synthetic winery wastewater: a mesocosm study. *Journal of Water*
-

Process Engineering, 3(C), 155-163.

Welz, P.J. Palmer, Z. Isaacs, S. Kirby, B. & la Roes-Hill, M. 2014. Analysis of substrate degradation, metabolite formation and microbial community responses in sand bioreactors treating winery wastewater: A comparative study. *Journal of Environmental Management*, 145 (2014), 147-156.

Welz, P.J., Holtman G., Haldenwang, R. & Le Roes-Hill, 2016. Characterisation of winery wastewater from continuous flow settling basins and waste stabilisation ponds over the course of 1 year: implications for biological wastewater treatment and land application. *WaterScience & Technology*, 74(9), 2036-2050

Welz, P.J., Ramond, J.-B., Cowan, D.A. & Burton, S.G. 2012. Phenolic removal processes in biological sand filters, sand columns and microcosms. *Bioresource Technology*, 119 (2012), 262–269.

Welz, P.J., Ramond, J.B., Cowan, D.A., Prins, A. & Burton, S.G., 2011. Ethanol degradation and the value of incremental priming in pilot scale constructed wetlands. *Ecological Engineering* 37 (2011), 1453 - 1459.

Welz, P.J., Ramond, J.B., Cowan, D.A., Smith, I., Palmer, Z., Haldenwang, R., Burton, S.G., Le Roes-Hill, M. (2015) Treatment of winery wastewater in unplanted constructed wetlands. WRC report no 2104/1/14 ISBN 978-1-4312-0647-6.

Wilson, E. 1990. *Engineering hydrology*. 4th ed. London, U.K.: Macmillan Press.

Wu, S. Wallace, S. Brix, H. Kuschik, P. Kipkemoi Kirui, W. Masi, F. Dong, R. 2015. Treatment of industrial effluents in constructed wetlands: Challenges, operational strategies and overall performance. *Environmental Population*, 201 (2015), 107-120.

Wu, S. Wallace, S. Kuschik, P. Brix, H. Vymazal, J. & Dong, R., 2014. Development of constructed wetlands in performance intensifications for wastewater treatment: A nitrogen and organic matter targeted review. *Water Research*, 57 (2014), 40-55.

Zhao, Y., Wei, Y., Zhang, Y., Wen, X., Xi, B., Zhao, X., Zhang, X. and Wei, Z. 2017. Roles of composts in soil based on the assessment of humification degree of fulvic acids. *Ecological Indicators*, 72 (2017), 473-480.

Zingelwa, N., Wooldridge, J., 2009. Tolerance of macrophytes and grasses to sodium and chemical oxygen demand in winery wastewater. *South African Journal Ecology and Viticulture*, 30 (2), 117-123.

Appendices

Appendix A. Flow calculations for sand filter modules

A. 1. Hydraulic conductivity

The intrinsic K of the Phillipi sand was determined by I. Smith (Unpublished) experimentally by means of a constant head method described by Ritzeman (1994) using the Darcy's equation (2.5). Three acrylic columns with a diameter of 300 mm were filled with Phillipi sand to the height of 0.62 m and three constant heads were used and the time to fill a known volumes of discharge of 0.02 m³. This resulted in a recorded K before ($K_{max} = 0.286$ mm/s) and 3 months after start up ($K_{min} = 0.144$ mm/s). The reduction in K was due to feeding of the sand with synthetic WWT to simulate the potential reduction in K due to biomass accumulation within a BSF. A sample calculation can be seen below and the results for the testes can be seen in Table B.1 and B.2.

$$Q = -KA \frac{dh}{dl} \tag{2.5}$$

$$0.02/841 = -K\pi \frac{0.3^2}{4} \left[\frac{-0.745}{0.62} \right]$$

$$K = 0.000280 \text{ m/s}$$

$$K = 0.280 \text{ mm/s}$$

Table A.1 Initial Hydraulic conductivity results from constant head by I. Smith

Head (m)	Colum 1				Colum 2				Colum 3 (Control)				
	t ₁ (s)	t ₂ (s)	t ₃ (s)	H/C (mm/s)	t ₁ (s)	t ₂ (s)	t ₃ (s)	H/C (mm/s)	t ₁ (s)	t ₂ (s)	t ₃ (s)	H/C (mm/s)	
0.745	841	841	841	0.280	790	790	790	0.299	892	892	892	0.265	
0.870	703	703	703	0.287	622	622	622	0.326	827	827	827	0.245	
1.120	553	553	553	0.283	550	550	550	0.307	554	554	554	0.285	
Average K				0.283	Average K				0.311	Average K			
The average hydraulic conductivity for Phillipi sand at start of filtration												0.286	

Table A.2 Hydraulic conductivity results from constant head by I. Smith after 3 months of filtration and control

Head (m)	Colum 1				Colum 2				Colum 3 (Control)				
	t ₁ (s)	t ₂ (s)	t ₃ (s)	H/C (mm/s)	t ₁ (s)	t ₂ (s)	t ₃ (s)	H/C (mm/s)	t ₁ (s)	t ₂ (s)	t ₃ (s)	H/C (mm/s)	
0.745	1500	1500	1500	0.157	1809	1809	1809	0.130	1022	1022	1022	0.231	
0.870	1455	1365	1365	0.144	1508	1508	1508	0.133	846	846	846	0.239	
1.120	1117	1042	1042	0.146	1285	1285	1285	0.130	616	616	616	0.256	
Average K				0.149	Average K				0.131	Average K			
The average hydraulic conductivity for Phillipi sand after 3 months of filtration												0.140	

A. 2. Properties of Phillipi sand and filter modules

The determination of the flow rate and velocity for a BSF was done using the Darcy's Law. The two hydraulic conductivities were used together with a sand height of 270 mm, which is the saturated height of sand at the outlet and a fall of 150 mm. The flow rate is calculated with the volume of sand at the outlet of the filter. The HRT used the full volume of sand.

Maximum Hydraulic conductivity	$K_{MAX} = 0.286 \text{ mm/s}$
Minimum Hydraulic conductivity	$K_{MIN} = 0.140 \text{ mm/s}$
Length of filter	$l = 1680 \text{ mm}$
Gradient of filter bed	$= 1\%$
Height of sand in filter	$= 420 \text{ mm}$
Change in head	$\Delta h = 150 \text{ mm}$
Height of saturated sand at filter outlet	$h = 270 \text{ mm}$
Flow type	<i>Horizontal subsurface flow</i>
Porosity of sand	$P_t = 0.292 \pm 0.02$

A.2.1. Cross-sectional area of sand within trapezoidal filter

The cross-sectional area of any height within the filter greater the 150 mm can be determined by Equation (3.1). This formula was derived from the actual dimensions within the filter module seen in Figure A.1. With the assumed change in water level from inlet to outlet can be seen in Figure A.2, with the outlet level of sand of 270 mm.

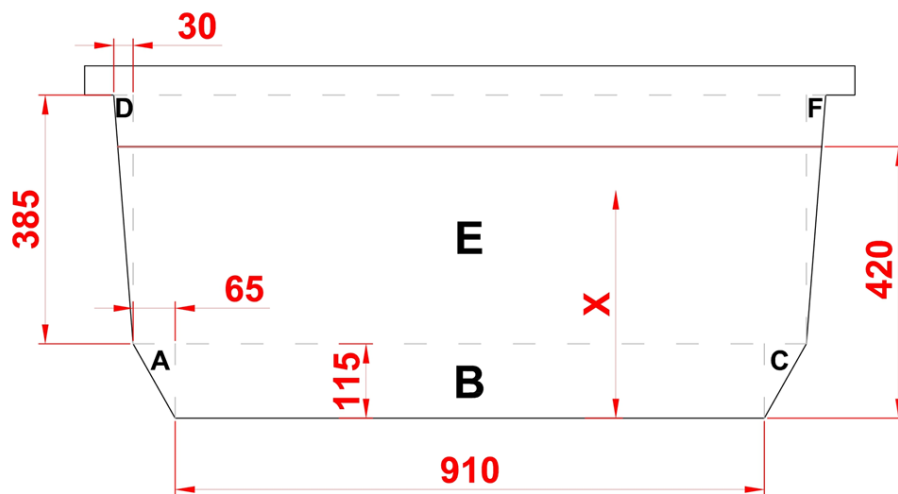


Figure A.1 Cross-section of a filter module, X represents the height of sand. ($115 \geq x \geq 500 \text{ mm}$)

$$\begin{aligned}
 A &= (910 + 65) \times 115 + (x - 115) \times 1040 + (x - 115) \times 30 \\
 \therefore A &= 1070x - 10925 \text{ [mm}^2\text{]} \\
 A &= 1070(270) - 10925 \\
 A &= 277975 \text{ mm}^2 \\
 A &= 0.278 \text{ m}^2
 \end{aligned}
 \tag{3.1}$$

A.2.2. Velocity and discharge using Darcy's Law for the maximum hydraulic conductivity

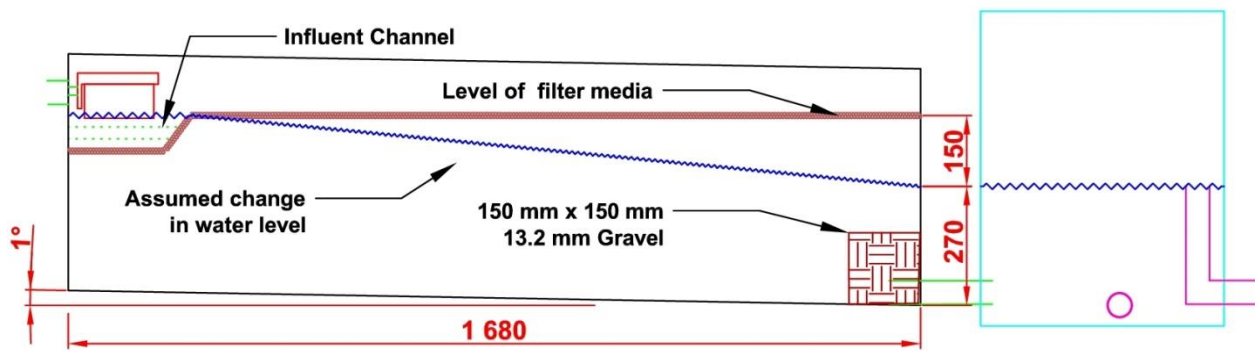


Figure A.2 Long-section of a filter module showing fall across filter.

$$U = -K \frac{dh}{dl} \quad (2.4)$$

$$U = -0.286 \div 1000 \times 60 \times 60 \times \left[\frac{-0.150 - \left(\frac{1}{100} \times 1.680\right)}{1.680} \right]$$

$$U = 0.102 \text{ m/hr}$$

$$Q = -KA \frac{dh}{dl} \quad (2.5)$$

$$Q = -0.286 \div 1000 \times 60 \times 60 \times 0.278 \times \left[\frac{-0.150 - \left(\frac{1}{100} \times 1.680\right)}{1.680} \right]$$

$$= 0.028 \text{ m}^3/\text{hr}$$

$$= 0.682 \text{ m}^3/\text{day.tank}$$

A.2.3. Discharge using Darcy's Law with the minimum hydraulic conductivity

$$U = -0.140 \div 1000 \times 60 \times 60 \times \left[\frac{-0.150 - \left(\frac{1}{100} \times 1.680\right)}{1.680} \right]$$

$$U = 0.050 \text{ m/hr}$$

$$Q = -0.140 \div 1000 \times 60 \times 60 \times 0.278 \times \left[\frac{-0.100 - \left(\frac{1}{100} \times 1.680\right)}{1.680} \right]$$

$$= 0.014 \text{ m}^3/\text{hr}$$

$$= 0.334 \text{ m}^3/\text{day.tank}$$

A. 3. Calculating hydraulic retention time

To calculate the hydraulic retention time must be done with the entire volume of the filter using a $P_t = 0.292$.

A.3.1. Cross-sectional area of sand within trapezoidal filter with a sand height 420mm

$$A = 1070(420) - 10925 \quad (3.1)$$

$$A = 438475 \text{ mm}^2$$

$$A = 0.438 \text{ m}^2$$

A.3.2. Calculating volume of water using full volume

$$\begin{aligned}
 V &= \text{Width} \times \text{Height} \times \text{Length} \\
 &= 0.438 \times 1.680 \\
 V &= 0.736 \text{ m}^3 \\
 V_{\text{water}} &= V \times P_t \tag{0.1} \\
 &= 0.736 \times 0.292 \\
 &= 0.215 \text{ m}^3
 \end{aligned}$$

A.3.3. Hydraulic retention time K maximum

$$\begin{aligned}
 HRT &= V_{\text{water}}/Q \tag{2.6} \\
 HRT &= 0.215/0.028 \\
 &= 7.67 \text{ hr} \\
 &= 0.3 \text{ days}
 \end{aligned}$$

A.3.4. Hydraulic retention time for K minimum

$$\begin{aligned}
 HRT &= 0.215/0.014 \tag{2.6} \\
 &= 15.35 \text{ hr} \\
 &= 0.6 \text{ days}
 \end{aligned}$$

A. 4. Hydraulic calculation for pipe flow from 500 L tank to filter

The hydraulic calculation for from 500 L tank to filter inlet was performed with differing heads and pipe diameters in order to calculate the correct influent flow rate to the filter module. An example is provided, while the complete integration is provided in Appendix B. The rationale around the calculation can be seen in Section 3.4.3. An example of the head provided by the 500 L tank can be seen in Figure A.3.

Assumed friction factor	$\lambda = 0.05$
Total head	$H = 0.4 \text{ m}$
Length of pipe	$l = 4 \text{ m}$
Water Density	$\rho = 1000 \text{ kg/m}^3$
Kinematic Viscosity at 15°C (Metcalf and Eddy, 2004)	$\nu = 1.14 \times 10^{-6} \text{ m}^2/\text{s}$
Pipe Diameter	$d = 25 \text{ mm}$
K-Values	
Sudden enlargement 25mm to 32mm	Calculate
Sudden contraction 32mm to 25mm x 2	Calculate
Exit loss	$K_{\text{Exit}} = 1$
Inlet Loss	$K_{\text{Inlet}} = 1$
Fully open gate valve	$K_{\text{open gate valve}} = 0.17$
¼ open gate valve	$K_{1/4 \text{ open gate valve}} = 24$
90° bend x 4	$K_{90^\circ \text{ bend}} = 0.75$

T flow through
T flow branch x 2

$$K_{T \text{ flow through}} = 0.4$$

$$K_{\text{flow branch}} = 1$$

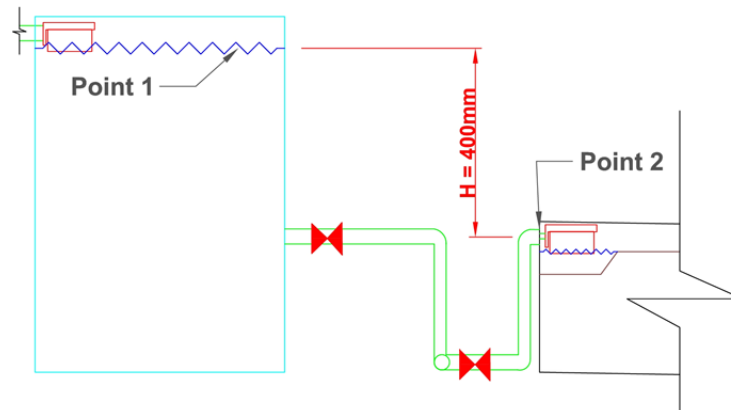


Figure A.3 Diagram depiction points used for the calculation of flow rate using the Bernoulli equation

A.4.1. K-Values

The sum of the K values must be calculated to determine the minor losses within the fittings.

Calculating sudden enlargement losses 25mm to 32mm

$$K_{\text{Enlargement}} = \left[\left(\frac{A_1}{A_2} \right) - 1 \right]^2 \quad (0.2)$$

$$K_{\text{Enlargement}} = \left[\left(\frac{\pi 0.025^2 \div 4}{\pi 0.032^2 \div 4} \right) - 1 \right]^2$$

$$K_{\text{Enlargement}} = 0.15$$

Sudden contraction losses 32mm to 25mm K read off table C.2 in Appendix C

$$\frac{D_2}{D_1} = \frac{0.025}{0.032}$$

$$\frac{D_1}{D_2} = 0.78$$

$$K_{\text{Contraction}} = 0.15$$

Calculating head loss due to minor losses.

$$h_{\text{Minor}} = K \left(\frac{U^2}{2g} \right) \quad (2.19)$$

$$h_{\text{Minor}} = (0.15 + 0.15 \times 2 + 1 + 1 + 0.17 + 24 + 0.75 \times 4 + 0.4 + 1 \times 2) \left(\frac{V^2}{2g} \right)$$

$$h_{\text{Minor}} = 32.02 \left(\frac{U^2}{2g} \right)$$

A.4.2. Calculate the new frictional factor

The Darcy-Weisbach equation is used to determine the head loss due to friction.

$$h_f = \frac{\lambda U^2}{2gD} \quad (2.15)$$

The starting point for the Bernoulli equation is point one which provide the head and the velocity at point 2 is calculated using the Bernoulli.

$$h_1 + \frac{p_1}{\rho g} + \frac{U_1^2}{2g} = h_2 + \frac{p_2}{\rho g} + \frac{U_2^2}{2g} + h_f + h_m \quad (2.14)$$

$$h_1 + 0 + 0 = 0 + 0 + \frac{U_2^2}{2g} + \frac{\lambda U^2}{2gD} + K \left(\frac{U^2}{2g} \right)$$

$$h_1 = \frac{U^2}{2g} \left(1 + \frac{\lambda l}{D} + K \right)$$

$$U^2 = \frac{2gh_1}{\left(1 + \frac{\lambda l}{D} + K \right)}$$

$$U = \sqrt{\frac{2gh_1}{\left(1 + \frac{\lambda l}{D} + K \right)}}$$

$$U = \sqrt{\frac{2 \times 9.81 \times 0.4}{\left(1 + \frac{0.05 \times 4}{0.025} + 32.02 \right)}}$$

$$U = 0.437 \text{ m/s}$$

The Reynolds number is calculated with the new calculated velocity.

$$Re = \frac{UD}{\nu} \quad (2.18)$$

$$Re = \frac{0.437 \times 0.025}{1.14 \times 10^{-6}}$$

$$Re = 9588$$

Then the frictional factor can be calculated using the Blasius yield relationship for smooth pipes with turbulent flow using the calculated Reynolds number.

$$\lambda = \frac{0.3164}{Re^{0.25}} \quad (2.17)$$

$$\lambda = \frac{0.3164}{9588^{0.25}}$$

$$\lambda = 0.032$$

This friction factor is used for the assumed friction factor

$$\text{Assumed friction factor} \quad \lambda = 0.032$$

$$h_1 + 0 + 0 = 0 + 0 + \frac{U_2^2}{2g} + \frac{\lambda U^2}{2gD} + K \left(\frac{U^2}{2g} \right)$$

$$U = \sqrt{\frac{2 \times 9.81 \times 0.4}{\left(1 + \frac{0.034 \times 4}{0.025} + 32.02\right)}}$$

$$U = 0.451 \text{ m/s}$$

Calculating the new Reynolds number

$$Re = \frac{UD}{\nu} \quad (2.18)$$

$$Re = \frac{0.453 \times 0.025}{1.14 \times 10^{-6}}$$

$$Re = 9896$$

$$\lambda = \frac{0.3164}{Re^{0.25}} \quad (2.17)$$

$$\lambda = \frac{0.3164}{9943^{0.25}}$$

$$\lambda = 0.032$$

When the assumed and the calculated friction factor are the same the integration is complete and the flow rate can be calculated.

$$Q = UA$$

$$Q = 0.453 \times \pi \times 0.025^2 \times 0.25$$

$$Q = 0.0002 \text{ m}^3/\text{s}$$

$$Q = 0.801 \text{ m}^3/\text{h}$$

$$Q = 19.230 \text{ m}^3/\text{day}$$

From the integration in Appendix B the desired flow rate of 0.709 m³/day was achieved by a 15 mm pipe together a ¼ open gate valve and a head of 200 mm and would feed the BSF at the correct rate.

A. 5. Design of gravity flow from holding tank to 500 L tank

In order to supply the 500 L tank, the sizing and flow rate of the pipe between the 5000 L holding tank and 500 L tank must be calculated in order to adequately fill the 500 L tank. An assumed K is used to determine the actual K as described in Section 3.4.4.

Assumed friction factor	$\lambda = 0.05$
Total head	$H = 4 \text{ m}$
Length of pipe	$l = 20 \text{ m}$
Water Density	$\rho = 1000 \text{ kg/m}^3$
Kinematic Viscosity at 15°C (Metcalf and Eddy, 2004)	$\nu = 1.14 \times 10^{-6} \text{ m}^2/\text{s}$
Pipe Diameter	$D = 25 \text{ mm}$

K-Values

Exit loss

$$K_{Exit} = 1$$

Inlet Loss

$$K_{Inlet} = 1$$

Fully open gate valve

$$K_{open\ gate\ valve} = 0.17$$

90° bend x 4

$$K_{90^\circ\ bend} = 0.75$$

A.5.1. K-Values

$$h_{Minor} = K \left(\frac{V^2}{2g} \right) \quad (2.19)$$

$$h_{Minor} = (1 + 1 + 0.17 + 0.75 \times 4) \left(\frac{V^2}{2g} \right)$$

$$h_{Minor} = 5.17 \left(\frac{V^2}{2g} \right)$$

A.5.2. Calculate the new frictional factor

$$h_1 + \frac{p_1}{\rho g} + \frac{U_1^2}{2g} = h_2 + \frac{p_2}{\rho g} + \frac{U_2^2}{2g} + h_f + h_m \quad (2.14)$$

$$h_1 + 0 + 0 = 0 + 0 + \frac{U_2^2}{2g} + \frac{\lambda U_2^2}{2gD} + K \left(\frac{U^2}{2g} \right)$$

$$U = \sqrt{\frac{2gh_1}{\left(1 + \frac{\lambda l}{D} + K\right)}}$$

$$U = \sqrt{\frac{2 \times 9.81 \times 4}{\left(1 + \frac{0.05 \times 20}{0.025} + 5.17\right)}}$$

$$U = 1.304\ m/s$$

$$Re = \frac{UD}{\nu} \quad (2.18)$$

$$Re = \frac{1.304 \times 0.025}{1.14 \times 10^{-6}}$$

$$Re = 28\ 591$$

$$\lambda = \frac{0.3164}{Re^{0.25}} \quad (2.17)$$

$$\lambda = \frac{0.3164}{28\ 591^{0.25}}$$

$$\lambda = 0.24$$

This friction factor is used for the assumed friction factor

Assumed friction factor $\lambda = 0.024$

$$U = \sqrt{\frac{2 \times 9.81 \times 4}{\left(1 + \frac{0.024 \times 20}{0.025} + 5.17\right)}}$$

$$U = 1.759 \text{ m/s}$$

$$Re = \frac{UD}{\nu} \quad (2.18)$$

$$Re = \frac{1.759 \times 0.025}{1.14 \times 10^{-6}}$$

$$Re = 38\,570$$

$$\lambda = \frac{0.3164}{38\,570^{0.25}}$$

$$\lambda = 0.023$$

This friction factor is used for the assumed friction factor

Assumed friction factor $\lambda = 0.023$

$$U = \sqrt{\frac{2 \times 9.81 \times 4}{\left(1 + \frac{0.023 \times 20}{0.025} + 5.17\right)}}$$

$$U = 1.787 \text{ m/s}$$

$$Re = \frac{UD}{\nu} \quad (2.18)$$

$$Re = \frac{1.787 \times 0.025}{1.14 \times 10^{-6}}$$

$$Re = 39\,193$$

$$\lambda = \frac{0.3164}{39\,193^{0.25}}$$

$$\lambda = 0.022$$

This friction factor is used for the assumed friction factor

Assumed friction factor $\lambda = 0.022$

$$U = \sqrt{\frac{2 \times 9.81 \times 4}{\left(1 + \frac{0.022 \times 20}{0.025} + 5.17\right)}}$$

$$U = 1.817 \text{ m/s}$$

$$Re = \frac{UD}{\nu} \quad (2.18)$$

$$Re = \frac{1.817 \times 0.025}{1.14 \times 10^{-6}}$$

$$Re = 39\,847$$

$$\lambda = \frac{0.3164}{39\,847^{0.25}}$$

$$\lambda = 0.022$$

Calculate discharge

$$Q = UA$$

$$Q = 1.817 \times \pi \times 0.025^2 \times 0.25$$

$$Q = 0.0010 \text{ m}^3/\text{s}$$

$$Q = 3.211 \text{ m}^3/\text{h}$$

The discharge is far greater than the flow rate of all 4 filters therefore a 25 mm pipe will adequately supply the 500 L tank and keep a constant head.

A. 6. Design of pumping main

The system curve must be calculated to plot against the pump curve to determine the duty point. The description of the method used to calculate can be found in Chapter 3.4.5. An assumed duty point was used to determine the friction factor and thus the system curve.

Total head	$H = 9.5 \text{ m}$
Length of pipe	$L = 25 \text{ m}$
Water Density	$\rho = 1000 \text{ kg/m}^3$
Kinematic Viscosity at 15°C (Metcalf and Eddy, 2004)	$\nu = 1.14 \times 10^{-6} \text{ m}^2/\text{s}$
Pipe Diameter	$D = 25 \text{ mm}$
K-Values	
Sudden enlargement 15 mm to 25 mm	Calculate
Sudden contraction 90 mm to 25 mm	Calculate
Sudden contraction 25 mm to 15 mm	Calculate
Exit loss	$K_{Exit} = 1$
Inlet Loss	$K_{Inlet} = 1$
Fully open gate valve	$K_{open \text{ gate valve}} = 0.17$
90° bend x 5	$K_{90^\circ \text{ bend}} = 0.75$

A.6.1. Using the assumed duty point to determine the friction factor

$$Q = \frac{U}{A}$$

$$U = \frac{Q}{A}$$

$$U = \frac{0.62 \div 60 \div 60}{\pi \left(\frac{0.025}{2}\right)^2}$$

$$U = 0.351 \text{ m/s}$$

$$Re = \frac{UD}{\nu} \quad (2.18)$$

$$Re = \frac{0.351 \times 0.025}{1.14 \times 10^{-6}}$$

$$Re = 7694$$

$$\lambda = \frac{0.3164}{Re^{0.25}} \quad (2.17)$$

$$\lambda = \frac{0.3164}{7694^{0.25}}$$

$$\lambda = 0.03$$

A.6.2. K-Values and Minor losses

Sudden enlargement losses 15 mm to 25 mm

$$K_{Enlargment} = \left[\left(\frac{A_1}{A_2} \right) - 1 \right]^2 \quad (0.2)$$

$$K_{Enlargment} = \left[\left(\frac{\pi 0.015^2 \div 4}{\pi 0.025^2 \div 4} \right) - 1 \right]^2$$

$$K_{Enlargment} = 0.41$$

Sudden contraction losses 90 mm to 25 mm and 25 mm to 15 mm and determination of K from table C.2

$$\frac{D_2}{D_1} = \frac{0.025}{0.090}$$

$$K_{Contraction} = 0.43$$

$$\frac{D_2}{D_1} = \frac{0.015}{0.025}$$

$$K_{Contraction} = 0.28$$

Calculating head loss due to minor losses

$$h_{Minor} = K \left(\frac{U^2}{2g} \right) \quad (2.19)$$

$$h_{Minor} = (0.41 + 0.43 + 0.28 + 1 + 1 + 0.17 + 0.75) \left(\frac{U^2}{2g} \right)$$

$$h_{Minor} = 4.04 \left(\frac{U^2}{2g} \right)$$

A.6.3. Major losses using Darcy-Weisbach equation

$$h_f = \frac{\lambda/4 \times l \times Q^2}{3.03 \times D^5} \quad (2.16)$$

A.6.4. Determine system curve using a system curve

$$h_{total} = h_{static} + h_f + h_m \quad (2.21)$$

$$h_{total} = \frac{\lambda U^2}{2gD} + K \left(\frac{U^2}{2g} \right)$$

$$h_{total} = \frac{\lambda/4 \times l \times Q^2}{3.03 \times D^5} + \frac{K \times 8 \times Q^2}{g \times \pi^2 \times D^4}$$

$$h_{total} = \frac{\frac{0.03}{4} \times 25 \times Q^2}{3.03 \times 0.025^5} + \frac{4.04 \times 8 \times Q^2}{9.81 \times \pi^2 \times 0.025^4}$$

$$h_{total} = 7191194 Q^2 \quad (4.1)$$

Equation (4.1) was used to determine the system curve with different flow rates.

Appendix B. Integration of flow rate

Table B.1 Integration of flow rate table 1 of 3

Supply Tank							Pipe				
Diameter (m)	Vol (m ³)	h (m)	K	Assume (λ)	Length (m)	v (m/s)	d (m)	a (m ²)	Q (m ³ /s)	Q (m ³ /hr)	Q (m ³ /day)
32 mm											
0.83	0.271	0.5	32.0	0.029	4	0.518	0.032	8E-04	0.0004	1.499	35.972
0.83	0.216	0.4	32.0	0.030	4	0.462	0.032	8E-04	0.0004	1.338	32.120
0.83	0.162	0.3	32.0	0.030	4	0.400	0.032	8E-04	0.0003	1.159	27.817
0.83	0.108	0.2	32.0	0.032	4	0.326	0.032	8E-04	0.0003	0.943	22.635
0.83	0.054	0.1	32.0	0.035	4	0.229	0.032	8E-04	0.0002	0.664	15.925
25 mm											
0.83	0.271	0.5	32.0	0.031	4	0.508	0.025	5E-04	0.0002	0.898	21.554
0.83	0.216	0.4	32.0	0.032	4	0.454	0.025	5E-04	0.0002	0.802	19.238
0.83	0.162	0.3	32.0	0.033	4	0.392	0.025	5E-04	0.0002	0.693	16.626
0.83	0.108	0.2	32.0	0.035	4	0.319	0.025	5E-04	0.0002	0.563	13.519
0.83	0.054	0.1	32.0	0.038	4	0.224	0.025	5E-04	0.0001	0.396	9.500
20 mm											
0.83	0.271	0.5	32.0	0.033	4	0.498	0.02	3E-04	0.0002	0.563	13.513
0.83	0.216	0.4	32.0	0.034	4	0.444	0.02	3E-04	0.0001	0.502	12.056
0.83	0.162	0.3	32.0	0.035	4	0.384	0.02	3E-04	0.0001	0.434	10.415
0.83	0.108	0.2	32.0	0.037	4	0.312	0.02	3E-04	1E-04	0.353	8.461
0.83	0.054	0.1	32.0	0.040	4	0.219	0.02	3E-04	7E-05	0.247	5.939
15 mm											
0.83	0.271	0.5	32.1	0.036	4	0.479	0.015	2E-04	8E-05	0.305	7.316
0.83	0.216	0.4	32.1	0.037	4	0.427	0.015	2E-04	8E-05	0.272	6.524
0.83	0.162	0.3	32.1	0.038	4	0.369	0.015	2E-04	7E-05	0.235	5.632
0.83	0.108	0.2	32.1	0.040	4	0.299	0.015	2E-04	5E-05	0.190	4.571
0.83	0.054	0.1	32.1	0.044	4	0.209	0.015	2E-04	4E-05	0.133	3.193
10 mm											
0.83	0.271	0.5	32.3	0.040	4	0.446	0.01	8E-05	4E-05	0.126	3.026
0.83	0.216	0.4	32.3	0.041	4	0.397	0.01	8E-05	3E-05	0.112	2.695
0.83	0.162	0.3	32.3	0.043	4	0.341	0.01	8E-05	3E-05	0.096	2.316
0.83	0.108	0.2	32.3	0.045	4	0.276	0.01	8E-05	2E-05	0.078	1.876
0.83	0.054	0.1	32.3	0.049	4	0.193	0.01	8E-05	2E-05	0.054	1.306

Table B.2 Integration of flow rate table 2 of 3

Head of Friction calculations				K - Values									
				Sudden Enlargment			Exit Loss		Sudden Contraction				
Viscosity	Re	Friction Final (λ)	hf (m)	D1 - Inlet (mm)	D2 (mm)	No (mm)	K	No	K	D1 (mm)	D2 (mm)	No	K
32 mm													
1.14E-06	14532	0.029	0.197	0.032	0.040	1	0.13	1	1	0.040	0.032	2	0.14
1.14E-06	12975	0.030	0.161	0.032	0.040	1	0.13	1	1	0.040	0.032	2	0.14
1.14E-06	11237	0.031	0.125	0.032	0.040	1	0.13	1	1	0.040	0.032	2	0.14
1.14E-06	9144	0.032	0.087	0.032	0.040	1	0.13	1	1	0.040	0.032	2	0.14
1.14E-06	6433	0.035	0.047	0.032	0.040	1	0.13	1	1	0.040	0.032	2	0.14
25 mm													
1.14E-06	11145	0.031	0.259	0.025	0.032	1	0.15	1	1	0.032	0.025	2	0.15
1.14E-06	9947	0.032	0.212	0.025	0.032	1	0.15	1	1	0.032	0.025	2	0.15
1.14E-06	8597	0.033	0.165	0.025	0.032	1	0.15	1	1	0.032	0.025	2	0.15
1.14E-06	6990	0.035	0.115	0.025	0.032	1	0.15	1	1	0.032	0.025	2	0.15
1.14E-06	4912	0.038	0.062	0.025	0.032	1	0.15	1	1	0.032	0.025	2	0.15
20 mm													
1.14E-06	8734	0.033	0.330	0.020	0.025	1	0.13	1	1	0.025	0.020	2	0.14
1.14E-06	7792	0.034	0.271	0.020	0.025	1	0.13	1	1	0.025	0.020	2	0.14
1.14E-06	6732	0.035	0.209	0.020	0.025	1	0.13	1	1	0.025	0.020	2	0.14
1.14E-06	5469	0.037	0.146	0.020	0.025	1	0.13	1	1	0.025	0.020	2	0.14
1.14E-06	3839	0.040	0.078	0.020	0.025	1	0.13	1	1	0.025	0.020	2	0.14
15 mm													
1.14E-06	6305	0.036	0.443	0.015	0.020	1	0.19	1	1	0.020	0.015	2	0.18
1.14E-06	5622	0.037	0.362	0.015	0.020	1	0.19	1	1	0.020	0.015	2	0.18
1.14E-06	4854	0.038	0.280	0.015	0.020	1	0.19	1	1	0.020	0.015	2	0.18
1.14E-06	3939	0.040	0.194	0.015	0.020	1	0.19	1	1	0.020	0.015	2	0.18
1.14E-06	2752	0.044	0.104	0.015	0.020	1	0.19	1	1	0.020	0.015	2	0.18
10 mm													
1.14E-06	3911	0.040	0.648	0.010	0.015	1	0.31	1	1	0.015	0.010	2	0.23
1.14E-06	3484	0.041	0.529	0.010	0.015	1	0.31	1	1	0.015	0.010	2	0.23
1.14E-06	2994	0.043	0.406	0.010	0.015	1	0.31	1	1	0.015	0.010	2	0.23
1.14E-06	2425	0.045	0.281	0.010	0.015	1	0.31	1	1	0.015	0.010	2	0.23
1.14E-06	1689	0.049	0.149	0.010	0.015	1	0.31	1	1	0.015	0.010	2	0.23

Table B.3 Integration of flow rate table 3 of 3

K - Values													Sum of all the K Values
Inlet losses			Gate Valve					Bends					
Inward	square	K	Fully open	3/4	1/2	1/4	K	90° Bend	45° Elbow	T flow through	T Flow Branch	K	
			0.17	0.9	4.5	24		0.75	0.35	0.4	1		
<u>32 mm</u>													
1	0	1	1	0	0	1	24.2	4	0	1	2	5.4	31.98
1	0	1	1	0	0	1	24.2	4	0	1	2	5.4	31.98
1	0	1	1	0	0	1	24.2	4	0	1	2	5.4	31.98
1	0	1	1	0	0	1	24.2	4	0	1	2	5.4	31.98
1	0	1	1	0	0	1	24.2	4	0	1	2	5.4	31.98
<u>25 mm</u>													
1	0	1	1	0	0	1	24.2	4	0	1	2	5.4	32.02
1	0	1	1	0	0	1	24.2	4	0	1	2	5.4	32.02
1	0	1	1	0	0	1	24.2	4	0	1	2	5.4	32.02
1	0	1	1	0	0	1	24.2	4	0	1	2	5.4	32.02
1	0	1	1	0	0	1	24.2	4	0	1	2	5.4	32.02
<u>20 mm</u>													
1	0	1	1	0	0	1	24.2	4	0	1	2	5.4	31.98
1	0	1	1	0	0	1	24.2	4	0	1	2	5.4	31.98
1	0	1	1	0	0	1	24.2	4	0	1	2	5.4	31.98
1	0	1	1	0	0	1	24.2	4	0	1	2	5.4	31.98
1	0	1	1	0	0	1	24.2	4	0	1	2	5.4	31.98
<u>15 mm</u>													
1	0	1	1	0	0	1	24.2	4	0	1	2	5.4	32.12
1	0	1	1	0	0	1	24.2	4	0	1	2	5.4	32.12
1	0	1	1	0	0	1	24.2	4	0	1	2	5.4	32.12
1	0	1	1	0	0	1	24.2	4	0	1	2	5.4	32.12
1	0	1	1	0	0	1	24.2	4	0	1	2	5.4	32.12
<u>10 mm</u>													
1	0	1	1	0	0	1	24.2	4	0	1	2	5.4	32.34
1	0	1	1	0	0	1	24.2	4	0	1	2	5.4	32.34
1	0	1	1	0	0	1	24.2	4	0	1	2	5.4	32.34
1	0	1	1	0	0	1	24.2	4	0	1	2	5.4	32.34
1	0	1	1	0	0	1	24.17	4	0	1	2	5.4	32.34

Appendix C. *K* values for minor losses

The *K* values for the various fittings have been expressed in Table C.1. For sudden enlargements, the *K* value must be calculated using equation (0.2) (Nalluri et al., 2009). For sudden contractions, the *K* value can be found on the following Table C.1.

Table C.1 *K* values for various fittings (Adapter from Nalluri et al., 2009; Upadhyay, 2010)

Description	<i>K</i> value
Exit loss	1
Inlet Loss	1
Fully open gate valve	0.17
¼ open gate valve	24
90° bend	0.75
T flow through	0.4
T flow branch	1

$$K_{Enlargment} = \left[\left(\frac{A_1}{A_2} \right) - 1 \right]^2 \quad (0.2)$$

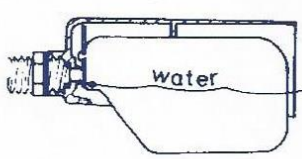
Table C.2 *K* values for sudden contraction in circular pipe (Adapter from Nalluri et al., 2009)

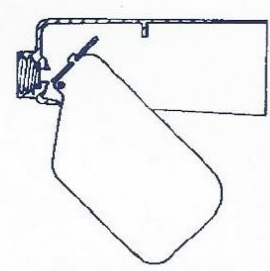
D_2/D_1	0	0.2	0.4	0.6	0.8	1.0
<i>K</i>	0.5	0.45	0.38	0.28	0.14	0

Appendix D. Brochure for Aqua-brooks float valve

Visit our website
www.aqua-brooks.co.za

"aqua-brooks"





FLOW - litres per hour VLOEI - liters per uur		
Class Colour Klas Kleur	Supply (kPa) Voorsiening	Flow Vloei
H.P. White	2000 max.	1200
" "	800	600
L.P. Red	800 max.	1800
" "	200	1100
X.L.P. Black	200 max.	2200
" "	100	1600
U.L.P. Grey	100 max.	2500
" "	50	1500

Veesuipingsklep more litres p.h.
 meer liters p.h.
Stockmans valve

Figure D.1 Brochure for Aqua-Brooks float valve

Appendix E. Costing for Biological Sand filter

The detailed cost of the different components used to build the BSF have been listed.

Table E.1 Initial setup costing for biological sand filter treatment system, February 2015.

Quantity	Description	Price	Sub Total
Solar Pump and Controls			R 19965.30
1	Shurflo 12V DC Diaphragm Premium Demand Pump Kit	R 10725.80	R 10725.80
1	TE101 12VDC LIQUID LEVEL RELAY 1C/O	R 204.49	R 204.49
1	ZRUV 11PIN BASE (RECTANGULAR)	R 80.21	R 80.21
2	ALB-80 12VDC AUTOMOTIVE RELAY 80A	R 45.38	R 90.76
1	BM00380/20 4-6MM YELLOW INS 6.3MM	R 11.90	R 11.90
1	KEY-P6 PANEL KEY 6MM SQ POLYCARB	R 5.56	R 5.56
1	RF-OV41 VERTICAL LEVEL SW M16 0.5A	R 265.34	R 265.34
1	CP2/C 2WAY CONDUCTIVE PROBE UNIT	R 187.53	R 187.53
2	BMF4001 ALUMINIUM PROFILE FOR S-PANEL	R 566.87	R 1133.74
2	BMF4301 TRIANGLE BRACKET FOR S/PANEL	R 658.35	R 1316.70
1	BMF4023 SOLAR PANEL END CLAMP 36MM	R 521.55	R 521.55
1	BMF4004 S/STEEL SCREW M8X20 H/HEAD	R 472.82	R 472.82
1	BMF4006 S/STEEL SCREW M8X20 HEX HEAD	R 198.36	R 198.36
1	EC23406 FLEXIBLE SLOTTED TRUNKING	R 134.67	R 134.67
1	DR35S-1M DIN 35 SLOTTED YELLOW RAIL	R 15.74	R 15.74
1	INSULATION TAPE 10M RED	R 7.00	R 7.00
1	INSULATION TAPE 10M BLK	R 7.00	R 7.00
1	STB10-BK 10MM 16A 12WAY S/CONNECTOR	R 10.84	R 10.84
1	STB10-BK 6MM 10A 12WAY S/CONNECTOR	R 8.15	R 8.15
1	SW103/5 6MM BLACK SOLAR CABLE /5M	R 117.71	R 117.71
10	16MM BLACK PERMOWELD CABLE P/M	R 31.57	R 315.70
10	16MM RED PERMOWELD CABLE P/M	R 31.57	R 315.70
10	CABLE HOUSE WIRE 6MM BLK (PER M)	R 12.60	R 126.00
10	CABLE HOUSE WIRE 6MM RED (PER M)	R 12.60	R 126.00
40	CABLE SURFIX 1.5MMX2CORE+E RND BLK (P/M)	R 11.20	R 448.00
1	TJ-MG-3040 ENCLOSURE 300X400X180 GR	R 696.26	R 696.26
1	MB-8060D320-O ORANGE STEEL ENCL.	R 1850.37	R 1850.37
10	6MM SOLAR CABLE Black (ALVERN)	R 22.23	R 222.30
2	P.V.C. 20MM CONDUIT (PER LENGTH)	R 14.95	R 29.90
1	P.V.C. 20MM 3WAY BOX "Y"	R 11.60	R 11.60
6	P.V.C. 20MM FEMALE ADAPTOR EA	R 1.70	R 10.20
1	P.V.C. WELD GLUE WITH BRUSH 200ML	R 23.70	R 23.70
1	P.V.C. BOX LID ROUND	R 1.70	R 1.70
10	BOLTS MACHINE SCREWS GALV.CSK 4X10MM	R 0.30	R 3.00
8	SURFIX GLANDS #1 ROUND WHITE"RED"	R 2.10	R 16.80

2	GLAND CONDUIT #0 "PUSH IN GLAND"	R	2.10	R	4.20
1	Circute Breaker 2P 16A D 6kA DIN MCB 2M	R	248.00	R	248.00
Pipes and Fittings				R	2947.67
25	0.75MM THREAD TAPE	R	2.25	R	56.25
4	20MM GATE VALVE	R	47.73	R	190.92
1	25 X 15 MM MI X FI	R	5.06	R	5.06
11	25MM PVC BALL VALVE	R	19.62	R	215.82
11	25MM STRAIGHT MI X P	R	3.00	R	33.00
15	40 X 25MM MI X FI	R	9.49	R	142.35
9	40MM PVC BALL VALVE	R	38.34	R	345.06
8	40MM STRAIGHT MI X P	R	7.89	R	63.12
1	50 X 32MM MI X FI	R	10.90	R	10.90
2	90 25 X 20MM MI X P	R	4.49	R	8.98
5	90 25MM FI X P	R	18.39	R	91.95
18	90 25MM MI X P	R	4.54	R	81.72
13	90 25MM P X P	R	3.55	R	46.15
13	NIPPLE 25 X 25MM MI X MI	R	5.38	R	69.94
70	Pipe 25mm LDPE class 3/m	R	2.92	R	204.40
35	Pipe 25mm LDPE class 6 /m	R	4.77	R	166.95
2	Pipe 40mm LDPE class 3 /m	R	5.32	R	10.64
2	Pipe 32mm LDPE class 6 /m	R	7.50	R	15.00
10	T 25MM FI X FI X FI	R	19.66	R	196.60
2	T 25MM P X MI X P	R	7.84	R	15.68
4	T 25MM P X P X P	R	4.75	R	19.00
100	TIE FOR 25MM PIPE	R	2.93	R	293.00
2	T 25 X 20 X 25MM P X MI X P	R	7.59	R	15.18
5	Aquabrooks Grey Ultra Low Pressure float valve	R	130.00	R	650.00
Tanks and Filters				R	21223.44
1	5000 L tank	R	3192.00	R	3192.00
4	1000L drinking through (J)	R	2514.00	R	10056.00
7	40mm FI Tank Connector	R	62.70	R	438.90
4	40mm MI Tank Connector	R	666.90	R	2667.60
4	100l Poly Drum	R	1060.20	R	4240.80
1	500L Tank	R	67.26	R	67.26
4	25mm MI Tank Connector	R	77.52	R	310.08
4	50mm X 40mm MI x FI Two way Tank Connector	R	62.70	R	250.80
General				R	6000.00
1	5 m ³ of Philippi, 10 m ^m Fill sand and delivery	R	3000.00	R	3000.00
10	Labour	R	200.00	R	2 000.00
1	Transport	R	1000.00	R	1000.00
Total				R	50136.41

Characterisation of winery wastewater from continuous flow settling basins and waste stabilisation ponds over the course of 1 year: implications for biological wastewater treatment and land application

P. J. Welz, G. Holtman, R. Haldenwang and M. le Roes-Hill

ABSTRACT

Wineries generate 0.2 to 4 L of wastewater per litre of wine produced. Many cellars make use of irrigation as a means of disposal, either directly or after storage. In order to consider the potential downstream impacts of storage/no storage, this study critically compared the seasonal organic and inorganic composition of fresh winery effluent with effluent that had been stored in waste stabilisation ponds. Ethanol and short chain volatile fatty acids were the main contributors to chemical oxygen demand (COD), with average concentrations of 2,086 and 882 mgCOD/L, respectively. Total phenolics were typically present in concentrations <100 mg/L. The concentration of sodium from cleaning agents was higher in the non-crush season, while the converse was true for organics. The effluent was nitrogen-deficient for biological treatment, with COD:N ratios of 0.09 to 1.2. There was an accumulation of propionic and butyric acid during storage. The composition of the pond effluent was more stable in character, and it is possible that bacterial and algal nitrogen fixation in such systems may enhance biological wastewater treatment by natural nitrogen supplementation. It is therefore recommended that if land requirements can be met, winery effluent should be stored in ponds prior to treatment.

Key words | characterisation, organics, seasonal variation, waste stabilisation pond, winery wastewater

INTRODUCTION

Studies have found that for each litre of wine that is produced, between 0.2 and 4 L of wastewater is generated (Vlyssides *et al.* 2005; Bolzonella & Rosso 2013). Most of this effluent originates from a variety of seasonal cleaning activities associated with winemaking, and typically has a high chemical oxygen demand (COD) concentration and low pH (Vlyssides *et al.* 2005; Bories & Sire 2010). The volume and chemical composition (inorganic and organic) of the wastewater are highly variable and depend on the grape varietal, the influent wash-water chemistry, the cellar activities from which it is generated, and the cleaning/sanitising products employed (Vlyssides *et al.* 2005;

Bolzonella & Rosso 2013). From an inorganic perspective, sodium-based cleaning and sanitising products are still used in most wineries (Bories & Sire 2010; Mosse *et al.* 2013). Caustic soda (NaOH), in particular, is very effective and affordable, a fact which is retarding the move to more environmentally friendly alternatives. From an organic perspective, cellar activities (e.g. grape crushing, fermentation, maturation/stabilisation, decanting and bottling) largely determine the effluent character (Bories & Sire 2010). For instance, the concentration of ethanol is high when vats are emptied and washed out, but low when crushing equipment is cleaned. The converse applies for sugars.

The grape varietal used to make the wine may also have a major impact on the organic character, especially during the crush season. For example, when comparing the crushing of late harvest white grapes with early harvest red varieties, fresh wastewater is characterised by high

P. J. Welz (corresponding author)
M. le Roes-Hill
Biocatalysis and Technical Biology (BTB) Research Group,
Institute of Biomedical and Microbial Biotechnology, Cape Peninsula University of Technology,
PO Box 1906,
Bellville 7535,
South Africa
E-mail: welzp@cput.ac.za

G. Holtman
R. Haldenwang
Department of Civil Engineering,
Cape Peninsula University of Technology,
PO Box 1906,
Bellville 7535,
South Africa

This is an Open Access article distributed under the terms of the Creative Commons Attribution Licence (CC BY 4.0), which permits copying, adaptation and redistribution, provided the original work is properly cited (<http://creativecommons.org/licenses/by/4.0/>).

doi: 10.2166/wst.2016.226

sugar/low total phenolic, or low sugar/high total phenolic concentrations, respectively (Malandra *et al.* 2003; Devesa-Rey *et al.* 2011; Bolzonella & Rosso 2013).

Most winery wastewater is discharged into municipal reticulation systems or irrigated onto agricultural or other nearby land. Chemical and/or biological treatment to enhance the 'quality' of the water may precede disposal (Aybar *et al.* 2007; Andreoletta *et al.* 2009; Mosse *et al.* 2011a). Ideally wineries should make it their responsibility to understand any adverse environmental impacts that may arise from discharging liquid and solid waste products, and institute measures to mitigate these.

Whether stemming from the need to comply with legislative requirements and/or an environmentally aware ethos of individual winemakers, most cellars test their effluent for selected parameters. The frequency of sampling and range of parameters differs from winery to winery and country to country, and results are not widely published and interpreted, or accessible. To assist wineries and wastewater treatment engineers/consultants to design and/or implement effective treatment systems, and government agencies to benchmark legislative discharge requirements, there is a need for more comprehensive studies on the characterisation and critical evaluation of different components of winery effluent. This study focused on the characterisation and comparison of winery effluent from: (i) waste stabilisation ponds (WSPs) at two large wineries that crush >10,000 tons of grapes/annum, (ii) 'fresh' wastewater from a small winery generating approximately 800 m³ wastewater per annum, and (iii) 'fresh' wastewater from a medium-sized winery generating approximately 5,000 m³ of wastewater per annum. Samples were taken monthly for a period of 1 year, with weekly samples being taken over the high crush season.

MATERIALS AND METHODS

Sample sites and collection

Four wineries in the Western Cape Province of South Africa were identified. In all instances, the effluent was disposed of via irrigation on adjacent grasslands/pastureland dedicated to this purpose. This is historically the primary means of effluent disposal at small to medium-sized wineries in South Africa. In order to compare the character of freshly produced effluent with stored effluent, samples were taken from two concrete settling basins ((SBs) Wineries A and B), where effluent was rapidly pre-settled and pH adjusted,

and from two WSPs into which effluent was pumped and stored prior to irrigation (Wineries C and D). All the study sites were located within a 50 km radius of one another. The wineries all crush grapes, and produce and bottle wines on the premises, which is typical of many wineries in South Africa. The ponds only serve as repositories for wastewater storage prior to irrigation, not as treatment systems, and are the only two such systems in the area. Likewise, the SBs only serve as rudimentary systems for settling larger particles that may otherwise block the irrigation infrastructure. The dimensions (length × width × depth) are as follows: Winery A (11 m × 5 m × 1 m), Winery B (8 m × 5 m × 1 m), Winery C (100 m × 40 m × 3 m), Winery D (50 m × 16 m × 3.5 m). The water column height, especially in the WSP at Winery C, varies throughout the year, depending on inflow and abstraction for irrigation, which is not routinely monitored. The retention times in all systems are highly variable, and it is assumed that they are lowest during the crushing and bottling seasons. Samples were taken each month for a period of 1 year, and each week during the 'high' crush season. Three samples were taken from each site at each sampling instance. For the ponds, three sites spread around the perimeter were identified and the same sites were used each month. For the SBs, samples were taken close to the inlet, at the middle of the basins, and close to the outlet. All samples were taken on the same day each month.

For total dissolved solids and total suspended solids, grab samples were taken in 1 L glass screw-capped Schott® bottles. For the remaining analyses, grab samples were taken in sterile 50 mL Falcon tubes. All samples were transported immediately to the laboratory for analysis.

Characterisation of effluent

pH

The pH was determined on the day of sample collection using a pH700 meter and probe (Eutech Instruments, Singapore), according to the manufacturer's instructions.

COD, total nitrogen, total phosphorus, nitrate, nitrite and ammonia

The COD, total nitrogen (TN), total phosphorus (TP), nitrate (NO₃⁻), nitrite (NO₂⁻) and ammonia (NH₃) were determined on unfiltered wastewater samples using a Merck Spectroquant® Pharo instrument (Merck, Darmstadt, Germany), together with Merck Spectroquant® cell tests or reagents

according to the manufacturer's instructions: COD (cell test: cat no. 1.14540 and 1.14541), TN (cell test: cat no. 1.14537), TP (cell test: cat no. 1.14543), NO_3^- (reagent kit: cat no. 1.09713), NO_2^- (cell test: 1.14547) and NH_3 (reagent kit: 1.00683). The COD was determined on the day of sampling. Due to time constraints, other parameters were determined the following day. All samples were kept at 4 °C until analysis.

Total phenolics

The concentration of total phenolics was determined on unfiltered wastewater samples using the Folin-Ciocalteu micro method for total phenolics in wine, based on the method reported by Slinkard & Singleton (1977), using Folin-Ciocalteu reagent (Merck).

Sodium and potassium

Concentrations of sodium and potassium were determined on unfiltered wastewater samples using a Varian[®] MPX ICP-OES spectrophotometer (Agilent Technologies, Santa Clara, USA) at Bemblab (Pty) Ltd (Strand, South Africa).

Volatile fatty acids (VFAs)

Two different methods were used to determine the concentrations of VFAs in the samples. Firstly, a spectrophotometric method was used to determine the overall VFA concentration in unfiltered samples, and secondly, high-performance liquid chromatography (HPLC) was used to quantify the concentrations of acetic, propionic and butyric acids in filtered samples. The unfiltered samples included possible contributions from organic solids, while the filtered samples did not. The total VFA concentration was determined using a Merck Spectroquant[®] Pharo spectrophotometer and the Hach (Loveland, USA) esterification method 8196, according to the manufacturer's instructions. Concentrations were determined using a graph prepared using standard solutions of acetic acid, and concentrations were given in mg acetate/L.

Sugars, ethanol, glycerol, VFAs and organic acids

Glucose, fructose, maltose, ethanol, lactic acid, tartaric acid, malic acid, succinic acid, acetic acid, propionic acid, butyric acid and glycerol were identified and quantified using reverse phase HPLC with filtered wastewater samples: samples were separated using a Phenomenex (Torrance, USA) Rezex RHM-monosaccharide H^+ (8% cross-linkage) column and an

Agilent Technologies 1100 series (Santa Clara, USA) equipped with a diode array ultraviolet detector set at 210 nm, and an Agilent Technologies 1200 series refractive index detector. The mobile phase consisted of 1 mM H_2SO_4 solution at pH 2.5 and the sample acquisition time and flow rate were set at 60 min and 0.550 mL/min, respectively.

The identities of the organic molecules were confirmed by spiking experiments. Standard graphs were prepared by plotting the absorbance against the concentrations of relevant standard solutions prepared from analytical grade chemicals obtained from Sigma-Aldrich (St Louis, USA). Concentrations were determined from the standard graphs using instrument software (EZChrom, Agilent Technologies). To determine the relative contributions of individual organics to the overall COD, all concentrations were converted into COD terms using the method described by Welz *et al.* (2011).

Statistical analyses

All statistical analyses were performed using Microsoft Excel 2010. Significance of temporal differences was determined using two-factor analysis of variance without replication. Correlations were determined using a two-tailed t-test (two samples of unequal variance, 95% confidence).

RESULTS AND DISCUSSION

Sampling bias

Due to low hydraulic retention times (HRTs), samples taken from the SBs during high flow periods were seen as snapshots of the total wastewater generated each month, and it was recognised that this commonly employed sampling strategy does not account for temporal variations. Conversely, it was assumed that the samples taken from the WSPs were a better reflection of the monthly average.

COD

COD concentrations in SBs and WSPs

In a recent review, Iaonnou *et al.* (2015) reported the average influent concentration of 40 systems being used to treat winery wastewater to be 11,886 mgCOD/L (range: 320 to 49,105 mgCOD/L). In this study, the lowest and highest COD concentrations were determined in samples taken from the SBs at the small winery (Winery A) and the

medium-sized winery (Winery B), respectively (Winery A: average 905 mgCOD/L, range 28 to 7,265 mgCOD/L; Winery B: average 10,906 mgCOD/L; range 675 to 76,900 mgCOD/L) (Figure 1(a) and 1(b)). The average COD concentration in the effluent at Winery B was similar to the literature average reported by Iannou *et al.* (2015), while the concentration at Winery A was considered low. There was one high outlier in the results from Winery B (January 2015). During this month, in order to de-sludge the basin before the crush season, no fresh wastewater was added at the inlet. Evaporation of the liquid fraction resulted in the concentration of solids leading to anomalously high results for most parameters at Winery B during January, particularly in the sample taken at the inlet. However, even with removal of the outlier, there was an average ten-fold difference in COD concentration between the two SBs (Wineries A and B), confirming the common perception that cellar practices can significantly improve the quality of wastewater produced by individual wineries.

The concentration of organics and inorganics in winery effluent is a direct reflection of cellar practices (Sheridan *et al.* 2011). A number of best practices to reduce the volume and/or 'strength' of wastewater are applicable to the wine industry. These range from simple procedures

such as mopping up spills before washing down with water, the installation of self-closing nozzles on hoses, installation of effective devices for trapping solids, and creating staff awareness about the need to conserve water, to more expensive options such as the installation of cleaning-in-place equipment. In some instances attempts to reduce water consumption lead to an increase in the concentration of the inorganic and/or organic fraction of the wastewater, unless this is addressed simultaneously.

In contrast to the results from the SBs, samples taken from the WSPs exhibited similar COD concentration averages (Winery C: 5,143 mgCOD/L, range 470 to 8,840 mg/L; Winery D: 5,534 mgCOD/L; range 700 to 13,730 mgCOD/L) (Figure 1(c) and 1(d)), which were lower than the literature average reported by Iannou *et al.* (2015).

Monthly variation in COD concentrations

In the case of the SBs, there were random monthly variations in COD concentrations (Figure 1). In contrast, similar monthly trends were exhibited by the samples from the WSPs. The highest concentrations in the WSP samples occurred during the crush season in 2015, and were notably

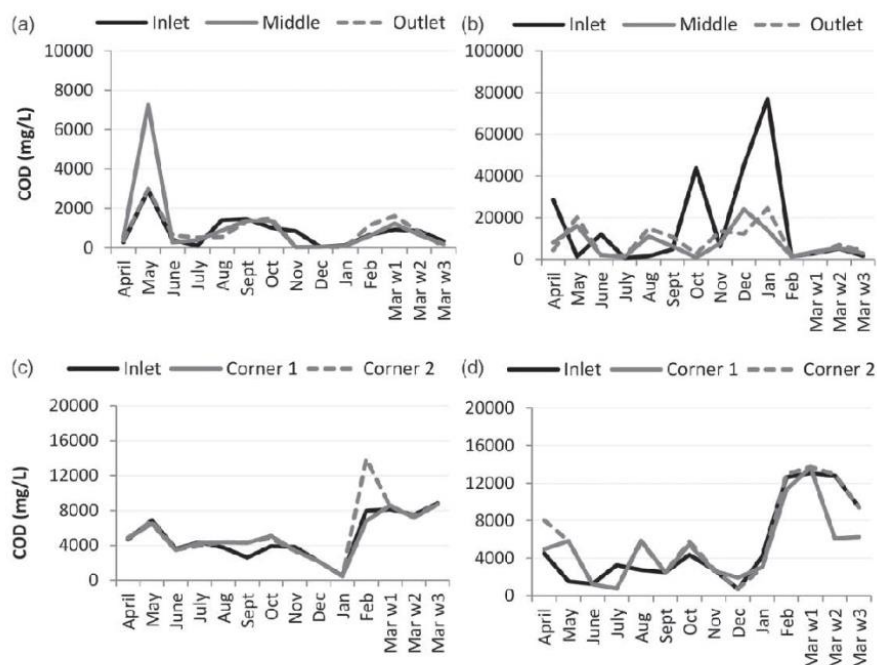


Figure 1 | COD concentrations measured in samples taken from the SBs at a small winery (a) and a medium-sized winery (b), and from WSPs at two large wineries (c) and (d) from April 2015 to March 2016.

higher at Winery D. In January 2015, there was an algal bloom in the pond at Winery C, which coincided with the lowest COD concentrations. It is postulated that the algae may have contributed to organic biodegradation at Winery C during this period. The algal growth abated during February 2015, and no visible growth was seen in either of the ponds at any other stage during the study period. This contrasts with ponds treating municipal effluent, where algae are typically abundant, and suggests that unless winery wastewater is dilute, it may be toxic to algae endemic to the area. It is unlikely that nutrient (N) limitation prevented algal growth in the winery ponds, as many algal species are capable of atmospheric nitrogen fixation.

The monthly variation in the COD concentration in samples taken from the SB at Winery A, and both WSPs (Wineries C and D) was highly significant ($p < 0.01$), but less significant in samples taken from the SB at Winery B ($0.01 < p < 0.05$), and it is postulated that this may have been related to the 'snapshot' sampling bias alluded earlier.

Compliance of COD concentrations with legislative requirements for irrigation

It has been shown that the typical biological oxygen demand (BOD_5)/COD ratio of winery wastewater is in the order of 0.5 to 0.8 (Quayle *et al.* 2009; Bolzonella & Rosso 2013), and is highest during the crush season (Oliveira & Duarte 2014). In South Africa, discharge standards are based on COD limits (and other parameters) applicable to the daily volume of wastewater that is applied via irrigation. In Australia, guidelines are based on BOD, take into account the area of land that is irrigated, and are applicable over a longer period (limit of 1,500 kgBOD/ha/month; Iannou *et al.* 2015). The Australian version is more complex for the wineries to calculate, but is more scientifically valid because the irrigation area is taken into account. This is important, because it has been shown that over-irrigation of land with winery wastewater results in significant soil degradation and microbial toxicity (Mosse *et al.* 2011b).

In terms of COD, the wastewater from 96% of samples from Winery A complied with South African legislative requirements for discharge via irrigation ($< 5,000$ mg COD/L for volumes < 500 m³/day or < 400 mg COD/L for volumes > 500 m³/day). Only 43%, 43% and 32% of samples from Wineries B, C and D complied with the upper COD discharge limit of 5,000 mg/L, and none with the lower limit of < 400 .

It is clear that winery wastewater should undergo more intensive treatment before being discharged to the

environment by irrigation or other means. Many different systems have been applied (with varying degrees of success) for the treatment of winery effluent, and have recently been reviewed by Lofrano & Meric (2016) and Inannou *et al.* (2015).

The organic fraction of winery wastewater

From an organic perspective, knowledge of COD concentration alone in winery effluent does not provide sufficient information for engineers wishing to design effective biological wastewater treatment systems, or for studying the functioning of such systems (Sheridan *et al.* 2011; Welz *et al.* 2012, 2014). This is because some of the organic components are highly biodegradable (e.g. sugars and alcohols), while others are recalcitrant and/or toxic to microbial communities and/or plants (e.g. many (poly)phenolics) (Arienzo *et al.* 2009a; Mosse *et al.* 2011b; Welz *et al.* 2012).

Non-phenolic organics

A variety of sugars, organic acids and alcohols contribute to the COD make-up of winery wastewater. In 'snapshot' samples taken from four wineries during the crush season, Malandra *et al.* (2003) identified 26 non-phenolic organics, and found that the fermentable sugars, glucose (0 to 1,800 mg/L), and fructose (0 to 1,530 mg/L) constituted almost half of the COD in some samples, but were absent in 33% and 11% ($n=9$), respectively. The authors also reported that acetic acid (27 to 663 mg/L) and ethanol (concentrations not given), contributed significantly to the overall COD. In a seasonal winery wastewater characterisation study, Sheridan *et al.* (2011) found ethanol and acetic acid to be the primary contributors to COD in two wineries, and did not detect glucose in any of the samples taken throughout the year. Apart from sugars, ethanol and acetic acid, other organics that have been reported to be present in relatively high concentrations are tartaric acid (0 to 530 mg/L), malic acid (0 to 70 mg/L), lactic acid (0 to 350 mg/L), succinic acid (40 to 80 mg/L), and glycerol (140 to 320 mg/L) (Mosse *et al.* 2011a; Bolzonella & Rosso 2013; Malandra *et al.* 2003). In light of previous findings, the range of non-phenolic organics quantified during this study was rationalised to short chain VFAs (acetic acid, propionic acid, butyric acid), ethanol, glycerol, tartaric acid, malic acid, lactic acid, succinic acid, glucose, fructose and maltose.

VFAs. For this study, the short chain VFAs commonly found in winery wastewater, namely acetic acid, propionic

acid and butyric acid, were considered. Previous studies have reported that acetic acid, which is a ubiquitous molecule involved in the central and subsidiary bacterial metabolic pathways, constitutes the major fraction of these VFAs (Malandra *et al.* 2003; Sheridan *et al.* 2011; Welz *et al.* 2014). Acetic acid can be absorbed and serve as a substrate for dissimilatory acetate utilisation, or assimilated and excreted by microorganisms (Wolfe 2005). It is the major substrate for the formation of propionic and butyric acid, and can be formed from the degradation of almost any organic molecule, including ethanol and (poly)phenolics (Welz *et al.* 2011, 2012). Although the short chain VFAs are generally considered as readily biodegradable molecules, this is not always the case; accumulation appears to be influenced significantly by the redox status of the environment (Conrad & Klose 2011; Welz *et al.* 2014).

VFAs can be formed from residuals in the winery, thereby constituting a fraction of the 'fresh' wastewater, or they can be formed from other organic molecules during the storage of wastewater. The high organic loads and HRTs in sedimentation basins and ponds in the absence of oxygen may favour anaerobic digestion, with concomitant VFA production. If anaerobic digestion is being considered as a method of COD reduction, it is important to note that acidification linked to high VFA concentrations can have a negative effect on methanogenic communities (Akuzawa *et al.* 2011).

In this study, VFAs were found in all of the samples from Wineries B, C and D, and in 75% of samples from the SB of (small) Winery A (Figure 2(a)). No hypotheses on the origin of VFAs in the samples from Wineries C and D are offered, because of the relatively long HRT in the ponds. Indeed, the results from Winery B, where there was a relatively short HRT, strongly suggest that significant formation occurred in the SB, because: (i) apart from samples taken in October 2014, December 2014 and January 2015, the concentration of VFAs was lowest in samples taken from the inlet, and highest in samples taken from the outlet of the SB (Figure 2(b)), suggesting sequential formation during wastewater movement through the SB; (ii) the highest concentrations of VFAs were found during the low flow/high HRT period in January 2015 (7,951–11,254 mg acetate/L), when VFAs were also the most substantial contributors to overall COD (Figure 2(a) and 2(c)); and (iii) low concentrations were found during the high flow/low HRT crush season.

However, there were three sampling instances when VFA concentrations were highest at the inlet of the SB basin at Winery B (demarcated by dotted circles in Figure 2(b)), indicating that VFAs were also formed in the cellar, and were

present in the incoming wastewater. On a monthly basis, the percentage of VFAs comprising the overall COD in the SBs was highly erratic, reflecting variable seasonal inputs from the cellar, when compared to the relative percentages in the WSPs, which were more stable (Figure 2(c) and 2(d)).

The concentrations of soluble short chain VFAs, acetic, propionic and butyric acids were measured and totalled. These molecules are considered to be readily biodegradable. In the SBs, there were instances where none of these molecules were detected, and also instances where only acetic acid was detected (Figure 3(a) and 3(b)). In contrast, all three VFAs were found in all of the samples from the WSPs, and propionic and butyric acid were typically found in higher concentrations than in the 'fresh' wastewater from the SBs (Figure 3(c) and 3(d)). The formation of propionic acid and the particularly malodorous butyric acid on storage of winery wastewater upon standing is problematic.

Ethanol. In this study, ethanol typically comprised a high fraction of the overall COD in the wastewater from both SBs and WSPs. If the origin of ethanol in winery wastewater could be definitely determined, it could be used as a proxy for product loss, and the need to identify best practices to reduce this. The highest concentrations determined were 2,377 mg/L, 21,000 mg/L, 1,539 mg/L and 4,896 mg/L from Wineries A through D, respectively. In samples from the SB at Winery A, the highest contributions to overall COD were seen out of crush season, constituting >50% of the COD in October and January (Figure 4(a)). In 'fresh' samples from the SB at Winery B, ethanol contributed to >50% of the overall COD in 50% of the samples, and >80% in 25% of the samples (Figure 4(a)). In these samples there was also a significant negative correlation between the contribution of VFAs and ethanol to the overall COD ($r = -0.76$; $p < 0.001$). In other words, when the VFA concentration was high, the ethanol concentration was relatively low, and vice versa.

Between 0 and 67% of the overall COD was comprised of ethanol in samples taken from the WSPs. Similar and clear seasonal changes were demonstrated at both wineries, with the lowest concentrations being seen in the non-crush period between September 2014 and January 2015 (Figure 4(b)). The contribution of ethanol to overall COD in the WSPs was typically lower than that from the 'fresh' wastewater at Winery B, and no negative correlation was seen between the % contribution of VFAs and ethanol.

These results highlight the fact that the complex organic formation/degradation kinetics has a notable impact on the composition of wastewater that has been exposed to the

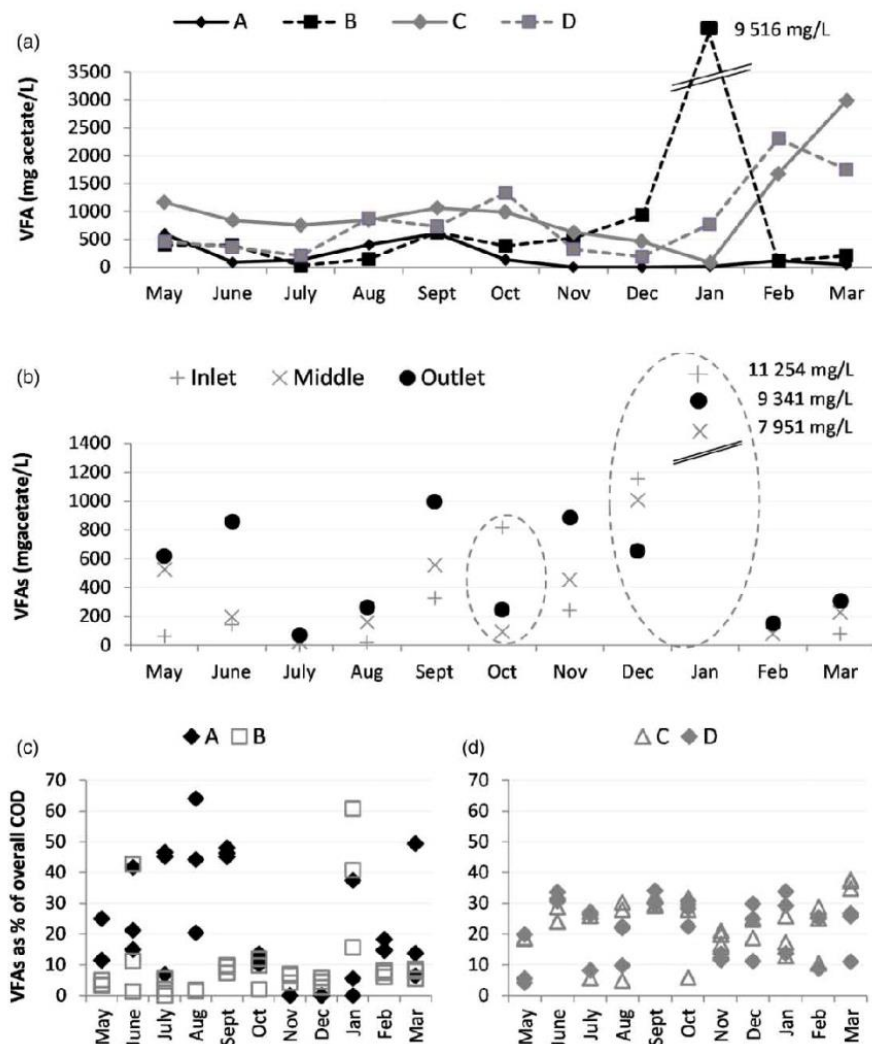


Figure 2 | Average monthly VFA concentrations (a), VFA concentrations at the inlet, middle and outlet of the SB at Winery B (b), % contribution of VFAs to overall COD in both SBs (c), and both WSPs (d).

environment for protracted time periods when compared to wastewater that has been recently generated. From a wastewater treatment perspective, ethanol, even in concentrations $>20,000$ mg/L, is readily biodegradable in biological wastewater treatment systems once the microbial community structure and function has acclimated to the prevailing chemical environment (Welz *et al.* 2011; Ma *et al.* 2013). Therefore, the presence of ethanol in the concentrations found in this study should not be deemed problematic.

Glycerol, organic acids and sugars. Holistically, ethanol and VFAs were major contributors to overall COD in the winery wastewater analysed during this study, while organic acids, glycerol and sugars were minor contributors (Table 1).

Of the minor organics, glycerol and tartaric acid were the most prevalent. The highest concentrations of glycerol ($>7,000$ mg/L) were found in the samples from the SBs, with the highest concentrations in both WSPs being notably lower ($<2,500$ mg/L), probably because of the highly biodegradable nature of this molecule. Malic acid, lactic acid and succinic acid were less prevalent, and found in lower concentrations in the samples from all sites. Relatively high concentrations of sugars (glucose, fructose and maltose) were typically only found around the crush period (results not shown). With the exception of Winery B, the sugars were prevalent in $<40\%$ of the samples. Although high concentrations of glucose were found during the crush period in the WSPs, this sugar

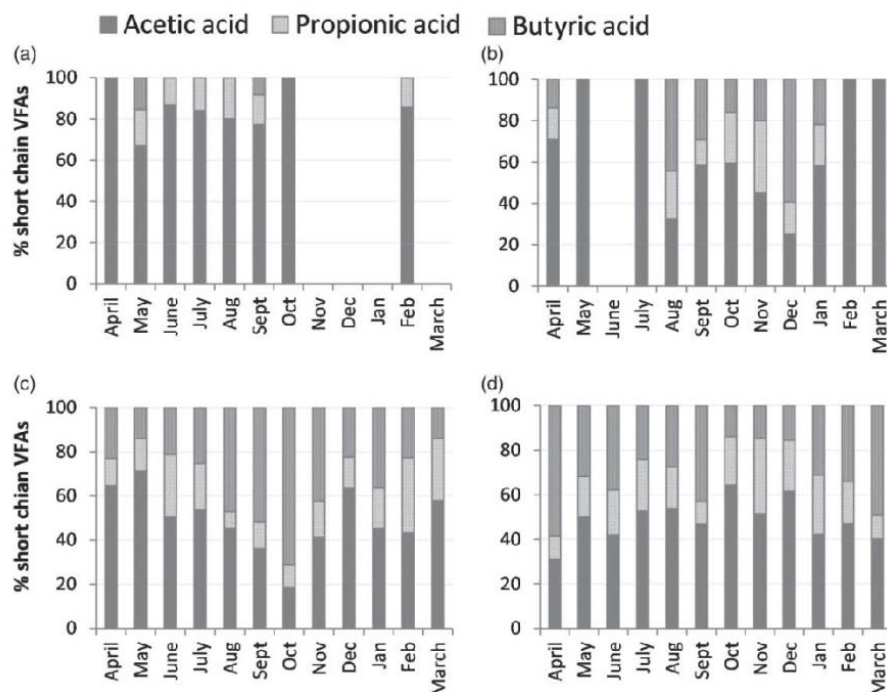


Figure 3 | Relative contributions of the short chain fatty acids from the SBs at Winery A (a) and Winery B (b), and from the WSPs at Winery C (c) and Winery D (d).

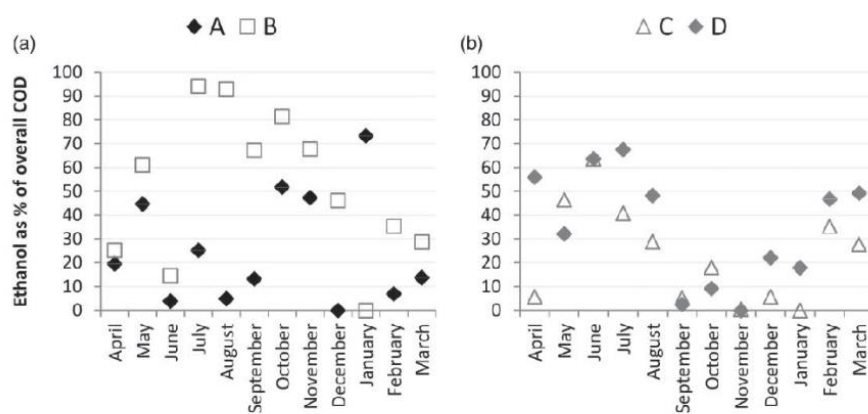


Figure 4 | Average % contribution of ethanol to the overall COD in both SBs (a) and both WSPs (b).

was only detected in samples taken from the inlet, reflecting the highly degradable nature of this molecule.

Total phenolics

It is generally accepted that the (poly)phenolic component of winery wastewater is the least degradable fraction. Once discharged to the environment, the different molecules can

polymerise/depolymerise, adsorb/desorb onto soil particles, undergo biotic and/or abiotic degradation, or remain recalcitrant to degradation (Coliarieti *et al.* 2002; Mutabaruka *et al.* 2007). Of concern to the wine industry is the fact that high concentrations of (poly)phenolics have been associated with phytotoxicity and microbial toxicity (Tharayil *et al.* 2006; Qu & Wang 2008, Welz *et al.* 2012). There are many factors that influence these toxic effects, most

Table 1 | Prevalence, concentration range and seasonality of minor non-phenolic organics in winery wastewater samples

		Winery A	Winery B	Winery C	Winery D
Glycerol	Prevalence (%)	50	94	50	67
	Conc. range (mg/L)	0 to 7,123	0 to 7,948	0 to 1,643	0 to 2,355
	Seasonality	No	No	No	No
Tartaric acid	Prevalence (%)	70	93	78	75
	Conc. range (mg/L)	0 to 392	0 to 1,794	0 to 165	0 to 352
	Seasonality	No	No	No	No
Malic acid	Prevalence (%)	22	64	14	22
	Conc. range (mg/L)	0 to 238	0 to 583	0 to 138	0 to 125
	Seasonality	No	No	No	No
Lactic acid	Prevalence (%)	8	11	17	22
	Conc. range (mg/L)	0 to 33	0 to 770	0 to 10	0 to 269
	Seasonality	No	Pre-crush	No	No
Succinic acid	Prevalence (%)	20	64	25	31
	Conc. range (mg/L)	0 to 230	0 to 1,121	0 to 938	0 to 333
	Seasonality	No	No	No	No
Glucose	Prevalence (%)	19	22	14	22
	Conc. range (mg/L)	0 to 1,596	0 to 653	0 to 1,450	0 to 626
	Seasonality	Crush	Crush	Crush*	Crush*
Fructose	Prevalence (%)	36	83	19	31
	Conc. range (mg/L)	0 to 412	0 to 238	0 to 12	0 to 506
	Seasonality	Crush	Crush	No	Crush
Maltose	Prevalence (%)	31	56	36	33
	Conc. range (mg/L)	0 to 889	0 to 718	0 to 45	0 to 14
	Seasonality	No	No	Crush	Crush

*Inlet samples.

notably the concentration and the chemical species of the particular molecule/s, and the physicochemistry of the soil horizon (Inderjit & Mallik 1997; Coliarieti *et al.* 2002; Tharayil *et al.* 2006; Chen *et al.* 2009).

In this study, the percentage contribution of total phenolics to the COD was small, ranging from 0.2 to 4.2%, with the highest percentages being found during the bottling season. There were significant correlations ($r=0.98, 0.82, 0.80, 0.50$; $p < 0.050$ from Wineries A through D, respectively) between COD and total phenolics in the samples. In keeping with elevated temporal COD values, 10 samples from Winery B, and 1 sample from Winery D, exhibited concentrations >100 mgGAE/L (110 to 3,531 mgGAE/L, and 110 mgGAE/L, respectively (GAE = gallic acid equivalents)). The total phenolic concentration in the remainder of the samples from Wineries A, C and D were <100 mgGAE/L throughout the study period.

Given the complexity of the subject, and the lack of available literature, it was beyond the scope of this study to determine the detailed phenolic profile and relate this to the potential environmental threat of the winery wastewater. Only one such study is reported in the literature,

where three hardy wetland macrophyte species (*Phragmites australis*, *Schoenoplectus validus*, *Juncus ingens*) were unable to survive in diluted winery wastewater with a total phenolic concentration as low as 2.5 mg/L (Arienzo *et al.* 2009a). However, it was not definitively established which component (or combinations) in the wastewater were responsible for the phytotoxicity. There is therefore a clear need for more in-depth research in this area. This would require formulating complex synthetic phenolic cocktails to mimic those found in 'typical' winery wastewaters. These cocktails would then need to be applied with and without other organic and inorganic fractions in toxicity assays.

The inorganic fraction of winery wastewater

Origin of inorganics in winery wastewater

Inorganics in winery wastewater originate from cleaning and sanitising agents, and from grape skins, juice and wine (Mosse *et al.* 2011a; Conradie *et al.* 2014; Versari *et al.* 2014). The range of inorganic cleaning products used in

wineries include alkalis (sodium hydroxide (NaOH), potassium hydroxide (KOH), sodium metasilicate (Na₂SiO₃), trisodium phosphate (Na₃PO₄), sodium carbonate (Na₂CO₃), and acids (phosphoric acid (H₃PO₄)). Caustic soda (NaOH) is also used as a sanitising agent. Other sanitising agents include quaternary ammonium compounds, peracetic acid compounds, hydrogen peroxide (H₂O₂), ozone, sulphur (S) compounds and heat. Depending on cellar practices, the cleaning and sanitising agents are expected to contribute mainly Na and/or K to the inorganic fraction of winery effluent, but some phosphorus/phosphate (P/PO₄³⁻), and NH₃/NH₄⁺ is also likely to originate from this source.

The concentration of inorganics in grapes varies according to the soil geochemistry, agricultural practices, and the plant uptake (which depends on the grape varietal and rootstock) (Versari *et al.* 2014; Bimpilas *et al.* 2015). In addition to Na, K, N and P, Bustamante *et al.* (2005) found high concentrations of Ca (286 mg/L), Mg (33 mg/L) and Fe (12 mg/L), as well as lower concentrations of Mn (310 µg/L), Cu (790 µg/L), Zn (580 µg/L), Co (170 µg/L), Cr (150 µg/L), Pb (1,090 µg/L), Cd (60 µg/L) and Ni (120 µg/L) in 21 samples of winery/distillery wastewater.

While the inorganic fraction emanating from the grapes, and to a large extent the influent wash-water, is unavoidable, the fraction from the cleaning and sanitising agents can be decreased by instituting best practice principles for wastewater management in wineries. This study therefore focussed on quantifying the inorganics that may have originated from cleaning and sanitising agents (Na and K), and those that can be present in cleaning agents and are also important nutrients in biological wastewater treatment processes (N and P).

Sodium and potassium concentrations in winery wastewater samples

NaOH is widely used as a cleaning and sanitising agent because it is inexpensive and effective. However, high concentrations of sodium in irrigation water can have a severe impact on the soil structure. In contrast, the addition of K in moderate concentrations is seen as beneficial, making KOH an environmentally-preferable alternative for cellar use. Unfortunately, it has not been widely adopted because it is significantly more expensive and is perceived to be less effective (Arienzo *et al.* 2009b).

To assist in preventing soil sodicity, the sodium adsorption ratio (SAR) was developed as a simplistic measure of the suitability of saline wastewater for irrigation (Equation (1), where cations are expressed in mmol/L). The World Health

Organization SAR guideline for this parameter for irrigation is 3 to 12 (Oliveira & Duarte 2014).

$$\frac{[\text{Na}]}{\sqrt{([\text{Ca}] + [\text{Mg}])}} \quad (1)$$

Oliveira & Duarte (2014) measured the SAR in treated winery wastewater from three wineries over a period of 3 years, and found the average to be 13 ± 2 (winery with lowest SAR) to 23 ± 6 (winery with highest SAR), all higher than the WHO recommendation.

In this study, the average winery effluent K concentrations were significantly higher ($p < 0.01$) than the Na counterparts at each winery (Table 2).

There were significant temporal trends in the concentrations of Na and K in the samples from all four wineries ($p < 0.01$) (Figure 5). In the case of Na, this contrasts with results obtained by Sheridan *et al.* (2011), who found that the Na concentration from one winery was relatively stable around the 50 mg/L mark ($n = 10$ samples over 1 year). In the WSP samples, elevated Na concentrations were found in all samples taken between August and December, and in the samples from Winery A, from August to November (Figure 5(a)). It was clear from the results that the highest concentrations of cleaning agents are found in winery wastewater during the non-crush season, which is expected as high concentrations of caustic soda are typically used for cleaning tanks/fermenters (Figure 5(b)).

Unlike Na, which emanates mainly from cleaning agents, significant quantities of K in winery wastewater can also be derived from grapes and wine. In all samples, the K concentrations remained < 150 mg after the crush season in spring and into early winter (April to July). In samples from the SBs, there was a sustained spike in K from August to October at Winery A, which correlated

Table 2 | Average sodium and potassium concentrations measured in the effluent from four wineries over a period of 1 year

	Na (mg/L)		K (mg/L)	
	Average $n = 36$ for each winery	Range	Average $n = 36$ for each winery	Range $n = 36$
Winery A	23 ± 19	5–67	59 ± 83	5–329
Winery B	73 ± 54	18–574	130 ± 96	11–383
Winery C	73 ± 35	24–116	265 ± 108	28–389
Winery D	55 ± 50	11–142	210 ± 106	43–334

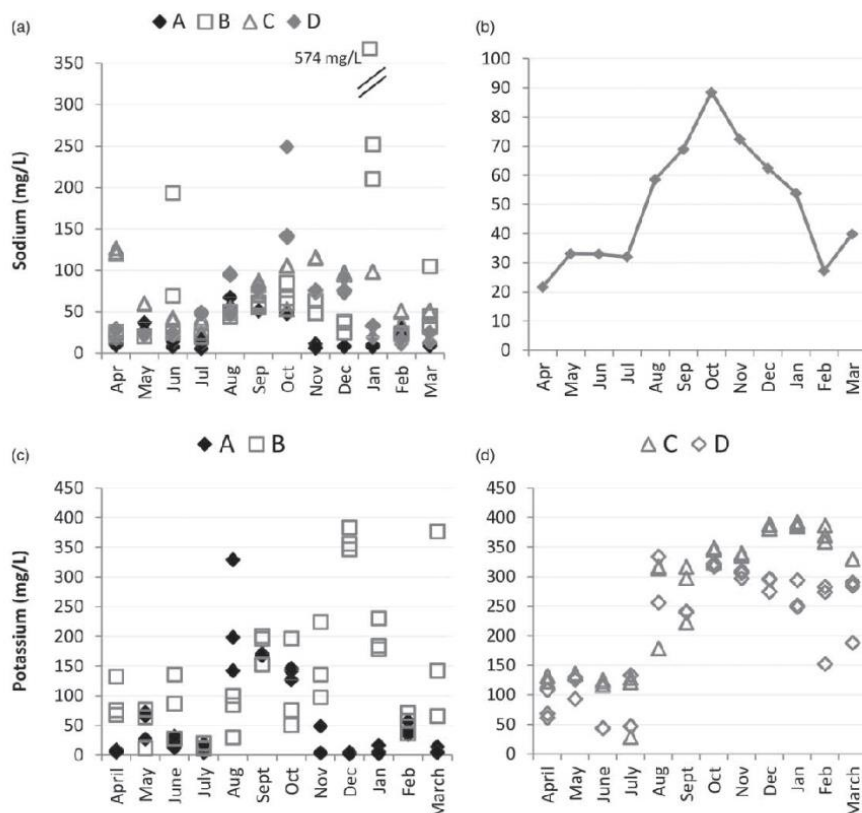


Figure 5 | Individual monthly wastewater sodium concentrations in all samples (a); average combined wastewater sodium concentrations from all sampling sites, with outliers removed [outliers: Winery B (January, June outlet); Winery C: April; Winery D: October site 3] (b); monthly wastewater potassium concentrations from all sampling sites in the SBs (c); and monthly wastewater potassium concentrations from all sampling sites in the WSPs (d).

with increased Na, but otherwise the monthly distribution was random (Figure 5(c)). In the WSPs (Figure 5(d)), which are a more accurate reflection of monthly trends, it is evident that the K levels in winery wastewater were affected by input from grape, grape juice and wine, as well as cleaning products, because as with Na, there was an increase in August. However, in contrast to the Na results, this was sustained during the crush period (February to March) when the COD values were highest.

Nitrogen and phosphorus in winery wastewater

If released to the environment, the presence of N and P in wastewater can lead to eutrophication and the death of aquatic organisms, including amphibians and fish (William *et al.* 2011). In this study, high concentrations of N (up to 176 mg/L), comprised mainly of different ratios of $\text{NH}_3/\text{NH}_4^+$ and NO_3^- , were found in the SB at Winery B (Figure 6(a)). The majority of the samples from the other

wineries fell below 10 mg/L (Figure 6(b)), with the notable exception of four samples from the WSP at Winery C taken in January and February (range: 10 to 40 mg/L). This coincided with an algal bloom in the pond. It is hypothesised that algal atmospheric N-fixation was responsible for the spike. Analysis of the TN results from the WSPs is confounded by the fact that microbial nitrogen fixation, nitrification and denitrification can take place in such systems, so that N can be both added and/or removed during storage.

Unlike N, P can neither be added to nor removed from a system by fixation or volatilisation via mineralisation. Concentrations >1 mg/L can lead to eutrophication of water bodies, but it is also an essential nutrient for plant growth (Correl 1998; William *et al.* 2011). It can precipitate into sediments in inland waters, become complexed with components of soil (e.g. iron), or be removed with microbial biomass in settled sludge of suspended growth wastewater treatment systems (Correl 1998; Wetzel 2001). The importance of P removal from winery wastewater is therefore dependent

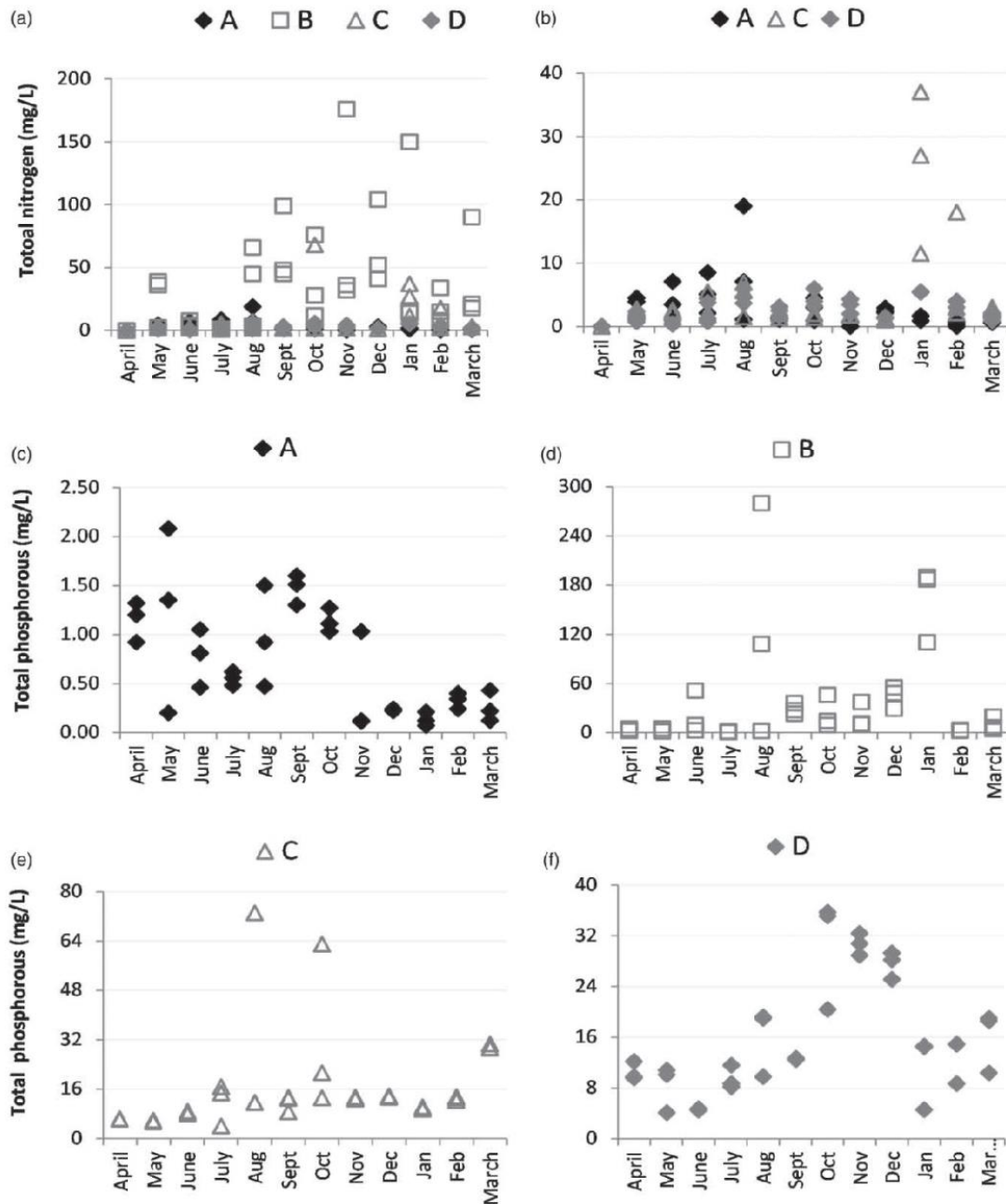


Figure 6 | Monthly wastewater TN concentrations in samples from all wineries (a), and all wineries except the SB at Winery B (b); and monthly total phosphorus concentrations in all samples from the SBs at Winery A and B (c) and (d), and WSPs at Winery C and D (e) and (f).

on a number of factors, most important being the destination of the final effluent. If the wastewater is being used for irrigation, the P concentrations and the soil properties will determine whether the seepage or run-off poses an environmental threat to inland water bodies. In this study, high

concentrations of P were intermittently found in the WSPs and the SB at Winery B, in the order of Winery B > Winery C > Winery D > Winery A (Figure 6(c)–6(f)). The concentration of this element is thus an important parameter to consider when monitoring winery wastewater for discharge.

Apart from the environmental significance of N and P, they are the most important functional nutrients required for biological systems treating organic-rich wastewaters, such as winery wastewater. In terms of the COD:N:P ratio, the ideal metabolic requirement is approximately 100:5:1, but differs according to the treatment system and the composition of the COD (O'Flaherty & Gray 2013). Winery wastewater may be nutrient-limited in terms of N and P. To remedy this, additional nutrients are sometimes added, or high C:N wastewater is treated simultaneously with domestic wastewater (Ganesh *et al.* 2009). However, addition of N and P may lead to excess nutrients in the treated effluent (Rodríguez-Caballero *et al.* 2012). In this study, the N, and to a lesser extent, P values were less than those suggested for biological wastewater treatment systems (Table 3). There is a possibility that N deficiency could be overcome by microbial nitrogen fixation in systems with relatively high HRTs, as has been shown with kraft mill wastewater in WSPs (Clark *et al.* 1997).

The pH of winery wastewater

Previous studies have reported the pH ranges of winery wastewater generated during the crush and non-crush as 4 to 6, and 6 to 8, respectively (Bolzonella & Rosso 2013). The lower values during the crush season have been linked to the presence of lower concentrations of caustic (alkaline) cleaning products. In samples taken from the SB at Winery A, the pH values fell in a relatively narrow range (between 5.0 and 7.2), but in the SB at Winery B, there were large monthly variations, ranging from 3.6 in August to 10.5 in June. There was no obvious distinction in the pH between the crush and non-crush seasons in the samples from the SBs. As expected, the pH changes in the samples taken from the WSPs were less erratic, and with

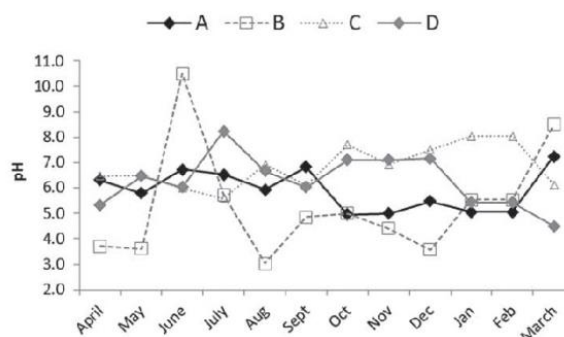


Figure 7 | Average ($n = 3$) monthly pH values in winery wastewater samples taken from SBs at Winery A and B, and the WSPs at Winery C and D.

the exception of the samples from Winery D in March, all monthly averages fell to between pH 5 and 8 (Figure 7).

CONCLUSIONS

In terms of wastewater remediation, the compositional variability of winery effluent presents a challenge during the design and operation of many physicochemical and biological treatment systems. In this study, it was shown that storage of effluent in ponds smoothed the variable nature of winery wastewater. Ponds can therefore potentially serve as both storage and equalisation basins to minimise fluctuations in pH, and volumetric and mass loading prior to further downstream remediation processes. Up-front equalisation could therefore be considered as best practice for winery wastewater treatment. In addition, previous studies have shown that when high C:N wastewater is treated in ponds, the environment becomes conducive for bacterial and/or algal nitrogen fixation. The nitrogen-deficient nature of winery effluent could potentially be overcome by nutrient 'self-balancing' in ponds. This would circumvent the common practice of adding nutrients to improve the performance of conventional biological treatment systems. Not only does nitrogen addition add to the cost and complexity of treatment, but residual nitrogen can result in eutrophication if the treated wastewater is discharged to the aquatic environment. Therefore, provided land requirements can be met, it is feasible to use ponds to pre-treat winery wastewater in order to improve the performance of downstream biological treatment systems.

The organic character of winery wastewater changes considerably during storage in ponds. In particular, there is a significant accumulation of VFAs. Research into (i) the reasons for this propensity, including the role of nitrogen

Table 3 | The ratio of essential nutrients measured in winery wastewater samples

	COD:N (100:X)		COD:P (100:X)	
	Average X $n = 36$ for each winery	Range	Average X $n = 36$ for each winery	Range
Winery A	1.20 ± 1.61	<0.01–6.3	0.41 ± 0.94	0.02–3.96
Winery B	0.65 ± 0.81	0.07–2.84	1.29 ± 2.79	0.01–12.47
Winery C	0.57 ± 1.61	0.04–7.18	0.59 ± 0.83	0.09–2.83
Winery C*	0.06 ± 0.05	0.04–0.16	N/A	N/A
Winery D	0.09 ± 0.06	0.01–0.21	0.70 ± 1.00	0.06–4.63

*Outliers from algal bloom period removed from Winery C. Ideal value of X for N = 5. Ideal value of X for P = 1 (O'Flaherty & Gray 2013).

limitation, (ii) the implications of high VFA concentrations on wastewater treatment processes, and (iii) the effect of VFA load on the environment, is recommended.

Finally, the results of this study reiterate previous research findings that: (i) although there are commonalities, the composition of winery wastewater is highly variable on a temporal and site basis, (ii) the highest concentrations of organics, and lowest concentrations of inorganics (from cleaning products) are found during the crush season, with the converse being true for the non-crush period, and (iii) without treatment, winery wastewater is generally not suitable for irrigation purposes in terms of current legislative requirements, and may lead to environmental degradation.

ACKNOWLEDGEMENTS

The authors would like to thank the National Research Foundation of South Africa for funding this project (P. Welz competitive support for unrated researchers grant number 91520), Jacques Rossouw from Distell for assistance with site selection, Ndimiso Mshicileli for assistance with the HPLC analyses, and the (unnamed) wineries involved.

REFERENCES

- Akuzawa, M., Hori, T., Haruta, S., Ueno, Y., Ishii, M. & Igarashi, Y. 2011 Distinctive responses of metabolically active microbiota in a thermophilic anaerobic digester. *Microbial Ecology* **61**, 595–605.
- Andreoletta, G., Foldari, P. & Ziglio, G. 2009 Biological treatment of winery wastewater: an overview. *Water Science and Technology* **5**, 1117–1125.
- Arienzo, M., Christen, E. W. & Quayle, W. C. 2009a Phytotoxicity testing of winery wastewater for constructed wetlands treatment. *Journal of Hazardous Materials* **169**, 94–99.
- Arienzo, M., Christen, E. W., Quayle, W. C. & Kumar, A. 2009b A review of the fate of potassium in the soil-plant system after land application of wastewaters. *Journal of Hazardous Materials* **164**, 415–422.
- Aybar, M., Carvallo, M., Fabacher, F., Pizarr, G. & Pastén, P. 2007 Towards a benchmarking model for wastewater treatment and disposal. *Water Science and Technology* **56**, 153–160.
- Bimpilas, A., Tsimogiannis, D., Balta-Brouma, K., Lympelopoulou, T. & Oreopoulou, V. 2015 Evolution of phenolic compounds and metal content of wine during alcoholic fermentation and storage. *Food Chemistry* **178**, 164–171.
- Bolzonella, D. & Rosso, D. 2013 *Proceedings of the 6th IWA conference on Viticulture and Winery wastes*. Narbonne, France.
- Bories, A. & Sire, Y. 2010 Impacts of winemaking methods on wastewaters and their treatment. *South African Journal of Enology and Viticulture* **31**, 38–44.
- Bustamante, M. A., Paredes, C., Moral, R., Moreno-Caselles, J., Perez-Espinosa, A. & Perez-Murcia, M. D. 2005 Uses of winery and distillery effluents in agriculture: characterisation of nutrient and hazardous components. *Water Science and Technology* **51**, 145–151.
- Chen, H., Yao, J., Wang, F., Choi, M. M. F., Bramanti, E. & Zaray, G. 2009 Study on the toxic effect of diphenol compounds on soil microbial activity by a combination of methods. *Journal of Hazardous Materials* **167**, 846–851.
- Clark, T. A., Dare, P. H. & Bruce, M. E. 1997 Nitrogen fixation in an aerated stabilization basin treating bleached kraft mill wastewater. *Water Environment Research* **69**, 1039–1046.
- Coliarieti, M. L., Toscano, G. & Greco, G. 2002 Soil-catalyzed polymerization of phenolics in polluted waters. *Water Research* **36**, 3015–3022.
- Conrad, R. & Klose, M. 2011 Stable carbon isotope discrimination in rice field soil during acetate turnover by syntrophic acetate oxidation or acetoclastic methanogenesis. *Geochimica et Cosmochimica Acta* **75**, 1531–1539.
- Conradie, A., Sigge, G. O. & Cloete, T. E. 2014 Influence of winemaking practices on the characteristics of winery wastewater and water usage of wineries. *Journal of South African Enology and Viticulture* **35**, 10–19.
- Correl, D. L. 1998 The role of phosphorus in the eutrophication of receiving waters: a review. *Journal of Environmental Quality* **27**, 261–266.
- Devesa-Rey, R., Bustos, G., Cruz, J. M. & Moldes, A. B. 2011 Optimisation of entrapped activated carbon conditions to remove coloured compounds from winery wastewaters. *Bioresource Technology* **102**, 6437–6442.
- Ganesh, R., Rajagopal, R., Thanikal, J. V., Ramanujin, R. A. & Torrijos, M. 2009 Anaerobic treatment of winery wastewater in a fixed bed reactor. *Bioprocess and Biosystems Engineering* **33**, 619–628.
- Inannou, L. A., Li Puma, G. & Fatta-Kassino, D. 2015 Winery wastewater treatment by physicochemical, biological and advanced processes: a review. *Journal of Hazardous Materials* **286**, 343–368.
- Inderjit, I. & Mallik, A. U. 1997 Effect of phenolic compounds on selected soil properties. *Forest Ecology and Management* **92**, 11–18.
- Lofrano, G. & Meric, S. 2016 A comprehensive approach to winery wastewater treatment: a review of the state-of-the-art. *Desalination and Water Treatment* **57**, 3011–3028.
- Ma, A., Ma, M., Ren, Q. & Li, W. 2013 Process research of ethanol wastewater treatment. *Advanced Materials Research* **807–809**, 1497–1500.
- Malandra, L., Wolfaardt, G., Zietsman, A. & Viljoen-Bloom, M. 2003 Microbiology of a biological contactor for winery wastewater treatment. *Water Research* **37**, 4125–4134.
- Mosse, K. P. M., Patti, A. F., Christen, E. W. & Cavagnaro, T. R. 2011a Review: winery wastewater quality and treatment options in Australia. *Australian Journal of Grape and Wine Research* **17**, 111–122.

- Mosse, K. P. M., Patti, A. F., Smernik, R. J., Christen, E. W. & Cavagnaro, T. R. 2011b Physicochemical and microbiological effect of long- and short-term winery wastewater application to soils. *Journal of Hazardous Materials* **201–202**, 219–228.
- Mosse, K. P. M., Lee, J., Leachman, B. T., Parikh, S. J., Cavagnaro, T. R., Patti, A. F. & Steenworth, K. L. 2013 Irrigation of an established vineyard with winery cleaning agent solution (simulated winery wastewater): vine growth, berry quality and soil chemistry. *Agricultural Water Management* **123**, 93–102.
- Mutabaruka, R., Hairiah, K. & Cadisch, G. 2007 Microbial degradation of hydrolysable and condensed tannin polyphenol-protein complexes in soils from different land-use histories. *Soil Biology and Biochemistry* **39**, 1479–1492.
- O'Flaherty, E. & Gray, N. F. 2013 A comparative analysis of the characteristics of a range of real and synthetic wastewater. *Environmental Science and Pollution Research* **20**, 8813–8830.
- Oliveira, M. & Duarte, E. 2014 Integrated approach to winery waste: waste generation and data consolidation. *Frontiers of Environmental Science and Technology* **10**, 1–9.
- Qu, X. H. & Wang, J. G. 2008 Effect of amendments with different phenolic acids on soil microbial biomass, activity, and community diversity. *Applied Soil Ecology* **39**, 172–179.
- Quayle, W. C., Fattore, A., Zandona, R., Christen, E. W. & Arienzo, M. 2009 Evaluation of organic matter concentration in winery wastewater: a case study for Australia. *Water Science and Technology* **60**, 2521–2528.
- Rodriguez-Caballero, A., Ramond, J. B., Welz, P. J., Cowan, D. A., Odlare, M. & Burton, S. G. 2012 Treatment of high ethanol concentration wastewater by biological sand filters: enhanced COD removal and bacterial community dynamics. *Journal of Environmental Management* **109**, 54–60.
- Sheridan, C., Glasser, D., Hildenbrandt, D., Petersen, J. & Rohwer, J. 2011 An annual and seasonal characterisation of winery effluent in South Africa. *South African Journal of Enology and Viticulture* **32**, 1–8.
- Slinkard, K. & Singleton, V. L. 1977 Total phenol analysis: automation and comparison with manual methods. *American Journal of Enology and Viticulture* **28**, 49–55.
- Tharayil, N., Prasanta, C. B. & Xing, B. 2006 Preferential sorption of phenolic phytotoxins to soil: implications for altering the availability of allelochemicals. *Agricultural and Food Chemistry* **54**, 3033–3040.
- Versari, A., Laurie, V. P., Ricci, A., Laghi, L. & Parpinello, G. P. 2014 Progress in authentication, typification, and traceability of grapes and wines by chemometric approaches. *Food Research International* **60**, 2–18.
- Vlyssides, A. G., Barampouti, E. M. & Mai, S. 2005 Wastewater characteristics from Greek wineries and distilleries. *Water Science and Technology* **51**, 53–60.
- Welz, P. J., Ramond, J. B., Cowan, D. A., Prins, A. & Burton, S. G. 2011 Ethanol degradation and the value of incremental priming in pilot scale constructed wetlands. *Ecological Engineering* **37**, 1453–1459.
- Welz, P. J., Ramond, J.-B., Cowan, D. A. & Burton, S. G. 2012 Phenolic removal processes in biological sand filters, sand columns and microcosms. *Bioresource Technology* **119**, 262–269.
- Welz, P. J., Palmer, Z., Isaacs, S., Kirby, B. & Le Roes-Hill, M. 2014 Analysis of substrate degradation, metabolite formation and microbial community responses in sand bioreactors treating winery wastewater: a comparative study. *Journal of Environmental Management* **145**, 147–156.
- Wetzel, R. 2001 *Limnology: Lake and River Ecosystems*, 3rd edn. Academic Press, London.
- William, M. L., Wurtsbaugh, W. A. & Paerl, H. W. 2011 Rationale for control of anthropogenic nitrogen and phosphorus to decrease eutrophication of inland waters. *Environmental Science and Technology* **45**, 10300–10305.
- Wolfe, A. J. 2005 The acetate switch. *Microbiology and Molecular Biology* **69**, 12–48.

First received 16 February 2016; accepted in revised form 27 April 2016. Available online 18 June 2016

Appendix G. Statistical analysis of final effluent flow rate

The statistical analysis of all the data point used of flow rate from BSF system.

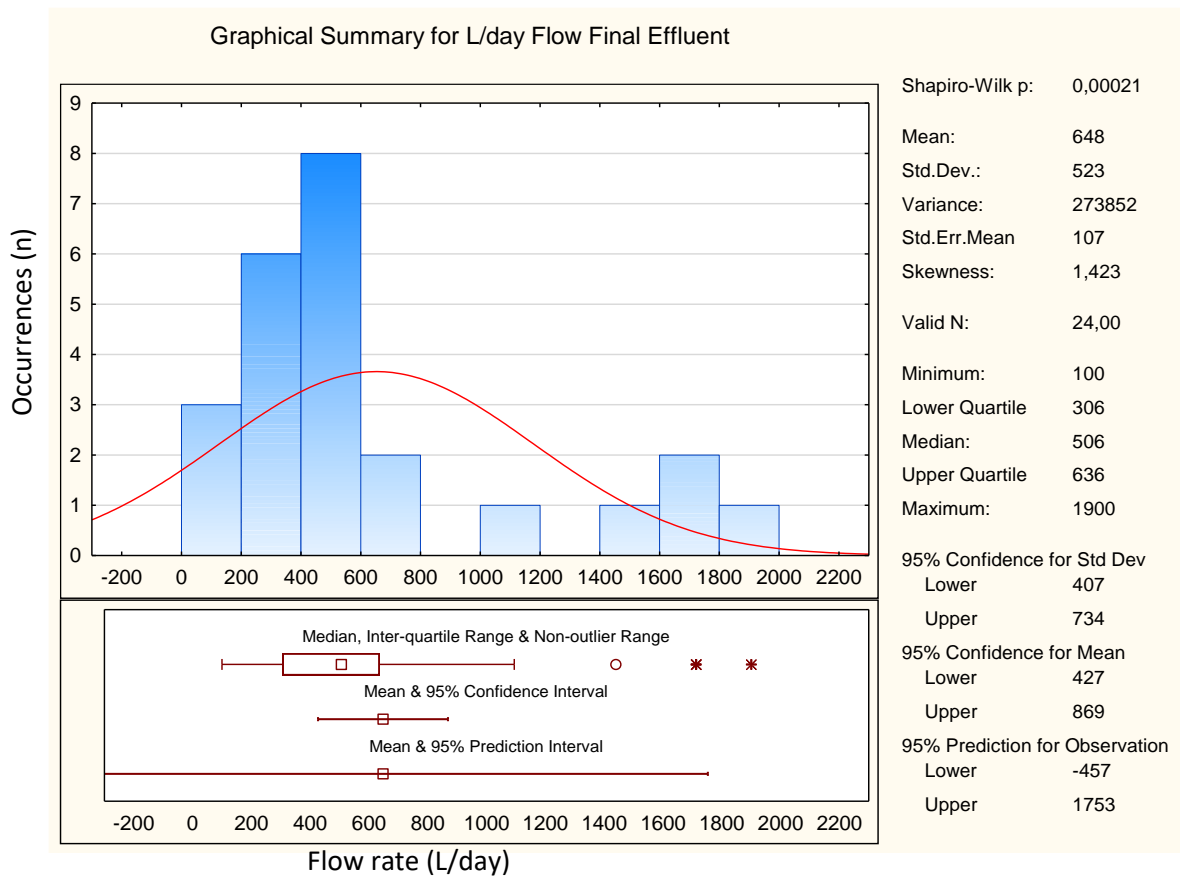


Figure G.1 Results of the statistical analysis of flow rates from the biological sand filtration system

Appendix H. Hydraulic retention time

H. 1. Hydraulic retention time for Filter modules using average discharge

The calculation of HRT for a filter with a flow rate of 413 L/day.

H.1.1. Hydraulic retention time for Q of 413 L/day for a filter module

$$\begin{aligned} HRT &= V_{\text{water}}/Q && (2.6) \\ &= 0.215/413 \div 1000 \div 4 \\ &= 49.98 \text{ hr} \\ &= 2.1 \text{ Days} \end{aligned}$$

H. 2. Calculation of systems hydraulic retention time

The calculations of the entire systems HRT for a flowrate of 413 L/day

H.2.1. Hydraulic retention time for 5000 L holding tank

$$\begin{aligned} HRT &= V/Q && (2.6) \\ &= 3.050/413 \div 1000 \div 24 \\ &= 177.24 \text{ hr} \\ &= 7.4 \text{ days} \end{aligned}$$

H.2.2. Hydraulic retention time for 500 L tank

$$\begin{aligned} HRT &= V/Q && (2.6) \\ &= 0.500/413 \div 1000 \div 24 \\ &= 29.06 \text{ hr} \\ &= 1.2 \text{ days} \end{aligned}$$

H.2.3. Hydraulic retention time for 100 L outlet structure

$$\begin{aligned} HRT &= V/Q && (2.6) \\ &= 0.050/413 \div 1000 \div 24 \div 4 \\ &= 11.62 \text{ hr} \\ &= 0.5 \text{ days} \end{aligned}$$

H.2.4. The total hydraulic retention time for the system

$$\begin{aligned} HRT_{\text{Total}} &= \sum HRT \\ &= 177.34 + 29.06 + 11.62 + 49.98 \\ &= 267.90 \text{ hr} \\ &= \pm 11.2 \text{ days} \end{aligned}$$

H.2.5. Hydraulic retention time between filling for 5000 L holding tank

$$\begin{aligned}
 HRT &= V/Q && (2.6) \\
 &= 1.3/413 \div 1000 \div 24 \\
 &= 75.54 \text{ hr} \\
 &= 3.1 \text{ days}
 \end{aligned}$$

H. 3. Calculation of Hydraulic retention time with adjusted volume

$$\begin{aligned}
 V &= \text{Width} \times \text{Height} \times \text{Length} \\
 &= [1070 (420 - 0.5(150) + 0.5(1/100 \times 1680)) - 10925] \times 1680 \\
 &= 616\,917\,840 \text{ mm}^3 \\
 V &= 0.617 \text{ m}^3 \\
 V_{\text{water}} &= V \times P_t \\
 &= 0.617 \times 0.292 \\
 &= 0.180 \text{ m}^3
 \end{aligned}$$

H.3.1. Hydraulic retention time for Q of 413 L/day and new volume

$$\begin{aligned}
 HRT &= V_{\text{water}}/Q && (2.6) \\
 HRT &= 0.180/413 \div 1000 \div 24 \div 4 \\
 &= 41.84 \text{ hr} \\
 &= 1.7 \text{ days}
 \end{aligned}$$

Appendix I. Achieved hydraulic conductivity calculations

The following calculations are used to determine the K achieved by the filter modules from on-site flow rates and the Darcy's equation.

Calculating the achieved hydraulic conductivity for the initial flow rate of 1900 L/day

$$Q = -KA \frac{dh}{dl} \tag{2.5}$$
$$1900 \div 24 \div 60 \div 60 \div 4 \div = -K \times 0.278 \times \left[\frac{-0.150 - (1/100 \times 1.680)}{1.680} \right]$$
$$= 0.199 \text{ mm/s}$$

Calculating the achieved hydraulic conductivity for the flow rate of 1094 L/day after 4 months of filtration

$$Q = -KA \frac{dh}{dl} \tag{2.5}$$
$$1094 \div 24 \div 60 \div 60 \div 4 \div = -K \times 0.278 \times \left[\frac{-0.150 - (1/100 \times 1.680)}{1.680} \right]$$
$$= 0.115 \text{ mm/s}$$

Calculating the achieved hydraulic conductivity for the average flow rate of 413 L/day

$$Q = -KA \frac{dh}{dl} \tag{2.5}$$
$$413 \div 24 \div 60 \div 60 \div 4 \div = -K \times 0.278 \times \left[\frac{-0.150 - (1/100 \times 1.680)}{1.680} \right]$$
$$= 0.043 \text{ mm/s}$$

Calculating the achieved hydraulic conductivity for the minimum recorded flow rate of 144 L/day

$$Q = -KA \frac{dh}{dl} \tag{2.5}$$
$$144 \div 24 \div 60 \div 60 \div 4 \div = -K \times 0.278 \times \left[\frac{-0.150 - (1/100 \times 1.680)}{1.680} \right]$$
$$= 0.015 \text{ mm/s}$$

Appendix J. Integration of outlet height optimization

The following calculations are used to determine the theoretical flow rate by reducing the theoretical outlet height and thus reducing the saturated area of sand within the filter. This was done to determine the optimum outlet height. The change in head together with the saturated height of sand was used in terms of the Darcy's equation. The Darcy's equation was combined with the cross-sectional area formula to determine the different discharge rates at different heights in an integrated formula. The theoretical K , determined in Section Appendix I, of 0.044 mm/s was used. This was used in an Excel spreadsheet to calculate the remaining data points at the different height, as seen in Table K.1.

$$Q = -KA \frac{dh}{dl} \quad (2.5)$$

$$A = 1070(x) - 10925 \quad (3.1)$$

$$Q = -K \times ((1070(x \times 1000) - 10925) \div 1000^2) \times \left[\frac{-(0.420 - x) - (1/100 \times 1.680)}{1.680} \right] \quad (0.3)$$

$$Q = -(0.044 \div 1000 \times 60 \times 60) \times ((1070(0.400 \times 1000) - 10925) \div 1000^2) \times \left[\frac{-(0.420 - 0.400) - (1/100 \times 1.680)}{1.680} \right] * 1000 * 24$$

$$Q = 34.7 \text{ l/day}$$

Table J.1 Flow rates of biological sand filter for changing outlet heights using a k of 0.044 mm/s

fall	Hight of sand column	cross-sect	Discharge	fall	Hight of sand column	cross-sect	Discharge
(mm)	(mm)	(m ²)	(L/day)	(mm)	(mm)	(m ²)	(L/day)
0	420	0.438	16.67	205	215	0.219	109.98
5	415	0.433	21.37	210	210	0.214	109.71
10	410	0.428	25.94	215	205	0.208	109.33
15	405	0.422	30.40	220	200	0.203	108.82
20	400	0.417	34.73	225	195	0.198	108.19
25	395	0.412	38.94	230	190	0.192	107.44
30	390	0.406	43.04	235	185	0.187	106.56
35	385	0.401	47.01	240	180	0.182	105.57
40	380	0.396	50.86	245	175	0.176	104.46
45	375	0.390	54.58	250	170	0.171	103.22
50	370	0.385	58.19	255	165	0.166	101.87
55	365	0.380	61.68	260	160	0.160	100.39
60	360	0.374	65.04	265	155	0.155	98.79
65	355	0.369	68.29	270	150	0.150	97.07
70	350	0.364	71.41	275	145	0.144	95.23
75	345	0.358	74.41	280	140	0.139	93.27
80	340	0.353	77.30	285	135	0.134	91.19
85	335	0.348	80.06	290	130	0.128	88.98
90	330	0.342	82.69	295	125	0.123	86.66
95	325	0.337	85.21	300	120	0.117	84.21
100	320	0.331	87.61	305	115	0.112	81.65
105	315	0.326	89.89	310	110	0.107	78.96
110	310	0.321	92.04	315	105	0.101	76.15
115	305	0.315	94.07	320	100	0.096	73.22
120	300	0.310	95.99	325	95	0.091	70.17
125	295	0.305	97.78	330	90	0.085	67.00
130	290	0.299	99.45	335	85	0.080	63.71
135	285	0.294	101.00	340	80	0.075	60.29
140	280	0.289	102.43	345	75	0.069	56.76
145	275	0.283	103.73	350	70	0.064	53.10
150	270	0.278	104.92	355	65	0.059	49.32
155	265	0.273	105.99	360	60	0.053	45.42
160	260	0.267	106.93	365	55	0.048	41.41
165	255	0.262	107.75	370	50	0.043	37.26
170	250	0.257	108.45	375	45	0.037	33.00
175	245	0.251	109.04	380	40	0.032	28.62
180	240	0.246	109.50	385	35	0.027	24.12
185	235	0.241	109.83	390	30	0.021	19.49
190	230	0.235	110.05	395	25	0.016	14.75
195	225	0.230	110.15	400	20	0.010	9.88
197	223	0.228	110.15	405	15	0.005	4.89
200	220	0.224	110.12	410	10	0.000	-0.22

Appendix K. Hydraulic and organic loading rate

Volume of filter module

$$\begin{aligned} Vol &= Area \times Length \\ &= (1070 \times 420 - 10925) \div 1000^2 \times 1.68 \\ &= 0.438 \times 1.680 \\ &= 0.736m^3 \end{aligned}$$

Hydraulic loading rate for August the 25th 2016

$$\begin{aligned} HLR &= Q \div Vol && (2.7) \\ &= \frac{403}{4} \div 0.736 \\ &= 137 L/m^3 \text{ of sand. day}^{-1} \end{aligned}$$

Organic loading rate for August the 25th 2016

$$\begin{aligned} OLR &= HLR \times COD && (2.10) \\ &= 137 \times 1905 \div 1000 \\ &= 261 gCOD/m^3 \text{ of sand. day}^{-1} \end{aligned}$$

Organic removal rate for August the 25th 2016

$$\begin{aligned} OLR &= HLR \times COD && (2.11) \\ &= 137 \times (1905 - 32) \div 1000 \\ &= 253 gCOD/m^3 \text{ of sand. day}^{-1} \end{aligned}$$

Appendix L. Correlations of flow rate and chemical oxygen demand

The correlations done using Dell Statistica between different measured parameters from the system.

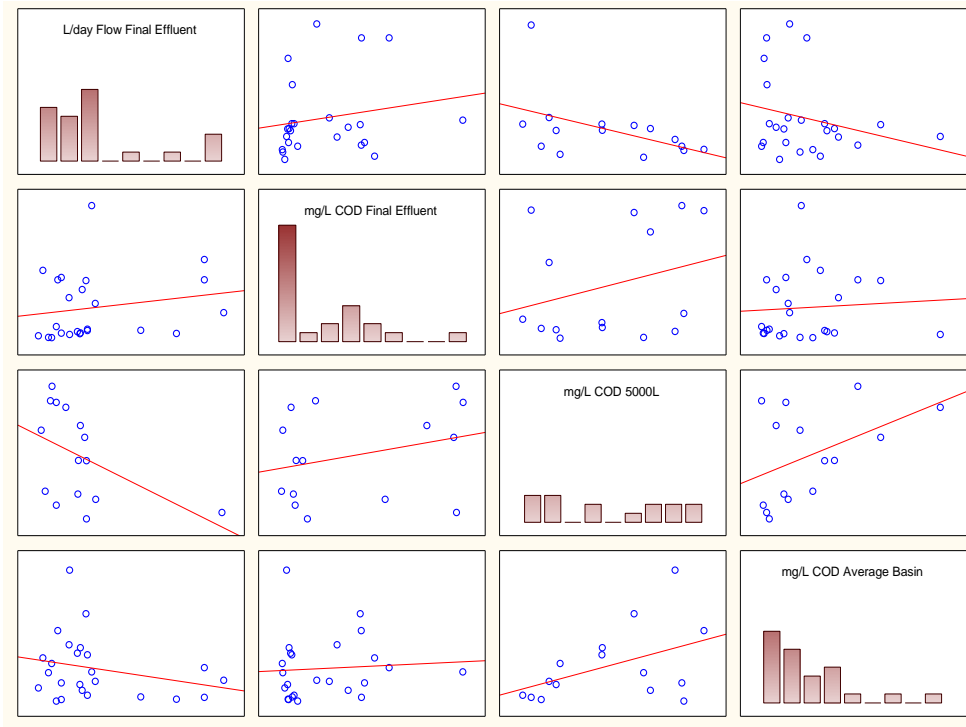


Figure L.1 Relationships between the following: final effluent flowrate and chemical oxygen demand, influent chemical oxygen demand (5000 L holding tank and average from settling basin)

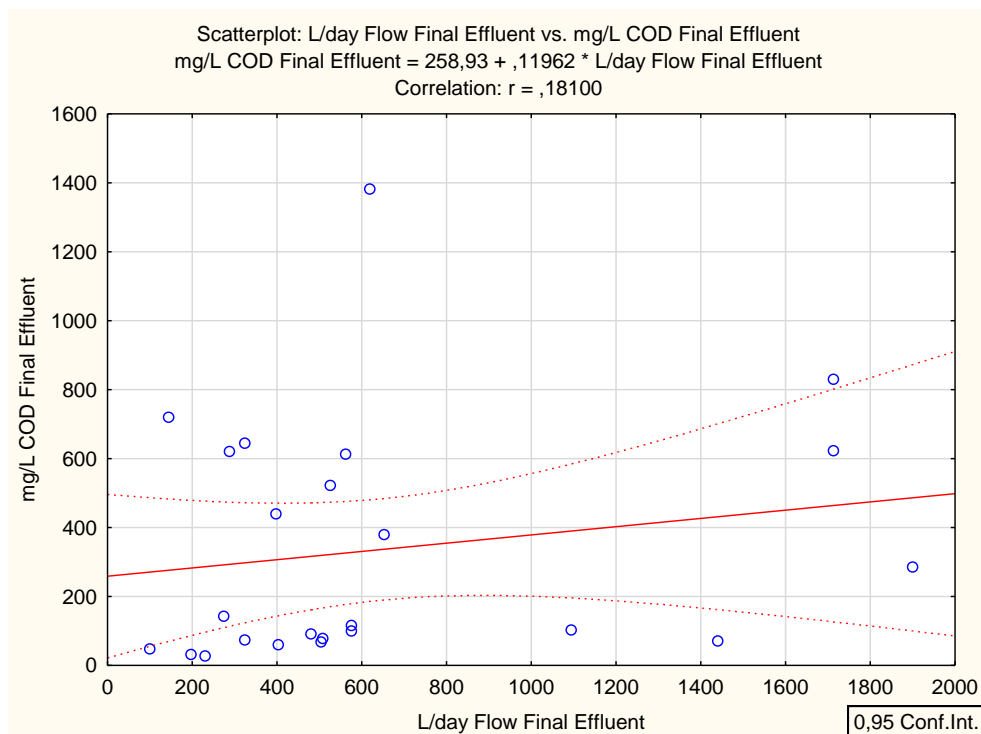


Figure L.2 Correlation between final effluent chemical oxygen demand and final effluent flow rate

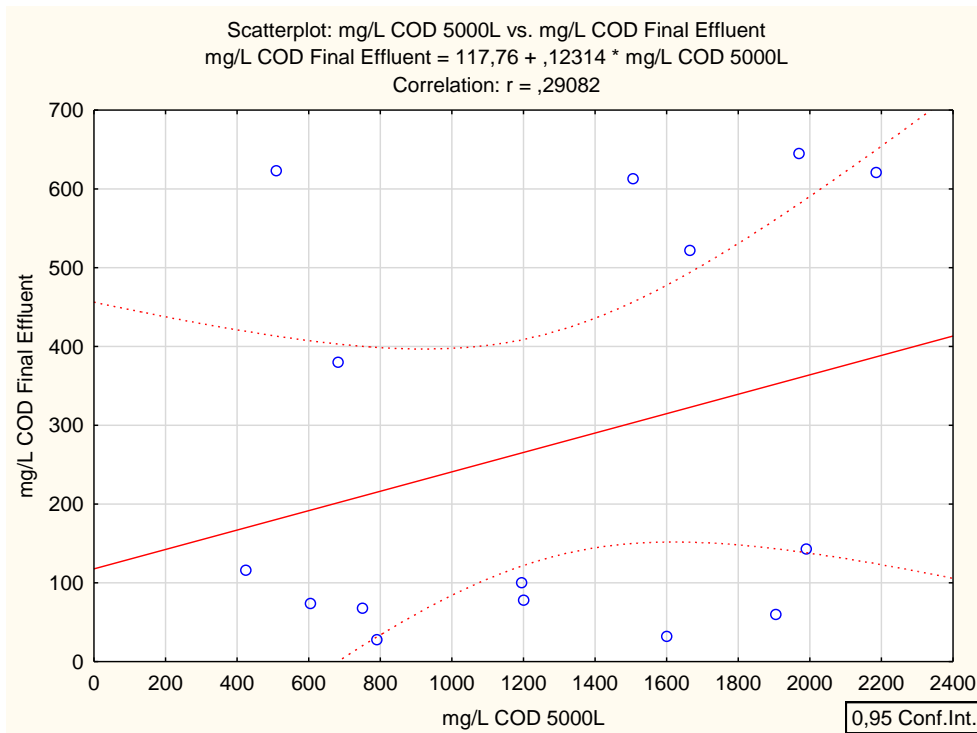


Figure L.3 Correlation between final effluent chemical oxygen demand and 5000 L holding tank COD

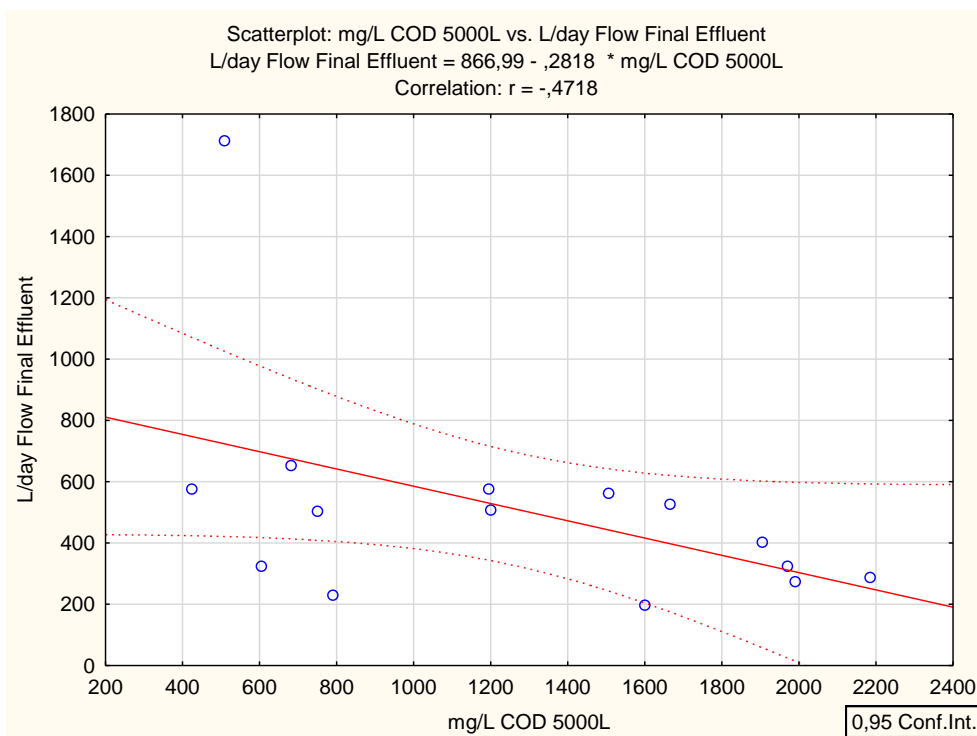


Figure L.4 Correlation between final effluent flow rate and 5000 L holding tank chemical oxygen demand

Appendix M. Hydrological data and discharge calculation

M. 1. Hydrological data for Jonkershoek weather station

The hydrological data near to the testing location was analysed. The information was gathered from The Department of Water and Sanitation of South Africa Hydrology page (<http://www.dwa.gov.za/Hydrology/Verified/HyDataSets.aspx?Station=G2E013>). The monitoring station is Jonkershoek@Manor with a station number of G2E013 and the drainage region of G22F and coordinates of 33°57'50"S 18°55'42"E. The station has been operational since 13th of August 1968, however only monthly values were taken before May 1984. The maximum precipitation from the 1st of May 1984 to 31st of September 2016 was 190.8 mm on the 11th of April 1993, the top ten instances of precipitation can be seen in Table M.1. The average monthly precipitation and evaporation can be seen in Table M.2. The maximum daily precipitation is higher than the any of the monthly averages, showing this was a uniquely high rainfall.

Table M.1 The ten maximum precipitation instances for Jonkershoek@Manor; G2E013 meteorology station from 13th of August 1968 to the end of August 2016

Ranking	1st	2nd	3rd	4th	5th	6th	7th	8th	9th	10th
Precipitation (mm)	190.8	114.2	113.9	100.0	94.0	88.3	88.0	85.0	84.9	82.5
Date	1993-04-11	1989-03-13	1992-04-27	2016-07-14	1991-07-10	1988-08-28	2003-08-18	2009-07-12	1995-08-20	2001-07-03

Table M.2 The average monthly precipitation and evaporation for Jonkershoek@Manor; G2E013 meteorology station in December 2016

Month	Oct	Nov	Dec	Jan	Feb	Mar	Apr	May	Jun	Jul	Aug	Sep	Total
Average Precipitation	49.2	35.9	25.8	22	16.8	33.8	82.8	126.4	162.2	154.6	127.8	76.3	929.3
Average Evaporation	113.8	148.3	175.9	188.8	164.1	138.3	84.7	56.5	36.3	37.1	48.9	66.7	1262.6

M. 2. Calculating the discharge and infiltration of a fully saturate biological sand filter

In order to determine the theoretical infiltration rate of a fully saturated BSF the discharge must be determined. The discharge will change depending on the point at which the water is infiltrating from, as the system is fully saturated the points at the inlet has the shortest distance to travel and thus the greatest flow rate and thus the greatest infiltration in terms of the Darcy's equation, Section 3.4.2. An integrated table was compiled with the different points of infiltration, Table M.3.

M.2.1. Discharge calculations for biological sand filter fully saturated due to precipitation at inlet

Calculating the cross-sectional area

$$\begin{aligned}
 A &= 1070(x) - 10925 & (3.1) \\
 &= 1070(420) - 10925 \\
 &= 438475 \text{ mm}^2 \\
 &= 0.438 \text{ m}^2
 \end{aligned}$$

Calculating the flow rate

$$Q = -KA \frac{dh}{dl} \quad (2.5)$$

$$\begin{aligned}
 Q &= -0.044 \div 1000 \times 60 \times 60 \times 0.438 \\
 &\quad \times \left[\frac{-(0.150 + 0.100) - (1/100 \times 1.680)}{1.680} \right]
 \end{aligned}$$

$$= 0.011 \text{ m}^3/\text{h}$$

$$= 11 \text{ l/hr}$$

$$= 0.264 \text{ m}^3/\text{day.tank}$$

M.2.2. Converting discharge into infiltration

$$\text{Surface area} = \text{lenght} \times \text{width} \quad (0.4)$$

$$= 1.680 \times 1.162$$

$$= 1.952 \text{ m}^2$$

$$\text{Infltration} = \frac{Q}{\text{Surface Area}} \quad (0.5)$$

$$= \frac{0.011}{1.952} \times 1000$$

$$= 6 \text{ mm/day}$$

Table M.3 The integrated flow rate of a fully situated biological sand filter with 100mm of surface water due to precipitation

Distance from inlet	Length of filter	Discharge	Infiltration rate	Distance from inlet	Length of filter	Discharge	Infiltration rate
(m)	(m)	(L/h)	(mm/h)	(m)	(m)	(L/h)	(mm/h)
0.00	1.68	11.0	5.6	0.84	0.84	22.1	11.3
0.02	1.66	11.2	5.7	0.86	0.82	22.6	11.6
0.04	1.64	11.3	5.8	0.88	0.80	23.2	11.9
0.06	1.62	11.4	5.9	0.90	0.78	23.8	12.2
0.08	1.60	11.6	5.9	0.92	0.76	24.4	12.5
0.10	1.58	11.7	6.0	0.94	0.74	25.0	12.8
0.12	1.56	11.9	6.1	0.96	0.72	25.7	13.2
0.14	1.54	12.0	6.2	0.98	0.70	26.5	13.6
0.16	1.52	12.2	6.2	1.00	0.68	27.3	14.0
0.18	1.50	12.4	6.3	1.02	0.66	28.1	14.4
0.20	1.48	12.5	6.4	1.04	0.64	29.0	14.8
0.22	1.46	12.7	6.5	1.06	0.62	29.9	15.3
0.24	1.44	12.9	6.6	1.08	0.60	30.9	15.8
0.26	1.42	13.0	6.7	1.10	0.58	31.9	16.4
0.28	1.40	13.2	6.8	1.12	0.56	33.1	16.9
0.30	1.38	13.4	6.9	1.14	0.54	34.3	17.6
0.32	1.36	13.6	7.0	1.16	0.52	35.6	18.2
0.34	1.34	13.8	7.1	1.18	0.50	37.1	19.0
0.36	1.32	14.0	7.2	1.20	0.48	38.6	19.8
0.38	1.30	14.3	7.3	1.22	0.46	40.3	20.6
0.40	1.28	14.5	7.4	1.24	0.44	42.1	21.6
0.42	1.26	14.7	7.5	1.26	0.42	44.1	22.6
0.44	1.24	14.9	7.7	1.28	0.40	46.3	23.7
0.46	1.22	15.2	7.8	1.30	0.38	48.8	25.0
0.48	1.20	15.4	7.9	1.32	0.36	51.5	26.4
0.50	1.18	15.7	8.0	1.34	0.34	54.5	27.9
0.52	1.16	16.0	8.2	1.36	0.32	57.9	29.7
0.54	1.14	16.3	8.3	1.38	0.30	61.8	31.6
0.56	1.12	16.5	8.5	1.40	0.28	66.2	33.9
0.58	1.10	16.8	8.6	1.42	0.26	71.3	36.5
0.60	1.08	17.2	8.8	1.44	0.24	77.2	39.5
0.62	1.06	17.5	9.0	1.46	0.22	84.2	43.1
0.64	1.04	17.8	9.1	1.48	0.20	92.7	47.4
0.66	1.02	18.2	9.3	1.50	0.18	102.9	52.7
0.68	1.00	18.5	9.5	1.52	0.16	115.8	59.3
0.70	0.98	18.9	9.7	1.54	0.14	132.4	67.8
0.72	0.96	19.3	9.9	1.56	0.12	154.4	79.1
0.74	0.94	19.7	10.1	1.58	0.10	185.3	94.9
0.76	0.92	20.1	10.3	1.60	0.08	231.6	118.6
0.78	0.90	20.6	10.5	1.62	0.06	308.8	158.1
0.80	0.88	21.1	10.8	1.64	0.04	463.3	237.2
0.82	0.86	21.5	11.0	1.66	0.02	926.5	474.4